

Some pages of this thesis may have been removed for copyright restrictions.

If you have discovered material in AURA which is unlawful e.g. breaches copyright, (either yours or that of a third party) or any other law, including but not limited to those relating to patent, trademark, confidentiality, data protection, obscenity, defamation, libel, then please read our [Takedown Policy](#) and [contact the service](#) immediately

MEASUREMENT OF OCULAR COMPONENT CONTRIBUTIONS TO
RESIDUAL ASTIGMATISM IN ADULT
HUMAN EYES

MOHAMED ELHASSAN ALI ELAWAD

Doctor of Philosophy

THE UNIVERSITY OF ASTON IN BIRMINGHAM

July 1995

Computing schemes were used to calculate the residual astigmatism arising from the combination of the following components: (1) calculation of cylindrical lens surface powers of the cornea and lens, (2) calculation of the residual astigmatism arising from the combination of the above components, (3) application of the vector method of analysis to calculate contributions to the residual astigmatism of ocular components with obliquely related cylinder axes, (4) calculation of the effect of random experimental errors on the calculated residual astigmatism data.

A complete set of biometric measurements were obtained from both eyes of 66 undergraduate students. Effectively due to optical factors such as the residual cylinder power contribution (up to 0.25DC) to residual astigmatism, induced by contributions of the anterior chamber depth (up to 0.25DC) and equatorial lens thickness (up to 0.10DC) to the total residual astigmatism were predominantly direct. Most astigmatism arose from the posterior corneal surface (up to 1.00DC) and from the anterior lens surface (up to 0.75DC). The astigmatic contributions of the posterior and anterior lens surfaces were found to be predominantly induced whilst direct astigmatism arose from the anterior lens surface. Very similar results were found for right versus left eyes and males versus females.

This copy of the thesis has been supplied on condition that anyone who consult it is understood to recognise that its copyright rests with its author and that no quotation from the thesis and no information derived from it may be published without proper acknowledgement.

The University of Aston In Birmingham

MEASUREMENT OF OCULAR COMPONENT CONTRIBUTIONS TO
RESIDUAL ASTIGMATISM IN ADULT HUMAN EYES

Mohamed Elhassan Ali Elawad

Ph.D. Thesis

July 1995

SUMMARY

The aim of this study was to determine whether an ophthalmophakometric technique could offer a feasible means of investigating ocular component contributions to residual astigmatism in human eyes.

Current opinion was gathered on the prevalence, magnitude and source of residual astigmatism. It emerged that a comprehensive evaluation of the astigmatic contributions of the eye's internal ocular surfaces and their respective axial separations (effectivity) had not been carried out to date.

An ophthalmophakometric technique was developed to measure astigmatism arising from the internal ocular components. Procedures included the measurement of refractive error (infra-red autorefractometry), anterior corneal surface power (computerised video keratography), axial distances (A-scan ultrasonography) and the powers of the posterior corneal surface in addition to both surfaces of the crystalline lens (multi-meridional still flash ophthalmophakometry).

Computing schemes were developed to yield the required biometric data. These included (1) calculation of crystalline lens surface powers in the absence of Purkinje images arising from its anterior surface, (2) application of meridional analysis to derive spherocylindrical surface powers from notional powers calculated along four pre-selected meridians, (3) application of astigmatic decomposition and vergence analysis to calculate contributions to residual astigmatism of ocular components with obliquely related cylinder axes, (4) calculation of the effect of random experimental errors on the calculated ocular component data.

A complete set of biometric measurements were taken from both eyes of 66 undergraduate students. Effectivity due to corneal thickness made the smallest cylinder power contribution (up to 0.25DC) to residual astigmatism followed by contributions of the anterior chamber depth (up to 0.50DC) and crystalline lens thickness (up to 1.00DC). In each case astigmatic contributions were predominantly direct. More astigmatism arose from the posterior corneal surface (up to 1.00DC) and both crystalline lens surfaces (up to 2.50DC). The astigmatic contributions of the posterior corneal and lens surfaces were found to be predominantly inverse whilst direct astigmatism arose from the anterior lens surface. Very similar results were found for right versus left eyes and males versus females.

Repeatability was assessed on 20 individuals. The ophthalmophakometric method was found to be prone to considerable accumulated experimental errors. However, these errors are random in nature so that group averaged data were found to be reasonably repeatable. A further confirmatory study was carried out on 10 individuals which demonstrated that biometric measurements made with and without cycloplegia did not differ significantly.

Key Words: Human, Ocular Biometry, Residual Astigmatism, Ocular Components, Ophthalmophakometry.

To my Parents

To my wife and my children for their patience and understanding

To all those who endeavour to promote the Sudan optometric profession

ACKNOWLEDGEMENTS

My gratefulness is due to Dr MCM. Dunne my supervisor for his valuable effort in preparing the computing programs, his friendship, encouragement and the knowledgeable guidance I experienced during this study. I would also like to thank A. Syed and all those who sacrificed their time to sit for the experiments. My gratitude is also due to all those who helped me in any way during this study.

I would also like thank The Institute of Optometry and Visual Sciences at Khartoum for the scholarship and my friend Mr H.A.Mangeil for his continuous support. Finally, I am grateful to Aston University hardship fund and the African Education fund for their valuable financial help.

List of Contents	Page
Title Page	1
Thesis Summary	2
Dedication	3
Acknowledgements	4

Chapter One

Scope of Study

1.1	Introduction	21
1.2	Residual Astigmatism	21
1.3	Biometric Methods and Experimental Protocol	21
1.4	Computing Schemes	22
1.5	Preliminary Study: Measurements of Residual Astigmatism	23
1.6	Main Study: Measurements of Internal Ocular Surface Astigmatism	23
1.7	Ocular Component Contributions to Residual Astigmatism	24
1.8	Conclusion and Future Work	24
1.9	Summary	24

Chapter Two

Residual Astigmatism

2.1	Introduction	26
2.2	Definition of Residual Astigmatism	26
2.3	Measurement of Residual Astigmatism	28
2.4	Prevalence and Magnitude of Residual Astigmatism	29

2.5	Possible Sources of Residual Astigmatism	33
2.5.1	Cornea	33
2.5.1.A	Anterior Surface of the Cornea	34
2.5.1.B	Corneal Thickness	34
2.5.1.C	Posterior Corneal Surface	36
2.5.2	The Anterior Chamber	37
2.5.3	Pupil	38
2.5.4	Crystalline Lens	38
2.5.4.A	Anterior Surface of the Lens	39
2.5.4.B	Lens Thickness	40
2.5.4.C	Posterior Surface of the Lens	41
2.5.4.D	Sectional Accommodation	41
2.5.5	Ocular Component Misalignment	42
2.5.6	Other Sources	45
2.5.6.A	Retinal Astigmatism	45
2.5.6.B	Perceptual Astigmatism	45
2.6	Summary	45

Chapter Three

Biometric Methods and Experimental Protocol

3.1	Introduction	48
3.2	Measurement of Refraction	49
3.3	Videokeratographic Measurements of Anterior Corneal Surface	50
3.4	Ultrasonic Measurements of Axial Distances	51
3.5	Ophthalmophakometric Measurements of Internal Ocular Surface Curvature	53
3.6	Experimental Protocol	61

3.6.1	Preliminary Study: Measurements of Residual Astigmatism	61
3.6.2	Main Study: Measurements of Internal Ocular Surface Toricity	62
3.6.3	Cycloplegic Study	63
3.7	Summary	63

Chapter Four

Computing Schemes

4.1	Introduction	66
4.2	Notional Meridional Power	67
4.3	Calculation of Meridional Data for Spectacle Refraction and Anterior Corneal Surface Radius of Curvature	67
4.3.1	Spectacle Refraction	67
4.3.2	Radius of Curvature of Anterior Corneal Surface	68
4.4	Calculation of Internal Ocular Surface Astigmatism	69
4.4.1	Review Meridional Analysis	70
i	Three Meridional Analysis	70
ii	Multi-meridional Analysis	70
4.4.2	Calculation of Meridional Surface Powers	72
i	Refractive and Catoptric Imaging Properties of the Anterior Corneal Surface	72
ii	Refractive and Catoptric Imaging Properties of the Posterior Corneal Surface	74
iii	Calculation of the Crystalline lens Surface Parameters	78
iv	Description of the Iterative Routine	83
4.4.3	Meridional Analysis	86

4.5	Calculation of Ocular Component Contribution to Residual Astigmatic Power	90
4.5.1	Astigmatic Decomposition	90
4.5.2	Vergence Analysis	92
4.5.3	Computing Scheme	93
4.6	Determination of Random Experimental Errors Involved in the Calculation of Meridional Powers	96
4.7	Determination of Random Experimental Errors Involved in the Calculation of Sphero-cylindrical Results	97
4.8	Calculation of Purkinje Image Positions, Ratios and Height	98
	i Anterior Corneal Surface (Purkinje image I)	99
	ii Posterior Corneal Surface (Purkinje image II)	99
	iii Anterior Lens Surface (Purkinje image III)	101
	iv Posterior Lens Surface (Purkinje image IV)	102
4.9	Summary	104

Chapter Five

Preliminary Study: Measurements of Residual Astigmatism

5.1	Introduction	106
5.2	Methods of Calculation	106
5.3	Repeatability	107
5.4	Population Study	111
5.5	Potential Errors of the Method	115
5.6	Summary	117

Chapter Six

Main Study: Measurements of Internal Ocular Surface Astigmatism

6.1	Introduction	119
6.2	Averaged Results and Estimated Precisions	119
6.3	Repeatability	123
6.4	Cycloplegic Study	127
6.5	Effect of not Measuring Corneal Thickness	131
6.6	Effect of using Fourth Meridian	131
6.7	Summary	133

Chapter Seven

Ocular Component Contributions to Residual Astigmatism

7.1	Introduction	136
7.2	Repeatability Study	136
7.3	Cycloplegic Study	138
7.4	Population Study	139
7.5	Summary	147

Chapter Eight

Summary and Future Work

8.1	Introduction	149
8.2	Review of Previous Chapters	149
8.3	Limitation of the Method	153

8.4	Suggestions for Future Work	154
8.4.1	How an Improvement could be Achieved	154
8.4.2	Possible Applications	154
8.4.3	Further Study	155

List of Tables

2.1	Age related residual astigmatism found by Tait (1956).	31
2.2	A summary of the findings of Grosvenor et al (1988).	32
4.1	Curvatures, axial distances and refractive indices used in calculations.	71
4.2	Symbols used in the computing scheme.	71
4.3	Input Parameter for the schematic eye of Le Grand (Bennett and Rabbetts, 1984) .	84
4.4	Effect of variation of F_3 upon Δh	85
5.1	Repeatability of measurements of residual astigmatic power made on two occasions in 20 male subjects.	109
5.2	Cumulative percentage of differences for residual astigmatic power measurements made on two occasions in 20 male subjects.	110
5.3	Cumulative percentage of differences for residual astigmatic power axis measurements made on two occasions in 20 male subjects.	110
5.4	Cumulative percentage of differences for torsion measurements made on two occasions in 20 male subjects.	110
5.5	Comparison of residual astigmatism measured in the right and left eyes of 70 subjects.	111
5.6	Comparison of residual astigmatism measured in the right and left eyes of 37 males and 33 females.	114
5.7	Comparison of residual astigmatism measured in the	

	right and left eyes of 25 Asians and 43 Caucasians.	114
6.1	Mean and estimated precisions of biometric measurements taken on 66 right and left eyes. All distances and radii are in millimetres. All powers are in dioptres.	120
6.2	Calculated means and estimated precisions of meridional ocular surfaces power derived from the average biometric data shown in Table 6.1 after the application of the computer program described in section 4.6.	121
6.3	Calculated means and estimated precisions of sphero-cylindrical ocular surface data derived from the meridional data shown in Table 6.2 after application of the computer program described in section 4.7.	121
6.4	Tscherning (1924) mean ocular components surface radius of curvature and their ocular powers measurements made in 3 eyes.	122
6.5	Cumulative percentages of the differences between internal ocular surface spherical components calculated for 20 right and left eyes from measurements made on two occasions.	124
6.6	Cumulative percentages of the differences between internal ocular surface cylindrical components calculated for 20 right and left eyes from measurements made on two occasions.	124
6.7	Cumulative percentages of the differences between internal ocular surface cylinder axis orientation calculated for 20 right and left eyes from measurements made on two occasions.	125
6.8	Internal ocular surface sphero-cylindrical components derived from the pooled data of 20 right and left eyes measured on two occasions.	126

6.9	Mean and estimated precision of measurements taken on left eyes of 10 male subjects (cycloplegics study). All distances and radii are in millimetres. All powers are in dioptres.	128
6.10	Internal ocular surface spherocylindrical components derived from the pooled biometric data of 10 left eyes measured with and without cycloplegia.	130
6.11	Sphero-cylindrical surface powers and their respective RMS errors calculated for 3 and 4 meridians using 66 subjects data.	132
7.1	Repeatability of ocular component astigmatic contributions to residual astigmatism calculated from biometric measurements made on two occasions in 20 subjects. An asterisk besides a value indicates that the bias was statistically significant to the 95% level (single sample t-test) this was the only the case for C_{45} components of d_3 ($df = 19$; $t = -2.17$) and F_4 ($df = 19$; $t = 2.13$)	137
7.2	Comparison of ocular component astigmatic contribution to residual astigmatism calculated from biometric measurement made with and without cycloplegia.	139
7.3	Comparison of ocular component astigmatic contributions to residual astigmatism calculated from biometric measurements in right and left eyes of 66 subjects. A statistically significant difference to the 95% level (unpaired t-test) was found for the C_{45} components of F_4 ($df = 65$; $t = -2.03$) only.	140
7.4	Comparison of ocular component astigmatic contribution to residual astigmatism(RAP) calculated from biometric measurements in the right and left eyes of 33 males and 33 females. A statistically significant difference to 95% level (unpaired t-test) was found for the C_{45} components of	

List of Figures

3.1	Photograph of the Multi-meridional still flash photographic ophthalmophakometer.	57
3.2	Diagrammatic representation of the fibre optic Purkinje image light sources (A- E) mounted in the 180° , 90° , 135° and 45° meridians. Light sources were placed at equal perpendicular distances (15 mm) from the axis (O) of the slit lamp objective (OB). The light array was operated at a working distance of 25mm from the subject's eye (S). Light sources were inclined (24.5°) towards the instrument axis so that light would strike the corneal surface normally.	58
3.3	Photograph of Purkinje images I, II, and IV taken along the 180° , 90° , 135° and 45° meridians using the apparatus depicted in Figure 3.1 and Figure 3.2. (see Figure 3.4 for diagrammatic representation of images).	59
3.4	Diagrammatic representation of Purkinje images (A' to E') corresponding to the light sources (A to E) shown in Figure 3.2. Images arising from the anterior corneal surface (a), posterior corneal surface (b) and the posterior crystalline lens surface (c) are highlighted separately for clarity and identified with Roman numerals I, II and IV, respectively (Note that Purkinje image IV is inverted). Reference centres (O') are also shown for each set of Purkinje images.	61
4.1	Catoptric imaging properties of the anterior corneal surface.	73
4.2	Finding the vertex of the posterior corneal equivalent mirror.	74
4.3	Finding the centre of curvature of the posterior corneal equivalent mirror.	75
4.4	Catoptric imaging properties of posterior corneal equivalent mirror.	76
4.5	Axial ray trace from the far point through the four surfaced eye.	78
4.6	Finding the vertex of the posterior lens equivalent mirror.	80

4.7	Finding the centre of curvature of the posterior lens equivalent mirror	81
4.8	Catoptric imaging properties of the posterior lens equivalent mirror	82
4.9	Graphical construction based on the combination of two cylinders C_0 and C_{45} at axis 0° and 45° respectively to produce an oblique cylinder of power C at axis \emptyset .	92
5.1	Frequency distribution of residual astigmatic powers measured in 70 right and left eyes.	112
5.2	Frequency distribution of residual astigmatic power axes measured in 70 right and left eyes.	112
5.3	Frequency distribution of torsion measured in 70 right and left eyes. Torsion represents the degree to which corneal and residual astigmatic power axes are mutually perpendicular. A value of zero indicates that both axes are mutually perpendicular. Negative or positive values indicate that both axes are, respectively, less than or greater than 90° apart.	113
7.1	Frequency distribution of ocular component cylinder power contributions to residual astigmatism of internal ocular distances d_1 (corneal thickness), d_2 (anterior chamber depth) and d_3 (lens thickness) measured in 66 right (A) and left eyes (B).	142
7.2	Frequency distribution of ocular component cylinder power contribution to residual astigmatism of internal ocular surfaces F_2 (posteriorcornea), F_3 (anterior lens) and F_4 (posterior lens) measured in 66 right (A) and left eyes (B).	143
7.3	Frequency distribution of ocular component cylinder axis contribution to residual astigmatism of internal ocular distances d_1 (corneal thickness), d_2 (anterior chamber depth) and d_3 (lens thickness) measured in 66 right (A) and left eyes (B).	144

7.4	Frequency distribution of ocular component cylinder axis contribution to residual astigmatism of internal ocular surfaces F_2 (posterior cornea), F_3 (anterior lens) and F_4 (posterior lens) measured in 66 right (A) and left eyes (B).	145
	References	156

Appendices

Appendix A: Computer Programs

A1	Calculation of Meridional Data (Notional Power) for Refraction and Anterior Corneal Surface Radius of Curvature.	168
A2	Calculation of Internal Ocular Surface Astigmatism.	171
A3	Calculation of the Contribution to Residual Astigmatism of the Internal Ocular Surfaces and their Axial separations.	175
A4	Determination of Random Experimental Errors involved in the Calculation of Meridional Surface Powers.	179
A5	Determination of Random Experimental Errors involved in the Calculation of Surface Powers in Spherocylindrical form.	183
A6	Calculation of Purkinje image Positions, Ratios and Heights (Program 6 List)	187

Appendix B: Biometric Data

B1	Subject Details	190
B2	Notional Meridional Refractive Errors	192

B2.1	70 right eyes	192
B2.2	20 right eyes repeated	193
B2.3	70 left eyes	194
B2.4	20 left eyes repeated	195
B2.5	10 left eyes with and without cycloplegia	196
B3	Notional Meridional Anterior Corneal Surface Radii	
B3.1	70 right eyes	197
B3.2	20 right eyes repeated	198
B3.3	70 left eyes,	199
B3.4	20 left eyes repeated	200
B3.5	10 left eyes with and without cycloplegia	201
B4	Preliminary Study: Residual Astigmatic Power	
B4.1	70 right eyes	202
B4.2	20 right eyes repeated	203
B4.3	70 left eyes	204
B4.4	20 left eyes repeated	205
B5	Ultrasonic Measurements of Axial Distances	
B5.1	66 right eyes	206
B5.2	20 right eyes repeated	207
B5.3	66 left eyes	208
B5.4	20 left eyes repeated	209
B5.5	10 left eyes with and without cycloplegia	210

B6 Ophthalmophakometric Measurements of Purkinje Image Heights

B6.1	Purkinje Image I (Anterior Corneal Surface)	211
B6.1.1	66 right eyes	211
B6.1.2	20 right eyes Repeated	213
B6.1.3	66 left eyes	214
B6.1.4	20 left eyes repeated	215
B6.1.5	10 left eyes with and without cycloplegia	216
B6.2	Purkinje Image II (Posterior Corneal Surface)	217
B6.2.1	66 right eyes	217
B6.2.2	20 right eyes repeated	218
B6.2.3	66 left eyes	219
B6.2.4	20 left eyes repeated	220
B6.2.5	10 left eyes with and without cycloplegia	221
B6.3	Purkinje Image IV (Posterior lens Surface)	222
B6.3.1	66 right eyes	222
B6.3.2	20 right eyes repeated	223
B6.3.3	66 left eyes	224
B6. 3.4	20 left eyes repeated	225
B6. 3.5	10 left eyes, with and without cycloplegia	226

B7 Computed Ocular surfaces Astigmatism

B7.1	20 right eyes repeated on two occasions	227
B7.2	20 left eyes repeated on two occasions	228
B7.3	10 left eyes with and without cycloplegia	229

B8 Computed Internal Ocular Component Contributions to Residual Astigmatism

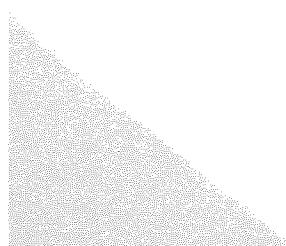
B8.1	Corneal Thickness	230
B8.1.1	66 right and left eyes	230
B8.1.2	20 right and left eyes repeated	232
B8.1.3	10 left eyes with and without cycloplegia	232
B8.2	Posterior Corneal Surface	233
B8.2.1	66 right and left eyes	233
B8.2.2	20 right and left eyes repeated	234
B8.2.3	10 left eyes with and without cycloplegics	235
B8.3	Anterior Chamber Depth	236
B8.3.1	66 right and left eyes	236
B8.3.2	20 right and left eyes repeated	237
B8.3.3	10 left eyes with and without cycloplegia	238
B8.4	Anterior Crystalline Lens Surface	239
B8.4.1	66 right and left eyes	239
B8.4.2	20 right and left eyes repeated	240
B8.4.3	10 left eyes with and without cycloplegia	241
B8.5	Crystalline Lens Thickness	242
B8.5.1	66 right and left eyes	242
B8.5.2	20 right and left eyes repeated	243
B8.5.3	10 left eyes with and without cycloplegia	244
B8.6	Posterior Crystalline Lens surface	245
B8.6.1	66 right and left eyes	245
B8.6.2	20 right and left eyes repeated	246
B8.6.3	10 left eyes with and without cycloplegia	247

B9 Residual Astigmatism Population Study

B9.1	66 right and Left eyes (Main Study)	248
B9.2	20 right and left eyes repeated	249
B9.3	10 left eyes with and without cycloplegia	250

Appendix C: Supporting Publications

C.1	A study of the Axis Orientation of Residual Astigmatism	252
C.2	A clinical trial of the SUN SK-2000 Computer-assisted Videokeratoscope	
C.3	Measurements of Astigmatism arising from the Internal Ocular Surfaces	259
C.4	Ocular Component Contributions to Residual Astigmatism (Submitted)	270



CHAPTER ONE
SCOPE OF STUDY

1.1 Introduction

This study was carried out to investigate the feasibility of an ophthalmophakometric method for measuring ocular component contributions to residual astigmatism. Funding was not available for developing the apparatus so that construction costs were kept to a minimum. This prevented the use of currently available but expensive techniques such as digital image capture and image analysis. The scope of the study was therefore confined to developing prototype, and somewhat unsophisticated, apparatus which would be used to gain a first approximation of the range of values likely to be encountered in a sample of human eyes against the errors of determination of these values. The following sections of this chapter provide an overview of the approach of this study by considering the topics covered in subsequent chapters.

1.2 Residual Astigmatism

Chapter two gathers together current opinion on the subject of residual astigmatism. The term residual astigmatism is first defined followed by a critical review of previous studies aimed at establishing its prevalence and magnitude. The potential sources of residual astigmatism are then considered starting with a description of the ocular components and leading on to the consideration of astigmatic accommodation, ocular component misalignments and finally the possibility of involvement of the retina and perception.

1.3 Biometric Methods and Experimental Protocol

The concept of functional ocular biometry and multi-meridional ultrasonic ophthalmophakometry is introduced in chapter three. Details of measuring refractive

errors using an infra-red autorefractor, anterior corneal surface curvature using computer assisted videokeratography and axial distances using A-scan ultrasonography are considered as well as the means of controlling accommodation. Measuring the internal ocular surface curvature needed special apparatus. The construction and use of the purpose built multi-meridional still-flash ophthalmophakometer is described.

An overall protocol for subjects recruitment, experimental design and the organisation of experimental sessions is considered.

1.4 Computing Schemes

Computing schemes were developed to allow determination of the astigmatic contributions of the ocular components towards residual astigmatism. A procedure was devised involving multi-meridional analysis, paraxial raytracing through optical systems including astigmatic surfaces at random axes, and making use of the principle of astigmatic decomposition.

Six computing programs were needed for the task. The first resolved refraction and keratometry measurements to notional powers along 180° , 90° , 135° , and 45° meridians. The second calculated meridional and spherocylindrical powers for each ocular surface. The third used the second program's results to generate ocular component contributions to residual astigmatism. The fourth and fifth dealt with accumulated experimental errors involved in the calculation of the meridional and the spherocylindrical powers generated by the second program. The sixth was designed to examine theoretically the positions and heights of Purkinje images measured in this study.

1.5 Preliminary Study: Measurements of Residual Astigmatism

Chapter five was designed to confirm the magnitude of residual astigmatism in addition to its ocular axis orientation, making use of the principle of the astigmatic decomposition.

The repeatability of measurements was examined followed by a population study. Statistical comparison of residual astigmatism arising from right versus left eyes, females versus males and from different racial groups was carried out making use of the calculated orthogonal (C_0) and oblique (C_{45}) cylinder components.

1.6 Main Study: Measurements of Internal Ocular Surface Astigmatism

Chapter 6 considers the results of the main study (66 subjects) aimed at measuring internal ocular surface toricity. Internal ocular surface astigmatism was measured applying multi-meridional ultrasonic still flash ophthalmophakometry. Results were averaged and an investigation was carried out into the precision of the technique by examining the influence of random independent errors from each measurement.

The repeatability of the method was assessed and a comparison was made between measurements made with and without cycloplegia.

Corneal thickness was assumed to be constant to remove the need for pachometry. The effect of this assumption was considered in addition to improvements in precision brought about by taking ophthalmophakometric measurements in four meridians when three would yield the results required.

1.7 Ocular Component Contributions to Residual Astigmatism

Chapter 7 considered the calculations of ocular components contributions to residual astigmatism. The precision and repeatability of the estimates was also considered. Comparisons were again made between results arising from data collected with and without cycloplegia.

1.8 Conclusion and Future Work

Main findings of this thesis were concluded in chapter 8. Beside the proposed future studies in the field. Limitations of the study were considered along with suggestions for improvement. Finally, possible clinical applications and future study were proposed.

1.9 Summary

An out line of this thesis has been given in this chapter. The following chapters will now cover each respect in greater details.

CHAPTER TWO
RESIDUAL ASTIGMATISM

2.1 Introduction

This chapter presents a review of previous studies which have investigated residual astigmatism. Section 2.2 defines the term residual astigmatism followed by a critical review of previous studies in section 2.3. The establishment of the prevalence and magnitude of residual astigmatism is considered in section 2.4. Possible sources of residual astigmatism are considered in section 2.5. Section 2.6 is the chapter summary.

2.2 Definition of Residual Astigmatism

The optical system of the human eye focuses light on the retina. When this optical system forms a point image, it is clinically defined as spherical or non-astigmatic. When it fails to do this, it is called astigmatic (Donders 1864; Emsley 1969; Duke Elder and Abrams 1970; Borish 1970).

Astigmatism largely depends on the presence of toroidal instead of spherical curvatures of the refracting surfaces of the eye. Therefore refractive power of the eye differs from one meridian to another instead of being equal in all meridians.

Residual astigmatism is defined as the component of ocular astigmatism that is not attributed to the anterior corneal surface (Mote and Fry 1939; Bannon and Walsh 1945; Kratz and Walton 1949; Neumueller 1953; Loper 1959; Carter 1963; Lyle 1971; Reading 1972; Grosvenor, Perrigin and Quintero 1988; Lyle 1991).

As residual astigmatism is the main issue of this study, it is necessary to establish specific definitions with regards to nomenclature and sign convention.

In this thesis total ocular astigmatism, referred to the anterior corneal surface vertex, is called the ocular astigmatic power (OAP) and is simply a plus-cylinder in the same axis as the spectacle correcting cylinder. For example if the spectacle correcting cylinder power and axis referred to the corneal vertex is $-0.25\text{DC axis } 180^\circ$, then OAP will be $+0.25\text{DC axis } 180^\circ$. When OAP plus cylinder axis is horizontal (axis $180^\circ \pm 20^\circ$) the ocular astigmatism is considered to be direct. When OAP plus cylinder axis is vertical (axis $90^\circ \pm 20^\circ$) it is considered to be inverse. It is referred to as oblique when it falls at axis $45^\circ \pm 25^\circ$ or $135^\circ \pm 25^\circ$. This convention applies to all ocular surface powers as well as that of residual astigmatism.

Corneal astigmatism is the power difference between the corneal principal meridians measured with a keratometer. Corneal astigmatic power CAP is derived from the measured principal corneal radii assuming a refractive index of 1.3771 taken from Le Grand schematic eye (Bennett and Rabbetts, 1989). For example, suppose the measured principal corneal radii are 7.80 mm meridian 180° and 7.68 mm meridian 90° their power will be 48.35D meridian 180° and 49.1D meridian 90° respectively. This yields a CAP of $+0.75\text{DC axis } 180^\circ$ (direct).

Since the residual astigmatism is the difference between OAP and CAP the formula shown below can be used to calculate its value which is referred to as residual astigmatic power (RAP).

$$\text{RAP} = \text{OAP} - \text{CAP} \quad (2.1)$$

In this expression all astigmatic powers are referred to the anterior corneal surface vertex and are represented in plus-cylinder form. When OAP and CAP axes coincide, as in the previous example, RAP is simply calculated by subtraction:

$$\text{RAP} = 0.25 - 0.75 = -0.50\text{DC}$$

In this example, RAP is seen to be $-0.50\text{DC axis } 180^\circ$ (inverse).

However, the OAP axes and CAP rarely coincide so that they need to be treated as obliquely crossed cylinders (Neumueller 1953; Gartner 1965; Carter 1980; Barnes 1984; Bennett 1984; Bennett and Rabbetts 1989). This aspect is considered in chapter 4.

2.3 Measurement of Residual Astigmatism

In the past, researchers were involved in the study of residual astigmatism for two main reasons. Firstly there had been a considerable interest in predicting the spectacle correcting cylinder from keratometric measurements of the anterior corneal surface (Javal, 1890; Mote and Fry, 1939; Kratz and Walton, 1949; Neumueller, 1953; Tait, 1956; Hofstetter and Baldwin, 1957; Carter, 1963; Gartner, 1965; Anstice, 1971; Carter, 1980; Bennett, 1984; Grosvenor, Quintero and Perrigin, 1988; Bennett and Rabbetts, 1989). Secondly clinicians were interested in fitting rigid spherical contact lenses on astigmatic cornea as an alternative means of optical correction. In this case residual astigmatism appeared to be one of the reasons behind the cause of unsatisfactory visual acuity (Bailey, 1961; Sarver, 1963, 1969, Dellande, 1970).

The results of the first type of study are of interest here because they involve measurements of residual astigmatism itself. Results of the second type of study are not considered due to the artifact induced by contact lens fitting; like astigmatism induced by the tear lens, poor contact lens centration and contact lens flexure.

The study of residual astigmatism has been complicated by the lack of coincidence between the corneal and ocular principal meridians. Most of those who studied residual astigmatism have selected their subjects to minimise the lack of coincidence

(Mote and Fry, 1939; Kratz and Walton, 1949; Tait, 1956; Hofstetter and Baldwin, 1957; Carter, 1963; Anstice, 1971; Grosvenor, Quintero and Perrigin, 1988).

2.4 Prevalence and Magnitude of Residual Astigmatism

Residual astigmatism is found in almost every human eye. Most studies have failed to demonstrate any significant differences in values measured in right and left eyes, males and females or among different age groups (Mote and Fry, 1939; Kratz and Walton, 1949; Tait, 1956; Carter, 1963; Anstice, 1971). The influence of racial variation has not been studied.

Most investigators found that the values of RAP ranged from 0.50DC to 0.75DC inverse astigmatism (Lyle, 1991).

Javal (1890) derived, from empirical data, a rule for computing the expected spectacle correcting cylinder from keratometric findings (Javal's Rule). In this rule Javal incorporates 0.50DC of inverse residual cylinder. This Rule is described below:

$$C = 1.25 A - 0.50 \quad (2.2)$$

Where C is the power of the correcting cylinder and A is the corneal astigmatism. If the latter is inverse, A is given a minus sign. Javal made clear that his rule was empirical and that the constants were only approximations. He pointed out that additional terms might have to be added (Bannon and Walsh, 1945 b; Bennett, 1984).

Since the time of Javal several studies on residual astigmatism have been published. These are described below.

Mote and Fry (1939) studied residual astigmatism in 146 eyes. The sample ages ranged between 5 and 79 years. Initially 100 subjects (200 eyes) were examined with the keratometer and with the fan and block technique subjective refraction to determine the relationship between the CAP and OAP. To avoid the problem of obliquely related cylinders, all eyes included in the study had been selected with the principal meridians of the keratometric astigmatism at or within 10° of 180° and 90° . The same axis criterion was followed in the selection of the spectacle correcting cylinder. This reduced the sample to 146 eyes. However, the 146 eyes included 5 eyes in which the discrepancy was 15° , 3 eyes with 20° and 1 eye in which it was 30° . In this study neither the gender nor the race of the included subjects were identified. The mean RAP was found to be 0.56DC of inverse astigmatism (range 0.02DC inverse to 1.30DC direct). They found that RAP did not vary with age or between the right and left eyes.

Kratz and Walton (1949) investigated RAP in a sample of 295 eyes and recorded the variance between the corneal cylinder and the subjective correcting cylinder. They reported a modal value of 0.50DC inverse residual astigmatism and values ranged from 3.00DC inverse to 2.00DC direct with no significant age dependence. The gender and races of subjects were again not identified.

Tait (1956) measured RAP in 2000 randomly selected eyes. Four age groups were considered; 5 to 10 years, 15 to 25 years, 30 to 45 years and 50 to 65 years. To keep equal numbers in each age group, 400 eyes were finally selected noting also the gender of each subject. Children were refracted under atropine cycloplegia and all young adults with homatropine. He found no gender difference and stated that there was a small but constant progression in the incidence of inverse RAP with age. Table 2.1 summarises his findings.

Age Group	RAP. Mean	RAP. Range
5 to 10 years	0.50D inverse	1.75D inverse to 0.80D direct
15 to 25 years	0.50D inverse	1.50D inverse to 0.50D direct
30 to 45 years	0.75D inverse	2.50D inverse to 0.75D direct
50 to 65 years	0.75D inverse	2.00D inverse to 1.00D direct

Table 2.1 Age related residual astigmatism found by Tait (1956)

Hofstetter and Baldwin (1957) measured RAP in 148 subjects from the files of two optometric practices. All cases with keratometric and total ocular cylinder axes of more than 30° from vertical or horizontal were excluded. They found calculated residual astigmatism using the following formula which is a modification of Javal's rule:

$$R = T - 1.25C \quad (2.3)$$

Here R is the residual cylinder, T the total ocular astigmatism at the corneal plane, 1.25 is a constant and C is the corneal astigmatism measured by keratometry. A mean value of 0.5DC inverse residual astigmatism with high level of correlation was found between the right and left eyes and no apparent trend with age was indicated.

Loper (1959) studied RAP in 55 optometry undergraduates in Indiana University. The average age for the group was 25.5 years and the range was from 20 to 56 years. Ocular astigmatic power OAP was found using Neumuller tables. RAP for the right eyes (0.57DC inverse, standard deviation ± 0.54DC) and left eyes (0.59DC inverse, standard deviation ± 0.41DC) were not significantly different.

Carter (1963) studied RAP in 100 subjects whose ages ranged from 17 to 50 years. He found the mean to be 0.60DC with a range of from 0.50DC direct to 2.00DC inverse. No variation was found due to age. Carter (1963) reported that 87% of the cases had inverse RAP with a modal value of 0.50DC axis 90° ± 20°. He found direct RAP in 2.3% of the sample whilst 10.7% had oblique astigmatism. He added

that if minus cylinders at axis 45° were referred to axis 180° while those at axis 135° were referred to axis 90° the arithmetic mean for RAP was 0.60DC with standard deviation ± 0.407 DC.

Anstice (1971) randomly selected records of 621 patients in New Zealand. He subdivided this group into age intervals of 5 years and determined the mean OAP and CAP for each age group. Comparison of the means revealed no trend with age until the 40 to 44 year old age group was reached, when the trend towards more inverse astigmatism began. From a series of correlation coefficients, he concluded that both OAP and CAP changed significantly with age and that RAP did not. The mean value for RAP was found to be 0.36DC inverse with a range of from 0.75DC direct to 2.00DC inverse.

Grosvenor, Quintero and Perrigin (1988) studied RAP in order to suggest a simple way of predicting spectacle correcting cylinder from keratometric readings. They used the right eyes of 791 subjects collected from different practices. The subjects were classified into three groups; 98 myopic children, 200 clinical patients and 493 optometric practice patients. Corneal and ocular principal meridians fell within 30° of 180° and 90° for all subjects. Further they were divided into age groups. Table 2.2 gives a brief summary of this study.

Groups	Age Range	Sample Size	Mean RAP	orientation
Myopic. Children Clinical PT	9 to 13 years	184 eyes	0.40D	Inverse
	6 to 20 years	102 eyes		
	21 to 40 years	161 eyes		
Optometric PT	41 and over	118 eyes	0.32D	Inverse
	5 to 20 years	109 eyes		
	21 to 40 years	107 eyes		
	41 to 60 years	204 eyes		
	60 to 84 years	73 eyes		

Table 2.2 A summary of the findings of Grosvenor et al (1988).

They compared their results with those obtained by applying Javal's rule(*equation 2*). They found that when + 0.50DC axis 180° was added to the keratometric astigmatism, leaving out the 1.25 the constant incorporated in Javal's rule the results showed a better fit. Their proposed version of Javal's rule as follows:

$$R_x = K + 0.50 \quad (2.4)$$

Where R_x is the spectacle correcting cylinder referred to the corneal vertex and K is the keratometric cylinder.

2.5 Possible Sources of Residual Astigmatism

2.5.1 Cornea

Optically, the cornea consists of three distinct refractive parts; the anterior surface; its axial thickness and its posterior surface.

The anterior surface of the cornea is covered by a thin tear film. The tear film consists of three layers; a thin oily layer, a watery layer and a mucin layer. This thin film forms the first line of defence, moisturises and maintains the smoothness of the anterior corneal surface which plays a major role in the refractive power of the eye.

The cornea is a relatively complex structure made up of 5 layers; the epithelium, Bowman's membrane, the stroma, Descemet's membrane and the endothelium. These layers are slightly different in their anatomical and optical structure, but unique in their function. The refractive indices of these layers vary slightly from one to another, causing light scatter which is optically used to visualize corneal structure with slit lamp microscopy.

Leary (1981), has analysed the refractive roles of the various ocular components in terms of their vergence contributions to the back vertex power of the anterior segment. He found that the corneal contribution is about 53% of the eye's back vertex power.

2.5.1.A Anterior Surface of the Cornea

The anterior corneal surface is typically steeper vertically giving the eye some degree of direct astigmatism. It provides most of the refractive power of the whole eye (approximately 49D), due to the large change in the refractive index from air to cornea. Its radius of curvature is typically 7.8 mm, and ranges from 7.0 to 8.6 mm in normal eyes (Stenstrom, 1946, 1948; Duke Elder and Wybar, 1961; Bennett and Rabbetts, 1989.)

The contour of the anterior corneal surface has been studied extensively. Some workers have attempted to describe it in qualitative terms. There are, however, wide variations in the topography of individual corneas. A common belief prevails that the cornea possesses an approximately spherical optical zone which extends horizontally about 4 mm and is decentred temporally and slightly inferiorly with respect to the line of sight. This zone is followed by progressive flattening towards the periphery. In some cases the surface curvature may steepen towards the periphery. Complete rotational symmetry is unusual (Helmholtz, 1924; Gullstrand, 1924; Prechtel and Wesley, 1970; Mandell and St Helen, 1971; Clark, 1972, 1974a, 1974b; Mandell, 1964; El Hage, 1976; Edmund and Sjontoft, 1985; Guillon, Lyndon and Wilson, 1986; Dingeldein and Klyce, 1989).

2.5.1.B Corneal Thickness

In the past corneal thickness measurements were only possible from post-mortem eyes the corneas of which tended to be swollen (Von Bahr, 1948). The stroma makes by

far the greatest contribution (about 90%) to the overall thickness of the cornea. The unique structure and arrangement of its collagen fibres and integrity of the endothelium and epithelium are of vital importance to maintain corneal transparency. In spite of differences and microscopic irregularities in the corneal thickness, the typical bulk refractive index is about 1.377, depending upon the wavelength and the temperature at which it is measured (Charman, 1991a).

The first attempt to take an *in vivo* measurement was made by Blix in 1880. Since then several studies have been carried out and average values of about 0.5 mm centrally and 0.7 mm peripherally have been suggested (Martola and Baum, 1968; Fatt and Harris, 1973; Hirji and Larke, 1978; Azen, Burg, Smith and Maguen, 1979).

It is generally assumed that physiological variation of the corneal refractive index is negligible. The validity of this assumption depends mainly on variations of the composition and concentration of substances dissolved in its water content. Patel (1987) studied the refractive index of the cornea to reach the conclusion that the anterior stromal refractive index is, on average, 0.007 units greater than the posterior endothelial refractive index. This is in an agreement with previous findings that the refractive index of the corneal stroma reduces along the antero-posterior direction (Kikkuhawa and Haryama, 1970; Lee and Wilson, 1981).

Further, available information (Tscherning, 1924; Gullstrand, 1924; Martola and Baum, 1968; Duke Elder and Abrams, 1970; (Kikkuhawa and Haryama, 1970; 1970; Fatt and Harris, 1973; Hirji and Larke, 1978; Azen, Burg, Smith and Maguen, 1979; Lee and Wilson, 1981; Patel, 1987) suggests that corneal refractive index and corneal thickness varies considerably from the corneal centre to the periphery. This must induce meridional power difference which potentially contribute to residual

astigmatism. The optical contribution of the corneal thickness to back vergence power will be considered in the chapters to follow.

2.5.1.C Posterior Corneal Surface

Measurement of the radius of the posterior corneal surface has attracted less attention compared to the anterior corneal surface due to measurement difficulties.

A number of workers have made measurements of the radius of the posterior corneal surface in one or two meridians. Gullstrand (1924) and Tscherning (1924) found that they could only measure the posterior corneal curvature peripherally. Tscherning (1924) discussed the optical importance of the posterior surface of the cornea indicating that it has negative power and contributes to ocular astigmatism (Bannon and Walsh, 1945). The mean radius of the posterior cornea is approximately 6.5 mm centrally and its back vertex power is about - 6.00D (Charman, 1991a).

Attempts to measure the radii of the posterior corneal surface in large samples have been made (Lowe and Clark, 1973a, 1973b; Sorsby, Benjamin and Sheridan, 1961; Hockwin et al, 1983). However, these readings were confined to the vertical meridian because measurements were taken from slit lamp section.

Bannon and Walsh (1945) examined the astigmatic contribution of the posterior corneal surface in eight aphakic eyes fitted with contact lenses. They found that three out of the eight cases showed no residual astigmatism with contact lens. However, the other five showed a residual astigmatism ranging from 0.25D to 1.50D inverse.

Recently, Royston, Dunne and Barnes (1990, 1991) and Dunne, Royston and Barnes (1991, 1992) have developed a method for measuring the toricity of the posterior corneal surface by taking measurements along three fixed meridians. They found that

the posterior corneal surface was steeper vertically than horizontally bringing about astigmatism opposite in sign to that of the anterior surface. They compared the toricity of both surfaces and concluded that if the posterior surface exhibited the same toricity as the anterior surface then a 5% reduction of total corneal astigmatism would arise. In fact, a reduction of 14% was found due to extra toricity of the posterior surface. Asphericity variation in the posterior corneal surface was found to have minimal effect on corneal astigmatism exhibited by a schematic eye (White, 1993).

2.5.2 The Anterior Chamber.

The anterior chamber separates the posterior surface of the cornea from the anterior surface of the lens. It is filled with a clear transparent liquid called the aqueous humour. Aqueous humour is formed and circulated continuously and normally constitutes an excellent optical medium. Its refractive index is about 1.337 (Charman, 1991a). The depth of the anterior chamber reduces during accommodation. It also reduces throughout adult life (from about 3.8 mm in early adult life to about 3.0 mm at around 70 years of age) due to the corresponding increase in the thickness of the lens (Weale, 1963). Changes in the refractive index of the aqueous humour or depth of the anterior chamber produce spherical changes in the back vertex power of the eye; for example reduction of the refractive index by 0.1% and 1.0% increases the refractive power to +0.08D and +0.81D respectively whilst an increase of 0.1% and 1.0% reduces the power by about -0.008D and -0.82D respectively. Also a depth reduction of 0.1 mm and an increase of 0.1 mm alters the power by +0.13D and -0.14D respectively (Erickson, 1991). Leary (1981) estimated that the anterior chamber contributes about 7% of the back vergence power of the eye.

2.5.3 Pupil

The pupil is a circular opening in the iris. It lies approximately tangential to the anterior surface of the lens and is the aperture stop of the eye. It thus not only controls the amount of light flux contributing to the retinal image but also affects the quality of the image through its influence on diffraction, ocular aberrations and depth-of-focus. A change in the pupil's location with respect to the optical centres of the optical components or a change in diameter must theoretically have an optical affect on the meridional power of the eye by exposing different zones of the ocular component surfaces. This is yet to be studied.

Although ambient lighting has, perhaps, the most important influence on pupil diameter, the latter is also affected by such factors as age, accommodation, emotion and drugs (Emsley, 1969; Hess, 1965; Lowenstein and Loewenfeld, 1969; Zinn, 1972; Janisse, 1973; Thompson 1987.)

2.5.4 Crystalline Lens

The crystalline lens is a transparent, deformable, biconvex structure enclosed within an elastic capsule which varies in thickness. The lens comprises of an epithelial layer which is confined to the anterior and the equatorial surfaces. Lens fibres, which are hexagonal in cross-section, stretch in arcuate fashion from the anterior to the posterior pole. Neighbouring fibres are rigidly linked through ball-and-socket joints along their edges so that relative movement cannot occur. It is, perhaps, the most remarkable of the optical components of the eye in that it continues to grow throughout life, through the addition of new lens fibres originating at the lens equator (Weale, 1963; 1982).

The crystalline lens is the seat of accommodation. Therefore, as it changes form during accommodation, its surfaces and refractive index distribution also change

form, making a full description of its dynamic optical behaviour particularly difficult to achieve (Patnaik, 1967; Brown, 1973; Koretz et al, 1984). The lens is often considered to be the source of residual astigmatism due to lens tilt and subluxation, surface toricity and refractive index variation throughout its thickness (Young, 1807; Donders, 1864; Tscherning, 1924; Le Grand and El Hage, 1980; Bennett, 1984; Campbell, 1984; Munger, Burns and Campbell, 1994).

2.5.4.A. Anterior lens surface

The most recent work on this surface has been reviewed by Smith, Pierscionek and Atchison (1991). Typically, the surface appears to flatten peripherally taking the form of a hyperbola (Parker, 1972; Howcroft and Parker, 1977). In normal eyes only the central area of the lens surface is exposed by the pupil. This area is not involved to any large extent in the peripheral flattening of the surface; the effect of each surface of the lens is therefore that of a toroidal refracting surface (Fletcher, 1951a).

According to Tscherning (1924), and others (Fletcher, 1951b; Duke Elder and Abrams, 1970; Lyle, 1971, 1991; Bennett and Rabbetts, 1989) the anterior surface is usually steeper vertically than horizontally so that it exhibits about 0.50DC of direct astigmatism. The shape of the anterior lens surface is subject not only to individual variations but also to alterations and adjustments in the same individual at various times. It is, therefore, even more difficult to give average values for the radius of curvature of its surfaces but a figures of 10 mm may be taken as being representative (Duke Elder and Abrams, 1970). Leary (1981) estimated that the vergence contribution of the anterior surface to the back vertex power of the eye was about 9.5%.

2.5.4.B Lens Thickness

At birth the crystalline lens is approximately 3.7 mm thick. This thickness diminishes up to about 15 years of age. Then it increases at a rate of about 0.02 mm per year (Ellerbrock, 1963; Luyckx-Bacus and Weekers, 1966; Luyckx-Bacus and Delmarcelle, 1969; Francois and Goes, 1969a, 1969b; Lowe, 1970; Weekers, Delmarcelle, Luyckx-Bacus and Collington, 1973, 1975; Howcroft and Parker, 1977). This increase is equally shared by shifts of the anterior and posterior pole. Accordingly lenticular power changes might be expected to occur with advancing age. The lens dimensions increase by about 50% between birth and the age of 70. Therefore the usually quoted thickness of 4 mm can only be considered as representative. A further consequence of this continued addition of new lens fibres is that the central region or nucleus of the lens is older than the outer layers, or cortex. The highest refractive index, about 1.41, is found in the nucleus and the lowest, about 1.38, in the cortex (Nakao et al, 1969)

The crystalline lens is a gradient index optical component whose properties cannot be completely described by classical eye models which assume homogenous refractive indices. The gradient index, together with the aspheric form of its external and iso-indical surfaces may help to reduce aberrations, particularly spherical aberration (Parker, 1972; Brown, 1973; 1974; Howcroft and Parker, 1977; Pomerantzeff, et al, 1984; Campbell, 1984). The gradient index structure of the crystalline lens is a matter of ongoing study (Henson, 1991; Munger, Campbell, Kroger and Burns, 1992; Munger, Burns and Campbell, 1994).

The lens thickness vergence contribution to the back vertex power of the eye amounts to about 13% (Leary, 1981).

2.5.4.C Posterior Lens Surface

The mean posterior lens radius is estimated to be 6 mm, (ranging between 4.6 to 8.3 mm) and flattens peripherally taking the form of a parabola (Ellerbrock, 1963; Parker, 1972; Howcroft and Parker, 1977). Usually the posterior lens surface exhibits astigmatism of about 0.50DC greater than that arising from the anterior lens surface (Tscherning, 1924; Fletcher, 1951b; Duke Elder and Abrams, 1970). The vergence contribution of this surface amounts to about 17.7% of the eye (Leary, 1981)

2.5.4.D Sectional Accommodation

Dobrowolsky (1868) is cited as being the originator of the term astigmatic accommodation. He stated that his crystalline lens tended to offset his corneal astigmatism during accommodation (Brzezinski, 1982). The phenomenon of astigmatic accommodation is defined as a lenticular compensatory astigmatism to the total astigmatism of the eye. It is believed that the eye has the ability to reduce its total astigmatism by sector contraction of ciliary muscle. This sector contraction produces lenticular astigmatism which either totally or partially corrects astigmatism. Although accommodative astigmatism might exist there has been some question about its employment to alter the degree of ocular astigmatism. Some workers feel that astigmatic accommodation is neither deliberate nor purposeful as a means of compensating for ocular astigmatism (Bannon, 1946; Fletcher, 1951a, 1952; Ukai and Ichihashi, 1991). Further, Duke Elder and Abrams (1970) concluded that all evidence indicates that in healthy normal eyes the ciliary muscles always contract as a whole.

Brzezinski (1982) attributed the change of astigmatism during accommodation to four major dynamic factors; (1) astigmatic accommodation; (2) accommodative astigmatism; (3) induced spectacle accommodative astigmatism; (4) corneal astigmatism resulting from convergence and accommodation. The first of these is

thought to arise from opposite sectors of the ciliary muscle being stimulated equally bringing about the desired sectional accommodation. The second is attributed to the involvement of accommodation. Here accommodative astigmatism is zero when no accommodation is exerted and increases with accommodation. It is a direct result of differential meridional contraction of the crystalline lens. The third is due to the effectivity change of spectacle correction from distance to near vision. The fourth is based on the possibility that accommodation and convergence alter the corneal curvature inducing astigmatism.

Recently Byakuno, Okuyama, Tokoro and Akizawa (1994) reported changes in astigmatism with changing accommodation. Whatever the causes or reasons behind this sort of astigmatism, the change was found to be neither clinically significant in degree nor in axis. The only significant differences reported have been associated with pathology (Lancaster and Walter, 1916; Weisz, 1978).

2.5.5 Ocular Component Misalignment

It is believed that none of the optical surfaces of the eye are exactly geometrically centred or share a common axis of symmetry . The fovea is eccentrically placed, being displaced 1.5 mm temporally and 0.5 mm downward relative to the posterior pole (Donders, 1864; Tscherning, 1924; Helmholtz, 1924; Gullstrand, 1924; Emsley, 1969; Duke Elder and Abrams, 1970). The astigmatism arising as a result of the misalignment of the optical system of the eye may also explain residual astigmatism (Tscherning, 1924; Bannon and Walsh, 1945; Fletcher, 1951b; Bennett, 1984).

Tscherning (1924), provided evidence for ocular component misalignment. He found that lens tilt was quite normal. The tilt of the crystalline lens was made up of two components. The first was a tilt or rotation of between 3° and 7° degrees around the vertical axis such that the temporal edge of the lens lies in front of the nasal edge.

This was combined with a horizontal tilt of between 0° and 3° degrees such that the upper edge of the lens lay in front of the lower edge, tending to cause an inverse astigmatism.

He was also quoted to have found that angle alpha (the angle between the optic and visual axis) varied from 4° to 7° degrees (Tscherning, 1924; Bannon and Walsh, 1945; Fletcher, 1951b). Although this implies that angle alpha is due to crystalline lens tilt, Shipley and Rawlings (1970) could find no clear statement from Tscherning's work that the existence of angle alpha necessitated lens tilt. This angle has been a source of disagreement between previous workers (Gullstrand, 1924; Lancaster, 1943), due to its confusing nature and its considerable variation in the population. Recent workers have found no significant astigmatic effect being produced as a result of variable angle alpha (Barnes, Dunne and Clement, 1986; Dunne and Barnes, 1989; Dunne, Misson, White and Barnes, 1993; Dunne, 1995). Dunne et al, (1993) questioned whether the optic axis (The optic axis is the line joining the optical centres of the of the refractive surfaces of the eye) and angle alpha exist.

Bennett (1984) considered that if both the lens surfaces were spherical or had axial symmetry, astigmatism could still arise if the lens were tilted with respect to the axis of the cornea. This prompted Bennett (1984) to ask whether such a tilt could be responsible for the 0.50DC of the inverse astigmatism implicit in Javal's rule.

He calculated that a lens tilt of about 14° was required to account for such an amount of astigmatism.

Sheard (1918) attempted to determine the corneal contribution that arises as a result of angle alpha. He calculated values of inverse astigmatism for 3 values of angles alpha 5° (0.53DC), 7° (0.66DC) and 9° (1.11DC).

Ludlam and Wittenberg (1966) also believed that corneal astigmatism could arise due to the cornea being tilted or rotated relative to the line of sight, even if it possessed spherical surfaces. They considered RAP to be an artifact of measurement of the anterior corneal surface astigmatism along the visual axis.

Recently, White (1993) tabulated the work of Barnes, Dunne and Clement (1987) who calculated the effect of rotation and translation of the cornea and crystalline lens on astigmatism to find that the effect of 5° nasal and inferior rotation of the cornea produces about 0.4DC inverse and 0.3DC direct astigmatism respectively. However, the same degrees of rotations when applied to the crystalline lens produced negligible astigmatism.

The possibility that the cornea and the crystalline lens are decentred with respect to each other raises a question about the optic and visual axes (the visual axis the line joining the object of regard to the fovea and passing through the nodal points. Strictly this line is not a single straight line as it consists of two parts one line connecting the object of regards to the first nodal point and the other line paralleled connecting the second nodal point to the fovea) (Emsley, 1969; Millodot, 1986). More real and practical axes are the pupillary axis (the line passing through the centre of the entrance pupil of the eye perpendicular to the surface of the cornea) and the line of sight (the line joining the point of fixation to the centre of the entrance pupil) (Gullstrand, 1924; Lancaster, 1943; Loper, 1959; Millodot, 1986).

Loper (1959) found that angle Lambda (the angle subtended at the centre of entrance pupil by the pupillary axis and line of sight) varied from 1.1° to 1.6° and concluded that it contributed little to RAP. However, angle Lambda was reported to vary considerably by London and Wick (1982).

2.5.6 Other Sources

2.5.6.A. Retinal Astigmatism.

Retinal astigmatism is concerned with retinal image deformity. The possibility that toricity of the retinal surface may be a cause of astigmatism has been noted by Bannon and Walsh (1945) and Le Grand (1967).

Retinal astigmatism has been reported following retinal detachment surgery, particularly by scleral buckling (Burton, 1973; Lyle, 1991). However, further studies are needed to confirm the influence of retinal toricity on residual astigmatism.

2.5.6.B. Perceptual Astigmatism.

Perceptual astigmatism refers to visual distortion that may be akin to aniseikonia, in that it occurs at higher centres of the brain. It has been discussed by Bannon and Walsh (1945) and Lyle (1991). Its contribution to residual astigmatism is also yet to be explored.

2.6 Summary.

Most eyes are known to be astigmatic. Usually a variance between total ocular and corneal astigmatism is found and is known by the name residual astigmatism.

Several studies have confirmed the existence of residual astigmatism. Residual astigmatism is found to be against-the-rule (inverse) for most eyes. In Carter's (1963) study 87% of the population had against-the-rule astigmatism (inverse), 2.3% had with -the-rule (direct) and 10.7% had oblique residual astigmatism. Most investigators

find residual astigmatism averages between 0.50D and 0.75D with similar results for right and left eyes and no gender or age related significant differences were found.

Residual astigmatism is thought to arise from a number of sources such as internal ocular component surface toricity, refractive index variations, astigmatic accommodation, ocular misalignments and probably the retina and the perception centres are also involved.

This study is confined to the measurement of ocular component contributions to residual astigmatism. The individual contribution of each of the components is not yet known. Means and methods concerning this task are to be discussed in the following chapters.

CHAPTER THREE
BIOMETRIC METHODS AND EXPERIMENTAL PROTOCOL

3.1 Introduction

Ocular biometry is the science of measuring the optical components of the eye. These measurements are either anatomical or functional. Anatomical biometry is concerned with ocular surface curvature, thickness and the relative distances of one component from the next. Functional biometry is concerned with the vergence contribution of each of the ocular components towards the back vertex power of the eye (Weekers et al, 1975; Leary, 1981). Both aspects are covered in this thesis.

Biometric techniques have received enormous attention and are undergoing continuous development due to their importance as tools in research and clinical investigations. This chapter presents a technique which is referred to as multi-meridional ultrasonic ophthalmophakometry. It utilizes measurements of refraction (section 3.2); anterior corneal radius (section 3.3); anterior chamber depth, lens thickness and vitreous depth (section 3.4); and ophthalmophakometric measurements of Purkinje images I, II and IV (section 3.5) in order to derive the toricity of the posterior corneal surface as well as the anterior and posterior lens surfaces.

The multi-meridional ultrasonic ophthalmophakometric technique involves resolving the measurements of refraction and anterior corneal curvature to four meridians (180° , 90° , 135° , 45°). These are combined with ultrasonic and phakometric measurements to determine internal ocular surfaces radii in the same meridians. Application of multi-meridional analysis then yields the toricity of the internal ocular surfaces. Experimental designs are considered in section 3.6. Section 3.7 is the chapter's summary.

3.2 Measurement of Refraction

Automatic infra-red refractometers have been the method of choice for numerous biometric studies (Zadnik, Mutti and Adams, 1992; Mutti, Zadnik and Adams, 1992 ; Mutti, Zadnik, Egashira, Kish, Twelker and Adams, 1994). They provide an objective assessment of refraction. Their precision is easily assessed, as the measurements are rapid and can be carried out repeatedly without discomfort (Wood, 1988; Howland, 1991). A Nidek AR800 autorefractometer was the instrument used in this study. This is an infra-red optometer based upon the Scheiner's disc principle. Its refractive measurement ranges from -18.00DS to +23.00DS, 0.00 to ± 8.00 DC in 0.25, 0.12 on 0.01D steps while the axis is measurable to intervals of 1°. measurements may be made at vertex distances of 0 mm, 12mm and 13.75mm in plus or minus cylinder form. The minimum pupillary diameter required for the autorefractor to operate is 2.9mm. Readings are taken and displayed in 0.3 seconds. Autorefractors of this kind are known to produce reliable and valid measurements of refraction (Wood, Papas, Burghardt and Hardwick, 1984).

Subjects were held still on a chin and a forehead rest. Fixation was guided to a target which was automatically fogged to relax accommodation. Accurate working distance and instrument alignment were achieved by ensuring that a corneally reflected fixation light was optimally focused and lined up with target circles seen on a TV monitor. For this purpose, instrument adjustment was controlled with a joystick. Five readings were taken from each eye. The instrument automatically determines refractive error in sphero-cylindrical form. Readings were referred to the anterior corneal surface vertex in minus-cylinder form. Each reading was resolved to notional power along the 180°, 90°, 135° and 45° meridians before calculating a mean and standard deviation in each meridian (see chapter 4 for computation procedure).

3.3 Videokeratographic Measurements of Anterior Corneal Surface

Measurements of the anterior corneal surface were made by means of keratometry or keratoscopy. There have been numerous studies involving measurements of the anterior surface of the cornea (see section 2.5.1.A). In this study the principal corneal radii were measured using a Sun SK2000 computer assisted videokeratographic device. Its measurements are based on the principle of keratoscopy. It has 15 concentric ring targets on an ellipsoid surface allowing the measurement of corneal curvature over a 2.5 mm diameter centrally and 8 mm peripherally. The results obtained have been found to compare well with conventional keratometry (Lam and Douthwaite, 1994).

Subjects were held still on a chin and forehead rest. Accurate instrument alignment was achieved by ensuring that two corneally reflected fixation lights were lined up with the target squares seen on a TV monitor. A joystick control was used for alignment as well as ensuring that the corneal reflections of the target rings were in optimal focus. In addition to this, a built in focusing system eliminated focusing errors.

The relevant dimensions of the reflected rings were automatically measured and processed to determine principal central corneal radii. Regular periodic calibrations were made with the calibration sphere provided (8mm radius of curvature).

Three readings were taken per eye. Each reading was converted to dioptric power and then resolved to notional power along the 4 meridians before calculating a mean and standard deviation in each (see chapter 4 for computation procedure).

3.4 Ultrasonic Measurements of Axial Distances

The ocular axial distances usually measured are corneal thickness, anterior chamber depth, crystalline lens thickness and vitreous depth. Addition of these distances yields the total axial length of the eye. Most often corneal thickness is included in the estimate of the anterior chamber depth.

The use of ultrasound for ocular measurements is based on the property of ultrasound waves reflected at boundary surfaces. When A-scan mode is used, an ultrasound pulse is emitted from a transducer (probe) and a return echo from each boundary (cornea, anterior lens capsule, posterior lens capsule and retina) is detected by the same transducer. The instrument records the elapsed time between the pulse and each echo along the horizontal axis whilst displaying the strength of the echoes as vertical lines of varying heights. The horizontal distance between vertical lines is calculated from the elapsed time and the assumed speed of the sound through the tissue examined. An average value of 1550 ms^{-1} was assumed in this study for the velocity of the ultrasound waves through the whole eye. The calculation formula can be expressed as:

$$D = R \times T \quad (3.1)$$

Where R is the speed of sound through the tissue, T is the elapsed time and D is the calculated intra-ocular distance. This calculation is usually carried out automatically.

As mentioned before the fraction of the incident beam reflected back as an echo at the interface of two tissues is depicted as the height of vertical lines shown on a display. The magnitude of the echo depends upon the acoustic impedance of the ocular tissues, the distance travelled and the angle of incidence. The acoustic impedance depends upon the density and elasticity of the substance. The greater the distance travelled, the

weaker the signal; most instruments provide circuitry to compensate for this by enhancing echo signals from a greater distance. The angle of incidence is controllable by the examiner and should, as closely as possible, be perpendicular to each boundary surface.

A-scan ultrasonic measurement of anterior chamber depth (including corneal thickness), crystalline lens thickness and vitreous length were made with the Storz Omega 20/20 Biometric Ruler. The automatic mode was used which automatically analyses and displays the results. This mode achieves a compromise between two basic requirements; (1) the need for a large number of repeated measurements to increase the accuracy and; (2) the need for a short measurement time to reduce the chances of movements of either the examiner or subject. The algorithm is also geared to account for the varying acoustical properties of the reflecting surfaces (the retina being a poor reflector while the sclera is much better).

Four returned echoes are required, one from each of the reflecting boundaries; the anterior corneal surface, the anterior and posterior crystalline lens capsule and the retina. These echoes must exceed a predetermined height and be spaced in conformance with expected human eye parameters. Echoes are automatically scanned for acceptable patterns. When acceptable echo patterns occur the machine takes and averages 64 consecutive readings in less than 50 milliseconds. This process is then repeated until 8 groups of readings are taken. Thus 512 readings are made in less than half a second. This provides a good balance between the desirability of a large number of readings and the advantage of taking them in a short time. It also provides a good statistical sample.

A foot switch was provided which, when depressed, initiated the measurement sequence and with continuous pressure successive blocks of 512 readings were

automatically made and stored in the instrument memory, where they could be reviewed.

A handheld hard probe containing a 10 MHz transducer was used. The probe was sterilised using Medi-Swabs (Smith and Nephew) and rinsed with normal saline. Subjects were seated comfortably fixating a light source placed 6 meters away. This type of fixation target was found to produce the best control for fixation and accommodation by Steele, Crabb and Edgar (1992). One drop of 0.4% benoxinate hydrochloride was instilled in each eye for anaesthesia. The probe was soaked with normal saline before being applied centrally and steadily to the eye. At least 10 measurements were made for each eye. Following each session, subjects were examined on a slit lamp. A mean and standard deviation was calculated from the 10 repeat measurements made of each axial distance.

3.5 Ophthalmophakometric Measurements of Internal Ocular Surface Curvature

The images which are used in the determination of the ocular radii were originally discovered in the late nineteenth century by Purkinje and later described by Sanson (Tscherning, 1924; Emsley, 1969; Duke Elder and Abrams, 1970; Bennett and Rabbetts, 1989). For this reason they are often called Purkinje or Purkinje-Sanson images. Bennett and Rabbetts (1989) provide a full account of the theoretical considerations involved in derivation of ocular surface radii from their respective Purkinje images. This is summarised below.

The small amount of incident light reflected from each refracting surface of the eye increases with the difference between the refractive indices of the media on either side of that surface. As the largest index change occurs at the front surface of the eye, the reflection from the anterior corneal surface (Purkinje image I) used for keratometry

and keratometry, is very much brighter than any of the others. Light entering the eye undergoes further partial reflection at the posterior corneal surface (Purkinje image II), anterior crystalline lens surface (Purkinje image III) and posterior crystalline lens surface (Purkinje image IV).

Theoretical calculations of the position and size of these images are made simpler by using the equivalent mirror theorem (see chapter 4). This states that a system comprising one or more refracting surfaces followed by a plane or spherical mirror can be simplified for calculation to an equivalent spherical mirror. The vertex and centre of curvature of the equivalent mirror then coincide, respectively, with the images of the vertex and centre of curvature of the actual mirror formed by the refracting elements.

Applying the equivalent mirror theorem in a schematic eye made up of typical human ocular parameters (Le Grand and El Hage, 1980; Bennett and Rabbetts, 1989), Purkinje image I is found to be virtual erect, diminished and positioned just in front of the anterior surface of the lens. Purkinje image II, is also virtual, erect, diminished and is positioned close to Purkinje image I. However, the relative brightness and proximity of Purkinje image I normally obscures Purkinje image II unless eccentric light sources are used. Purkinje image III is nearly twice the size of Purkinje image I and is virtual, diminished erect and situated in the vitreous chamber. Finally Purkinje image IV is real, diminished, inverted and lies close to Purkinje image I, being about three quarters of its size.

Tscherning is credited with the invention of visual ophthalmometry (Tscherning, 1924). He used a graduated circular arc supported on a stand with an observing telescope mounted in a central aperture. The subject's eye was placed at the centre of the curvature of the arc on which various sets of lamps were fixed.

Still flash photographic ophthalmophakometry was introduced to overcome the drawback of eye movements (Sorsby, Benjamin and Sheridan, 1961; Sorsby, Leary and Richards, 1962a; Sorsby, Sheridan and Leary, 1962b; Francis, 1962 and Ludlam, Weinberg, Twarowski and Ludlam, 1972; Dunne, 1987; Van Veen and Goss, 1988). Here the Purkinje images are photographed from a known angle and the spot separations appearing on photographic negatives are measured. The apparent radii are then derived by the method of comparison phakometry. This states that, for objects at infinity the size of the image formed by reflection is proportional to the focal length of the equivalent mirror, which is one half of its radius of curvature. It then follows that the ratio between the height of Purkinje image I to either III or IV is the same as the ratio between their respective apparent radii. The values of the latter are then simply calculated following determination of the corneal radius by keratometry.

The draw back of still flash photography is that two separate photographs need to be taken; one with Purkinje image I and IV in focus, the other with Purkinje image III in focus (Sorsby et al, 1961; Francis, 1962; Ludlam et al, 1965). The necessity to take two photographs brings in possible errors due to factors such as eye movements and accommodation fluctuations. Other authors have taken single photographs in which Purkinje images I and IV are very nearly in focus whilst III is out of focus (Dunne ,1987; Van Veen and Goss, 1988). This approach, however, brings in partial errors due to defocus of Purkinje image III.

Video ophthalmophakometry was introduced by Mutti, Zadnik and Adams (1992) to overcome the problems of still flash photography. The objective lens attached to the video camera could be adjusted to optimise focusing of all the Purkinje images. Improvement in repeatability was found using this video system compared to still flash photography.

To date, most ophthalmophakometric methods have been confined to one meridian and have neglected the posterior corneal surface (Sorsby et al, 1961; Dunne, 1987; Van Veen and Goss, 1988; Mutti et al, 1992). In contrast, the present study involves measurements of ocular surface toricity including the posterior corneal surface. This necessitates measurements in more than one meridian. For this purpose, a computing scheme was developed (see chapter 4) which allowed the lens surface curvature to be calculated without the need to measure Purkinje image III (Dunne, 1991). The advantages that this allowed were that it made use of Purkinje images (I, II and IV) which were positioned close to one another (just in front of the anterior crystalline lens surface), thereby reducing the potential defocusing errors arising from measurement of Purkinje image III when taking a single still flash photographs. Further, observation of Purkinje image II, for determination of posterior corneal curvature, necessitates that the Purkinje image light sources are placed in more eccentric positions (Tscherning, 1924). This means that Purkinje image III becomes obscured behind the pupil preventing its measurement.

A multi-meridional still flash photographic ophthalmophakometer was built by modifying a Zeiss Jena photographic slit lamp (model 110, that used by Dunne, 1987). The method was necessarily limited to hardware made available to avoid excessive construction cost. The slit lamp mirror, which normally served to deflect illumination in the direction of the subject's eye, was removed so that light could be guided down five fibre optic cables with tips masked with 2 mm apertures (Figure 3.1). These served as Purkinje image light sources and were positioned 25 mm in front of the subject's eyes and 15 mm above the instrument axis (see figure 3.2). They were angled 24.5° towards the instrument axis in order to strike a corneal surface of 8 mm normally. Two light sources were placed in the 180° meridian and one in each of the 135° , 90° and 45° meridians. The original intention was to place a pair of light sources in each meridian but this produced too much light at the cornea resulting in pupil constriction which obscured Purkinje image IV.

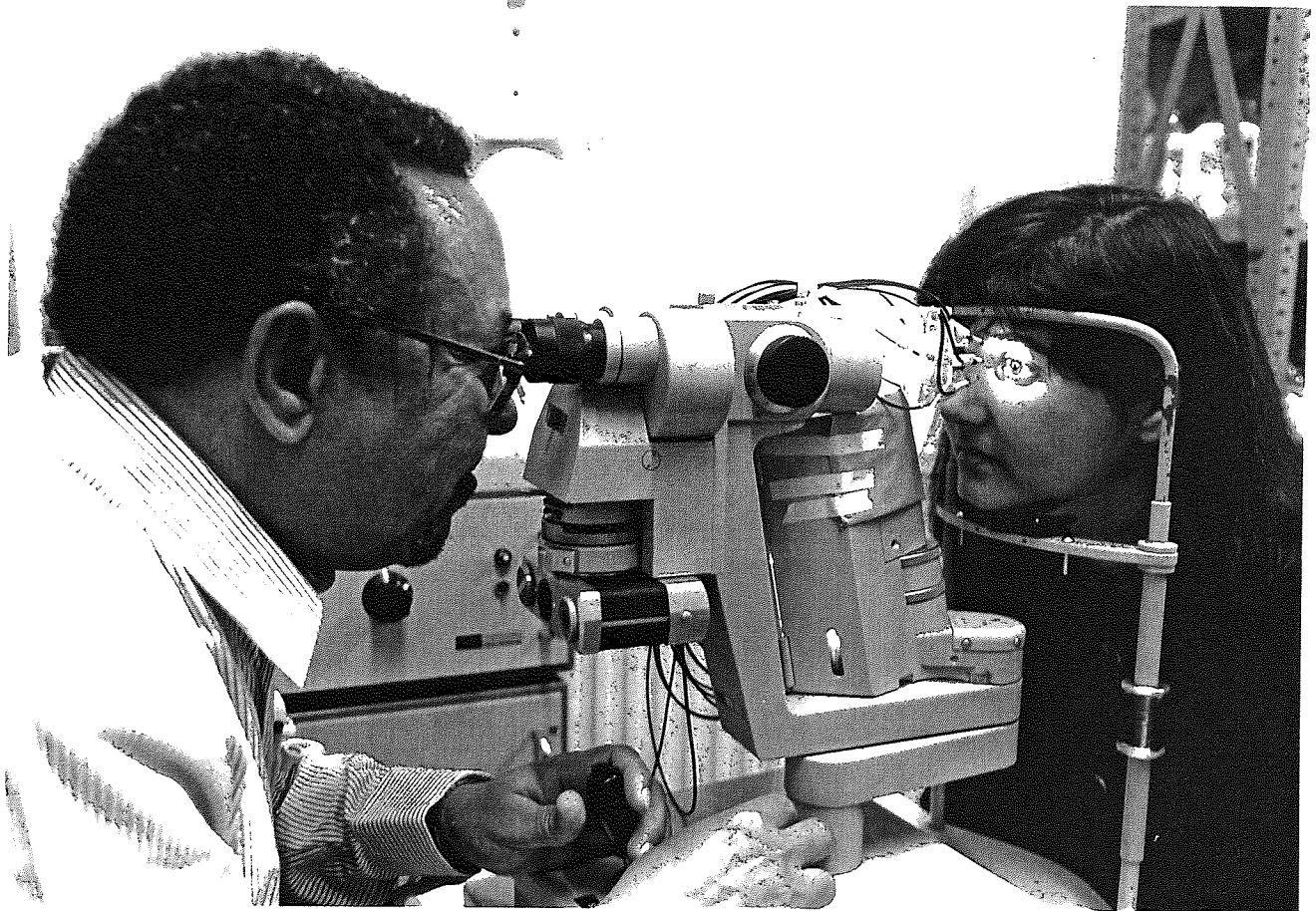


Figure 3.1 Photograph of the multi-meridional still flash photographic ophthalmophakometer.

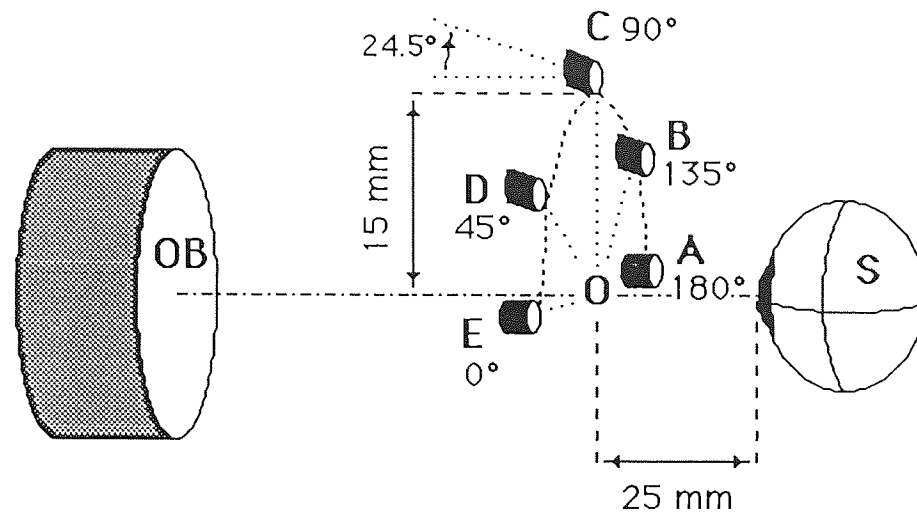


FIGURE 3.2. Diagrammatic representation of the fibre optic Purkinje image light sources (A - E) mounted in the 180°, 90°, 135° and 45° meridians. Light sources were placed at equal perpendicular distances (15 mm) from the axis (O) of the slit lamp objective (OB). The light array was operated at a working distance of 25 mm from the subject's eye (S). Light sources were inclined (24.5°) towards the instrument axis so that light would strike the corneal surface normally.

Subjects were stabilised on a chin and forehead rest. Fixation was directed to a weak reflection of the subject's own eye seen in the centre of the objective lens. By this means, the subject's visual axis was made to coincide with the axis of the slit lamp objective. In the event of Purkinje image overlap, small amount of lateral displacement of the light array mounting relative to the slit lamp objective were essential. In this case slightly off axis photographs were taken. Purkinje Images I, II and IV, were successfully photographed in all subjects included in this study. Figure 3.3 is an example photograph.

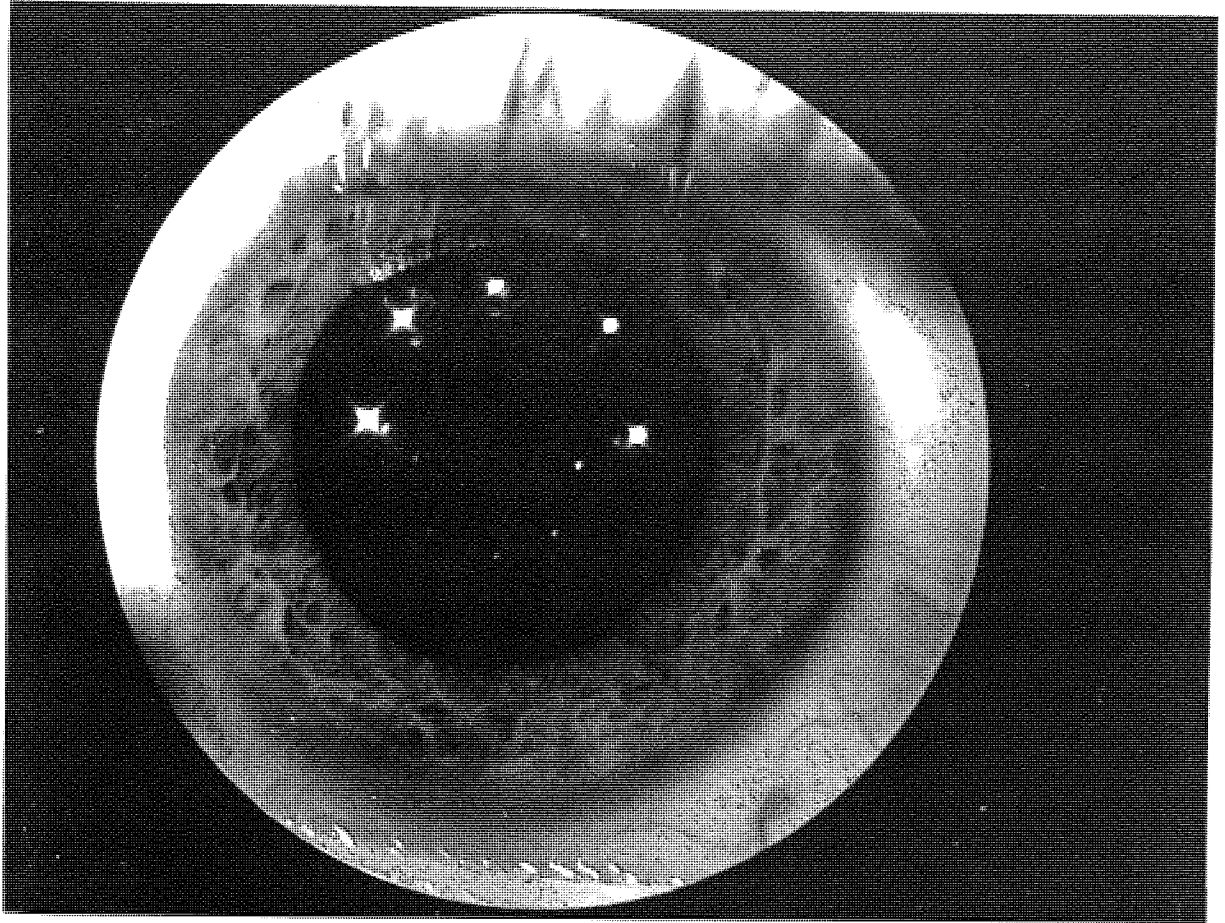


Figure 3.3 Photograph of Purkinje images I, II, and IV taken along the 180°, 90°, 135° and 45° meridians using the apparatus depicted in Figure 3.1 and Figure 3.2. (see Figure 3.4 for diagrammatic representation of images)

Accommodation could not be controlled by means of a fixation target because this would obstruct or interfere with Purkinje image photography. However, it was unlikely that the weak light reflection used for fixation would act as a strong accommodation stimulus. In addition to this, measurements were taken with the room lights off and pupil fluctuations were monitored as a safe guard against accommodation. Potential errors due to accommodation are considered in chapter 6.

For best results, the photographic flash was set at a maximum intensity of 480 W s^{-1} . The camera was adjusted for an exposure time of 0.04 seconds, an aperture ratio of 1:1.79 and reproduction ratio of 1:1.6. Photographic negatives (ILFORD HP5 400 ASA black and white film) were processed using standard procedures.

Each of the negatives was projected against a screen and thereby magnified by X37.5. Previous experience with the same apparatus revealed that negligible distortion arises from this approach (Dunne, 1987; Royston, 1990). Purkinje images were measured using a precision rule to the nearest $\pm 0.5 \text{ mm}$ (a scaled down interval of $\pm 0.01 \text{ mm}$). The procedure adopted for Purkinje image measurements is depicted in Figure 3.4. Purkinje images A' to E' correspond to the light sources (A and E) shown in Figure 3.2. Images arising from the anterior corneal surface (Figure 3.4a), posterior corneal surface (Figure 3.4b) and the posterior crystalline lens surface (Figure 3.4c) are presented this way for simplicity and are identified with the Roman numerals I, II and IV, respectively. For each set of Purkinje images, reference centre (O') was located by bisecting a line drawn between A' and E'. Image heights along 180° (A'O'), 135° (B'O'), 90° (C'O') and 45° (D'O') were then measured with respect to the centre. If all the ocular components were centred with respect to the visual axis then (O'_I, O'_{II}, O'_{IV}) would coincide but this was rarely the case.

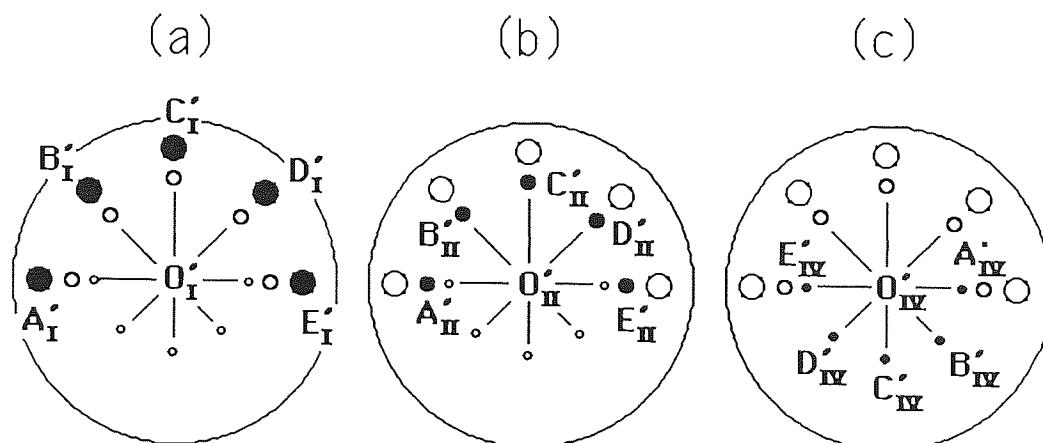


FIGURE 3.4. Diagrammatic representation of Purkinje images (A' to E') corresponding to the light sources (A to E) shown in Figure 3.2. Images arising from the anterior corneal surface (a), posterior corneal surface (b) and the posterior crystalline lens surface (c) are highlighted separately for clarity and identified with Roman numerals I, II and IV, respectively (Note that Purkinje image IV is inverted). Reference centres (O') are also shown for each set of Purkinje images.

A mean and standard deviation was calculated from nine repeat measurements, three repeat measurements of each Purkinje image height from all three photographs taken on each eye. Purkinje image heights were utilized for the calculation of the ocular surface power as described in chapter 4.

3.6 Experimental Protocol

3.6.1 Preliminary Study: Measurements of Residual Astigmatism

In this part of the study residual astigmatism was measured to establish its magnitude and axis orientation.

Previous studies have shown that the refractive components of the human eyes undergo considerable changes with age (Hirsch, 1959; Lyle, 1971; Anstice, 1971; Baldwin and Mills, 1981; Saunders, 1981, 1984; Lyle, 1991 and Erickson, 1991; Grosvenor, 1994). For this reason, subjects who participated in the study fell within a narrow age range. Members of the undergraduate population attending the optometry course in the Vision Sciences Department of Aston University were therefore recruited for the sample. Measurements of refraction and anterior corneal curvature (see section 3.2 and 3.3) were taken from the right and left eyes of 70 students (37 males, 33 females) whose ages ranged from 18 to 30 years. The sample included 25 Asians (12 males, 13 females), 43 Caucasians (23 males, 20 females) and 2 males from other racial groups. All eyes were free from ocular abnormality and contact lens wearers were excluded.

Being optometry students, these subjects were accustomed to relaxing their accommodation and maintaining steady fixation when measurements were taken.

Repeatability was assessed by taking readings from the right and left eyes of 20 males on two occasions at least one week apart.

3.6.2 Main Study: Measurement of Internal Ocular Surface Toricity

The full complement of biometric measurements was carried out on both eyes of 66 subjects (4 of the 70 subjects included in the preliminary study dropped out before completing the required measurements). The sample were of mixed race and consisted of 33 males (age range 18-30 years, 12 Asians, 21 Caucasians) and 33 females (Age range 18- 25 years, 13 Asians, 20 Caucasians).

Repeatability was again assessed by taking readings from the right and left eyes of 20 males on two occasions at least a week apart.

3.6.3 Cycloplegic Study

The intention of the previously described parts of this study was to measure ocular components under natural conditions, not under the influence of cycloplegic drugs. However, the non-cycloplegic approach raises questions about the potential influence of uncontrolled accommodation on the results. This part of the study was therefore designed to test the effect of controlling accommodation. Measurements were taken from the left eyes of 10 healthy males free from any ocular abnormality. Subjects were examined with and without the use of cycloplegic drugs.

Amplitudes of accommodation were measured using RAF rule before and after cycloplegic drugs were instilled. Two drops of cyclopentolate (1%), were instilled in the left eye 5 minutes apart followed by biometric measurements 60 minutes later. The same eyes were measured again under natural conditions (no cycloplegia), at least one week later.

3.7 Summary

This chapter has described the biometric methods chosen to measure *in vivo* ocular components of the human eye (multi-meridional ultrasonic ophthalmophakometry). Automated infra-red autorefractometry was used to estimate refractive error. Corneal curvatures were measured using a computerised video keratographic device. A-scan Ultrasonography was used to measure intra-ocular axial distances. Measurements of Purkinje images I, II, IV in four meridians were made by means of a purpose built still flash photographic ophthalmophakometer.

A protocol involving preliminary (right and left eyes of 70 subjects), main (right and left eyes of 66 subjects), repeatability (right and left eyes of 20 male subjects) and Cycloplegic studies (left eyes of 10 male subjects) was laid down.

All measurements were taken along the line of sight under natural conditions. The line of sight is the only logical axis where all the components function jointly (Gullstrand, 1924).

The calculation schemes using the biometric measurements described in this chapter are considered in the chapter 4.

CHAPTER FOUR
COMPUTING SCHEMES

4.1 Introduction

This chapter describes the computing schemes used in conjunction with the measurements described in chapter three. Computing schemes start with determining notional power in section 4.2 for meridional spectacle refraction and anterior corneal surface radius of curvature in section 4.3 which in turn is divided into subsections (1) spectacle refraction and (2) radius of curvature of anterior corneal surface. Calculation of internal ocular surface astigmatism is considered in section 4.4 and subsection (1) review of meridional analysis and (i) three meridional analysis (ii) multi meridional analysis. In subsection 4.4.2 calculation of meridional surface power is considered under the following headings: (i) refractive and Catoptric imaging properties of the anterior corneal surface; (ii) refractive and Catoptric imaging properties of the posterior corneal surface, (iii) calculation of the crystalline lens surface parameters and (iv) description of the iterative routine. Subsection 4.4.3 deals the meridional analysis.

Calculation of ocular components contributions to residual astigmatic power is looked at in section 4.5 followed by 3 subsections: (1) astigmatic decomposition; (2) vergence analysis and (3) computing scheme.

Calculation of random experimental errors involved in the calculation of meridional powers and spherocylindrical results are covered in section 4.6 and 4.7 respectively. Finally the Purkinje image positions, ratios and heights are described in section 4.8 considering the following: (i) anterior corneal surface (Purkinje image I); (ii) posterior corneal surface (Purkinje image II); (iii) anterior lens surface (Purkinje image III) and (iv) posterior lens surface (Purkinje image IV). The chapter ends with summary in section 4.9.

4

4.2 Notional Meridional Power

An essential part of the overall computational procedure was the calculation of power in meridians which did not necessarily coincide with the principal power meridians of the eye or its constituent surfaces. The concept of power in any meridian other than principal power meridians is purely notional. There is a persistent fallacy that a spherocylindrical lens has a focal power equal to $(S + C \sin^2 \emptyset)$ in the meridian at \emptyset° from the cylinder axis. Bennett and Rabbetts (1978) addressed this matter and suggested the term notional power for the quantity $(S + C \sin^2 \emptyset)$ which has been used by previous workers to derive spectacle correction (Bennett and Rabbetts, 1978, 1989) and was used in this project to calculate ocular surface powers. It also provided means to overcome the problems of averaging spherocylindrical data raised by Harris (1992a, 1992b).

4.3 Calculation of Meridional Data for Spectacle Refraction and Anterior Corneal Surface Radius of Curvature

A computer program was written to resolve repeat measurements of refractive error (section 3.2) and anterior corneal radius of curvature (section 3.3) to four meridians 180° , 90° , 135° and 45° (appendix A1). A mean and standard deviation is automatically calculated for each set of repeat readings.

4.3.1 Spectacle Refraction

Symbols used:

N	Number of repeat measurements	
F_{spS}	Spherical power	(D)
F_{spC}	Cylindrical power	(D)
F_{spA}	Cylinder axis	($^\circ$)

The sphero-cylindrical data were resolved to the four required meridians using the following equations (Laurance, 1920; Brubaker et al., 1969):

$$F_{sp180} = F_{spS} + \{F_{spC} \cdot \sin^2 (F_{spA} - 180)\} \quad (1.A_1)$$

$$F_{sp90} = F_{spS} + \{F_{spC} \cdot \sin^2 (F_{spA} - 90)\} \quad (2.A_1)$$

$$F_{sp135} = F_{spS} + \{F_{spC} \cdot \sin^2 (F_{spA} - 135)\} \quad (3.A_1)$$

$$F_{sp45} = F_{spS} + \{F_{spC} \cdot \sin^2 (F_{spA} - 45)\} \quad (4.A_1)$$

The program looped until all the repeated measurements have been entered and resolved to four meridians.

Calculation of a statistical mean and standard deviation for repeat estimates of spectacle refraction along each meridian was then carried out (Bailey, 1983). If x is taken to be F_{sp180} , F_{sp90} , F_{sp135} or F_{sp45} , then the calculations start by determining $\sum x$ and $\sum x^2$ to determine mean values as follows :

$$\text{Mean} = (\sum x / N) \quad (5.A_1)$$

Next, $\sum(x - \text{mean})^2$ is calculated using the following equation :

$$\sum(x - \text{mean})^2 = \sum x^2 - \{(\sum x)^2 / N\} \quad (6.A_1)$$

Finally, the standard deviation was calculated as follows :

$$\text{Standard deviation} = \sqrt{\{\sum(x - \text{mean})^2 / (N - 1)\}} \quad (7.A_1)$$

4.3.2 Radius of Curvature of Anterior Corneal Surface

Symbols used:

N	Number of repeat measurements	
r_1 flat	Radii of curvature along the flattest meridian	(mm)
r_1 steep	Radii of curvature along the steepest meridian	(mm)
r_1A	Axis of the flattest meridian	($^{\circ}$)
r_1S	Spherical power	(D)
r_1C	Cylindrical power	(D)
r_1A	Cylinder axis in minus-cylinder form	($^{\circ}$)

The measured anterior corneal curvature values were converted to spherocylindrical form. Although conversion of radii into spherocylindrical form yielded quantities which were only theoretical, this process was still mathematically correct and offered one of the simplest means of resolving radii of curvature to specific meridians (Fowler, 1989; Royston, 1990). The conversion was carried out in the following manner which yielded a sphere (r_1S), cylinder (r_1C) and cylinder axis (r_1A) in minus-cylinder form :

$$r_1S = r_1\text{flat} \quad (8.A_1)$$

$$r_1C = r_1\text{steep} - r_1\text{flat} \quad (9.A_1)$$

$$r_1A = r_1\text{flatter} \quad (10.A_1)$$

The calculation of notional radii r_1180° , r_190° , r_1135° and r_145° followed the same procedure as described for spectacle refraction (equations 1.A₁ to 4.A₁). Likewise, the calculation of a statistical mean and standard deviation for repeat estimates of anterior corneal surface radius along each meridian was identical to the procedure adopted for spectacle refraction (equations 5.A₁ to 7.A₁) except that x was now taken to be r_1180° , r_190° , r_1135° or r_145° .

4.4 Calculation of Internal Ocular Surface Astigmatism

Another computer program was written (appendix A.2) which utilised the meridional refractive and keratometric data in conjunction with measurements of axial distances (section 3.4) and Purkinje image heights (section 3.5) to determine the spherocylindrical powers of the internal ocular surfaces after applying a technique called meridional analysis. This program provided the option to carry out meridional analysis on data collected along three (180° , 90° and 135°) or four (180° , 90° , 135° and 45°) meridians. Three meridians are the minimum number required to specify the spherocylindrical power of a surface. The benefit of using a fourth meridian could be tested using the option provided by the this computer program.

4.4.1 Review of Meridional Analysis

Most of the work involving meridional analysis techniques has been related to refraction and spectacle correction of the eye. The equations used for meridional analysis are based on an approximation relating to the meridional power of a cylindrical lens derived by Laurance (1920). Bennett (1960) was the first to propose determination of spectacle correction from readings taken in pre-selected meridians.

(i) Three Meridional Analysis

Three meridional analysis is the method used to derive a sphero-cylindrical correction from measurements taken in three meridians. Brubaker, Reinecke and Copeland (1969) used Bennett's (1960) equations to determine a sphero-cylindrical correction from refractive measurements made on 90° , 135° , 180° meridians opening the door for other researchers to follow (Reinecke, Carroll, Beyer and Montross, 1972; Haine, Long and Reading, 1973; Malacara, 1974; Haine, Long and Reading, 1976; Worthey, 1977; Whitefoot and Charman, 1980). Fowler (1989) was the first to produce a method to derive sphero-cylindrical power from meridional curvatures (90° , 180° , 45°) and Burek (1990) has developed set of equations which enables measurements from any set of three meridians to be used. The meridional power and meridional curvature methods were found to function equally well (Royston, 1990).

(ii) Multi-meridional Analysis

Long (1974) demonstrated that a small error in the initial measurements can lead to significantly large difference in the final prescription regarding the cylindrical power and axis orientations. To overcome this he suggested a mathematical method which involved measurements taken along four or more meridians. The method predicted

close answers to the measured meridional values and provided an indication of which meridian should be re-evaluated when the estimated accuracy was inadequate.

Number allocated to F, L, L', d, h, n..		d	n
1	anterior cornea	corneal thickness	cornea 1.3771
2	posterior cornea	anterior chamber	aqueous 1.3374
3	anterior lens	lens thickness	lens 1.42
4	posterior lens		Vitreous 1.336

Table 4.1 Curvatures, axial distances and refractive indices (n_1 air) used in the calculations.

Parameter	Symbol	Units
Ocular surface power	F	(D)
Catoptric ocular surface power	F_c	(D)
Ocular vertex distance	v	(mm)
Radius of curvature of ocular surface	r	(mm)
vergence of light striking an ocular surface	L	(D)
vergence of light after refraction by an ocular surface	L'	(D)
Purkinje image height	h	(mm)
Purkinje image distance	l'	(m)
Purkinje image magnification	m	
Intraocular distances	d	(m)
Distance of the object light source	d_s	(m)
Centre of curvature of the equivalent mirror	C	(m)
Equivalent mirror vertex	A	(m)
Refractive indices	n	
Number allocated to F, L, L', d, n, e t c. in sequence:	i	
spherical component of F, L, and L'	S	(D)
cylindrical component of F, L and L'	C	(D)
cylinder axis orientation of F, L and L'	A	(°)
mean refractive power of F, L and L'	MRP	(D)
orthogonal cylindrical component of F, L and L'	C_o	(D)
oblique cylindrical component of F, L and L'	C_{45}	(D)

Table 4.2 Symbols used in the computing scheme.

Ultrasonically measured (section 3.4) anterior chamber depths, lens thicknesses and vitreous lengths (in millimetres) were called for first. These data were automatically converted to meters in preparation for biometric calculations. Corneal thickness was assumed to be 0.5 mm (section 3.4) and was automatically subtracted from the anterior chamber depth. The ophthalmophakometer working distance was taken to be 25 mm in accordance with design parameters (section 3.5). The refractive indices were assumed to be 1.3771 for the cornea, 1.3374, for the aqueous humour, 1.42 for the crystalline lens and 1.336 for the vitreous humour. Secondly, the meridional data calculated for spectacle refraction and anterior corneal radius of curvature was called for. Meridional corneal radii stored in millimetre were automatically converted to meters. Heights (in millimetres) of Purkinje images arising from the anterior corneal surface (Purkinje I), posterior corneal surface (II) and posterior lens surface (IV) were then prompted for. It was unnecessary to convert these values into meters as will be seen later.

4.4.2 Calculations Meridional Surface Powers

The meridional powers of the anterior and posterior corneal and lens surfaces were calculated using a computing scheme developed by Dunne (1992). This is described in this section.

(i) Refractive and Catoptric Imaging Properties of the Anterior Corneal Surface

The refractive power, F_1 , of the anterior corneal surface is found using the following well known equation :

$$F_1 = (n_2 - n_1) / r_1 \quad (1.A_2) \text{----- (step 1)}$$

Purkinje image I is produced by mirror reflection from this surface. The catoptric power, F_{1c} , of the anterior corneal surface acting as a mirror is calculated as follows :

$$F_{1c} = (-n_1 - n_1)/r_1 \quad (2.A_2) \text{----- (step 2)}$$

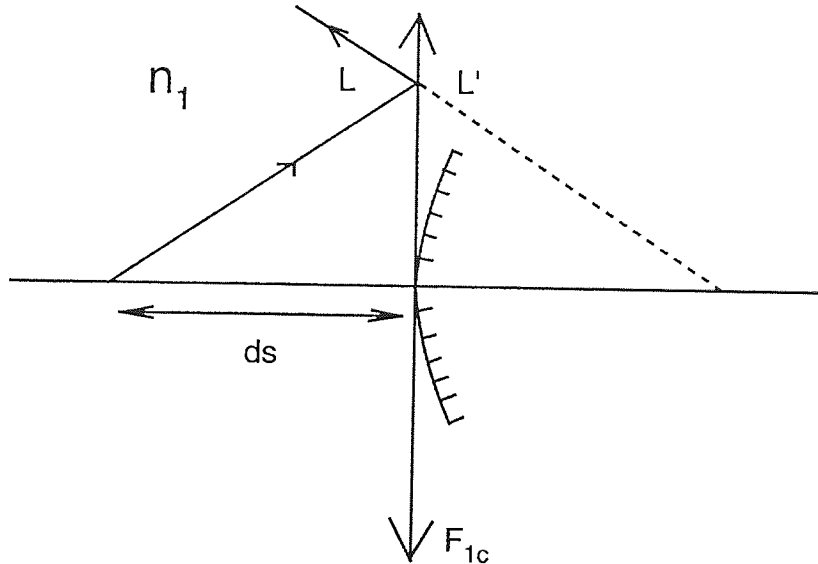


Figure 4.1 Catoptric imaging properties of the anterior corneal surface

The transverse magnification of Purkinje image I, m_1 is then required. This is given by the following equation where L and L' are object and image vergences, respectively.

$$m_1 = L/L' \quad (3.A_2)$$

It can be seen from figure 1 that the object giving rise to Purkinje image I is at a known distance, d_s , in front of the anterior corneal surface vertex. The object vergence is thus :

$$L = n_1/-d_s \quad (4.A_2)$$

the image vergence is then :

$$L' = L + F_{1c} \quad (5.A_2)$$

By combining equation 3 - 5.A₂ into one expression we have :

$$m_1 = (1/-d_s) / \{ (1/-d_s) + F_{1c} \} \quad (6.A_2) \text{----- (step 3)}$$

(ii) Refractive and Catoptric Imaging Properties of the Posterior Corneal Surface :

It is necessary to calculate the transverse magnification of Purkinje image II, m_2 , which is formed by the posterior corneal surface acting as a mirror. Clearly, the ratio of Purkinje image magnifications for both corneal surfaces is the same as the ratio between their respective image heights. The value of m_2 is thus derived from the following expression :

$$m_2 = (h_2/h_1)m_1 \quad (7.A_2)\text{----- (step 4)}$$

Now, calculation of the refractive properties of the posterior corneal surface requires calculation of its catoptric imaging properties first of all. Calculations for the latter are simplified by application of the equivalent mirror theorem. Here, a system comprising one or more refracting surfaces followed by a plane or spherical mirror can be simplified for calculation to an 'equivalent' spherical mirror. The vertex and spherical curvature of the equivalent mirror coincide, respectively, with the images of the vertex and centres of curvature of the actual mirror formed by the refracting elements (Bennett and Rabbetts, 1984).

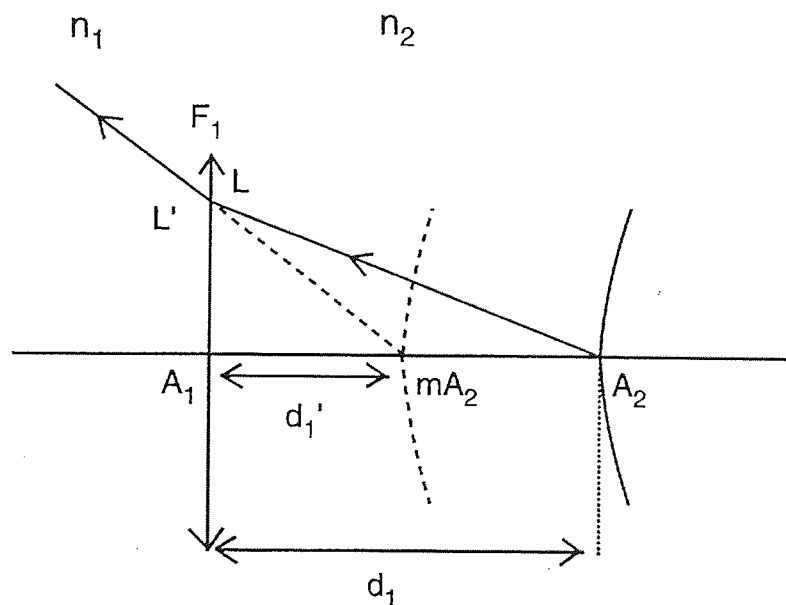


Figure 4.2 Finding the vertex of the posterior corneal equivalent mirror

The position of the vertex of the equivalent mirror for the posterior corneal surface, mA_2 , is calculated as depicted in (Figure 4.2). The true posterior corneal surface vertex, at A_2 , is treated as an object which forms an image at mA_2 after refraction through the cornea at A_1 . The distance A_1A_2 thus corresponds to the true corneal thickness, d_1 , whilst the distance A_1mA_2 corresponds to the apparent corneal thickness, d_1' , as seen through the anterior corneal surface.

Now the object vergence, L , is given by :

$$L = n_2/d_1 \quad (8.A_2)$$

and the image vergence, L' , is :

$$L' = L - F_1 \quad (9.A_2)$$

so that d_1' represents the image distance, l' , which is :

$$d_1' = l' = n_1/L' \quad (10.A_2)$$

Combination of equations 8 - 10.A₂ yields the following expression :

$$d_1' = n_1 / \{ (n_2/d_1) - F_1 \} \quad (11.A_2) \text{----- (step 5)}$$

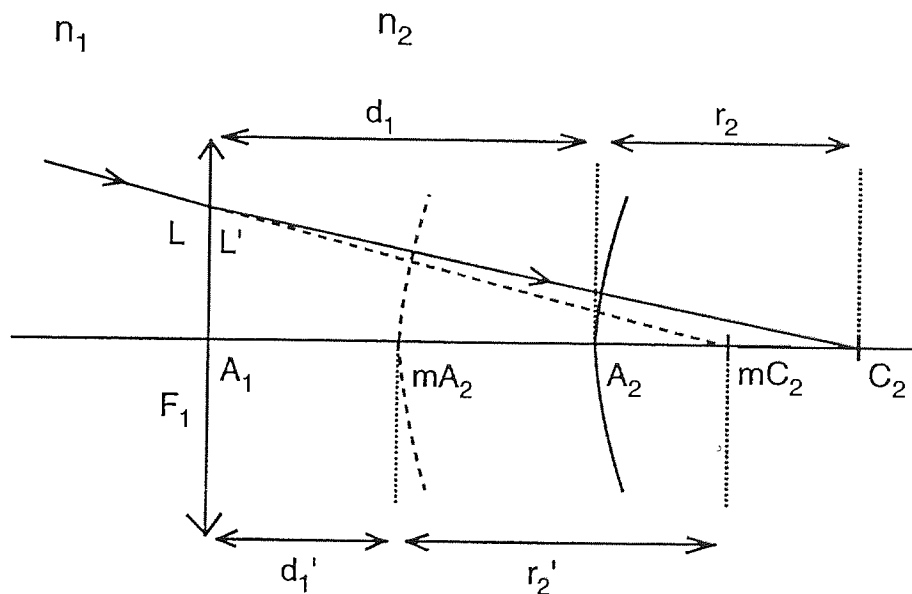


Figure 4.3 Finding the centre of curvature of the posterior corneal equivalent mirror.

The position of the centre of curvature of the equivalent mirror for the posterior corneal surface, mC_2 , may be derived in a similar fashion to the calculations just described. That is, the true posterior corneal surface centre of curvature, C_2 , is treated as an object which after refraction through the anterior corneal surface is imaged at mC_2 . The distances A_2C_2 and A_2mC_2 are then, respectively, the true, r_2 , and apparent, r_2' , posterior corneal surface radii (Figure 4.3). A problem arises, however, because r_2 is not known.

The problem is solved by consideration of the imaging properties of the equivalent mirror for the posterior corneal surface (Figure 4.4).

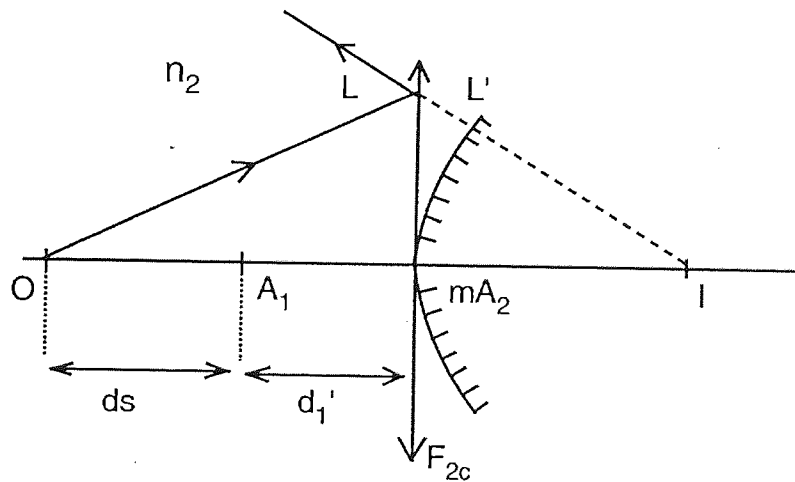


Figure 4.4 Catoptric imaging properties of posterior corneal equivalent mirror.

Clearly the object light source at O is imaged at I to form Purkinje image II after reflection by the equivalent mirror corresponding to the posterior corneal surface.

Now, the object vergence, L , is given by :

$$L = n_1 / -(ds + d_1') \quad (12.A_2)$$

Also, rearrangement of the well known equation relating object and image vergences to transverse image magnification, m_2 , allows the calculation of image vergence, L' :

$$L' = L / m_2 \quad (13.A_2)$$

It then follows that the dioptric difference between L and L' must necessarily be the catoptric power of the equivalent mirror, F_{2c} :

$$F_{2c} = L' - L \quad (14.A_2)$$

Equations 12 - 14.A₂ may be combined to produce the following expression :

$$F_{2c} = [n_1/(ds+d_1')] - \{ [n_1/(ds+d_1')] / m_2 \} \quad (15.A_2)----- \text{ (step 6)}$$

This, in turn, yields the radius of the equivalent mirror :

$$r_2' = (-n_1 - n_1) / F_{2c} \quad (16.A_2)----- \text{ (step 7)}$$

With reference to (Figure 4.3), the value calculated for r_2' now allows the position of the centre of curvature of the equivalent mirror, at mC_2 , to be determined. This is then treated as an object to be imaged at C_2 , the centre of curvature of the true posterior corneal surface, after refraction by the anterior corneal surface.

The object vergence, L, is now :

$$L = n_1 / (d_1' + r_2') \quad (17.A_2)$$

and the image vergence, L', is given by :

$$L' = L + F_1 \quad (18A_2)$$

the image distance, l', is then :

$$l' = n_2 / L'. \quad (19.A_2)$$

Now, in figure 4.3 it is clear that l' is equal to the quantity $(d_1 + r_2)$ so that the true posterior corneal surface radius, r_2 , is given by :

$$r_2 = l' - d_1. \quad (20.A_2)$$

Again, equations 17 - 20.A₂ can be combined to produce the following expression :

$$r_2 = \{ n_2 / [(n_1 / (d_1' + r_2')) + F_1] \} - d_1 \quad (21.A_2)----- \text{ (step 8)}$$

Finally, the power of the posterior corneal surface is calculated :

$$F_2 = (n_3 - n_2) / r_2 \quad (22.A_2)----- \text{ (step 9)}$$

(iii) Calculation of the Crystalline Lens Surface Parameters

A considerable complication now exists. If the Purkinje image heights of the anterior (III) and posterior (IV) crystalline lens surfaces were known then their respective radii could be readily calculated. However, it is only the height of Purkinje image IV which is known and this image is formed by reflection from the posterior crystalline lens surface after refraction through each of the other refracting surfaces including that of the anterior crystalline lens - the parameters of which are not known.

The simplest remedy is to start off with an arbitrary value for the anterior lens surface power, F_3 . This allows derivation of an initial value for the radius, r_4 and power, F_4 , of the posterior crystalline lens surface. Application of the equivalent mirror theorem then yields a computed value for the height of Purkinje image IV, $h_{4(\text{estimate})}$. This is compared to the measured height of Purkinje image IV, h_4 . Any difference will indicate that the original choice of F_3 was incorrect. F_3 is then altered until good agreement between the measured and computed Purkinje image IV heights occurs at which point the required values of F_3 and F_4 will have been found.

The first step is then to chose an arbitrary value for F_3 :

F_3 ----- (step 10)

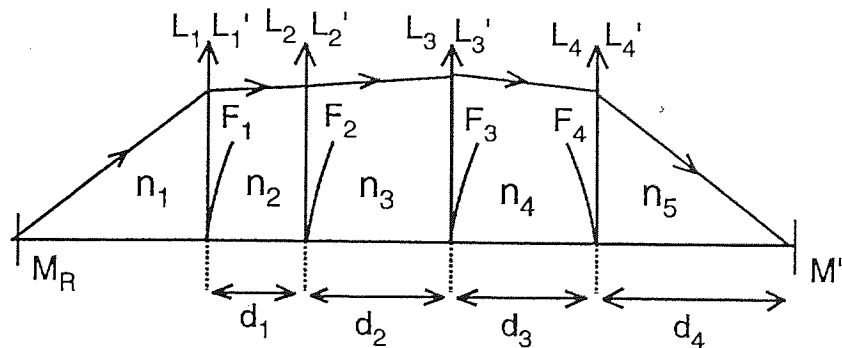


Figure 4.5 Axial ray trace from the far point through the four surfaced eye.

F_4 and r_4 are now determined by carrying out a step along ray trace (Bennett and Rabbetts, 1989) from the eye's far point, M_R , to its focus at the retina, M' (Figure 4.5). Tracing from M_R yields the vergence of the rays incident upon the posterior crystalline lens surface, L_4 . Tracing from M' then yields the vergence of rays emerging from the same surface, L_4' . The dioptric difference between incident and emergent vergences gives the power, F_4 , of this surface from which r_4 is then calculated. The steps involved are as follows :

$$L_1 = F_{sp} / (1 - v.F_{sp}) \quad (23.A_2) \text{----- (step 11)}$$

$$L_1' = L_1 + F_1 \quad (24.A_2) \text{----- (step 12)}$$

$$L_2 = L_1' / \{ 1 - (d_1/n_2).L_1' \} \quad (25.A_2) \text{----- (step 13)}$$

$$L_2' = L_2 + F_2 \quad (26.A_2) \text{----- (step 14)}$$

$$L_3 = L_2' / \{ 1 - (d_2/n_3).L_2' \} \quad (27.A_2) \text{----- (step 15)}$$

$$L_3' = L_3 + F_3 \quad (28.A_2) \text{----- (step 16)}$$

$$L_4 = L_3' / \{ 1 - (d_3/n_4).L_3' \} \quad (29.A_2) \text{----- (step 17)}$$

Now L_4' is found by :

$$L_4' = n_5 / d_4 \quad (30.A_2) \text{----- (step 18)}$$

so that the posterior crystalline lens surface power, F_4 , is :

$$F_4 = L_4' - L_4 \quad (31.A_2) \text{----- (step 19)}$$

and the posterior crystalline lens radius, r_4 , is :

$$r_4 = (n_5 - n_4) / F_4 \quad (32.A_2) \text{----- (step 20)}$$

Next, the equivalent mirror for the posterior crystalline lens surface is derived in order to simplify calculation of the computed height of Purkinje image IV.

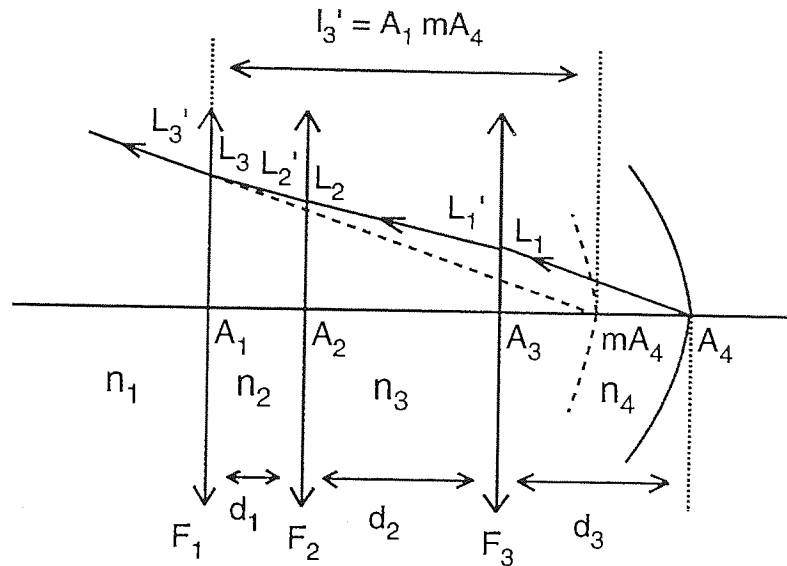


Figure 4.6 Finding the vertex of the posterior lens equivalent mirror

Figure 4.6 outlines the procedure adopted for calculation of the position of the equivalent mirror vertex, mA_4 . Here, the vertex of the true posterior lens surface, A_4 , is treated as an object which forms an image at mA_4 after refraction by the anterior lens surface at A_3 , the posterior corneal surface at A_2 and the anterior corneal surface at A_1 .

A step along back raytrace is required. The following equations include alterations made in accordance with the sign convention (Bennett and Rabbetts, 1989), as rays are being traced back out of the eye:

$$L_1 = n_4 / d_3 \quad (33.A_2)\text{----- (step 21)}$$

$$L_1' = L_1 - F_3 \quad (34.A_2)\text{----- (step 22)}$$

$$L_2 = L_1' / \{ 1 + (d_2/n_3).L_1' \} \quad (35.A_2)\text{----- (step 23)}$$

$$L_2' = L_2 - F_2 \quad (36.A_2)\text{----- (step 24)}$$

$$L_3 = L_2' / \{ 1 + (d_1/n_2).L_2' \} \quad (37.A_2) \text{----- (step 25)}$$

$$L_3' = L_3 - F_1 \quad (38.A_2)\text{----- (step 26)}$$

The position of equivalent mirror vertex with respect to the anterior corneal surface vertex is A_1mA_4 and is found as follows :

$$A_1mA_4 = l_3' = n_1 / L_3' \quad (39.A_2) \text{----- (step 27)}$$

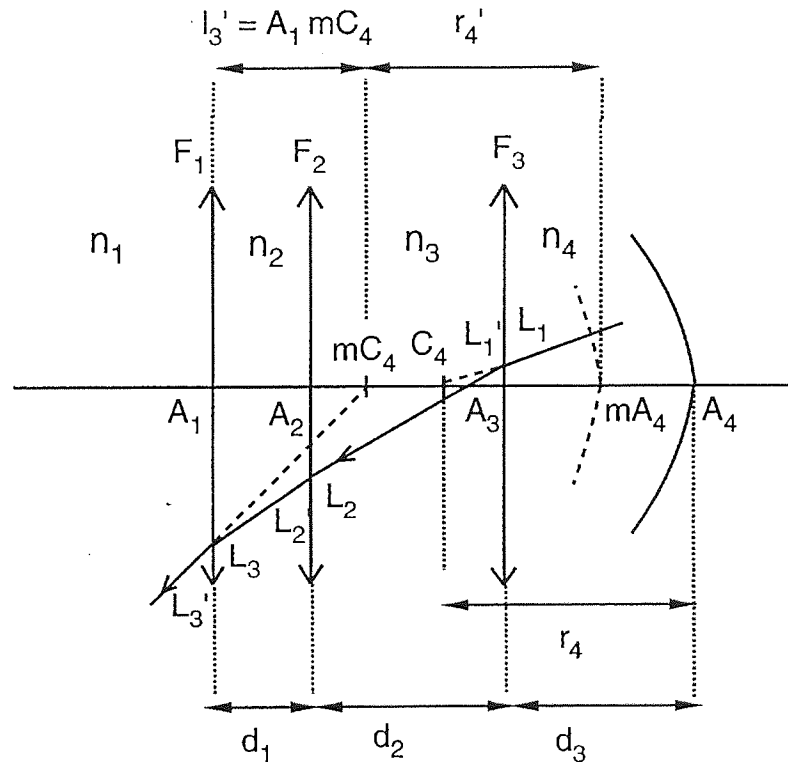


Figure 4.7 Finding the centre of curvature of the posterior lens equivalent mirror

The centre of curvature of the equivalent mirror, mC_4 , is derived in a similar fashion by treating the true centre of curvature of the posterior crystalline lens surface, C_4 , as an object (Figure 4.7).

As Bennett and Rabbetts (1989) pointed out, the posterior lens surface vertex, A_4 , and centre of curvature, C_4 , lie on opposite sides of the anterior lens surface vertex at A_3 . Therefore C_4 becomes a virtual object which gives rise to a real image after refraction through the front lens surface (Figure 4.7).

A step along back raytrace is again required as follows :

$$L_1 = n_4 / (r_4 + d_3) \quad (40.A_2) \text{----- (step 28)}$$

$$L_1' = L_1 - F_3 \quad (41.A_2) \text{----- (step 29)}$$

$$L_2 = L_1' / \{ 1 + (d_2/n_3).L_1' \} \quad (42.A_2) \text{----- (step 30)}$$

$$L_2' = L_2 - F_2 \quad (43.A_2) \text{----- (step 321)}$$

$$L_3 = L_2' / \{ 1 + (d_1/n_2).L_2' \} \quad (44.A_2) \text{----- (step 32)}$$

$$L_3' = L_3 - F_1 \quad (45.A_2) \text{----- (step 33)}$$

The position of equivalent mirror centre of curvature with respect to the anterior corneal surface vertex is A_1mC_4 and is found as follows :

$$A_1mC_4 = l_3' = n_1 / L_3' \quad (46.A_2) \text{----- (step 34)}$$

It now follows that the radius of the equivalent mirror, r_4' , is given by :

$$r_4' = A_1mC_4 - A_1mA_4 \quad (47.A_2) \text{----- (step 35)}$$

from which the catoptric power of the equivalent, F_{4c} , mirror is derived :

$$F_{4c} = (-n_1 - n_1) / r_4' \quad (48.A_2) \text{----- (step 36)}$$

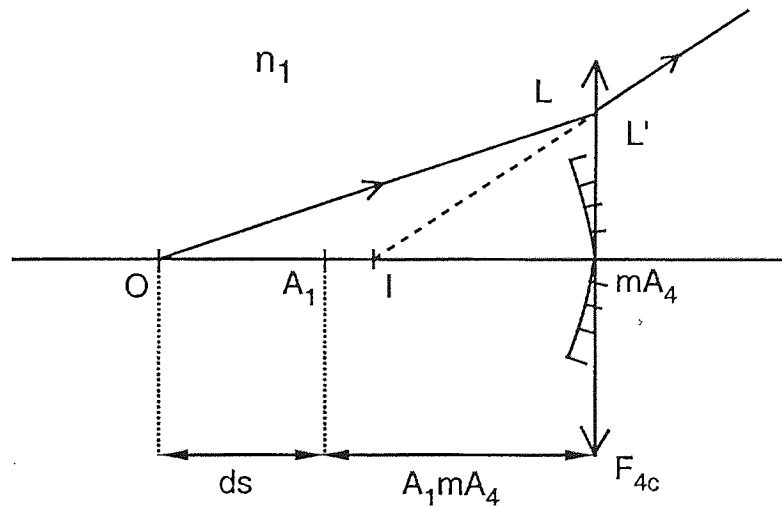


Figure 4.8 Catoptric imaging properties of the posterior lens equivalent mirror.

The advantages offered by the equivalent mirror theorem now really come to light as the catoptric imaging properties of the posterior lens equivalent mirror are simply depicted as in figure 4.8. Here, the object light source at O is imaged at I to form Purkinje image IV. The transverse magnification, m_4 , of this image is now :

$$m_4 = L / L', \quad (49.A_2)$$

where the object vergence, L , is :

$$L = n_1 / -(ds + A_1 m A_4) \quad (50.A_2)$$

and the image vergence, L' , is :

$$L' = L + F_{4c}. \quad (51.A_2)$$

Combination of equations 49 - 51 A.2 gives the following expression :

$$m_4 = \{ n_1 / -(ds + A_1 m A_4) \} / \{ \{ n_1 / -(ds + A_1 m A_4) \} + F_{4c} \} \quad (52.A_2) \text{----- (step 37)}$$

The computed height of Purkinje image IV, $h_{4(\text{estimate})}$, is then :

$$h_{4(\text{estimate})} = (m_4 / m_1) \cdot h_1 \quad (53.A_2) \text{----- (step 38)}$$

The computed height of Purkinje image IV, $h_{4(\text{estimate})}$, may now be compared to the measured value, h_4 . If agreement exists between the two, then we have the correct dioptric powers for the anterior (F_3) and posterior crystalline (F_4) lens surfaces. If not, then a new value of F_3 is chosen (step 10) and steps 11 - 38 repeated. This "trial and error" approach was made easier by incorporating an appropriate iterative routine into the computer program.

(iv) Description of the Iterative Routine

The iterative routine simply involved raising or lowering the initial value of F_3 dependent upon the sign of the difference, Δh , recorded between the computed and measured Purkinje image IV heights:

$$\Delta h = h_4 - h_{4(\text{estimate})} \quad (54.A_2) \text{----- (step 39)}$$

To observe the effect of different initial values of F_3 upon Δh , the calculations described in steps 1 to 39 have been carried out on the schematic eye of Le Grand (Bennett and Rabbetts, 1989), the input parameters of which are shown in table 4.3. The distance of the object light source, d_s , giving rise to Purkinje images I, II and IV is taken to be 500mm. Values for relative Purkinje image heights h_1 , h_2 and h_4 are those calculated by Bennett and Rabbetts (1984).

Parameter	Value
F_{sp}	-0.01 D
v	0 m
r_1	0.0078 m
h_1	1
h_2	0.821
h_4	-0.762
d_s	0.5 m
d_1	0.00055 m
d_2	0.00305 m
d_3	0.00400 m
d_4	0.01660 m
n_1	1.0000
n_2	1.3771
n_3	1.3374
n_4	1.42
n_5	1.336

Table 4.3 Input Parameter for the schematic eye of Le grand (Bennett and Rabbetts, 1984)

The actual value of F_3 for this schematic eye is 8.10 D. Table 4.4 shows the effect that higher and lower initial values of F_3 have upon the sign of Δh .

Parameter		Values		
F_1	(step 1)	48.35 D		
F_{1c}	(step 2)	-256.41 D		
m_1	(step 3)	0.00774		
m_2	(step 4)	0.00635		
d_1'	(step 5)	0.000407 m		
F_{2c}	(step 6)	-312.71 D		
r_2'	(step 7)	0.006396 m		
r_2	(step 8)	0.0065 m		
F_2	(step 9)	-6.11 D		
F_3	(step 10)	7 D	8.10 D	9 D
L_1	(step 11)	-0.01 D	-0.01 D	-0.01 D
L_1'	(step 12)	48.34 D	48.34 D	48.34 D
L_2	(step 13)	49.29 D	49.29 D	49.29 D
L_2'	(step 14)	43.18 D	43.18 D	43.18 D
L_3	(step 15)	47.90 D	47.90 D	47.90 D
L_3'	(step 16)	54.90 D	56.00 D	56.90 D
L_4	(step 17)	64.95 D	66.50 D	67.76 D
L_4'	(step 18)	80.48 D	80.48 D	80.48 D
F_4	(step 19)	15.53 D	14.00 D	2.72 D
r_4	(step 20)	-0.00540 m	-0.00600 m	0.00660 m
L_1	(step 21)	355.00 D	355.00 D	355.00 D
L_1'	(step 22)	348.00 D	346.90 D	346.00 D
L_2	(step 23)	194.02 D	193.68 D	193.40 D
L_2'	(step 24)	200.10 D	199.78 D	199.50 D
L_3	(step 25)	185.31 D	185.02 D	184.79 D
L_3'	(step 26)	136.97 D	136.67 D	136.43 D
A_1mA_4	(step 27)	0.00730 m	0.00732 m	0.00733 m
L_1	(step 28)	-1009.54 D	-709.15 D	-545.27 D
L_1'	(step 29)	-1016.54 D	-717.26 D	-554.27 D
L_2	(step 30)	771.12 D	1128.23 D	2099.28 D
L_2'	(step 31)	777.23 D	1134.34 D	2105.38 D
L_3	(step 32)	593.11 D	780.66 D	1143.69 D
L_3'	(step 33)	554.77 D	732.32 D	1095.34 D
A_1mC_4	(step 34)	0.00184 m	0.00137 m	0.00091 m
r_4'	(step 35)	-0.00546 m	-0.00595 m	-0.00642 m
F_{4c}	(step 36)	365.94 D	336.07 D	311.69 D
m_4	step 37)	-0.00542 m	-0.00590 m	-0.00636 m
$h_4(\text{estimate})$	(step 38)	-0.700	-0.762	-0.822
Δh	(step 39)	-0.062	0.000	+0.060

Table 4.4 Effect of variation of F_3 upon Δh .

Table 4.2 clearly indicates that if the initial value of F_3 is too low then Δh will be negative; if it is too high then Δh will be positive. The amount by which F_3 is incrementally raised or lowered then depends upon the accuracy required. The author requires calculation of the crystalline lens radii to the nearest ± 0.01 mm which is achieved by altering F_3 in 0.01D increments.

The iteration routine then proceeds during which time Δh becomes successively smaller in value. The author finds that when F_3 is within ± 0.01 D of the true value, Δh does not exceed ± 0.0005 units. At this point, the iteration routine ceases.

4.4.3 Meridional Analysis

Having calculated the anterior and posterior corneal and lens surface powers along the 180° , 90° , 45° and 135° meridians as described in section 4.4.2, multi-meridional analysis was automatically applied to this data in order to generate surface powers in spherocylindrical form. The equations adopted in the computing scheme were originally derived by Long (1974).

The computing scheme was written for a BBC microcomputer by Armstrong (1991). This program was then adapted for the Apple Macintosh computer for the purposes of the present study (appendix A.2).

Meridional analysis is carried out for meridional power data relating to the refractive error followed by the anterior corneal surface, the posterior corneal surface, the anterior lens surface and finally the posterior lens surface. The multi-meridional analysis computing scheme of Long (1974) involves the equation :

$$F_{xq} = F_s + F_c \cdot \cos^2 (q - a) \quad (55.A_2)$$

where F_{xq} is the measured power with axis at q , F_s is the sphere power, F_c is the cylinder power and a is the cylinder axis. However, the meridional calculations

described in section 4.4.2 yield powers along power meridians. The power meridian is simply perpendicular to the power axis. Therefore, the program changes the power recorded along the 180° meridian to power at axis 90° and so on for the other meridians.

Before saying anything else about the computer program, it is necessary to describe the basis of the computing scheme. To start with, section 4.4.2 provides values of F_{xqi} (notional meridional power) and q_i (meridian axis - after conversion) in each meridian, i . The value of i varies from 1, ... , M where M denotes the number of meridians being considered. The program needs to determine F_S (sphere), F_C (cylinder) and a (cylinder axis) such that $F_S + F_C \cdot \cos^2(q - a)$ is as close as possible to F_{xqi} for all values of i . This is achieved by means of a least squares fit. Long (1974) described how this could be carried out. First of all, F_{xq} can be rewritten in the form:

$$F_{xq} = A + B\sin 2q + C\cos 2q. \quad (56.A_2)$$

where :

$$A = F_S + 0.5 F_C$$

$$B = 0.5 F_C \sin 2a$$

$$C = 0.5 F_C \cos 2a$$

Long (1974) explained that this forms the function :

$$h = \sum_{i=1}^M [F_{xqi} - F_S - F_C \cos^2(q - a)]^2 \quad (57.A_2)$$

and that by applying the minimizing condition described below :

$$\partial h / \partial A = \partial h / \partial B = \partial h / \partial C = 0 \quad (58.A_2)$$

a matrix equation is derived :

$$WU = V. \quad (59.A_2)$$

where W is a symmetric 3 x 3 matrix, the components of which are :

$$W_{11} = M \quad (60.A_2)$$

$$W_{22} = \sum_{i=1}^M \sin^2 2q_i \quad (61.A_2)$$

$$W_{33} = \sum_{i=1}^M \cos^2 2q_i \quad (62.A_2)$$

$$W_{12} = W_{21} = \sum_{i=1}^M \sin 2q_i \quad (63.A_2)$$

$$W_{13} = W_{31} = \sum_{i=1}^M \cos 2q_i \quad (64.A_2)$$

$$W_{23} = W_{32} = \sum_{i=1}^M \sin 2q_i \cos 2q_i \quad (65.A_2)$$

V is a column vector, the components of which are :

$$V_1 = \sum_{i=1}^M F_{xq_i} \quad (66.A_2)$$

$$V_2 = \sum_{i=1}^M F_{xq_i} \sin 2q_i \quad (67.A_2)$$

$$V_3 = \sum_{i=1}^M F_{xq_i} \cos 2q_i \quad (68.A_2)$$

U is also a column vector in which :

$$U_1 = A$$

$$U_2 = B$$

$$U_3 = C$$

Matrix W is inverted to find column vector U so that :

$$U = W^{-1}V \quad (69.A_2)$$

This yields A, B and C which, in turn, yield F_S , F_C and a.

The program commences by calculating the components of matrix W (W_{11} to W_{33}) and column vector V (V_1 to V_3). Next, inversion of matrix W (W^{-1}) is carried out which involves several steps :

(i) **Form transpose matrix (W^T)** - in actual fact, matrix W^T is identical to the original matrix W due to the fact that W is symmetrical.

(ii) **Replace components of W^T with their respective cofactors to produce an adjoint or adjugate matrix (W^*)** - Calculation of the cofactors of components W_{11} to W_{33} is performed. A cofactor of a particular

component is the minor of that component together with its associated sign. The minor is determined by deleting the row and column passing through the component in the 3x3 matrix. What remains is a 2x2 matrix, the components of which constitute the minor. The associated sign, + or -, depend upon the position of the original component in the 3 x 3 matrix. It is in this manner that the cofactors of components W_{11} to W_{33} , shown below, were derived :

$$W_{11}\text{cofactor} = + \{(W_{22} \cdot W_{33}) - (W_{23} \cdot W_{32})\} \quad (70.A_2)$$

$$W_{21}\text{cofactor} = - \{(W_{12} \cdot W_{33}) - (W_{13} \cdot W_{32})\} \quad (71.A_2)$$

$$W_{31}\text{cofactor} = + \{(W_{12} \cdot W_{23}) - (W_{13} \cdot W_{22})\} \quad (72.A_2)$$

$$W_{12}\text{cofactor} = - \{(W_{21} \cdot W_{33}) - (W_{23} \cdot W_{31})\} \quad (73.A_2)$$

$$W_{22}\text{cofactor} = + \{(W_{11} \cdot W_{33}) - (W_{13} \cdot W_{31})\} \quad (74.A_2)$$

$$W_{32}\text{cofactor} = - \{(W_{11} \cdot W_{23}) - (W_{13} \cdot W_{21})\} \quad (75.A_2)$$

$$W_{13}\text{cofactor} = + \{(W_{21} \cdot W_{32}) - (W_{22} \cdot W_{31})\} \quad (76.A_2)$$

$$W_{23}\text{cofactor} = - \{(W_{11} \cdot W_{32}) - (W_{12} \cdot W_{31})\} \quad (77.A_2)$$

$$W_{33}\text{cofactor} = + \{(W_{11} \cdot W_{22}) - (W_{12} \cdot W_{21})\} \quad (78.A_2)$$

(iii) **Calculation of the determinant of matrix W^*** - The determinant of matrix W^* , $|W|$, is defined as the sum of the products of the components of the first row of W^T with their respective cofactors.

$$|W| = (W_{11} \cdot W_{11}\text{cofactor}) + (W_{21} \cdot W_{21}\text{cofactor}) + (W_{31} \cdot W_{31}\text{cofactor})$$

(iv) **Calculation of W^{-1}** - This is carried out by dividing matrix W^* by its determinant so that :

$$W^{-1} = 1 / |W| \cdot W^* \quad (78.A_2)$$

It follows that column vector U becomes :

$$U = 1 / |W| \cdot W^* \cdot V \quad (79A_2)$$

Components U_1 to U_3 are now found by multiplication as shown below :

$$U_1 = \{(W_{11}\text{cofactor} \cdot V_1) + (W_{21}\text{cofactor} \cdot V_2) + (W_{31}\text{cofactor} \cdot V_3)\} / |W| \quad (80.A_2)$$

$$U_2 = \{(W_{12}\text{cofactor} \cdot V_1) + (W_{22}\text{cofactor} \cdot V_2) + (W_{32}\text{cofactor} \cdot V_3)\} / |W| \quad (81.A_2)$$

$$U_3 = \{(W_{13}\text{cofactor} \cdot V_1) + (W_{23}\text{cofactor} \cdot V_2) + (W_{33}\text{cofactor} \cdot V_3)\} / |W| \quad (82.A_2)$$

As mentioned before, $A = U_1$, $B = U_2$ and $C = U_3$. These are solved to find F_S , F_C and a as shown below :

$$\text{Cylinder axis, } a = \tan^{-1} (B / C) / 2 \quad (84.3A_2)$$

$$\text{Cylinder power, } F_C = 2C / \cos 2a \quad (84.A_2)$$

$$\text{Sphere power, } F_S = A - 0.5F_C \quad (85.A_2)$$

The sphero-cylindrical results are expressed in minus-cylinder form. Occasionally, the program generates a negative cylinder axis in which case 180° is added to it. Finally, a print out of the sphero-cylindrical results for refractive error along with the anterior and posterior surfaces of the corneal and crystalline lens. (For program list see appendix A.2).

4.5 Calculation of the Ocular Component Contributions to Residual Astigmatic Power.

This section describes the application of astigmatic decomposition and vergence analysis to determine the ocular components contributions to residual astigmatic power.

4.5.1 Astigmatic Decomposition

Astigmatic decomposition was first introduced by Humphrey in 1977, as a method of remote subjective refraction employing continuously variable sphero-cylindrical correction in the Humphrey Vision Analyser. Following that, Bennett (1977) mathematically explained the method and eased its understanding. Further he demonstrated its statistical application to astigmatic prescriptions (Bennett, 1984).

Astigmatic decomposition is a vector method of analysis. It works on the basis that any given cylinder (C) of axis (\emptyset) is the resultant of two components, C_0 at axis 0° (orthogonal) and C_{45} at axis 45° (oblique). The combined effect of any number of

obliquely crossed cylinders may then be determined by decomposing each of the given cylinders into these components. By this means, the components of one cylinder may be added to or subtracted from the next, as appropriate, followed by re-conversion to orthodox notation to give the resultant cylinder and axis (Barnes, 1984; Bennett, 1984). The required equations arise from the construction shown in Figure 4.9 (Bennett and Rabbetts, 1984). Line OA represents C_0 and AR represents C_{45} . This method is based upon conventional graphical techniques which require that \emptyset is doubled. Therefore AR is at right-angles to OA. The length OR represents the resultant cylinder, its axis being half the angle AOR. From this diagram it follows that the orthogonal and oblique components are calculated using equations 1 and 2.A₃.

$$C_0 = C \cos 2\emptyset \quad (1.A_3)$$

$$C_{45} = C \sin 2\emptyset \quad (2.A_3)$$

and may be re-converted to a cylinder and axis using equations 4.3 and 4.A₃ (add 180° to \emptyset if it turns out to be negative).

$$C = + \sqrt{(C_0^2 + C_{45}^2)} \quad (3.A_3)$$

$$\emptyset = \arctan\{(C - C_0) / C_{45}\} \quad (4.A_3)$$

As an example of how astigmatic decomposition may be applied to residual astigmatic power (RAP), suppose the corneal astigmatic power (CAP) is +3.00 DC axis 180° and the ocular astigmatic power (OAP) is +2.50 DC axis 175°. Subtraction of CAP components ($CAP_0 = +3.00$ DC, $CAP_{45} = 0.00$ DC) from OAP components ($OAP_0 = +2.46$ DC, $OAP_{45} = -0.43$ DC) yields the required RAP components ($RAP_0 = -0.54$ DC, $RAP_{45} = -0.43$ DC). After re-conversion to orthodox notation RAP is +0.69 DC axis 109.4°.

The problem of statistically analysing cylinder power of varying axes of orientation is also overcome by the use of astigmatic decomposition because statistical comparisons can be made with the components of astigmatic decomposition (C_0 and C_{45}) rather than involving the complications of cylinder axis (\emptyset) which represent the cylindrical nature which cannot be treated statistically (Bennett, 1984). Hence, in this thesis

calculations and comparisons of the residual astigmatism arising from the different ocular components were made possible.

Figure 4.9 below illustrates the graphical method of resolving two cylinders:

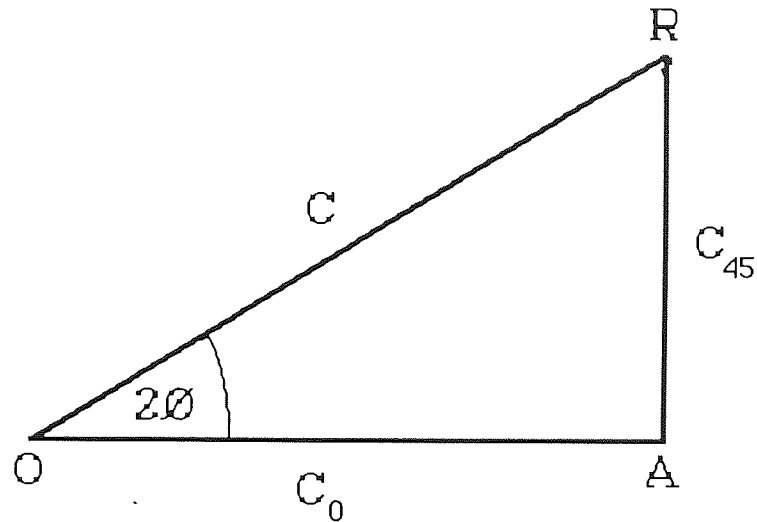


Figure 4.9 Graphical construction based on the combination of two cylinders C_0 and C_{45} at axis 0° and 45° respectively to produce an oblique cylinder of power C at axis θ .

4.5.2 Vergence Analysis

Traditionally, the ocular components of refraction have been analysed in terms of surface powers and linear separations in the eye (Sorsby et al 1961; McBrien and Millodot, 1987; Bullimore, Gilmartin and Royston, 1992; Grosvenor and Scott, 1993; Grosvenor, 1994). A suggestion has been made that refractive effects of these components are better studied in the terms of their vergence contributions (Leary, 1981; Erickson, 1984).

Leary (1981) has suggested that a more direct and appropriate form of analysis is accomplished by tracing wavefronts through the ocular components. The contribution

of each component to ocular refraction is described as percent of the back vertex power of the anterior segment of the eye. The back vertex power is determined by tracing the change in vergence through the eye, beginning with parallel wavefronts impinging on the cornea. The vergence exiting the posterior lens surface is defined as the back vertex power of the anterior segment. Dioptric values are assigned to path lengths by calculating the change in wavefront vergence over the distance involved. However, Leary's method failed to include the effect of vitreous chamber depth, although this ocular dimension is a major determiner of refractive status of the eye (Leary, 1981; Erickson, 1984).

Erickson (1984) suggested another approach to overcome the limitation experienced in Leary's method. He assumed that, if the refractive status of the eye is known, wavefronts can be traced from the far point of the eye rather than infinity. Vergence exiting the posterior lens surface will then incorporate the effect of vitreous chamber depth as contribution to the refractive status. This can also be achieved by assuming a divergent dioptric value to the vitreous chamber and tracing wavefronts to the front of the eye. Components analysis by direct vergence contribution can be done in away similar to that described by Leary (1981). Refracting surfaces contribute according to their refracting power and ocular distances contribute according to the change in vergence over the distance involved. Vitreous chamber depth contributes according to the divergence associated with its optical path (Erickson, 1984).

4.5.3 Computing Scheme

The biometric data derived as described in section 4.4 provided the ocular surface curvatures and axial separations. Ocular component contributions to residual astigmatism were calculated based upon the biometric data derived. These calculations are now described in detail. The symbols and values used were listed in Table 4.2.

Equations (5.A₃) to (21.A₃) were based upon the computing scheme developed by Bennett (1986). Bennett in 1986 has developed a ray tracing method through astigmatic surfaces applicable for deriving each component contribution to the total power of the eye. The method involved two stages: (1) Apply astigmatic decomposition to derive the refractive power of the ocular components. (2) Back trace the light from the retina through each of the components. This required, refractive powers, refractive indices as well as the axial distances of the ocular components.

Astigmatic decomposition was carried out on the spherocylindrical components of the vergence of light striking the i^{th} ocular surface :

$$L_i \text{MRP} = L_i S + L_i C / 2 \quad (5.A_3)$$

$$L_i C_0 = L_i C \cdot \cos(2 \cdot L_i A) \quad (6.A_3)$$

$$L_i C_{45} = L_i C \cdot \sin(2 \cdot L_i A) \quad (7.A_3)$$

Astigmatic decomposition was also carried out on the spherocylindrical components of the i^{th} ocular surface :

$$F_i \text{MRP} = F_i S + F_i C / 2 \quad (8.A_3)$$

$$F_i C_0 = F_i C \cdot \cos(2 \cdot F_i A) \quad (9.A_3)$$

$$F_i C_{45} = F_i C \cdot \sin(2 \cdot F_i A) \quad (10.A_3)$$

This procedure overcame the frequent lack of coincidence between the cylinder axes of light vergences and ocular surfaces. The vergence of light after refraction by the i^{th} ocular surface was calculated using the well known general formula $L' = L + F$.

Hence :

$$L_i' \text{MRP} = L_i \text{MRP} + F_i \text{MRP} \quad (10.A_3)$$

$$L_i' C_0 = L_i C_0 + F_i C_0 \quad (12.A_3)$$

$$L_i' C_{45} = L_i C_{45} + F_i C_{45} \quad (13.A_3)$$

In order to calculate the change in vergence (effectivity) as light passed from one ocular surface to the next, it was necessary to consider the vergence of light separately in its principal meridians. This required conversion of the vergence L' to spherocylindrical form :

$$L_i' C = \sqrt{(L_i' C_0)^2 + (L_i' C_{45})^2} \quad (14.A_3)$$

$$L_i' S = L_i' \text{MRP} - (L_i' C / 2) \quad (15.A_3)$$

$$L_i' A = \tan^{-1}\{(L_i' C - L_i' C_0) / L_i' C_{45}\} \quad (16.A3)$$

$$L_i' S+C = L_i' S + L_i' C \quad (17.A3)$$

Here, $L_i' S$ and $L_i' S+C$ are vergences in the principal meridians. The vergence of light striking the next surface was then calculated using the well known general effectivity relationship $L_x = L_o / \{1 - (d/n) L_o\}$ where L_x and L_o are vergences at two points O and X separated by a distance d. Hence:

$$L_{i+1}S = L_i' S / \{1 - (d_i/n_i)L_i' S\} \quad (18.A3)$$

$$L_{i+1}S+C = L_i' S+C / \{1 - (d_i/n_i)L_i' S+C\} \quad (19.A3)$$

The cylinder and axis of vergence L_{i+1} is then :

$$L_{i+1}C = L_iS+C - L_iS \quad (20.A3)$$

$$L_{i+1}A = L_i' A \quad (21.A3)$$

Equations 22 - 25.A3 were used to the calculate astigmatic contributions of ocular surfaces and intraocular distances towards residual astigmatic power. These equations were added to the computing scheme developed by Bennett (1986) for the purposes of the present study. The astigmatic contribution of ocular surfaces as already derived from calculations described in section 4.4 was simply equal to F_iC axis F_iA . The astigmatic contribution of intraocular distance (effectivity) was equal to the difference between the vergences of light before and after traversing that intraocular distance (i.e $L_{i+1} - L_i'$). Equation (21.A3) indicates that effectivity brings about a change in the size of the cylindrical component of vergence whilst the cylinder axis orientation remains unchanged. Hence :

$$d_i C = L_{i+1}C - L_i'C \quad (22.A3)$$

$$d_i A = L_{i+1}A \quad (23.A3)$$

Here, the astigmatic contribution of intraocular distance d_i was denoted by d_iC axis d_iA . Although cylinders and axes are more meaningful in ophthalmology and optometry, they do not lend themselves to statistical analysis. Therefore, it was also necessary to express the astigmatic contributions of F_i and d_i in terms of orthogonal and oblique cylindrical components (C_0 and C_{45}), after astigmatic decomposition, which could be statistically analysed (Bennett, 1984). This was carried out with equations 9-10.A3 for F_i . and equations (24-25.A3) for d_i .

$$d_i C_0 = d_i C \cdot \cos(2 \cdot d_i A) \quad (24.A_3)$$

$$d_i C_{45} = d_i C \cdot \sin(2 \cdot d_i A) \quad (25.A_3)$$

Equations (5 to 25.A₃) were used for all four ocular surfaces and their respective axial separations. For program list see appendix A.3.

4.6 Determination of Random Experimental Errors involved in the Calculation of Meridional Surface Powers

The influence of random independent errors of each measurement on the errors propagated in the computed anterior and posterior corneal and lens surface meridional powers (section 4.4.2) is considered in this section.

The general approach adopted was based upon that of Ludlam, Wittenberg and Rosenthal (1965). Briefly, the level of uncertainty of each measurement was gained from the distribution of repeat measurements made on one occasion using the instrument chosen to make that measurement. This involved calculating the standard deviation of the mean for the repeat measurements made. The level of uncertainty was then taken to be equal to two standard deviations (representing 95% of the distribution of repeat measurements). Ludlam et al (1965) determined the influence of measurement uncertainties on calculated ocular components by carrying out differentiation of Sorsby's equations (Sorsby et al, 1961) of photographic ophthalmophakometry. This resulted in a series of differentials describing the direction and order of magnitude of all measurement uncertainties involved with a given ocular component. Multiplication of the differentials by their respective levels of uncertainty gave the magnitude of random independent errors for specified levels of experimental uncertainty. As the resulting random independent errors had an equal probability of occurring in either a positive or a negative direction, the standard deviation for a calculated ocular component was calculated as the square root of the sum of the squares of the independent errors (the root mean square, RMS, error).

Differentiation was readily applied to Sorsby's equations (Ludlam et al, 1965). However, the calculations described in section 4.4.2 were complicated by the fact that the final results were obtained after an iterative loop. It was therefore difficult to apply differentiation to determine the experimental errors involved in this process. In actual fact differentiation is only a mathematical short cut for a graphical means of examining experimental errors. The graphical method simply involves altering individual parameters by known amounts and observing the changes which arise in the final calculated results. The gradients of the graphs describing the changes exhibited by the calculated results in response to changes in each parameter are equivalent to the differentials derived by Ludlam et al (1965) as mentioned in the previous paragraph.

A computer program was therefore written (appendix A.4) which was based on the graphical method. Calculation of meridional surface powers was carried as described in section 4.4.2 but the program was designed to repeat calculations after raising and lowering each of the entered measured biometric parameters, consecutively, by their respective measurement uncertainties. Averages were taken of the magnitude of errors exhibited by calculated meridional surface powers when each of the biometric measurements are raised or lowered by their estimated experimental uncertainties. These averaged values were squared and added to errors derived in the same manner for all of the other biometric measurements upon which each calculated meridional surface power depended. The square root of the sum of the errors (RMS error) for each meridional surface power is then calculated. For program list see appendix A.4.

4.7 Determination of Random Experimental Errors involved in the Calculation of Sphero-cylindrical Results

This program (appendix A.5) was designed to determine the influence of random independent errors associated with the estimated meridional surface powers, these

errors as described in section 4.6, calculated on the errors propagated in the computed surface spherocylindrical results. Calculation of spherocylindrical surface results involved meridional analysis as described in section 4.4.3. However the procedure was repeated after raising and lowering each of the entered meridional surface powers consecutively by their respective R.M.S errors (calculated as described in section 4.6). This was followed by calculation of R.M.S errors for the spherocylindrical results adopting the procedure described in section 4.6.

4.8 Calculation of Purkinje Image Positions, Ratios and Heights

This program (appendix A.6) was written to provide a first order (paraxial) approximation of the positions, ratios and heights of Purkinje images I, II, III and IV. The input data required were the surface curvatures and axial separations of any four surfaced schematic eye in addition to the height and position (in front of the anterior corneal surface vertex) of the light source giving rise to the Purkinje images. Purkinje image positions represent their respective distances from the anterior corneal surface vertex. Purkinje image ratios (II/I, III/I and IV/I) are also calculated along with the heights of each Purkinje image above or below the optic axis. The computing scheme adopted was based upon that outlined by Bennett and Rabbetts (1984) and could be used to examine systematic errors which may influence the determination of surface curvature from Purkinje image measurements. The program allowed the user to decide whether or not the refractive indices were defaulted to those of Le Grand's schematic eye (Bennett and Rabbetts, 1984).

In fact, the program was not used in this thesis but has been included as it may be of use to the reader involved in this field of research.

The symbols used follow those adopted in section 4.4.2.

(i) Anterior Corneal Surface Purkinje image I

The program used equations 1 and 2.A₆ to calculate the dioptric (F_1) and catoptric (F_{1c}) powers of the anterior corneal surface:

$$F_1 = (n_2 - n_1) / r_1 \quad (1.A_6)$$

$$F_{1c} = (-n_1 - n_1) / r_1 \quad (2.A_6)$$

Object (L) and image (L') vergences of light arising from the object light source and being reflected by the anterior corneal surface were calculated using equations 3 and 4.A₆ see also Figure 4.1.

$$L = n_1 / -d_s \quad (3.A_6)$$

$$L' = L + F_{1c} \quad (4.A_6)$$

The position of Purkinje image I (l') was calculated using equations 5 and 6.A₆.

$$l' = -n_1 / L' \quad (5.A_6)$$

The magnification of Purkinje image I (m_1) was then calculated using equation 6.A₆.

$$m_1 = L / L' \quad (6.A_6)$$

Finally the height of Purkinje I (h_1) was obtained by multiplying the original object height (h) by the image magnification (m_1):

$$h_1 = h \cdot m_1 \quad (7.A_6)$$

The calculated height of Purkinje image I, is in millimetres.

(ii) Posterior Corneal Surfaces Purkinje image II

The dimensions of the Purkinje image II were calculated making use of the equivalent mirror theorem (section 4.4.2.ii). The calculation of the object (L) and image (L') vergences and image distance (l') of an imaginary ray of light arising from the vertex of the posterior corneal surface (which was treated as the object), traversing the

corneal media and refracted by the anterior corneal surface was made as follows (see also Figure 4.3.).

$$L = n_2 / d_1 \quad (8.A_6)$$

$$L' = L - F_1 \quad (9.A_6)$$

$$l' = n_1 / L' \quad (10.A_6)$$

The sign of F_1 was reversed as the imaginary ray was being traced out of the eye. The calculated image distance (l') provided the position of the equivalent mirror vertex distance. In later stages of computation this was denoted A_1mA_2 as shown below:

$$A_1mA_2 = l' \quad (11.A_6)$$

The centre of curvature of the equivalent mirror was determined in much the same way. In this case, the calculation the object (L) and image (L') vergence and image distance (l') of an imaginary ray of light arising from the centre of curvature of the posterior corneal surface (an object distance equal to $d_1 + r_2$), traversing the corneal media and refracted by the anterior corneal surface was calculated s as follows:

$$L = n_2 / (d_1 + r_2) \quad (12.A_6)$$

$$L' = L - F_1 \quad (13.A_6)$$

$$l' = n_1 / L' \quad (14.A_6)$$

The calculated image distance (l') provided the position of the equivalent mirror centre of curvature (A_1mC_2).

$$A_1mC_2 = l' \quad (15.A_6)$$

The radius of the equivalent mirror was determined by simply subtracting the position of its vertex from that of its centre of curvature.

$$r_2' = A_1mC_2 - A_1mA_2 \quad (16.A_6)$$

The catoptric power (F_{2c}) of the equivalent mirror was:

$$F_{2c} = (-n_1 - n_1) / r_2' \quad (17.A_6)$$

The object (L) and image (L') vergences of light arising from the object light source and being reflected by the posterior corneal surface equivalent mirror were calculated using equations 18 and 19.A₆ (see also Figure 4.4).

$$L = n_1 / -(d_s + A_1mA_2) \quad (18.A_6)$$

$$L' = L + F_{2c} \quad (19.A_6)$$

The position of Purkinje image II (I') relative to the anterior corneal vertex was calculated using equation 20.A6a.

$$I' = (-n_1 / L') + A_1 m A_2 \quad (20.A_6)$$

The magnification of Purkinje image II (m₁) was calculated using equation 21.A6.

$$m_2 = L / L' \quad (21.A_6)$$

Finally the ratio (II/I) of Purkinje image II was found using equation 22.A6.

$$\text{Purkinje image II ratio} = m_2 / m_1 \quad (22.A_6)$$

Then the height of Purkinje II (h₂) was:

$$h_2 = h \cdot m_2 \quad (23.A_6)$$

Calculation of Purkinje images arising from the crystalline lens surfaces was conducted along the same lines as the posterior corneal surface except that further ray tracing steps were required as progressively more refractive elements lay in front of their respective equivalent mirrors.

(iii) Anterior Lens Surface Purkinje image III .

The dioptric power (F₂) of the posterior corneal surface was calculated in preparation for later calculations using equation 24.A6.

$$F_2 = (n_3 - n_2) / r_2 \quad (24.A_6)$$

A "step along" ray trace (Bennett and Rabbetts, 1984) of an imaginary ray of light arising from the vertex of the anterior lens surface, traversing the anterior chamber, refracted by the posterior corneal surface, traversing the corneal media and refracted by the anterior corneal surface was followed as outlined by equations 25 to 29.A6.

$$L_1 = n_3 / d_2 \quad (25.A_6)$$

$$L_1' = L_1 - F_2 \quad (26.A_6)$$

$$L_2 = L_1' / \{1 + [(d_1 / n_2) \cdot L_1']\} \quad (27.A_6)$$

$$L_2' = L_2 - F_1 \quad (28.A_6)$$

$$l_2' = n_1 / L_2' \quad (29.A_6)$$

The calculated image distance (l₂') provided the position of the anterior lens equivalent mirror vertex. This was denoted A₁mA₃ for the purposes.

$$A_3 = l_2' \quad (30.A_6)$$

The centre of curvature of the equivalent mirror was then determined. Here the anterior lens surface was treated as an object distance equal to $d_2 + r_3$:

$$L_1 = n_3 / (d_2 + r_3) \quad (31.A_6)$$

$$L_1' = L_1 - F_2 \quad (32.A_6)$$

$$L_2 = L_1' / \{1 + [(d_1 / n_2) \cdot L_1']\} \quad (33.A_6)$$

$$L_2' = L_2 - F_1 \quad (34.A_6)$$

$$l_2' = n_1 / L_2' \quad (35.A_6)$$

The calculated image distance (l_2') provided the position of the equivalent mirror centre of curvature (A_1mC_3).

$$A_1mC_3 = l_2' \quad (36.A_6)$$

Equations 37 - 44.A₆ were used to calculate the catoptric properties of the equivalent mirror and the required Purkinje image data in precisely the same manner as carried out for the posterior corneal surface:

Equivalent mirror radius (r_3')

$$r_3' = A_1mC_3 - A_1mA_3 \quad (37.A_6)$$

Equivalent mirror catoptric power (F_{3c})

$$F_{3c} = (-n_1 - n_1) / r_3' \quad (38.A_6)$$

Purkinje image III position (l')

$$L = n_1 / -(d_s + A_3) \quad (39.A_6)$$

$$L' = L + F_{3c} \quad (40.A_6)$$

$$l' = -n_1 / L' \quad (41.A_6)$$

Purkinje image III magnification (m_3)

$$m_3 = L / L' \quad (42.A_6)$$

Purkinje image III ratio

$$m_3 / m_1 \quad (43.A_6)$$

Purkinje image III height (h_3)

$$h_3 = h \cdot m_3 \quad (44.A_6)$$

(iv) Posterior Lens Surface Purkinje image IV

Equations 46- 49A₆ were those used for calculations relating the posterior lens surface and Purkinje image IV. The scheme followed that adopted to anterior lens surface dioptric power (F_3).

$$F_2 = (n_3 - n_2) / r_2 \quad (46.A_6)$$

Equivalent mirror vertex (A_1mA_4):

$$L_1 = n_4 / d_3 \quad (47.A_6)$$

$$L_1' = L_1 - F_3 \quad (47.A_6)$$

$$L_2 = L_1' / \{1 + [(d_2 / n_3) \cdot L_1']\} \quad (48.A_6)$$

$$L_2' = L_2 - F_2 \quad (49.A_6)$$

$$L_3 = L_2' / \{1 + [(d_1 / n_2) \cdot L_2']\} \quad (50.A_6)$$

$$L_3' = L_3 - F_1 \quad (51.A_6)$$

$$l_3' = n_1 / L_3' \quad (52.A_6)$$

$$A_1mA_4 = l_3' \quad (53.A_6)$$

Equivalent mirror centre of curvature (A_1mC_4)

$$L_1 = n_4 / (d_3 + r_4) \quad (54.A_6)$$

$$L_1' = L_1 - F_3 \quad (55.A_6)$$

$$L_2 = L_1' / \{1 + [(d_2 / n_3) \cdot L_1']\} \quad (56.A_6)$$

$$L_2' = L_2 - F_2 \quad (57.A_6)$$

$$L_3 = L_2' / \{1 + [(d_1 / n_2) \cdot L_2']\} \quad (58.A_6)$$

$$L_3' = L_3 - F_1 \quad (59.A_6)$$

$$l_3' = n_1 / L_3' \quad (60.A_6)$$

$$A_1mC_4 = l_3' \quad (61.A_6)$$

Calculation of required Purkinje image IV data

Equivalent mirror radius (r_4')

$$r_4' = A_1mC_4 - A_1mA_4 \quad (62.A_6)$$

Equivalent mirror catoptric power (F_{4c})

$$F_{4c} = (-n_1 - n_1) / r_4' \quad (63.A_6)$$

Purkinje image IV position (l')

$$L = n_1 / - (d_s + A_4) \quad (64.A_6)$$

$$L' = L + F_{4c} \quad (65.A_6)$$

$$l' = -n_1 / L' \quad (66.A_6)$$

Purkinje image IV magnification (m_4)

$$m_4 = L / L' \quad (67.A_6)$$

Purkinje image IV ratio

$$m_4 / m_1 \quad (68.A_6)$$

Purkinje image IV height (h_4)

$$h_4 = h \cdot m_4 \quad (69.A_6)$$

For program list see appendix A.6.

4.9 Summary

The computing schemes described in this chapter were designed to derive results from biometric data discussed in subsequent chapters of this thesis. Calculations included: (1) notional meridional powers from refractive and keratometric measurements; (2) crystalline lens surface power in the absence of III Purkinje image arising from the anterior lens surface; (3) application of meridional analysis to derive spherocylindrical powers from notional powers calculated along 4 pre-selected meridians; (4) application of stigmatic decomposition and vergence analysis to calculate contributions to residual astigmatism of ocular components with obliquely related cylinder axes and (5) calculation of effect of random experimental errors on the calculated data.

An important conceptual point must be made at this stage. It will be noted that no attempt was made to either measure or calculate the degree of misalignment (tilt or decentration) of any of the ocular surfaces in respect to one another. Such misalignment can contribute to the measurement of astigmatism exhibited by any surface (see section 2.5.5).

Therefore, whilst calculations performed in this study may be used to estimate the astigmatism exhibited by a particular ocular surface, it is not possible to determine the exact contributions that surface toricity or misalignment make towards the astigmatism exhibited by that surface.

The measured and calculated experimental results are to proceed in the following chapters.

CHAPTER FIVE
PRELIMINARY STUDY: MEASUREMENTS OF RESIDUAL
ASTIGMATISM

5.1 Introduction

The results of the preliminary study (introduced in section 3.6.1) aimed at measuring residual astigmatism and its axis of orientation are presented in this chapter. Section 5.2 describes the calculation methods. Calculations were carried out applying the principle of astigmatic decomposition on refractive and keratoscopic data collected from healthy young subjects (see section 3.6 and appendix B1). The principle of astigmatic decomposition overcame the problem of statistically analysing cylinder powers of varying axes of orientation (see section 4.5.1). By these means values of residual astigmatism arising from measurements repeated on two occasions, from right versus left eyes, from males versus females and from different racial groups were compared. Repeatability is covered in section 5.3, population study in section 5.4 and potential errors in section 5.5. Section 5.6 presents the chapter's summary.

5.2 Methods of Calculation

Mean refractive values (appendices B2.1- B2.4) were calculated from five repeat readings taken from each eye and converted to ocular astigmatic power (OAP) ; a straight forward operation as OAP is simply a plus-cylinder in the same axis as the ocular corrective cylinder (see section 2.2). Astigmatic decomposition was then used to derive residual astigmatic power (see section 4.5).

Mean values of anterior corneal curvatures (appendices B3.1- B3.4) were calculated from three repeat readings taken from each eye. Radii were converted to powers, assuming a corneal refractive index of 1.3333. The chosen refractive index makes little difference to calculated cylinder power. For example, Dunne et al (1992) derived maximum (1.3305) and minimum (1.3251) corneal refractive indices calculated to account for the dioptric effects of corneal thickness and the full range of posterior

corneal radii measured in normal eyes. Applying both values to a cornea exhibiting 0.2 mm difference in radii of curvature between principal meridians (roughly equivalent to 1 D of keratometric astigmatism) produced a clinically undetectable cylindrical error (0.02 D). Corneal astigmatic power (CAP) was then derived from the calculated principal corneal powers (see section 2.2). Astigmatic decomposition was applied for the calculation of residual astigmatism (see section 4.5 and appendices B4.1- B4.4).

The RAP axis may be expressed in terms of its departure from the CAP axis. Previous research indicates that the axes of corneal and residual astigmatism tend to be mutually perpendicular. Therefore it seems logical to assess the degree to which this holds true. The value derived, for the want of a better term, may be called the torsion (T) and is calculated as in equation 5.1.

$$T = (\text{ØCAP} - \text{ØRAP}) - 90^{\circ} \quad (5.1)$$

In the example illustrated in (4.5.1), $T = -19.4^{\circ}$. A value of zero would indicate that both axes were mutually perpendicular. Negative or positive values would occur if the separation between both axes was, respectively, less than or greater than 90° .

5.3 Repeatability

One of the most commonly used methods for evaluating the repeatability of measurements in ophthalmic literature is the product-moment correlation coefficient (r). The product-moment correlation coefficient may be used as an indicator of the agreement between the results of two measurements made on two occasions. However, the results of this technique can be misleading (Bland and Altman 1986). (Bland and Altman (1986) stated that: (1) r measure the strength of the relation between two variables, not the agreement between them. A perfect agreement will be

found if the plotted points lie along the line of equality whilst a correlation will arise if they fall along a straight line; (2) a change in the scale of measurement does not affect the level of correlation, but it certainly affects the agreement; (3) a high correlation depends on the range of the sample, if it is wide the correlation will be greater than if it is narrow; (4) the test of significance may show that two methods are related, even if they are not because test of significance is irrelevant to the question of agreement; (5) data which seem to be in poor agreement can produce a high correlation.

Another technique is to estimate the instrument precision by multiplying the standard deviations of the distribution of repeated measures on one occasion by ± 1.96 or ± 2 (Mutti et al, 1992; Zadnik et al, 1992; Rudnicka et al, 1992). However, the precision determined on one occasion is likely to overestimate the repeatability for measurements made on two occasions because the separation in time brings about additional variability from examiner's technique and the quantity being measured. For example, diurnal variations would reduce the repeatability but not affect precision on one occasion.

In the present study, the repeatability was determined by comparing measurements made on two different occasions. The degree of repeatability, or limits of agreement, was taken to be the interval over which 95% of the differences between measurements taken on two occasion lay. This was assumed to be approximately equal to 1.96 multiplied by the standard deviation of that distribution (Mutti et al, 1992; Zadnik et al, 1992; Rudnicka et al, 1992).

Measurements of refraction (section 3.2, appendices B2.1 - B2.4) and anterior corneal curvature (section 3.3, appendices B3.1 - B3.4) were taken on two occasions from the right and left eyes of 20 male subject (see section 3.6.1). Residual astigmatism

(RAP) was calculated from these measurements using the astigmatic decomposition method as described in section 5.2.

The components of astigmatic decomposition (C_0 and C_{45}) were then used to investigate repeatability (see appendices B4.1- B4.4).

Repeatability was determined using the orthogonal (ΔC_0) and oblique (ΔC_{45}) components of residual astigmatism (Table 5. 1).

Element	Bias	Standard Deviation	95% Limit of Agreement
Right Eyes			
Orthogonal, ΔC_0	+0.01D	$\pm 0.37D$	+0.74 to -0.72D
Oblique, ΔC_{45}	-0.03D	$\pm 0.28D$	+0.52 to -0.58D
Left Eyes			
Orthogonal, ΔC_0	+0.09D	$\pm 0.35D$	+0.77 to -0.59D
Oblique, ΔC_{45}	+0.06D	$\pm 0.26D$	+0.57 to -0.45D

Table 5.1. Repeatability of measurements of residual astigmatic power made on two occasions in 20 male subjects.

In this table, the bias refers to the mean difference found between measurements made on two occasions. The standard deviation was that of the bias. In all cases, the calculated bias showed no statistically significant departure from zero (single sample t-tests) at the 95% level. This indicates that a high level of repeatability may be expected when comparing averaged data collected from a sample of eyes. However, the limits of agreement indicate that the repeatability, for some individual eyes, can exceed 0.75D which is greater than expected levels of residual astigmatism. This point is further illustrated by the distribution of differences for measurements of residual astigmatic power (table 5.2) and axis (table 5.3). The level of variability found for repeat axis measures is reflected by repeated estimates of torsion (table 5.4).

Difference	Left Eye	Right Eye
$\pm 0.10D$	45	20
$\pm 0.25D$	80	40
$\pm 0.50D$	85	80
$\pm 1.00D$	95	100

Table 5.2. Cumulative percentage of differences for residual astigmatic power measurements made on two occasions in 20 male subjects.

Difference	Left Eye	Right Eye
$\pm 1^\circ$	5	20
$\pm 5^\circ$	40	40
$\pm 10^\circ$	60	55
$\pm 20^\circ$	85	85

Table 5.3. Cumulative percentage of differences for residual astigmatic power axis measurements made on two occasions in 20 male subjects.

Difference	Left Eye	Right Eye
$\pm 1^\circ$	15	5
$\pm 5^\circ$	40	40
$\pm 10^\circ$	70	55
$\pm 20^\circ$	100	65

Table 5.4. Cumulative percentage of differences for torsion measurements made on two occasions in 20 male subjects.

These tables presented clinically acceptable difference; 80% of the subjects lay within $\pm 0.50D$. However, the axes and the torsion were not showing similar results, that

could be due to the clinically negligible cylindrical powers involved (estimation of the axis of a small cylinder is usually very difficult).

5.4. Population Study

This section considers the results of measurements made on 70 subjects (see section 3.6.1. and appendices B4.1 and B4.3). Table 5. 5 summarised the values of residual astigmatism obtained from the right and left eyes studied. Mean and standard error values are shown for orthogonal and oblique components of residual astigmatism. No statistically significant differences were found for the right and left eyes at the 95% level (Paired t-tests). Table 5.5 also shows calculated mean residual astigmatic powers and axes for both eyes after re conversion to orthodox notation.

Mean \pm standard error	C ₀	C ₄₅	Cylind er	Axis
Right Eye	-0.473 \pm 0.05D	-0.161 \pm 0.04D	0.50D	99.4 ^o
Left Eye	-0.441 \pm 0.05D	-0.130 \pm 0.03D	0.46D	98.2 ^o

Table 5.5. Comparison of residual astigmatism measured in the right and left eyes of 70 subjects.

Frequency distribution graphs are shown for residual astigmatic powers (Figure 5.1), axes (Figure 5.2) and torsion (Figure 5.3).

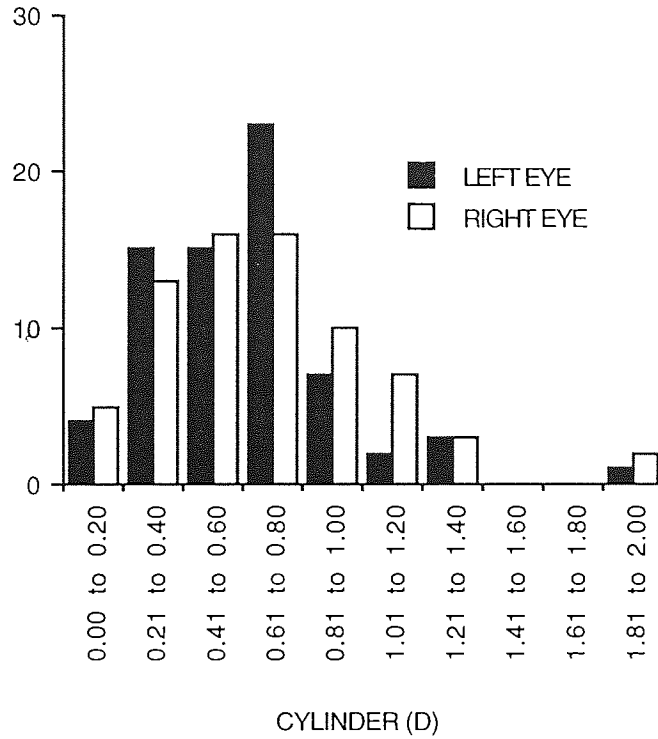


Figure 5.1. Frequency distribution of residual astigmatic powers measured in 70 right and left eyes.

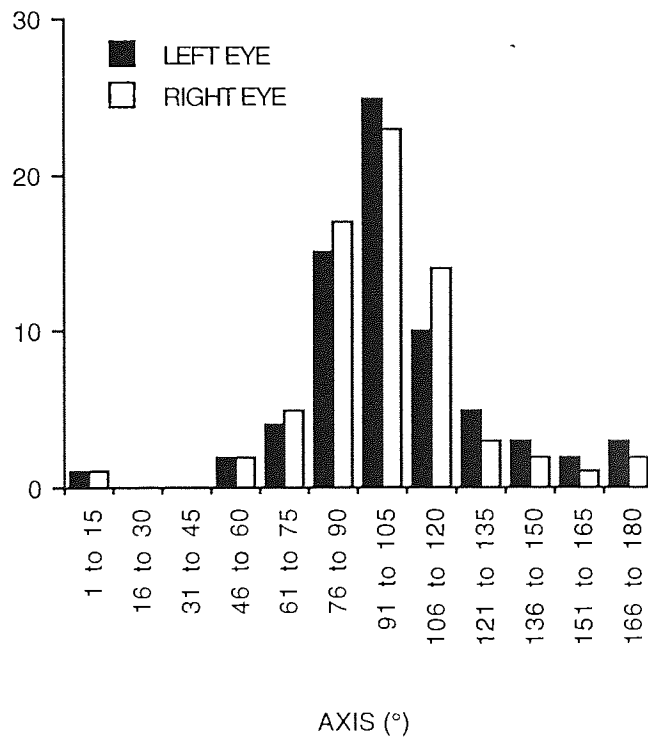


Figure 5.2. Frequency distribution of residual astigmatic power axes measured in 70 right and left eyes.

As for torsion, the residual and corneal astigmatic power axes lay within $\pm 20^\circ$ of being mutually perpendicular in 64% of right eyes and 66% of left eye

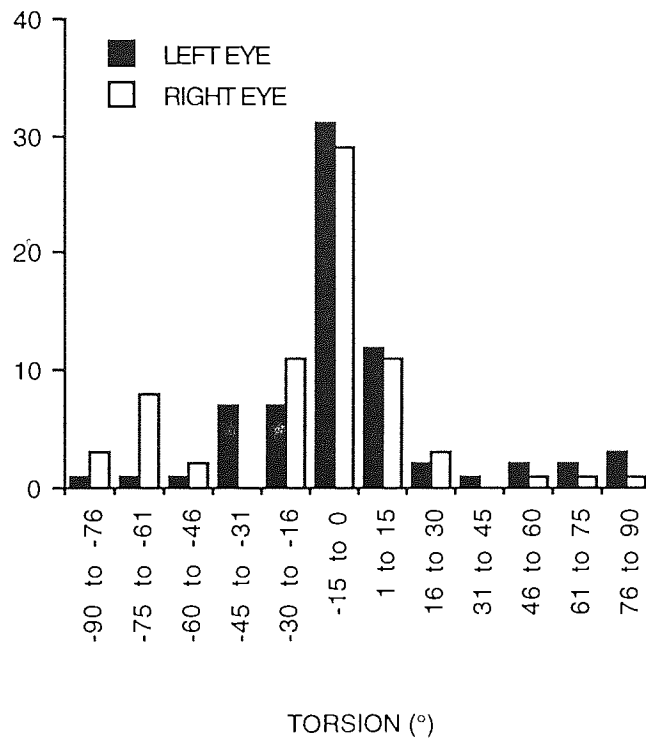


Figure 5.3. Frequency distribution of torsion measured in 70 right and left eyes. Torsion represents the degree to which corneal and residual astigmatic power axes are mutually perpendicular. A value of zero indicates that both axes are mutually perpendicular. Negative or positive values indicate that both axes are, respectively, less than or greater than 90° apart.

The residual astigmatic power was found to vary from 0.03 D to 1.88 D for right eyes and from 0.06 D to 1.86 D for left eyes.

The astigmatic axes may be referred to as being against-the-rule or inverse (axis $90^\circ \pm 20^\circ$), with-the-rule or direct (axis $180^\circ \pm 20^\circ$) or oblique (axis $45^\circ/135^\circ \pm 25^\circ$). Using these criteria, residual astigmatism was found to be against-the-rule in 83% and 66% of right and left eyes, respectively; with-the-rule in 6% and 7% of right and left eyes, respectively; and oblique in 11% and 27% of right and left eyes, respectively.

Tables 5. 6 and 5. 7 compare mean values of residual astigmatism found in the right and left eyes of males versus females (Table 5.6) and Asians versus Caucasians (Table 5.7).

Mean \pm standard error	C ₀	C ₄₅	Cylind er	Axis
Right Eyes				
Males	-0.449 \pm 0.07	-0.169 \pm 0.05	0.48D	100.3°
Females	-0.488 \pm 0.09	-0.149 \pm 0.06	0.51D	98.5°
Left Eyes				
Males	-0.433 \pm 0.06	-0.121 \pm 0.05	0.45D	97.8°
Females	-0.449 \pm 0.07	-0.139 \pm 0.05	0.47D	98.6°

Table 5.6. Comparison of residual astigmatism measured in the right and left eyes of 37 males and 33 females.

Mean \pm standard error	C ₀	C ₄₅	Cylind er	Axis
Right Eyes				
Asians	-0.441 \pm 0.09	-0.130 \pm 0.06	0.46D	98.2°
Caucasians	-0.467 \pm 0.07	-0.179 \pm 0.06	0.50D	100.5°
Left Eyes				
Asians	-0.296 \pm 0.07	-0.168 \pm 0.03	0.34D	104.8°
Caucasians	-0.508 \pm 0.07	-0.110 \pm 0.05	0.52D	96.1°

Table 5. 7. Comparison of residual astigmatism measured in the right and left eyes of 25 Asians and 43 Caucasians.

The results indicate that females exhibited slightly more residual astigmatism compared to males whilst Asians exhibited slightly less residual astigmatism compared to Caucasians. Comparison of orthogonal and oblique cylinder components, however, failed to reveal any statistically significant differences to the 95% level (paired t-tests).

5.5 Potential Errors of the Method

This chapter has described the application of astigmatic decomposition to the calculation of residual astigmatism and its axis of orientation when, as most often occurs, the corneal and refractive cylinder axes are obliquely related. The use of astigmatic decomposition as a means of carrying out statistical analysis of residual astigmatism has also been demonstrated.

An important point regarding the application of astigmatic decomposition to the calculation of residual astigmatism relates to a point made by Bennett (1984) that the axes of astigmatism in the right and left eyes tend to be disposed about a vertical meridian line. This brings about a difference in the sign of the C_{45} component. He added that this may be a disadvantage in studies of right and left eyes as a pair, particularly if mean values are being extracted. He therefore suggested that bilateral symmetry may be introduced by expressing the oblique component of the left eye in terms of C_{135} . This approach was not adopted in the present study as an investigation of the eyes measured revealed that the percentage of individuals exhibiting symmetrically disposed corneal and ocular astigmatic axes was 59% and 51%, respectively. This fell to 26% for residual astigmatism, meaning that Bennett's alternative procedure would only apply to a minority of the eyes measured. In any case, adoption of either procedure leads to exactly the same mean residual astigmatic powers and axes as shown in tables 5.5, 5.6 and 5.7.

Another relevant point of interest is the height above the corneal apex at which the corneal surface is sampled during measurements of corneal radius and refractive error. Differences between sampling heights of keratometry and autorefractometry could lead to systematic errors in residual astigmatism. Precise information as to the sampling heights of the instruments used in this study could not be obtained. However, autorefractometer instructions do indicate that the minimum pupil diameter

required for measurements is 2.9 mm which implies that this is the region over which refractive error is measured. This coincides approximately to a sampling height of 1.5 mm, typically adopted by conventional keratometers.

The question arises as to how the astigmatism measured from an aspheric cornea varies from its apex to a point at any given height from the apex. The keratoscopic study of Guillon et al. (1986) provides data upon which calculations may be based. Their study applied the conic section formula to specify the apical radius (r_o) and asphericity (p) of the corneal surface:

$$2r_o x - px^2 - y^2 = 0 \quad (5.2)$$

where surface intersection co-ordinates refer to distances along the corneal axis (x) and heights above the corneal apex (y). The value of p (a dimensionless unit) determines whether the peripheral corneal surface radius remains constant ($p = 1$), becomes progressively flatter ($p < 1$) or steeper ($p > 1$). By this means corneal profiles along the flattest ($r_o = 7.87$ mm; $p = 0.83$) and steepest ($r_o = 7.70$ mm; $p = 0.81$) principal meridians were found for 110 subjects. Given a corneal refractive index of 1.3333, the corresponding apical powers are 42.35 D and 43.29 D yielding a corneal astigmatic power of 0.94 DC.

According to Bennett and Rabbetts (1989), keratometers and keratoscopes measure sagittal surface radii (r_s) which may be calculated using the following formula :

$$r_s = \{r_o^2 + (1 - p) y^2\}^{1/2} \quad (5.3)$$

For a height of 1.5 mm above the corneal apex the principal sagittal radii become 7.89 mm (42.22D) and 7.73 mm (43.13 D) yielding astigmatism of 0.91DC. At this height, the change in measured corneal astigmatism amounts to only 0.03 DC. For a

height of 3 mm above the corneal apex the sagittal radii become 7.97 mm (41.84 D) and 7.81 (42.67 D) yielding astigmatism of 0.83 DC. Even at this height, the change in corneal astigmatism amounts to only 0.11 DC. As corneal astigmatism varies little for sampling heights up to 3 mm, it is unlikely that differences in the corneal region measured by the keratoscope and autorefractometer will give rise to significant systematic errors in calculated residual astigmatism.

5.6 Summary

In general, the results presented in this chapter support previous findings that the human eye possesses approximately 0.50 D of residual astigmatism (see section 2.4). The proportion of eyes exhibiting against-the-rule ($180^\circ \pm 20^\circ$ inverse) in 83% and 66% of the right left eyes respectively, with-the-rule ($90^\circ \pm 20^\circ$ direct) in 6% and 8% of the right and left eyes respectively and oblique ($135^\circ/45^\circ \pm 25^\circ$) in 25% and 27% of the right and left eyes respectively, these matched what had been reported. An additional finding of the present study is that for over two thirds of the sample the corneal and residual astigmatic power axes were mutually perpendicular to within $\pm 20^\circ$ (64% and 66% of right and left eyes respectively) Further, the level of residual astigmatism exhibited (0.46DC axis 98.2 for Asians RE and 0.50DC axis 99.4 Caucasians RE) is comparable to what had been reported and was not significantly affected by gender or race.

However, whilst the repeatability of estimates of residual astigmatism individual eyes was found to be poor, mean values taken from samples as small as 20 individuals proved to be reasonably repeatable. It is therefore concluded that measurements of residual astigmatism made in this study may only be reliable for averaged data or greater number of repeat measurements.

Chapter 6 takes this study to the next stage by investigating the astigmatism arising from individual ocular surfaces and their axial separations.

CHAPTER SIX

*MAIN STUDY: MEASUREMENTS OF INTERNAL OCULAR
SURFACE ASTIGMATISM*

6.1 Introduction

This chapter considers the results of the main study aimed at measuring internal ocular surface toricity. It is important to remember that the astigmatism exhibited by a particular ocular surface may include contributions from surface toricity as well as tilt and decentration (see sections 2.5.5 and 4.9). Internal ocular surface astigmatism was measured applying multi-meridional ultrasonic ophthalmophakometry. This involved making biometric measurements described in chapter 3 and applying calculations described in chapters 4. Results are averaged in section 6.2 and an investigation is carried out into the precision of the technique by examining the influence of random independent errors from each measurement and the errors propagated in the estimates of ocular surface astigmatism. Section 6.3 considers the repeatability of the method from measurements made on separate occasions. The influence of accommodation on the results is covered in section 6.4, whilst the evaluation of the effect of not measuring corneal thickness is provided in section 6.5. The benefit of using a fourth meridian is considered in section 6.6 and the chapter summary is in section 6.7.

6.2 Averaged Results and Estimated Precisions

Sample details were considered in section 3.6.2. The results of the biometric methods (described in chapter 3) are shown in the appendices B2 (refractive errors), B3 (anterior corneal surface radii), B5 (axial distances) and B6 (Purkinje image heights).

The means and estimated precisions of biometric measurements shown in Table 6.1 were calculated from the above mentioned appendices. Mean values represent the average of the 66 right and left eyes measured. Estimated precisions were calculated by multiplying averaged standard deviations by 2 and represented the level of uncertainty of each measurement as described in section 4.6.

These means and estimated precisions were then entered into the computer program described in section 4.6 (appendix A4) to determine the influence of experimental uncertainty upon the errors propagated in the computed ocular surface meridional powers. The results of this procedure are shown in Table 6.2. Meridional ocular surface power data were, in turn, entered into the computer program described in section 4.7 (appendix A5) to determine the accumulation of experimental errors propagated in the computed ocular surface sphero-cylindrical results. these results are shown in Table 6.3.

Parameter	Meridian	R	L
Anterior Chamber		3.49 ± 0.15	3.39 ± 0.16
Lens thickness		3.55 ± 0.15	3.54 ± 0.12
Vitreous depth		16.62 ± 0.14	16.61 ± 0.18
Refractive error	180°	-1.20 ± 0.18	-0.91 ± 0.14
	90°	-1.20 ± 0.21	-1.10 ± 0.16
	135°	-1.14 ± 0.19	-1.01 ± 0.14
	45°	-1.23 ± 0.20	-1.01 ± 0.15
Anterior Corneal Surface Radius	180°	7.89 ± 0.04	7.89 ± 0.03
	90°	7.79 ± 0.03	7.77 ± 0.03
	135°	7.84 ± 0.03	7.83 ± 0.03
	45°	7.84 ± 0.03	7.85 ± 0.03
Purkinje image I	180°	74.84 ± 0.73	75.15 ± 0.69
	90°	79.14 ± 0.72	79.34 ± 0.79
	135°	84.93 ± 0.69	85.43 ± 0.86
	45°	83.52 ± 0.80	83.92 ± 0.83
Purkinje image II	180°	63.35 ± 0.71	63.76 ± 0.68
	90°	65.49 ± 0.76	65.84 ± 0.82
	135°	71.57 ± 0.81	72.48 ± 0.79
	45°	69.55 ± 0.78	69.89 ± 0.76
Purkinje image VI	180°	-50.84 ± 0.64	-51.43 ± 0.69
	90°	-59.32 ± 0.64	-59.23 ± 0.80
	135°	-61.33 ± 0.63	-60.66 ± 0.90
	45°	-58.73 ± 0.66	-59.36 ± 0.77

Table 6.1 Means and estimated precisions of biometric measurements taken on 66 R and L eyes. All distances and radii are in millimetres. All powers are in dioptres.

Ocular Surface Power	Meridian	Right Eye	Left Eye
Anterior Corneal Surface	180°	47.79 ± 0.24	47.79 ± 0.18
	90°	48.41 ± 0.19	48.53 ± 0.19
	135°	48.10 ± 0.18	48.16 ± 0.18
	45°	48.10 ± 0.18	48.04 ± 0.18
Posterior Corneal Surface	180°	-5.91 ± 0.08	-5.90 ± 0.08
	90°	-6.11 ± 0.08	-6.11 ± 0.09
	135°	-5.98 ± 0.08	-5.95 ± 0.08
	45°	-6.04 ± 0.08	-6.03 ± 0.08
Anterior Lens Surface	180°	10.39 ± 0.84	10.38 ± 0.87
	90°	10.89 ± 0.82	10.80 ± 0.88
	135°	10.68 ± 0.84	10.45 ± 0.88
	45°	10.54 ± 0.82	10.70 ± 0.87
Posterior Lens Surface	180°	15.09 ± 0.32	14.89 ± 0.31
	90°	13.68 ± 0.27	13.73 ± 0.30
	135°	14.17 ± 0.27	14.42 ± 0.34
	45°	14.62 ± 0.30	14.42 ± 0.31

Table 6.2 Calculated means and estimated precisions of meridional ocular surfaces power derived from the averaged biometric data shown in Table 6.1 after the application of the computer program described in section 4.6.

Surface	Eye	Sphere (D)	Cylinder (D)	Axis (°)
Posterior Cornea	R	-6.12 ± 0.13	+0.21 ± 0.22	81.6 ± 31.1
	L	-6.11 ± 0.13	+0.22 ± 0.22	79.6 ± 30.8
Anterior Lens	R	10.36 ± 1.23	+0.52 ± 2.36	7.8 ± 79.1
	L	10.34 ± 1.30	+0.49 ± 2.59	164 ± 78.9
Posterior Lens	R	13.65 ± 0.54	+1.48 ± 0.82	98.9 ± 15.5
	L	13.79 ± 0.54	+1.16 ± 0.90	90.0 ± 20.7

Table 6.3 Calculated means and estimated precisions of sphero-cylindrical ocular surface data derived from the meridional data shown in table 6.2 after application of the computer program described in section 4.7.

Several points can be raised from the results shown in Table 6.3. It is shown that the spherical component is least affected by accumulated experimental errors (± 0.13 to 1.30 DS) followed by the cylinder component (± 0.22 to ± 2.59 DC) and cylinder axis orientation ($\pm 15.5^\circ$ to 79.1°). This appears to be due to use of meridional analysis to generate results in spherocylindrical form as the same trends have been reported for an instrument which derives refractive error by meridional analysis (McBrien & Millodot, 1985). Accumulated experimental errors are loaded onto the anterior crystalline lens surface. This has been reported before and results from the calculation of meridional surface powers in the absence of Purkinje image data from the anterior crystalline lens surface (Dunne and Barnes, 1993).

Not shown in Table 6.3 are the mean spherocylindrical results for the anterior corneal surface of the right (47.79 DS / $+0.62$ DC axis 180°) and left (47.75 DS / $+0.75$ DC axis 4.6°) eyes (see appendices B8.1.1, B8.2.1). It appears that the typical cylinder axis orientations (plus-cylinder) of the anterior corneal and crystalline lens surfaces are horizontal whilst those of the posterior corneal and crystalline lens surfaces are vertical. Further, almost identical amounts of astigmatism occur in right and left eyes.

Tscherning (1924) measured 3 eyes where he found the ocular surfaces to be as follows:

Surface	Horizontal radius (mm)	vertical radius (mm)	Cylinder (D)	Axis orientation
Anterior Cornea	$8.02 = (47.02D)$	$7.94 = (47.49D)$	$+0.47$	W.T.R (direct)
Posterior Cornea	$6.02 = (-7.05D)$	$5.51 = (-7.59D)$	-0.46	A.T.R (inverse)
Anterior Lens	$10.2 = (8.10D)$	$10.1 = (8.18D)$	$+0.08$	W.T.R (direct)
Posterior Lens	$6.17 = (-13.61D)$	$6.13 = (-13.70D)$	-0.09	A.T.R (inverse)

Table 6.4 Tscherning (1924) mean ocular components surface radius of curvature and their ocular powers measurements made in 3 eyes.

However, Tscherning (1924) was not satisfied by the out come of his measurements. He commented on the findings saying that, "*We must not deceive ourselves as to the exactness of these measurements; excepting those of the anterior corneal surface, they are not very exact. In fact the crystalline images are very feeble, and those of anterior surface of the crystalline lens very diffuse, which causes the measurements to become less certain; there are also other sources of errors, such as that made by comparing the surfaces to spherical surfaces*". In spite of that, it prevailed for a long time and still reflects a similar trend to what has been found in this study.

6.3 Repeatability

Repeat measurements were taken in 20 male right and left eyes as explained in sections 3.6.1 and 3.6.2. The repeat data are presented in the appendices B2 (refractive errors), B3 (anterior corneal surface radii), B5 (ultrasonic axial distances), B6 (Purkinje image heights), B7 (ocular surface spherocylindrical power).

The reproducibility of the technique is illustrated in Tables 6.5 to 6.8. Results for data taken from individual eyes are shown first in the form of cumulative percentages of the differences between measurements made on two occasions of spherical components (Table 6.5), cylindrical components (Table 6.6) and cylinder axis orientations (Table 6.7). Results for pooled data are then shown in Table 6.8. Here, the biometric measurements made on each occasion were averaged and used to calculate a set of internal ocular surface sphero-cylindrical components for each occasion.

Cumulative percentages

Difference between readings made on the two occasions	Posterior cornea	Anterior lens	Posterior lens
Right eyes			
± 0.25D	95	20	15
± 0.50D	100	35	60
± 0.75D		55	90
± 1.00D		80	95
>±1.00D		100	100
Left eyes			
± 0.25D	90	35	45
± 0.50D	100	70	80
± 0.75D		75	85
± 1.00D		85	90
>±1.00D		100	100

Table 6.5 Cumulative percentages of the differences between internal ocular surface spherical components calculated for 20 right and left eyes from measurements made on two occasions.

Cumulative percentages

Difference between readings made on the two occasions	Posterior cornea	Anterior lens	Posterior lens
Right eyes			
± 0.25DC	95	20	30
± 0.50DC	100	50	60
± 0.75DC		90	60
± 1.00DC		90	65
>±1.00DC		100	100
Left eyes			
± 0.25DC	80	55	30
± 0.50DC	100	85	70
± 0.75DC		95	90
± 1.00DC		95	90
>±1.00DC		100	100

Table 6.6 Cumulative percentages of the differences between internal ocular surface cylindrical components calculated for 20 right and left eyes from measurements made on two occasions.

Cumulative percentages

Difference between readings made on the two occasions	Posterior cornea	Anterior lens	Posterior lens
Right eyes			
$\pm 5^\circ$	20	20	30
$\pm 10^\circ$	40	40	45
$\pm 15^\circ$	60	45	65
$\pm 20^\circ$	70	55	80
$>\pm 20^\circ$	100	100	100
Left eyes			
$\pm 5^\circ$	30	15	30
$\pm 10^\circ$	60	25	45
$\pm 15^\circ$	75	35	50
$\pm 20^\circ$	75	40	60
$>\pm 20^\circ$	100	100	100

Table 6.7 Cumulative percentages of the differences between internal ocular surface cylinder axis orientations calculated for 20 right and left eyes from measurements made on two occasions.

Ocular Surface	Sphere (D)	Cylinder (D)	Axis (°)
Right Eyes			
<i>Posterior corneal surface</i>			
1st occasion	-6.05	+0.26	78.3
2nd occasion	-6.04	+0.28	77.2
Absolute difference	0.01	0.02	1.1
<i>Anterior lens surface</i>			
1st occasion	10.39	+0.37	1.6
2nd occasion	10.27	+0.64	179.5
Absolute difference	0.12	0.27	2.1
<i>Posterior lens surface</i>			
1st occasion	13.11	+1.33	97.9
2nd occasion	13.12	+1.35	97.7
Absolute difference	0.01	0.02	0.2
Left eyes			
<i>Posterior corneal surface</i>			
1st occasion	-6.10	+0.32	78.8
2nd occasion	-6.08	+0.33	83.0
Absolute difference	0.02	0.01	4.2
<i>Anterior lens surface</i>			
1st occasion	10.00	+0.71	1.8
2nd occasion	9.85	+0.74	4.3
Absolute difference	0.15	0.03	2.5
<i>Posterior lens surface</i>			
1st occasion	13.12	+1.37	91.9
2nd occasion	12.91	+1.50	97.6
Absolute difference	0.21	0.13	5.7

Table 6.8 Internal ocular surface sphero-cylindrical components derived from the pooled data of 20 right and left eyes measured on two occasions.

Although the accumulated experimental errors shown in Table 6.3 were clinically considerable, this method may still be suitable for large samples of eyes (or large numbers of repeat readings made in individual eyes) in which the experimental errors, being random in nature, tend to cancel themselves out. This is supported by the results shown in Tables 6.5 to 6.8. For example, differences for repeat estimates of crystalline lens surface power in individual eyes exceed $\pm 1.00\text{D}$ spherical component in 5 - 20% of cases (Table 6.5), $\pm 1.00\text{D}$ cylindrical component in 5 - 35% of cases

(Table 6.6) and $\pm 20^\circ$ cylinder axis in 20-60% of cases (Table 6.7). However, differences for repeat estimates made from pooled data never exceeded $\pm 0.21\text{D}$ spherical component, $\pm 0.27\text{D}$ cylindrical component and $\pm 5.7^\circ$ cylinder axis (Table 6.8).

One could therefore be reasonably confident about the mean levels of internal ocular astigmatism recorded in Table 6.3.

6.4 Cycloplegic Study

This study was carried out as explained in section 3.6.3, to examine the influence of accommodation on the results. Measurements were taken on 10 left eyes with and without cycloplegia. Biometric data collected under these conditions (shown in appendices B2, B3, B5, B6 and B7) were used to derive ocular surface astigmatism, expressed in spherocylindrical form applying the computer program described in section 4.4 (appendix A2). Table 6.9 shows mean values and estimated precisions of measurements taken.

Parameter	Meridian	No Cyclo	Under Cyclo
Anterior chamber		3.56 ± 0.07	3.73 ± 0.11
Lens thickness		3.71 ± 0.12	3.66 ± 0.11
Vitreous depth		16.54 ± 0.12	16.28 ± 0.20
Refractive error	180°	+0.21 ± 0.12	+0.66 ± 0.13
	90°	+0.04 ± 0.13	+0.45 ± 0.09
	135°	+0.15 ± 0.13	+0.57 ± 0.11
	45°	+0.10 ± 0.13	+0.54 ± 0.13
Anterior corneal radius	180°	7.96 ± 0.02	7.95 ± 0.02
	90°	7.83 ± 0.02	7.84 ± 0.01
	135°	7.90 ± 0.02	7.90 ± 0.03
	45°	7.89 ± 0.02	7.88 ± 0.01
Purkinje image I	180°	113.77± 0.86	114.10 ± 0.58
	90°	138.18± 0.54	138.15 ± 0.70
	135°	147.92± 0.96	148.60 ± 0.78
	45°	133.57± 0.66	133.88± 0.64
Purkinje image II	180°	97.90 ± 0.90	97.58 ± 0.60
	90°	115.97± 0.93	116.52 ± 0.77
	135°	127.03± 0.88	126.73 ± 0.82
	45°	113.72± 0.68	113.94 ± 0.82
Purkinje image IV	180°	-79.12 ± 0.58	-84.79 ± 0.73
	90°	-101.50± 0.83	-107.43 ± 0.82
	135°	-102.67± 0.63	-109.52 ± 0.90
	45°	-96.20 ± 0.53	-101.77 ± 0.71

Table 6.9 Means and estimated precisions of biometric measurements taken on the left eyes 10 male subjects with and without cycloplegia. All distances and radii are in millimetres. All powers are in dioptres.

Table 6.9 shows means and estimated precisions of the biometric measurements made with and without cycloplegia. It is noticeable that the lens was thicker and the anterior chamber shallower for the non-cycloplegic data. Therefore accommodation was not being completely relaxed without cycloplegia. However, paired t-tests revealed no statistically significant differences (to the 95% level) between ultrasonic measurements made under both conditions.

That accommodation was not fully relaxed was also supported by the findings that the non-cycloplegic refractive data (not shown in the table, see appendix B7.3) exhibited relatively less hypermetropia. When paired t-tests was carried out, it was found to be statistically significant ($t = -3.223$, $df = 9$ and $P = 0.010$).

As expected, only very small differences were found for the anterior corneal radii and the heights of Purkinje images I and II. Paired t-test revealed no statistical significant difference (to the 95% level). This finding was clearly due to the lack of corneal involvement in the accommodation process.

The heights of Purkinje IV images were found to be relatively small in the non-cycloplegic data, the difference being statistically significant (99% level) along all four meridians ($180^\circ t = -5.477$, $df = 9$, $P = 0.00$; $90^\circ t = -5.765$, $df = 9$, $P = 0.00$; $135^\circ t = -4.613$, $df = 9$, $P = 0.001$ and $45^\circ t = 6.393$, $df = 9$ and $P = 0.00$ paired t-test). That is again an indication that accommodation was not fully relaxed bringing about steeper lens surface curvature.

The data shown in Table 6.8 were used to calculate the internal ocular surfaces spherocylindrical powers shown in Table 6.9.

Elements compared	Sphere (D)	Cylinder (D)	Axis (°)
<i>Anterior corneal surface</i>			
Non-cycloplegic	48.19	+0.82	88.46
Cycloplegic	48.17	+0.77	89.46
Absolute difference	0.02	0.05	1.00
<i>Posterior corneal surface</i>			
Non-cycloplegic	-5.75	+0.28	120.00
Cycloplegic	-5.77	+0.26	127.78
Absolute difference	0.02	0.02	7.78
<i>Anterior lens surface</i>			
Non-cycloplegic	9.56	+0.77	58.91
Cycloplegic	10.65	+0.65	66.16
Absolute difference	1.09	0.12	7.25
<i>Posterior lens surface</i>			
Non-cycloplegic	14.92	+0.88	126.36
Cycloplegic	14.09	+0.94	125.76
Absolute difference	0.83	0.06	0.6

Table 6.10 Internal ocular surface sphero-cylindrical components derived from the pooled biometric data of 10 left eyes measured with and without cycloplegia.

Table 6.10 shows clearly that, the corneal surfaces data were little effected by cycloplegia, whilst both of the crystalline lens surfaces showed decreased spherical component power under the influence of cycloplegia. When paired t-test was carried out, the spherical components of the anterior lens surfaces were found to be statistically significant ($t = -4.27$, $df = 9$ and $P = 0.002$ and the posterior lens surfaces $t = -4.362$, $df = 9$ and $p = 0.002$) whilst the cylindrical and axes components were not. The anterior lens surface was more effected (1.09D), than the posterior surface (0.83D) and that is due to the accommodative changes (Fletcher, 1951b, 1952; Duke Elder and Abrams, 1970) and accumulated experimental errors loaded onto anterior lens surface (Dunne and Barnes, 1993).

However, clinically negligible differences to the astigmatic cylinders and axes were detected. As these are the elements that influence residual astigmatism, the conclusion

is that cycloplegia has little effect upon ocular surface astigmatism measured using multi-meridional ultrasonic ophthalmophakometry.

6.5 Effect of not Measuring Corneal Thickness

Previous research indicates that the corneal thickness varies from approximately 0.4 to 0.6mm (Olsen and Ehlers, 1984; Royston, 1990).

Failure to account for such variation is likely to have negligible effect upon the calculated surface powers. For example, consider an emmetropic eye which has an anterior corneal radius of 7.8mm, an anterior chamber depth of 3.6mm, a lens thickness of 4mm and a vitreous chamber depth of 16.6mm. Suppose that a light source placed 15mm above the optic axis and 25mm in front of the cornea gives rise to posterior corneal (I : II) and lenticular (I : IV) surface Purkinje image ratios of 0.83 and -0.75, respectively. It then emerges that alteration of corneal thickness by ± 0.1 mm only changes the calculated power of the posterior corneal, anterior lens and posterior lens surfaces by ± 0.03 D, ± 0.02 D and ± 0.01 D respectively. Further, as the same corneal thickness is used to calculate surface powers in all selected meridians, it follows that the calculated surface astigmatism would be effected to a much lesser extent.

6.6 Effect of using Fourth Meridian

This study has been designed to measure ocular components along 4 meridians. The computing programs used give the options of deriving results from 3 or 4 meridians (see sections 4.6, 4.7 and appendices A4 and A5). This opportunity was used to access the differences on the accumulated experimental errors (RMS) using the averaged data of the main study in Tables 6.1 and 6.2. The results of comparing

sphero-cylindrical surface powers and their respective RMS errors calculated for three and four meridians are shown in following table.

Element	Meridian	Sphere	RMS	cylinder	RMS	Axis	RMS
Right eye							
F ₁	3	48.41	±0.19	-0.62	±0.30	90.00	±21.4
F ₁	4	48.41	±0.17	-0.62	±0.31	90.00	±11.5
Difference		0.0	0.02	0.0	0.01	0.0	10.1
F ₂	3	-5.91	±0.07	-0.21	±0.12	171.7	±24.6
F ₂	4	-5.91	±0.07	-0.21	±0.11	171.6	±15.3
Difference		0.0	0.0	0.0	0.0	0.1	9.3
F ₃	3	10.89	±0.91	-0.51	±1.61	94.5	±62.7
F ₃	4	10.88	±0.59	-0.52	±0.94	97.8	±67.5
Difference		0.01	0.32	0.01	0.67	0.33	4.8
F ₄	3	15.12	±0.37	-1.47	±0.46	8.5	±12.5
F ₄	4	15.13	±0.27	-1.48	±0.45	8.9	±7.8
Difference		0.01	0.1	0.01	0.01	0.4	4.7
Left eye							
F ₁	3	48.53	±0.19	-0.74	±0.27	90.0	±16.7
F ₁	4	48.50	±0.16	-0.75	±0.26	94.6	±9.6
Difference		0.03	0.03	0.01	0.01	4.6	7.1
F ₂	3	-5.89	±0.07	-0.24	±0.14	166.2	±21.4
F ₂	4	-5.89	±0.07	-0.22	±0.12	169.6	±14.6
Difference		0.0	0.0	0.02	0.02	3.4	6.8
F ₃	3	10.84	±1.03	-0.50	±1.71	73.2	±66.3
F ₃	4	10.83	±0.63	-0.49	±0.92	74.6	±66.6
Difference		0.01	0.4	0.01	0.79	1.4	0.3
F ₄	3	14.90	±0.29	-1.18	±0.45	174.6	±18.4
F ₄	4	14.95	±0.27	-1.16	±0.44	180.0	±11.1
Difference		0.05	0.02	0.02	0.01	5.4	7.1

Table 6.11 Spherocylindrical surface powers and their respective RMS errors calculated for 3 and 4 meridians using the 66 subject data.

Table 6.11 is reflecting the benefit of using a fourth meridians in the computations of the biometric data. The difference showed up clearly in the axis orientations of all the astigmatic components ranging between $\pm 0.3^\circ$ and $\pm 10.1^\circ$. In the cylindrical components the range was between 0.00 to $\pm 0.79D$ and the least differences were

those arising from the spherical components where it ranged between 0.00 to $\pm 0.40D$. The crystalline lens surfaces were more effected than the corneal surfaces and the anterior lens surface was the one most benefited from the use of fourth meridian.

6.7 Summary

Accumulated experimental errors were loaded onto the anterior crystalline lens surface. This has been reported before and results from use of Purkinje images I, II and IV excluding Purkinje image III (Dunne and Barnes, 1993).

The spherical component was least effected by errors (± 0.07 - 1.03 DS) followed by the cylinder component (± 0.11 - 1.71 DC) and cylinder axis orientation (± 7.8 - 67.5°). This has been reported before (McBrien and Millodot, 1985).

With the possible exception of the posterior corneal surface, accumulated experimental errors were such that this method would only lend itself to studies of individual eyes if a large number of repeat observations were made. Only then would the experimental errors, being random in nature, tend to cancel themselves out.

Utilization of 4 meridians instead of 3 tends to alleviate the effects of accumulated experimental errors to some extent. The effects are most noticeable for cylinder axis orientation followed by cylinder component and spherical component.

It is interesting to note that anterior:posterior corneal radius ratios calculated for the 180° (RE = 0.8504; LE = 0.8517) and 90° (RE = 0.8331; LE = 0.8353) meridians confirm a previous observation (Dunne, Royston and Barnes, 1991; Dunne and Barnes, 1993) that the posterior corneal surface is steeper vertically relative to the anterior corneal surface. This has the effect of greater effective compensation of

anterior corneal surface astigmatism than would occur if the ratios were the same in both meridians (see section 2.5.1.C).

In conclusion the method described in this thesis allows reasonably reproducible estimates of the astigmatism arising from the internal ocular surfaces to be made, as measured along the visual axis, in large samples data. Errors of the technique tend to manifest themselves in the calculated anterior lens surface power.

Asphericity and misalignment (see section 2.55) of the ocular components has been considered to be a major source of discrepancy in the results of ocular biometric measurements (Sheard, 1920; Tscherning, 1924; Ludlam and Wittenberg, 1966; Bennett, 1984; Barnes, et al, 1987; White, 1993). One could argue that surface toricity measured along the visual axis relates to the functional astigmatism experienced at the fovea. In this sense, no matter what the level of surface misalignment, the interest is only in the resulting astigmatism along the visual axis. In other words, rather than considering the apical toricity and of a surface separately, it is only necessary to consider the toricity of that surface at the point of intersection with the visual axis.

Nevertheless the importance of the subject (asphericity and misalignment of ocular component) warrants further study.

Contributions of the internal ocular surfaces and their axial separations towards residual astigmatism (RAP) are to be discussed in chapter 7.

CHAPTER SEVEN
OCULAR COMPONENT CONTRIBUTIONS TO RESIDUAL
ASTIGMATISM

7.1 Introduction

This chapter considers the contributions of the ocular surfaces and their axial separations to residual astigmatism utilizing the computing scheme described in section 4.5 (appendix A5). Section 7.2 investigates the repeatability of the method considering the accumulation of experimental errors in the estimates of ocular surface astigmatism considered in section 6.2. Section 7.3 investigates the influence of the accumulated errors on the computed results considering the noticeable differences in the anterior chamber depth and lens thickness measured with and without cycloplegia in section 6.4. Although the findings of section 6.2 and 6.3 indicted that the data of individual subjects were not that reliable, section 7.4 examines the distributions of ocular components astigmatic contributions to residual astigmatism. A summary of the chapter is in section 7.5.

7.2 Repeatability Study

Whilst section 6.3 considered the repeatability of estimates of ocular surface astigmatism, no evaluation of the astigmatic contribution of the axial distances were carried out. The repeatability of both surface and effectivity are covered in this section.

Repeat measurements were taken in 20 male right and left eyes as described in section 3.6.1 and 3.6.2. The calculated astigmatic contribution of each of ocular component were shown in the appendices B8.1 to 8.6.3. Orthogonal C_0 and oblique C_{45} components of the calculated astigmatic contributions of each ocular component were used to determine estimates of repeatability using the procedure described in section 5.2. Table 7.1 shows the bias, the standard deviation and 95% limits of agreement between repeated estimates of the astigmatic contributions arising from corneal

thickness (d1), posterior corneal surface (F2), anterior chamber depth (d2), anterior lens surface (F3), lens thickness (d3) and posterior lens surface (F4).

Element	Astigmatic component	Bias (D)	Standard deviation	95% limit	of	agreement (D)
Right eyes						
d ₁	C ₀	0.00	±0.01	+0.02	to	-0.02
	C ₄₅	0.00	±0.01	+0.02	to	-0.02
F ₂	C ₀	-0.09	±0.29	+0.47	to	-0.65
	C ₄₅	0.00	±0.19	+0.38	to	-0.38
d ₂	C ₀	+0.01	±0.09	+0.19	to	-0.17
	C ₄₅	0.00	±0.07	+0.14	to	-0.14
F ₃	C ₀	+0.13	±0.88	+1.59	to	-1.85
	C ₄₅	+0.02	±0.50	+1.00	to	-0.96
d ₃	C ₀	-0.04	±0.23	+0.40	to	-0.48
	C ₄₅	-0.05	±0.15	+0.25	to	-0.35
F ₄	C ₀	+0.13	±0.84	+1.76	to	-1.61
	C ₄₅	+0.19	±0.57	+1.30	to	-0.92
Left eyes						
d ₁	C ₀	0.00	±0.01	+0.03	to	-0.03
	C ₄₅	0.00	±0.01	+0.02	to	-0.02
F ₂	C ₀	+0.02	±0.24	+0.49	to	-0.45
	C ₄₅	+0.02	±0.17	+0.36	to	-0.33
d ₂	C ₀	+0.02	±0.07	+0.15	to	-0.11
	C ₄₅	-0.02	±0.06	+0.10	to	-0.12
F ₃	C ₀	-0.21	±0.53	+0.84	to	-1.26
	C ₄₅	-0.20	±0.68	+1.12	to	-1.52
d ₃	C ₀	-0.04	±0.14	+0.23	to	-0.31
	C ₄₅	-0.08*	±0.16	+0.24	to	-0.40
F ₄	C ₀	+0.14	±0.52	+1.16	to	-0.88
	C ₄₅	+0.31*	±0.65	+1.59	to	-0.97

Table 7.1 Repeatability of ocular component astigmatic contributions to residual astigmatism calculated from biometric measurements made on two occasions in 20 subjects. An asterisk besides a value indicates that the bias was statistically significant to the 95% level (single sample t-test). This was only the case for C₄₅ components of d₃ (df = 19; t = - 2.17) and F₄ (df = 19; t = 2.13).

From Table 7.1 it can be seen that the calculated bias for the data of right eyes showed no statistically significant departure from zero (single sample t-test) at the 95% level. For the left eye data, however, a statistically significant difference was found for the repeated estimates of C_{45} relating to d_3 (lens thickness) and F_4 (posterior lens surface power). Nevertheless, the bias calculated for all parameters measured in both eyes fell within ± 0.25 D with the exception of the C_{45} component of F_4 measured in left eyes which only amounted to $+0.31$ D. This indicates that a reasonably high level of repeatability may be expected when comparing averaged data. On the other hand, the limits of agreement shown in Table 7.1 indicate that measurements made in individual eyes are less repeatable, especially for estimates of the astigmatic contributions of both lens surfaces. For this reason, the comparisons between right versus left eyes (Table 7.2) and males versus females (Table 7.3) of the main study are carried out on group averaged data.

7.3 Cycloplegic Study

As previously mentioned in section 3.6.3, this study was carried out to examine the influence of accommodation on the results. Measurements were repeated in 10 left eyes with and without cycloplegia. Ocular component contributions towards residual astigmatism were calculated from each set of biometrics measurements made under those conditions. Calculated data were shown in appendices B8.1 to B8.6.

In table 7.2 the results of all 10 eyes were pooled to give a mean set of results for measurements taken with and without cycloplegia. For both conditions orthogonal (C_0) and oblique (C_{45}) components of astigmatic decomposition were compared using paired t-tests and revealed no statistically difference to the 95% level. Cylinders and axes were also shown for all ocular components astigmatic contributions to give a clear clinical picture. Difference in cylinders never exceeded ± 0.06 D whilst axes differences fell with $\pm 11^\circ$. The conclusion was therefore that cycloplegia had little

effect on the astigmatism exhibited by each ocular component measured using this method.

Component	Cycloplegics	C ₀ Mean	Standard error	C ₄₅ Mean	Standard error	Cylinder (D)	Axis (°)
d ₁	without	+0.021	±0.014		±0.009	+0.02	179.91
	with	+0.019	±0.010	+0.001	±0.012	+0.02	1
F ₂	without	-0.227	±0.216	+0.053	±0.109	+0.23	83.38
	with	-0.162	±0.210	+0.014	±0.135	+0.16	87.51
d ₂	without	+0.067	±0.125	+0.013	±0.056	+0.07	1.32
	with	+0.079	±0.039	+0.007	±0.074	+0.08	8.13
F ₃	without	-0.038	±0.648	-0.373	±0.493	+0.37	132.43
	with	-0.081	±0.425	-0.387	±0.074	+0.40	128.82
d ₃	without	+0.165	±0.125	-0.127	±0.146	+0.21	160.49
	with	+0.138	±0.153	-0.139	±0.178	+0.22	149.46
F ₄	without	-0.591	±0.419	-0.439	±0.501	+0.74	108.25
	with	-0.475	±0.050	-0.491	±0.620	+0.68	112.99

Table 7.2 Comparison of ocular component astigmatic contribution to residual astigmatism calculated from biometric measurements. Made with and without cycloplegia.

7.4 Population Study

The aim of this section was to examine the distribution of ocular components contributions to residual astigmatism. It should be remembered that individual data has been found to be less reliable than pooled data (see sections 6.3 and 7.2). Therefore though it would appear unwise to look at frequency distributions based on unreliable individual data, this approach does at least provide an approximation of the distributions from which mean values arise.

The following tables and histograms were derived from calculated data shown in Appendices B8.1 to B8.6. These calculated data were based upon biometric measurements taken on right and left eyes of 66 subjects.

Component	Eye	C ₀	Standard	C ₄₅	Standard	Cylinder (D)	Axis(°)
		Mean	error	Mean	error		
d ₁	R	+0.021	±0.01	+0.005	±0.01	+0.02	6.7
	L	+0.019	±0.01	+0.002	±0.01	+0.02	3.0
F ₂	R	-0.199	±0.02	+0.044	±0.02	+0.20	83.8
	L	-0.190	±0.03	+0.077	±0.02	+0.21	79.0
d ₂	R	+0.099	±0.01	+0.038	±0.01	+0.11	10.5
	L	+0.075	±0.01	+0.029	±0.01	+0.08	10.6
F ₃	R	+0.313	±0.09	-0.038	±0.07	+0.32	176.5
	L	+0.423	±0.09	-0.118	±0.09	+0.44	172.2
d ₃	R	+0.309	±0.03	+0.061	±0.02	+0.31	5.6
	L	+0.307	±0.03	+0.022	±0.02	+0.31	2.0
F ₄	R	-1.153	±0.10	-0.226	±0.07	+1.17	96.5
	L	-1.156	±0.10	-0.062	±0.07	+1.16	91.5
RAP	R	-0.613	±0.05	-0.129	±0.04	+0.62	95.9
	L	-0.557	±0.04	-0.073	±0.05	+0.56	93.7

Table 7.3 Comparison of ocular component astigmatic contributions to residual astigmatism calculated from biometric measurements in right and left eyes of 66 subjects. A statistically significant difference to the 95% level (unpaired t-test) was found for the C₄₅ components of F₄ (df = 65; t = -2.03) only.

component	Gender	Mean		Mean		Cylinder	Axis
		C ₀ (D)		C ₄₅ (D)			
Right eye							
d ₁	Males	+0.020	±0.01	+0.004	±0.01	+0.02	5.7
	Females	+0.023	±0.01	+0.006	±0.01	+0.02	7.3
F ₂	Males	-0.214	±0.04	+0.052	±0.03	+0.22	83.2
	Females	-0.185	±0.03	+0.036	±0.04	+0.19	84.5
d ₂	Males	+0.093	±0.02	-0.033	±0.01	+0.10	9.8
	Females	+0.104	±0.01	+0.042	±0.02	+0.11	11.0
F ₃	Males	+0.296	±0.12	-0.096	±0.11	+0.31	171.0
	Females	+0.329	±0.13	+0.021	±0.10	+0.33	1.9
d ₃	Males	+0.282	±0.04	+0.025	±0.03	+0.28	2.5
	Females	+0.335	±0.04	+0.098	±0.02	+0.35	8.2
F ₄	Males	-1.080	±0.15	-0.104	±0.10	+1.08	92.8
	Females	-1.227	±0.12	-0.348	±0.09	+1.28	97.9
RAP	Males	-0.601	±0.06	-0.109	±0.06	+0.61	95.1
	Females	-0.625	±0.07	-0.149	±0.06	+0.64	96.7
Left eyes							
F ₂	Males	-0.230	±0.04	+0.052	±0.03	+0.24	83.6
	Females	-0.151	±0.05	+0.102	±0.04	+0.18	73.0
d ₂	Males	+0.063	±0.01	+0.024	±0.02	+0.07	10.4
	Females	+0.088	±0.01	+0.034	±0.02	+0.09	10.6
F ₃	Males	+0.465	±0.15	-0.089	±0.13	+0.47	174.6
	Females	+0.380	±0.10	-0.147	±0.12	+0.41	169.4
d ₃	Males	+0.288	±0.05	+0.019	±0.03	+0.29	1.9
	Females	+0.326	±0.03	+0.024	±0.02	+0.33	2.1
F ₄	Males	-1.107	±0.15	-0.060	±0.12	+1.11	91.6
	Females	-1.205	±0.09	-0.065	±0.08	+1.21	91.5
RAP	Males	-0.508	±0.06	-0.068	±0.07	+0.51	93.8
	Females	-0.605	±0.06	-0.078	±0.06	+0.61	93.7

Table 7.4 Comparison of ocular component astigmatic contributions to residual astigmatism(RAP) calculated from biometric measurements in the right and left eyes of 33 males and 33 females. A statistically significant difference to 95% level (unpaired t-test)) was found for the C₄₅ components of d₃ (df = 64; t = 2.14) in the right eye.

In Table 7.4 males and females showed almost similar results over the whole measurements.

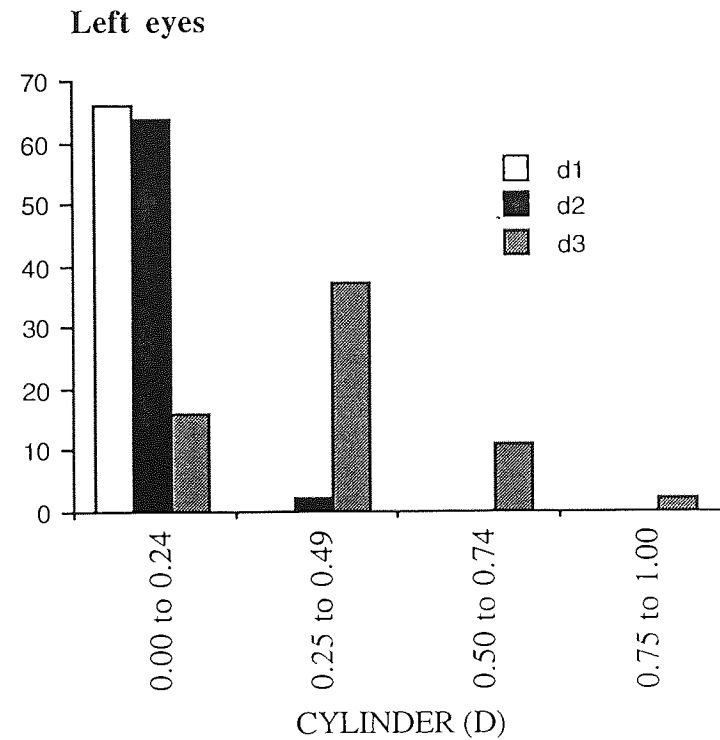
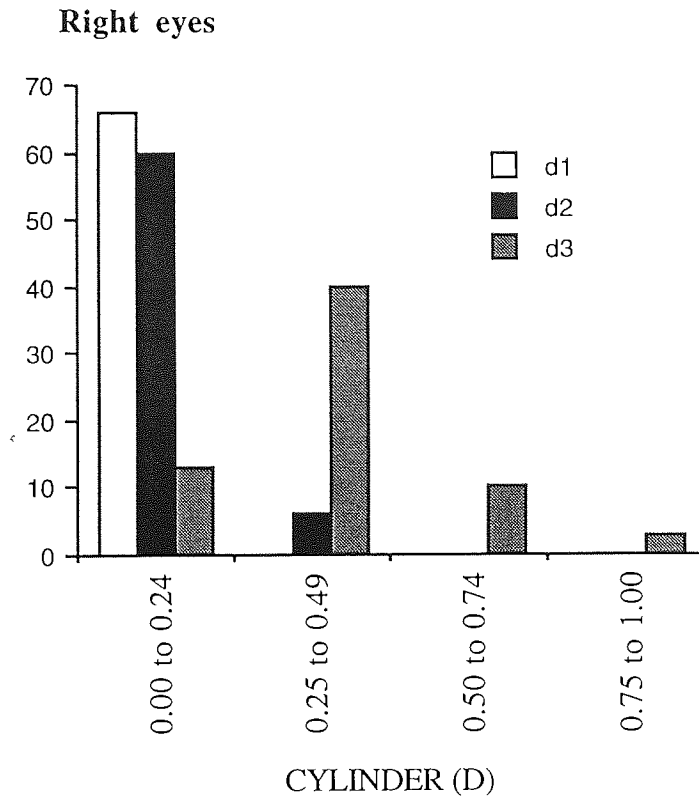
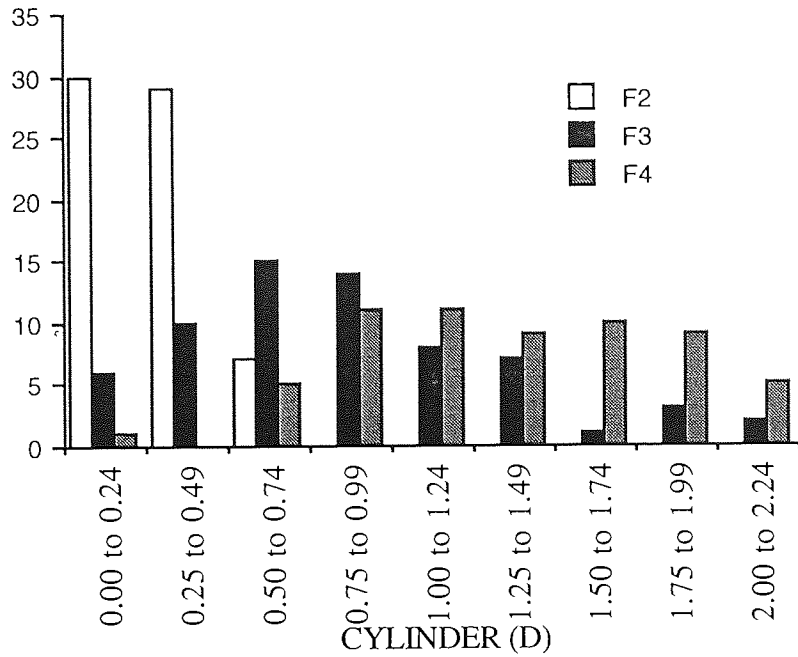


Figure 7.1 Frequency distributions of ocular component cylinder power contributions to residual astigmatism of internal ocular distances d_1 (corneal thickness) d_2 (anterior chamber depth) and d_3 (lens thickness) measured in 66 right (A) and left eyes (B).

Right eyes



Left eyes

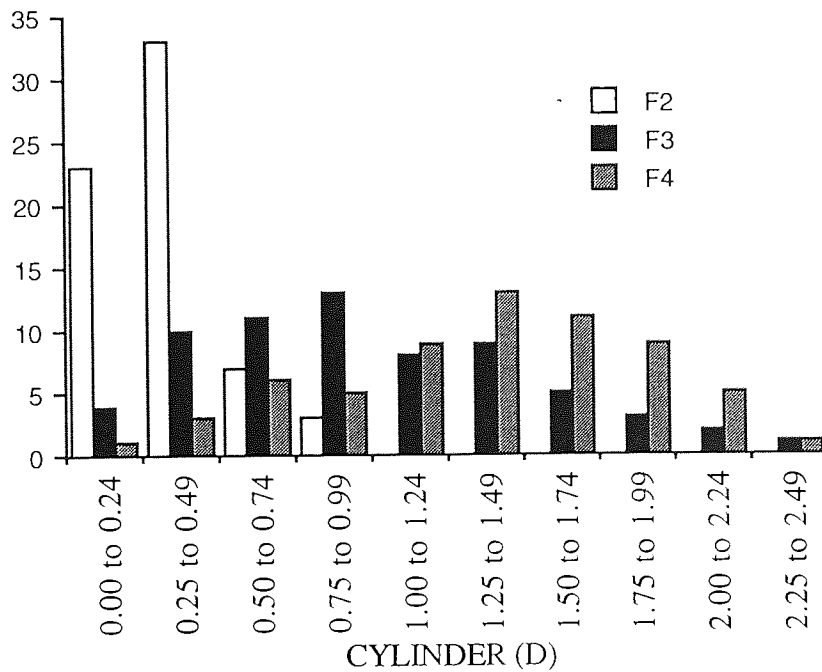


Figure 7.2 Frequency distributions of ocular component cylinder power contributions to residual astigmatism of internal ocular surfaces F₂ (posterior cornea) F₃ (anterior lens) and F₄ (posterior lens) measured in 66 right (A) and left eyes (B).

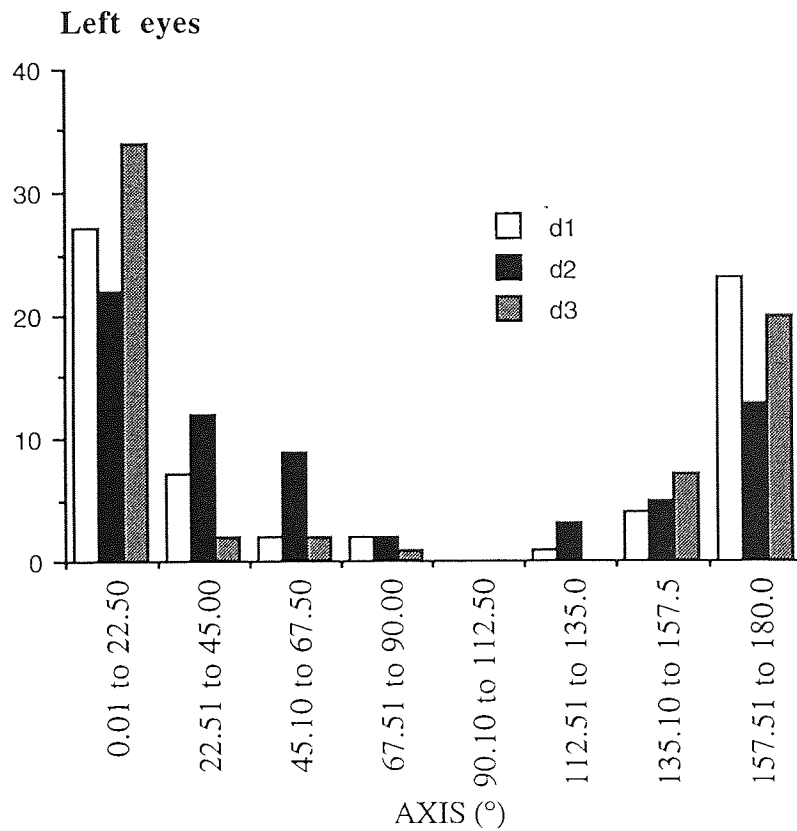
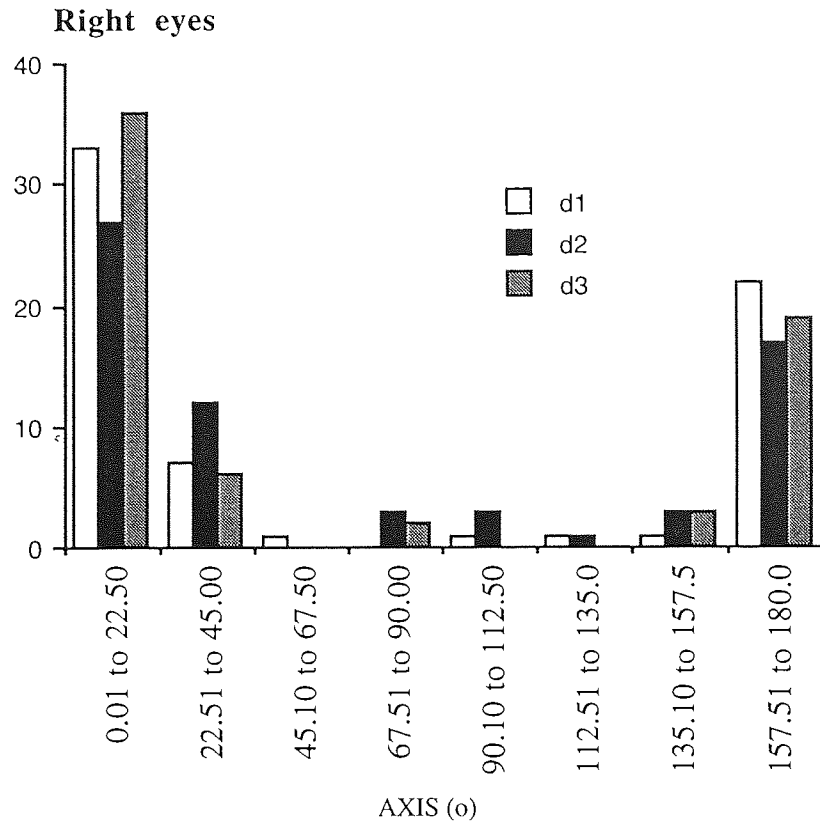


Figure 7.3 Frequency distributions of ocular component cylinder axis contributions to residual astigmatism of internal ocular distances d_1 (corneal thickness) d_2 (anterior chamber depth) and d_3 (lens thickness) measured in 66 right (A) and left eyes (B).

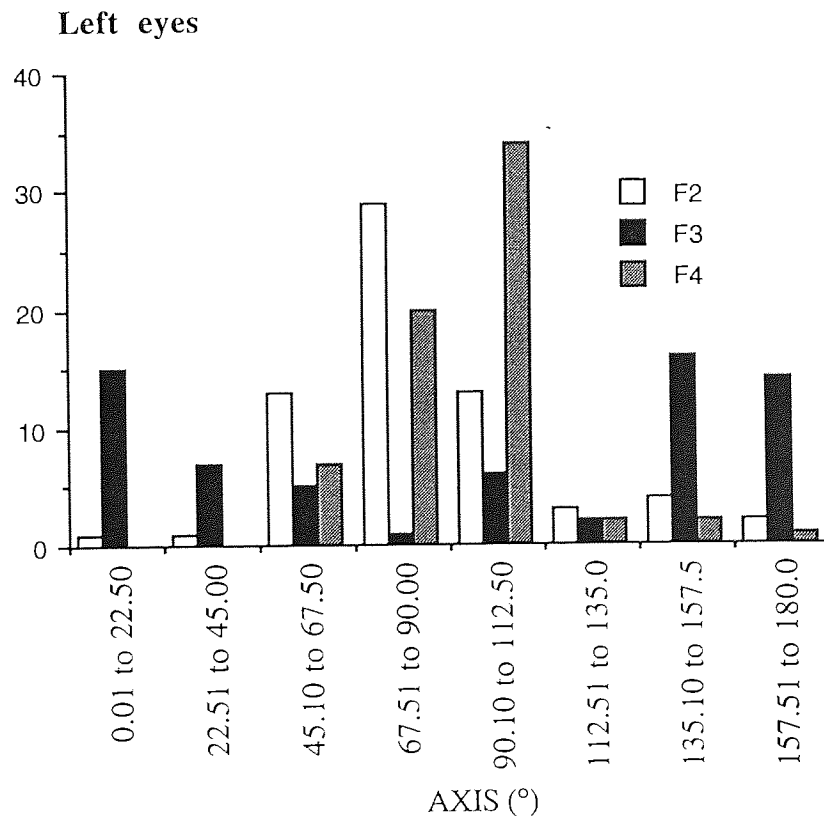
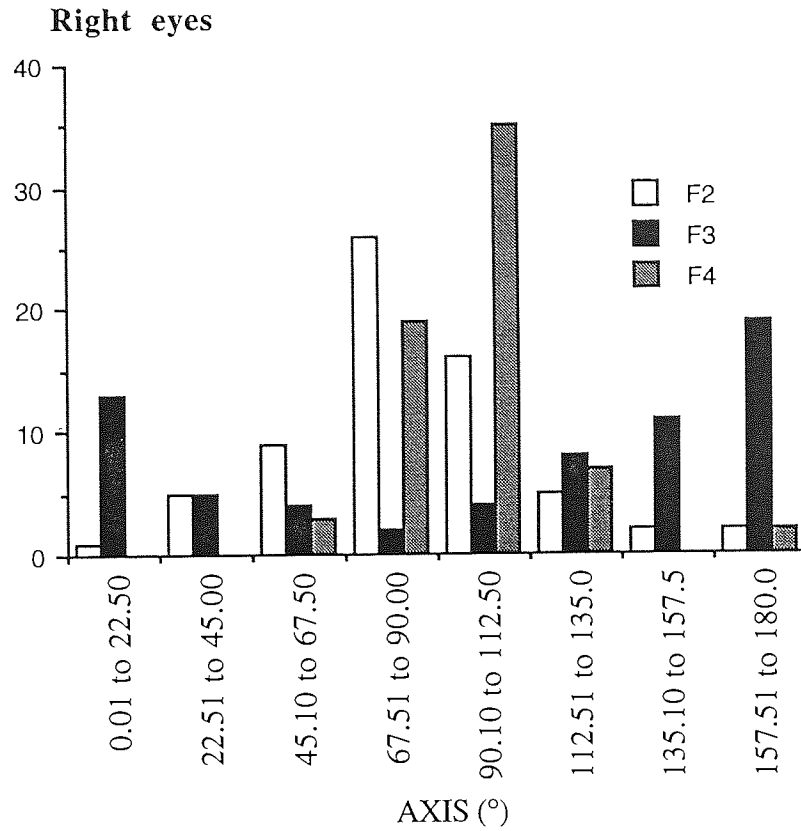


Figure 7.4 Frequency distributions of ocular component cylinder axis contributions to residual astigmatism of internal ocular surfaces F₂ (posterior cornea) F₃ (anterior lens) and F₄ (posterior lens) measured in 66 right (A) and left eyes (B).

Frequency distributions of ocular component cylinder power and axis contributions to residual astigmatism are shown in Figures 7.1 to 7.4. As far as the author is aware, no such data exists elsewhere. With regard to cylinder power, corneal thickness effectivity (d_1) makes the smallest contribution (less than 0.25DC) to residual astigmatism. This is followed by anterior chamber depth effectivity (d_2), the contribution of which falls within 0.50DC. Crystalline lens effectivity (d_3) makes by far the largest contribution which may reach 1.00DC. More substantial cylinder power arise from the internal ocular surfaces; up to 1.00DC arises from the posterior corneal surface while both lens surfaces exhibit up to 2.50DC. If plus cylinder axes are classified as being with-the-rule (direct) astigmatism (axis $180^\circ \pm 20^\circ$), against-the-rule (axis $90^\circ \pm 20^\circ$) inverse or oblique (axis $45^\circ / 135^\circ \pm 25^\circ$), the with-the-rule (direct) astigmatism tends to arise from corneal thickness effectivity (in 83% of right eyes and 76% of the left eyes), anterior chamber depth effectivity (in 67% of right eyes and 53% of left eyes), lens thickness effectivity (in 83% of right eyes and 82% of left eyes), anterior lens surface toricity (in 64% of right and left eyes). Against-the-rule (inverse) astigmatism tends to arise from the posterior surface of the cornea (in 48% of right eyes and 44% of the left eyes) and lens (in 82% of right and left eyes), (see section 2.5 and 6.2).

An additional facility of the computing scheme used in this chapter is that the components of astigmatic decomposition (C_0 and C_{45}) may be simply added to one another in order to calculate the astigmatism resulting from two or more ocular elements. for example, the astigmatic contribution of the lens treated as a single element, is simply calculated by finding the sum of the C_0 and C_{45} components of its anterior surface (F_3), axial thickness (d_3) and posterior surface (F_4) followed by conversion to spherocylindrical form.

Hence, from Table 7.2, the lens is found to have C_0 values of -0.531D (right eyes) and -0.426D (left eyes) with C_{45} values of -0.203D (right eyes) and -0.158D (left

eyes) which yields spherocylindrical values of +0.57DC axis 100.5° (right eyes) and +0.45DC axis 100.2° (left eyes). These values may be compared to the residual astigmatic power shown in Table 7.2, for the right eyes +0.62DC axis 95.4° and left eyes +0.52DC axis 92.7°. This confirms the traditional assumption that residual astigmatism is typically almost entirely lenticular.

7.5 Summary

The determination of the individual internal ocular component contributions to residual astigmatism was carried out in this chapter. Effectivity due to corneal thickness (d_1) made the smallest cylinder power contribution (< 0.25 DC) followed by that due to the anterior chamber depth (d_2) which amount to (< 0.50 DC) and the crystalline lens thickness (d_3) about (< 1.00 DC). More cylinder power arose from (F_2) the posterior corneal surface (< 1.00 DC) and both (F_3 and F_4) lens surfaces (< 2.50 DC).

Predominantly with-the-rule (direct) astigmatism arose from effectivity due to corneal thickness (R 83%; L 76%), anterior chamber depth (R 67%; L 53%) and lens thickness (R 83% L 82%) as well as the anterior lens surface toricity (R and L 64%). Predominantly against-the-rule (inverse) astigmatism arose from posterior surfaces of the cornea (R 48%; L 44%) and lens (R and L 82%). Very similar results were found for right versus left eyes and males versus females.

Pooled data was found to have higher level of repeatability than individual subjects and unwanted accommodation had little influence on the results.

Frequency distribution graphs indicated that the pooled mean values of ocular components astigmatic contributions reflected the general population trends.

CHAPTER EIGHT
SUMMARY AND FUTURE WORK

8.1 Introduction

A review of the previous chapters is presented in section 8.2. Limitations of the method are covered in section 8.3, while suggestions for further work are discussed in section 8.4.

8.2 Review of Previous Chapters

In the first chapter the scope of the study and the outlines of the thesis were laid down.

The second chapter has reflected that most eyes are known to be astigmatic. Usually a variance between total ocular, and corneal astigmatism, is found and is known by the name residual astigmatism.

Several studies have confirmed the existence of residual astigmatism. Residual astigmatism is most often found to be against-the-rule (inverse) for most eyes. Most investigators find residual astigmatism averages between 0.50D and 0.75D.

Residual astigmatism is thought to arise from a number of sources such as internal ocular component surface toricity, refractive index variations, astigmatic accommodation, ocular misalignments and probably the retina and the perception centres are also involved.

The third chapter has described the biometric methods chosen to measure *in vivo* ocular components of the human eye (multi-meridional ultrasonic ophthalmophakometry). Automated infra-red autorefractometry was used to estimate refractive error. Corneal curvatures were measured using a computerised video keratographic device. A-scan Ultrasonography was used to measure intra-ocular axial

distances. Measurements of Purkinje images I, II and V in four meridians were made by means of a purpose built still flash photographic ophthalmophakometer.

A protocol involving preliminary, main, repeatability and Cycloplegic studies were laid down.

All measurements were taken along the line of sight under natural conditions. The line of sight is the only logical axis where all the components function jointly (Gullstrand, 1924).

The computing schemes utilized in this study were described in this chapter 4. Calculations included: (1) notional meridional powers from refractive and keratometric measurements; (2) crystalline lens surface power excluding III Purkinje image arising from the anterior lens surface; (3) application of meridional analysis to derive spherocylindrical powers from notional powers calculated along 4 pre-selected meridians; (4) application of astigmatic decomposition and vergence analysis to calculate contributions to residual astigmatism of ocular components with obliquely related cylinder axes and (5) calculation of effect of random experimental errors on the calculated data.

An important conceptual point must be made that no attempt was made to either measure or calculate the degree of misalignment (tilt or decentration) of any of the ocular surfaces in respect to one another. Such misalignment can contribute to the measurement of astigmatism exhibited by any surface (see section 2.5.5). Therefore, whilst calculations performed in this study may be used to estimate the astigmatism exhibited by a particular ocular surface, it is not possible to determine the exact contributions that surface toricity or misalignment make towards the astigmatism exhibited by that surface.

In general, the results presented in chapter 5 supported previous findings that the human eye possesses approximately 0.50 D of residual astigmatism. The majority of eyes exhibited against-the-rule (inverse) residual astigmatism in keeping with what had been previously reported. An additional finding of the present study was that for over two thirds of the sample the residual astigmatic power axes were mutually perpendicular to within $\pm 20^\circ$. Further, the level of residual astigmatism exhibited was not significantly effected by gender or race.

However, whilst the repeatability of estimates of residual astigmatism in individual eyes were found to be poor, mean values taken from samples of as little as 20 individuals proved to be reasonably repeatable. Therefore, measurements of residual astigmatism may only be reliable for averaged data or greater numbers of repeat measurements.

In chapter six, the findings indicated that accumulated experimental errors were loaded onto the anterior crystalline lens surface. This had been reported before and results from use of Purkinje images I, II and IV and excluding Purkinje image III (Dunne and Barnes, 1993) during ophthalmophakometry.

The spherical component was least affected by errors (± 0.07 - 1.03 DS) followed by the cylinder component (± 0.11 - 1.71 DC) and cylinder axis orientation (± 7.8 - 67.5°). This had been reported before (McBrien and Millodot, 1985).

With the possible exception of the posterior corneal surface, accumulated experimental errors were such that this method would only lend itself to studies of individual eyes if a large number of repeat observations were made. Only then would the experimental errors, being random in nature, tend to cancel themselves out.

Utilization of 4 meridians instead of 3 tended to alleviate the effects of accumulated experimental errors to some extent. The effects were most noticeable for cylinder axis orientation.

The anterior:posterior corneal radius ratios calculated for the 180° and 90° meridians confirmed a previous observation (Dunne, Royston and Barnes, 1991; Dunne and Barnes, 1993) that the posterior corneal surface is steeper vertically relative to the anterior corneal surface. This has the effect of greater effective compensation of anterior corneal surface astigmatism than would occur if the ratios were the same in both meridians.

Asphericity and misalignment of the ocular component was been considered to be a major source of discrepancy in the results of ocular biometric measurements (Sheard, 1920; Tscherning, 1924; Ludlam and Wittenberg, 1966; Bennett, 1984; Barnes, et al, 1987; White, 1993). One could argue that surface toricity measured along the visual axis relates to the functional astigmatism experienced at the fovea. In this sense, no matter what the level of surface misalignment, the interest is only in the resulting astigmatism along the visual axis. In other words, rather than considering the apical toricity and misalignment of a surface separately, it is only necessary to consider the astigmatism arising from that surface at the point of intersection with the visual axis. Nevertheless the importance of the subject (asphericity and misalignment of ocular component) warrants further study.

The determination of individual internal ocular component contributions to residual astigmatism was carried out in chapter 7. Effectivity due to corneal thickness made the smallest cylinder power contribution (< 0.25DC) followed by that due to the anterior chamber depth which amount to (< 0.50DC) and the crystalline lens thickness about (< 1.00DC). More cylinder power arose from the posterior corneal surface (< 1.00DC) and both lens surfaces (< 2.50DC).

Predominantly with-the-rule (direct) astigmatism arose from effectivity due to corneal thickness anterior chamber depth and lens thickness as well as the anterior lens surface toricity. Predominantly against-the-rule (inverse) astigmatism arose from posterior surfaces of the cornea and lens. Very similar results were found for right versus left eyes and males versus females.

Pooled data was found to have higher level of repeatability than individual subjects and the use of cycloplegia had little influence on the results.

Frequency distribution graphs indicated that the pooled mean values of ocular components astigmatic contributions reflected the general population trends.

8.3 Limitations of the Method

Although a successful determination of the astigmatic power and the cylinder axis orientation arising from each of the internal ocular components of the human eye has been achieved, the method has its limitations which can be summarised as follows:

- 1 The method is highly repeatable with pooled data, but relatively poor with individual cases.
- 2 The use of notional power for meridional calculations.
- 3 The accumulation of experimental errors to anterior crystalline lens surface.
- 4 The obtained results seemed to have been influenced by the ocular surfaces asphericity due the positioning of the Purkinje light sources (widely separated to insure the visibility of the Purkinje image II).
- 5 The time factor (a long time is needed for each case).

8.4 Suggestions for Future Work

8.4.1 How an Improvement could be Achieved

- 1 The use of a Video Camera and collimated light sources to include III Purkinje image.
- 2 The use of Purkinje light sources in a Placido disc form pattern (two concentric rings of spot light sources, to test for central and peripheral radii).
- 3 The use of digital image capture and image analysis systems.
- 4 The use of high numbers of repeat measurements (not less than 10 repeats).

8.4.2 Possible Applications

From the obtained results the ocular components of the human eye have shown a unique arrangement of its individual components contributing to astigmatic powers. The axis orientations of each of the ocular surfaces are at right angle to one another bringing about a compensatory effect. The result of this compensatory phenomenon is stigmatic eye or a clinically negligible cylinder (called physiological astigmatism). Beside this, the optical performance of the cornea, the pupil, the misaligned ocular component, components separation and refractive indices variations, could only be a purposeful creation enhancing the optical performance of the eye; apart of a complex visual task. The compensatory phenomenon of the eye as a visual apparatus is yet to be investigated.

Applying the suggested improvements the method could be used to:

- 1 Assess the growth of the crystalline lens and curvature ametropia;
- 2 Study (the disputed) sectional accommodation;

- 3 Study ocular components misalignment;
- 4 Study lenticular changes, associated with diabetes melitis, early cataract and glaucoma;
- 5 Assessment of astigmatism arising from intra ocular lens implant in situ;
- 6 Study internal ocular components asphericity.

8.4.3 Further Study

The present thesis has not attempted to examine ocular component asphericity, crystalline lens tilt (ocular misalignment), astigmatic accommodation, retinal and perceptual astigmatism. Beside these, there seems to be a compensatory mechanism enhancing the visual performance of the seeing eye, these are yet to be investigated.

The author hopes sincerely that the points mentioned above lead to a fruitful research to disclose the purposeful nature of creating the eye and the visual system the way it exists.

REFERENCES

- Anstice J. (1971) Astigmatism-its components and their changes with ages . Am J. Optom Arch Am Acad Optom; 48:1001-1006.
- Armstrong P. (1991). An investigation into the accuracy of tri-meridional and multi-meridional analysis of the anterior corneal surface. Unpublished dissertation for the Ophthalmic Optics honours degree program. Aston University.
- Azen S.P., Burg K.A., Smith R.E. and Maguen E.(1979) A comparison of three methods for the measurement of corneal thickness. Invest Ophthalmol Vis Sci; 18:535 -538.
- Baily Neal J.(1961) Residual astigmatism with contact lenses, Pt 1. Incidence Opt J and Rev. Optm; 98 (1):30-31.(Cited by Sarver 1963).
- Bailey T.J.(1983) Statistical Methods in Biology, 2nd Edn, Hodder and Stoughton, London, pp 14-17.
- Baldwin W.R. and Mills A.(1981) A longitudinal study of corneal astigmatism and total astigmatism. Am J Optom Physiol Opt ; 58: 206-211.
- Banks M.S.(1980) Infant refraction and accommodation, Int Ophthalmol Clin, 20 (1): 205-232.
- Bannon R.E and Walsh R.(1945) On astigmatism (Part II.) Am J Optom Arch Am Acad Optom; 22: 162-181.
- Bannon R.E.(1946) A study of astigmatism the near point with special reference to astigmatic accommodation. Am J Optom Arch Acad Am Optom; 23: 53-75.
- Barnes D.A (1984) Astigmatic decomposition: an alternative Subjective refraction test employing conventional instrumentation. Ophthal Physiol Opt ;4:359-364
- Barnes D.A., Dunne M.C.M. and Clement R.A. (1987)A schematic eye model for the effects of translation of ocular components on peripheral astigmatism. Oph Physiol Opt; 7:153-158.
- Bennett A.G. (1960) Refraction by automation ? New application of the scheiner disc. Optician; 139:5-9
- Bennett A.G. (1961) Appendix D. The computation of the optical dimensions . In Sorsby A., Benjamin B. and Sceridan M. (1961) Refraction and its components during growth of the eye from the age of three . Medical Research Council Special report series No. 301, London. pp 55- 64.
- Bennett A.G.(1977) Some novel optical features of the Humphrey Vision Analyser. Optician; 173(4481), 8-16.
- Bennett A.G. (1984) Astigmatic effect of a tilted crystalline lens . Ophthalmic Optician, 24:793-794.
- Bennett A.G.(1984) A new approach to statistical analysis of ocular astigmatism and astigmatic prescriptions. The Frontiers of optometry: First International Congress 2:35-42.

- Bennett A.G (1986) Two simple calculating schemes for use in ophthalmic optics - II. Tracing axial pencils through systems including astigmatic surfaces at random axes. *Ophthal Physiol Opt* 6:419-429.
- Bennett A.G and Rabbetts R.B (1978) Refraction in oblique meridians of the astigmatic eye, *Br J Physiol Opt*; 32:59-77.
- Bennett A.G. and Rabbetts R.B.(1984) *Clinical Visual Optics*. Butterworth, London.
- Bennett A.G. and Rabbetts R.B.(1989) *Clinical Visual Optics*. Butterworth, London.
- Bland J.M and Altman D.G. (1986) Statistical method for assessing agreement between two methods of clinical measurements. *The Lancet* 1(8746): 307-310.
- Berstein N.L.(1984) Quoted by Maurice D.M. In Davson M.(Ed) *The cornea and the sclera in the eye*, 3rd edn . Vol 1 B: 64. Academic press, London.
- Borish I.M.(1970) *Clinical Refraction*. Professional Press;Chicago.
- Brown N.(1973) The change in shape and internal form of the lens of the eye on accommodation. *Exp Eye Res*; 15: 441-460.
- Brown N.(1974) The shape of the lens equator. *Exp Eye Res*;19: 571-576.
- Brubaker R.F., Reinecke R.D. and Copeland J.C. (1969) Meridional refractometry, 1. derivation of equations. *Arch Ophthalmol* 81:849-853.
- Brzezinski M.A. (1982) Review: astigmatic accommodation(Sectional Accommodation) a form of Dynamic Astigmatism. *Aust J Optom*; 65: 5-11.
- Bullimore M.V., Gilmartin B and Royston J.M (1992) Steady-state accommodation and ocular biometry in late-onset myopic eyes. *Doc Ophthalmol*; 80: 143-155.
- Burton T.C.(1973) Irregular Astigmatism following episcleral buckling procedure with use of silicone rubber sponges. *Arch Ophthalmol*; 90: 447-448.
- Burek H. (1990) Tri-meridional analysis using arbitrary meridians. *Ophthal Physiol Opt*; 10 : 280-285.
- Byakuno I.E, Okuyama F., Tokoro T. and Akizawa Y. (1994) Accommodation in astigmatic eyes. *Optom Vis Sci*; 71(5):323-331.
- Campbell M.C.W (1984) Measurement of refractive index in an intact crystalline lens. *Vision Research*;24:409-415.
- Carter J.H.(1963) Residual astigmatism of the human eye . *Optom Weekly*. 54 :1271-1272.
- Carter J. H. (1980) Ophthalmometric prediction of correcting cylinder axis. *Am J Optom Physiol Opt*; 57:15-24.
- Charman W.N.(1991a) Optics of the human eye.(Chapter 1) In *Vision and Visual Dysfunction*;Vol 1. General Editor: J.R. Cronly Dillon. M. Macmillan Press scientific & Medical.
- Clark B.A.J.(1972) Autocollimating photokeratoscope. *J Opt Soc Am* ;62:169-176.

- Clark B. A. J.(1973a) Keratometry :a review. Australian J Optm , 56:94-100.
- Clark.B. A.J.(1973b) Conventional keratometry-a critical review. Aust J Optom, 56:140-155.
- Clark B.A. J.(1974a)Topography of some individual cones. Aust J Optom, 57:65-69.
- Clark B. A. J.(1974b) Mean topography of corneas. Aust J Optom, 57:107-114.
- Cui C. Campbell M.C.W.(1994) Two methods of measuring the tilt and Decentration of the crystalline lens in vivo. Inves Ophthal Vis Sci; Vol 35(4)
- Dellande W.D.(1970) A comparison of predicted and measured residual astigmatism in corneal contact lens wearers, Am J optom Arch Am acad Optom; 47 (6):459-463.
- Dingeldein S.A and Klyce S.D.(1989) The topography of the normal corneas. Arch Ophthalmo ; 107:512-518.
- Dobrowolsky K.M. (1868) Veber verschiedene Weranderungen des Astigmatismus unter dem Einfluss Accommodation; Arch Ophthalm;14: 51-105. Cited by Brzezinski (1982).
- Donders F.C.(1864) On the Anomalies of Accommodation and Refraction of the Eye.(Translated by Moore WD) London: New Sydenham Society. Hatton Press edition, 1952.
- Duke Elder and Wybar K.C. (1961) The anatomy of the visual system. In system of ophthalmology, Vol. II. Kimpton, London.
- Duke-Elder S. and Abrams D. (1970) Ophthalmic optics and refraction. In Duke-Elder S, ed. System of ophthalmology . St. Louis: CV Mosby, Vol 5.p:274-295.
- Dunne M.C.M. (1987) An optical study of human ocular dimensions. Unpublished (PhD thesis). Aston University.
- Dunne M.C.M. (1991) Scheme for calculation of ocular components in a four-surface eye without need for measurement of the anterior crystalline lens surface Purkinje image. Ophthal Physiol Opt;12: 370-375.
- Dunne M.C.M, (1995) A computing scheme for determination of retinal contour from peripheral refraction, keratometry and A-scan ultrasonography. Ophthal Physiol Opt, 15:(in press)
- Dunne M.C.M., Barnes D.A. (1989) Modelling angle alpha.Ophthal Physiol Opt ; 9: 338-339.
- Dunne M.C.M. and Barnes D.A. (1993) A comparison of the errors arising from three methods of phakometric computation. In Ophthalmic and Visual Optics Noninvasive assessment of the visual system Technical Digest; P 66-65. Optical society of America, Washington DC.
- Dunne M.C.M., Royston J.M. and Barnes D.A.(1991) Posterior corneal surface toricity and total corneal astigmatism . Optom Vis Sci, 68:708-710.
- Dunne M.C.M., Royston J M. and Barnes D.A.(1992) Normal variation of the posterior corneal surface. Acta Ophthalmologica. 70:255-261.

- Dunne MCM, Misson G.P, White E.K. and Barnes D.A, (1993) Peripheral astigmatic asymmetry and angle alpha. *Ophthal Physiol Opt*;13: 303-305.
- Edmund C. and Sjontoft E. (1985) The central-peripheral radius of the corneal curvature. *Acta Ophthalmologica*. 63:670-677.
- EL Hage S.G.(1976) The three- dimensional configuration of the cornea, *Nouv Rev. Optique*; 7: 205-209.(Cited by Charman 1991).
- Ellerbrock V.J. (1963) Developmental, congenital and hereditary anomalies of the eye. In Hirsch M.J. and Wick R.E. (Eds) *Vision of children*, Chapter 2: 79-98. Chilton Book Co., Philadelphia.
- Emsley H.H.(1969) *Visual optics*. Vol. 1. Hatton, London.
- Erickson P. (1984) Complete ocular components analysis by vergence contribution. *Am J Optom Physiol Opt* .61:469-472.1
- Erickson P. (1991) Optical component contributing to refractive anomalies. In Grosvenor T. and Flom M.C. *Refractive Anomalies Research and Clinical Application*. Butterworth Heineman p:199-218.
- Fatt I. and Harris MG.(1973) Refraction of the cornea as a function of its thickness. *Am J Optom Arch Am Acad Optom*; 60:383-386.
- Francois J. and Goes F. (1969a) Oculometry in emmetropia and ametropia. In *Ultrasonographica Medica*; pp 473-515. Verlag der Akademie, SIDU III.
- Francois J. and Goes F. (1969b) Echographic study of the lens thickness as a function of the axial length in emmetropic eyes of the same age. In *Ultrasonographica Medica*; pp 531-538. Verlag der Akademie, SIDU III.
- Fletcher R.J .(1951a) Astigmatic accommodation. *Br J Physiol Opt*; 8: 73-94, 129-160,193-224.
- Fletcher R.J .(1951b)The utility of the third Purkinje image for studies of changes of accommodation in the human eye. *Trans. Int. Oph Opt Congress*. pp 121-136.
- Fletcher R.J. (1952) Astigmatic accommodation. *Br J Physiol Opt*; 9: 8-32.
- Fowler C.W.(1989) Assessment of toroidal surfaces by the measurements of curvature in three fixed meridians. *Ophthal Physiol Opt*; 9: 79-80.
- Francis J.L.(1962) Some measurements on myopic eyes . In *Transactions of the International Ophthalmic Optics Congress*: 406-416. Hafner publishing Company, New York.
- Gartner W F. (1965) Astigmatism and optometric vectors. *Am J Optom Arch Am Acad Optom*; 42: 459-463.
- Grosvenor T, Perrigin D Mand Quintero S.(1988) Predicting refractive astigmatism: a suggested simplification of Javal's rule. *Am J Optom Physiol Opt*; 65:292-297.
- Grosvenor T. and Scott R.(1993) Three-year changes in refraction and its components in youth- onset and early adult-onset myopia. *Optom Vis Sci*; 70: 677-683.

- Grosvenor T.(1994) Refractive component changes in adult-onset myopia: evidence from five studies. *Clinical and Experimental Optometry*; 77.5: 196-205.
- Guillon M., Lyndon D..P.M. and Wilson C.(1986) Corneal topography : a clinical model. *Ophth Physiol Opt*; 6:47-56.
- Gullstrand A. (1924) Appendices to *Physiological Optics .Vo 1* by Helmholtz (translated by Southall J.B.C.) Optical Society of America, Rochester.
- Haine C.L., Long W.F and Reading R.W. (1973) Laser meridional refractometry: a preliminary report. *Optom Weekly*; 64: 1064-1067.
- Haine C.L., Long W.F and Reading R.W. (1976) Laser meridional refractometry. *Am J Optom Physiol Opt*;53: 194-204.
- Harris W.F.(1992a) Calculation and least- squares estimation of surface curvature and dioptric power from meridional measurements. *Ophthal Physiol Opt*; 12:58-63.
- Harris W.F.(1992b) Constrained least-squares estimation of surface curvature and dioptric power from meridional measurements. *Ophthal Physiol Opt*; 12:64-68.
- Helmholtz H.(1924) *Physiological optics Vol 1.* (Trans. Southall J.P.C.) Optical society of America ,Rochester.
- Henson D.B.(1991) Optical methods for measurement of ocular parameters. (Chapter 17) In *Vision and Visual Dysfunction*;Vol 1. General Editor: J.R. Cronly Dillon. M. Macmillan Press scientific & Medical.
- Hess E.H.(1965) Attitude and pupil size. *Sci . Am*;212(4):46-54. Cited by Charman W.N.(1991).
- Hirji N.K. and Larke J.R.(1978) Thickness of the human cornea measured by topographic pachometry. *Am J Optom Physiol Opt*; 55:97-100.
- Hirsch M.J.(1959) Changes in astigmatism after the age of forty. *Am J Optom Arch Am Acad Optom* ;36:395-405.
- Hockwin O, Weigelin E, Laser H. and Dragmoriscu V.(1983) Biometry of the anterior eye segment by Scheimpflug photography. *Ophthalmic eye Res* ,15:102 -108.
- Hofstetter HW. and Baldwin W.(1957) Bilateral Correlation of Residual Astigmatism. *Am J Optom Arch Am Acad Optom*;34:388-391.
- Howcroft M.J. and Parker J.A.(1977) Aspheric curvature for the human lens . *Vision Res*; 17: 1217-1223.
- Howland H.C.(1991) Determination of ocular refraction (Chapter 18). In *Vision and Visual Dysfunction*. Vol 1. General Editor: J.R. Cronly .Dillon. M. Macmillan Press Scientific & medical.
- Humphrey W.E. (1977) Automatic retinoscopy: The Humphrey Vision Analyser. A remote Subjective refractor employing continuously variable sphere-cylinder corrections. *Optician*;173: 17-18,23-25 and 27.
- Janisse M.P. (1973) *Pupillary Dynamics and Behaviour*. Plenum Press: New York.
- Javal E. (1890) *Memories d' Ophthalmologie*. G. Masson.Paris, pp 627.(Cited by Bannon and Walsh 1945).

- Kikkuhawa Y., and Harayama K. (1970) Uneven swelling of the corneal stroma. *Invs Ophthalmol Vis Sci*; 9: 735-741.
- Koretz J.F., Handelman G.H. and Brown N.P. (1984) Analysis of Human crystalline lens as a function of accommodation and age. *Vision Res*; 14: 1141-1151.
- Kratz J.D. and Walton W.G. (1949) A modification of Javal's Rule for the correction of astigmatism. *Am J Optom Arch Am Acad Optom*, 259-306.
- Lam A.K.C., Douthwaite W.A. (1994) Derivation of corneal flattening factor, p-value. *Ophthal Physiol Opt*; 14: 423-427.
- Lancaster and Walter B. (1916) A case of Botulism. *Tras Amer Ophthal soc*; 14: 648-660. Cited by Brzezinski (1982).
- Lancaster W.B. (1943) Terminology in ocular motility and allied subjects. *Am J Ophthalmol*, 26: 122-132.
- Larsen J.S. (1971) The sagittal growth of the eye . IV. Ultrasonic measurement of the axial length of the eye from birth to puberty. *Acta Ophthalmol*; 49: 873-886.
- Laurance L. (1920) *General and Practical Optics*, 3rd Edn, The School of Optics, London, pp 153, 593-602. Cited by Brubaker et al (1969).
- Le Grand Y. (1967) *From and Space Vision*. Revised ed. Translated by Millodot M. and Heath G.G. Bloomington: Indiana University; 108-128.
- Le Grand Y. and El Hage S.G. (1980) *Physiological Optics*. Springer, Berlin.
- Leary G.A. (1981) Ocular component analysis by vergence contribution to the back vertex power of the anterior segment. *Am J Optom Physiol Opt*; 58: 899-909.
- Lee D. and Wilson G. (1981) Non-uniform swelling properties of the corneal stroma. *Curr. Eye Res*; 1: 457-461.
- London R. and Wick B.C. (1982) Changes in angle lambda during growth: theory and clinical implications. *Am J Optom Physiol Opt* ;59: 568-572.
- Long W.F. (1974) A mathematical analysis of multi-meridional refractometry. *Am J Optom Physiol Opt*; 51: 260-263.
- Loper L.R. (1959) The relationship between angle lambda and the residual astigmatism of the eye. *Am J Optom Arch Am Acad Optom*. p:365-377.
- Lowe R.F. (1970) Aetiology of the anatomical basis of primary angle closure glaucoma. *Bri J Ophthalmol*; 54: 161-169.
- Lowe R.F. and Clark B.A.J. (1973a) Posterior corneal curvature . Correlation in normal eyes and eyes involved with primary angle-closure glaucoma. *Bri J Ophthalmol*. 57:464-470.
- Lowe R.F. and Clark B.A.J. (1973b) Radius of curvature of the anterior lens surface correlation in normal eyes and in eyes involved with primary angle -closure glaucoma. *Bri J Ophthalmol*. 57: 471-474.
- Lowenstein O. and Lowenfeld I.E. (1969) The pupil. In *The Eye*. Vol 3 ed. Davson H. New York: Academic Press.

- Ludlam W.M and Wittenberg S., Rosenthal J.(1965) Measurements of ocular dioptric elements utilizing photographic methods. PT.1. Errors analysis of Sorsby' photographic Ophthalmophakometry. Am J Optom Arch Am Acad Optom; 42:394-416.
- Ludlam WM. and Wittenberg S.(1966) Measurements of the ocular dioptric elements utilizing photographic methods . PT 11. Cornea -theoretical considerations. Am J Optom Arch Am Acad Optom ,43:249-267.
- Ludlam W.M., Weinberg S.S., Twarowski C.J. and Ludlam DP.(1972) Comparison of cycloplegic and non-cycloplegic ocular component measurement in children. Am J Optom Arch Am Acad Optom; 49: 805-818.
- Luyckx-Bacus J. and Weekers J. (1966) Etude biometrique de l'oeil humain par ultrasonographie. I. Les ametropies. Bulletin de la Societe Belege d'Ophthalmologie;143: 552-567. Cited by Weekers et al. (1973).
- Luyckx-Bacus J. and Delmarcelle Y. (1969) Influence des alterations biometries du cristallin sur la profondeur de la chambre anterieure. Bulletin de la Societe Belege d'Ophthalmologie;152: 507-513 Cited by Weekers et al. (1973).
- Lyle W.M. (1971) Changes in corneal astigmatism with age .Am J Optom Arch Am Acad Optom; 48:467-478.
- Lyle W.M. (1991) Astigmatism. In Grosvenor T.and Flom M.C. Refractive Anomalies Research and Clinical Application. Butterworth Heineman. 146-172.
- Malacara D. (1974) Measurements of visual refractive defects with a gas laser. Am J Optom Physiol Opt; 51: 15-23.
- Mandell R.B.(1964) Corneal areas utilised in ophthalmometry. Am J Optom Arch Am Acad Optom; 41:150-153.
- Mandell R.B. and St Helen R. (1971) Mathematical model of corneal contour. Bri J Physiol Opt; 26: 183-197.
- Martola E.L. and Baum J.L.(1968) Corneal and peripheral corneal thickness: a clinical study. Arch Ophthalmol; 79:28 -30.
- Maurice D.M.(1957) The structure and transparency of the cornea. J Physiol; 136:263-286.
- McBrien N.A. and Millodot M.(1985) Clinical evaluation of the Canon Autorefractometer R-1. Am J Optom Physiol Opt;62: 786-792.
- Millodot M. (1986) Dictionary of optometry. Butterworth & Co (publishers)
- Mote HG. and Fry GA. (1939) The significance of Javal's Rule. Am J Optom Arch Am Acad Optom, 16:362-365.
- Munger R., Burns C. and Campbell M.C.W.(1994) Symmetry of refractive index profiles in mammalian crystalline lenses. Invest Ophthalmol Vis Sci; 35(4)
- Munger R., Campbell M.C.W., Koroger R.H.H., and Burns C.(1992)Refractive index profiles of crystalline lens with a visible region of opacity. Invest Ophthalmol Vis Sci; 33(4): 1169.

- Mutti D. O, Zadnik k. and Adams A.J.(1992) Video technique for phakometry of the human crystalline lens. *Invst Ophthalmol Vis Sci*; 33: 1771-1782.
- Mutti D. O, Zadnik k, Egashira S., Kish L., Twelker J.D. and Adams A.J.(1994) The effect of cycloplegia on measurement of the ocular components. *Invst Ophthalmol Vis Sci*; 35: 515-527.
- Nakao S., Mine K. and Kamiya S. (1969) The distribution of their refractive indices in the human crystalline lens. *Jap J Clin Ophthalmol*, 23:41-44.
- Neumueller J.(1953) Optical, physiological and perceptual factors influencing the ophthalmometric findings . *Am J Optom Arch Am Acad Optom*. 30:281-291.
- Olsen T. and Ehlers N.(1984) The thickness of the human eye cornea as measured by the specular method. *Acta Ophthalmol(Copenh)*; 62: 859-871.
- Parker J.A.(1972) Aspheric optics of the human lens. *Can J Ophthalmol*;7: 168-175.
- Patel S.(1987) Refractive index of the mammalian cornea and its influence during pachometry, *Ophth Physiol Opt*; 7:(4)503-506.
- Patnaik B.(1967) A photographic study of accommodative mechanisms; changes in the lens nucleus during accommodation. *Invest Ophthalmol*; 6: 601-611.
- Pomerantzeff O., Pankratov M., Wang G. and Dufault P. (1984) Wide-angle optical model of the eye. *Am J Optom Physiol Opt*; 61: 166-176.
- Prechtel L.A. and Wesley N.K. (1970) Corneal topography and its application to contact lenses. *Bri J Physiol Opt*; 25:117-126.
- Reading V.M.(1972) Corneal curvature. *The Contact Lens*. 3)6):23-25.
- Reinecke R.D, Caroll J., Beyer C.K.and Montross R.T.(1972) An innovation in eye care. *Sight saving Rev*; 42: 35-41.
- Royston J.M.(1990) The influence of posterior corneal surface astigmatism on residual astigmatism. Unpublished "Ph.D. thesis" Aston University.
- Royston J.M., Dunne M.C.M. and Barnes D.A. (1990) Measurement of the posterior corneal radius using slit lamp and Purkinje image techniques. *Ophthalmol Physiol Opt*. 10 : 385-388.
- Royston J.M., Dunne M.C.M. and Barnes D.A.(1991) Measurements of posterior corneal surface toricity . *Optom Vis Sci*, 67:757-763.
- Rudnicka A.R., Steele C.F., Crabb D.P. and Edgar D.F.(1992) Repeatability , reproducibility and intercession variability of the Allergan Humphery ultrasonic biometer. *Acta Ophthalmologica*; 70:327-334.
- Sarver M.D (1963) The effect of contact lens tilt upon residual astigmatism. *Am J Optom Arch Am Acad Optom*; 40: 730-744.
- Sarver M.D. 1969) A study of residual astigmatism. *Am J Optom Arch Am Acad Optom*;46: 578-582.
- Saunders H. (1981) Age dependence of human refractive errors. *Ophthal Physiol Opt*; 1:159-174.

- Saunders H. (1984) The astigmatic modulus and its age-dependence. *Ophthal Physiol Opt*; 4: 215-222.
- Sheard C.(1918) *Physiological Optics*. Chicago: Cleveland Press. p:36-67,139-146-236. Cited by Lyle(1990).
- Sheard W.(1920) Ophthalmometry and its application to ocular refraction and eye examination . *Am J Physiol Opt*. 4:357-397. Cited by Ludlam and Wittenberg(1967).
- Shipley T. and Rawlings S.C.(1970) The nonius horopter-II. An experimental report. *Vision Res*; 10: 1263 - 1290.
- Smith W.J., Pierscionek B.K.and Atchison D.A. (1991) The optical modelling of the human lens. *Oph Physiol Opt*; 11: 359-396.
- Sorsby A., Benjamin B. and Sheridan M. (1961) Refraction and its components during growth of the eye from the age of three . Medical Research Council Special report series No. 301, London.
- Sorsby A., Leary G.A. and Richards M.J.(1962a) Correlation ametropia and component ametropia. *Vision Research*; 2: 309-313.
- Sorsby A., Sheridan M. and Leary G.A. (1962b) Refraction and its components in twins. Medical Research Council Special Report Series No. 303. HMSO, London.
- Steele C.E., Crabb D.P. and Edgar D.F.(1992) The effect of different ocular fixation conditions on A-scan biometry measurements. *Ophthal Physiol Opt*; 12: 491-495.
- Stenstrom S.(1946) Investigation of the variation and correlations of the optical elements of human eyes . (Trans. 1948 Wooldf ,D.) *Am J Optom Mongraph* 58.
- Stenstrom S.(1948) Variation in the size and shape of the eye. *Acta Ophthalmologica*; 26: 559-567.
- Tait E.F.(1956) Intraocular astigmatism. *Amer J Ophthal*; 41: 813-825.
- Tate F.W., Safir A., Mills C.Z., Bowling J.E. Mc Donald J.I. and Carig M.R. (1987) Accuracy and reproducibility of keratometer reading. *CIAO J*; 13:50.
- Thompson H.S.(1987) The pupil. In *Adler's Physiology of the Eye: Clinical application*. eds. Moses R.A. and Hart W.M. Chapter 12. St Louis: Mosby.
- Tscherning M. (1924) *Physiological optics* (trans. Weiland C.) Keystone, Philadelphia.
- Ukai k. and Ichihaashi Y. (1991) Changes in ocular astigmatism over the whole range of accommodation. *Optom Vis Sci* 68: 813-818.
- Van Veen H.G. and Goss D.A. (1988) Simplified system of Purkinje image photography for phakometry. *Am J Otom Physiol Opt*; 65: 905.
- Von Bahr G.(1948) Measurements of the thickness of the cornea. *Acta Ophthalmologica (Basel)*; 26: 247-265.
- Weale R.A.(1963) *The Ageing Eye*. London: HK. Lewis.
- Weale R.A.(1982) *A Biography of the Eye*. London: Lewis.

- Weekers R., Delmarcelle Y.Luyckx-Bacus J. and Collington J. (1973) Morphological changes of the lens with age and cataract. Ciba foundation symposium; 19: 25-40. Elsevier Experta Medica, North Holland.
- Weekers R., Delmarcelle Y.Luyckx-Bacus J. and Collington J. (1975) Biometric of the crystalline lens. IN Bellows J G, (Ed) Cataract and abnormalities of the lens : 134-147. Grune and Stratton Inc. , London.
- Weisz and Caren L.(1978) Induced Against-the-rule Astigmatism in accommodative Disorders. J Am Optom Assoc.; 49: 335-336.
- White E.K.(1993) Modelling Ocular monochromatic aberrations using schematic eyes with homogenous media. Unpublished (PhD thesis) Aston university.
- Whitefoot H.D and Charman W.N.(1980) A comparison between laser and conventional subjective refraction. Ophthalmic Optician; 20: 169-173.
- Wood I.C.J, Papas F., Burghardt D.and Hardwick G. (1984) A clinical evaluation of the Nidek autorefractor. Ophthal Physiol Opt; 4: 169-178.
- Wood I.(1988) Computerised refractive examination. In Optometry, eds Edwards K. and Llewellyn R. London Butterworth.
- Worthey J.A. (1977) Simplified analysis of meridional refraction data.Am J Optom physiol Opt; 54: 771-775.
- Young T, (1807) Course of lectures in natural Philosophy and mechanical arts. Vol. 2 pp 588-589. Johnson, London.(Cited by Charman , 1983).
- Zadnik k, Mutti D. O. and Adams A.J.(1992) The repeatability of measurement of the ocular components. Invest Ophthalmol Vis Sci ,33: 2325-2333.
- Zinn K.M. (1972) The Pupil. Thomas: Springfield, Illinois.

APPENDICES

APPENDIX A: COMPUTER PROGRAMS

Appendix A1

CALCULATION OF MERIDIONAL DATA (NOTIONAL POWER) FOR REFRACTION AND ANTERIOR CORNEAL SURFACE RADIUS OF CURVATURE

Written in BASIC for the Macintosh computer using Microsoft Basic(d) (see section 4.3 for details).

```
10 REM - PROGRAM 1 : CALCULATES MEAN ± SD REFRACTION AND KERATOMETRY
20 REM - TAKES REPEAT READINGS IN FORM MEASURED (SPH/CYL(RX) OR XCYL(K))
30 REM - CALCULATES MERIDIONAL VALUES
40 REM- CALCULATES MEAN ± SD FOR EACH READY FOR INPUT INTO PROGRAM 2

50 REM ----- REFRACTION -----
60 REM - INPUT DATA
70 INPUT "NUMBER OF RX REPEATS";REP:PRINT :PRINT

80 FOR LOOP = 1 TO REP
90 CLS
100 PRINT"DATA SET ";LOOP:PRINT
110 PRINT"INPUT REFRACTIVE DATA IN NEGATIVE CYLINDER FORM":PRINT
120 INPUT"REFRACTIVE SPHERE (D)";RXSPH:PRINT
130 INPUT"REFRACTIVE CYLINDER (D)";RXCYL:PRINT
140 INPUT"REFRACTIVE CYLINDER AXIS (°)";RXAXIS:PRINT

150 REM - MERIDIONAL CALCULATIONS

160 RX180(LOOP)=RXSPH+(RXCYL*((SIN((RXAXIS-180)*.01745329278#))^2))
170 RX90(LOOP)=RXSPH+(RXCYL*((SIN((RXAXIS-90)*.01745329278#))^2))
180 RX135(LOOP)=RXSPH+(RXCYL*((SIN((RXAXIS-135)*.01745329278#))^2))
190 RX45(LOOP)=RXSPH+(RXCYL*((SIN((RXAXIS-45)*.01745329278#))^2))

200 NEXT LOOP

210 REM - STATISTICS
220 SUMRX180=0:SUMRX90=0:SUMRX135=0:SUMRX45=0
230SUMRX180SQUARE=0:SUMRX90SQUARE=0:SUMRX135SQUARE=0:SUMRX45SQUA=0

240 FOR LOOP = 1 TO REP

250 REM - CALCULATE SUMX
260 SUMRX180=SUMRX180+RX180(LOOP)
270 SUMRX90=SUMRX90+RX90(LOOP)
280 SUMRX135=SUMRX135+RX135(LOOP)
290 SUMRX45=SUMRX45+RX45(LOOP)

300 REM - CALCULATE SUMXSQUARE
310 SUMRX180SQUARE=SUMRX180SQUARE+(RX180(LOOP)^2)
320 SUMRX90SQUARE=SUMRX90SQUARE+(RX90(LOOP)^2)
330 SUMRX135SQUARE=SUMRX135SQUARE+(RX135(LOOP)^2)
340 SUMRX45SQUARE=SUMRX45SQUARE+(RX45(LOOP)^2)

350 NEXT LOOP

360 REM - CALCULATE MEANS
370 RX180MEAN =SUMRX180/REP
380 RX90MEAN =SUMRX90/REP
390 RX135MEAN =SUMRX135/REP
400 RX45MEAN =SUMRX45/REP
```

```

430 SUMDIFRX90SQUARE=SUMRX90SQUARE-(SUMRX90^2/REP)
440 SUMDIFRX135SQUARE=SUMRX135SQUARE-(SUMRX135^2/REP)
450 SUMDIFRX45SQUARE=SUMRX45SQUARE-(SUMRX45^2/REP)

460 REM - CALCULATE STANDARD DEVIATION (SD)
470 SDRX180= SQR(SUMDIFRX180SQUARE/(REP-1))
480 SDRX90= SQR(SUMDIFRX90SQUARE/(REP-1))
490 SDRX135= SQR(SUMDIFRX135SQUARE/(REP-1))
500 SDRX45= SQR(SUMDIFRX45SQUARE/(REP-1))

510 REM - PRINTOUT
520 CLS
530 PRINT "MERIDIONAL RESULTS":PRINT :PRINT
540 PRINT "MEAN RX 180 = ";INT(10000*RX180MEAN)/10000
550 PRINT "STANDARD DEVIATION ="; INT(100*SDRX180)/100: PRINT
560 PRINT "MEAN RX 90 = ";INT(10000*RX90MEAN)/10000
570 PRINT "STANDARD DEVIATION ="; INT(100*SDRX90)/100: PRINT
580 PRINT "MEAN RX 135 = ";INT(10000*RX135MEAN)/10000
590 PRINT "STANDARD DEVIATION ="; INT(100*SDRX135)/100: PRINT
600 PRINT "MEAN RX 45 = ";INT(10000*RX45MEAN)/10000
610 PRINT "STANDARD DEVIATION ="; INT(100*SDRX45)/100: PRINT

620 INPUT"ANY NUMBER TO PROCEED";NUM

630 REM ----- KERATOMETRY -----

640 REM - INPUT DATA
650 CLS
660 INPUT "NUMBER OF K REPEATS";REP:PRINT :PRINT

670 FOR LOOP = 1 TO REP
680 CLS

690 PRINT"DATA SET ";LOOP: PRINT
700 PRINT"INPUT KERATOMETRIC DATA IN CROSS CYLINDER FORM":PRINT
710 INPUT"RADIUS ALONG FLATTEST MERIDIAN (MM)";KFL:PRINT
720 INPUT"RADIUS ALONG STEEPEST MERIDIAN (D)";KST:PRINT
730 INPUT"FLATTEST MERIDIAN (°)";KFLA:PRINT

740 REM- CONVERT TO SPHERO CYLINDRICAL FORM
750 KSPH=KFL
760 KCYL=KST-KFL
770 KAXIS=KFLA

780 REM - MERIDIONAL CALCULATIONS

790 RX180(LOOP)=KSPH+(KCYL*((SIN((KAXIS-180)*.01745329278#))^2))
800 RX90(LOOP)=KSPH+(KCYL*((SIN((KAXIS-90)*.01745329278#))^2))
810 RX135(LOOP)=KSPH+(KCYL*((SIN((KAXIS-135)*.01745329278#))^2))
820 RX45(LOOP)=KSPH+(KCYL*((SIN((KAXIS-45)*.01745329278#))^2))

830 NEXT LOOP

840 REM - STATISTICS
850 SUMRX180=0:SUMRX90=0:SUMRX135=0:SUMRX45=0
860
SUMRX180SQUARE=0:SUMRX90SQUARE=0:SUMRX135SQUARE=0:SUMRX45SQUARE=0

870 FOR LOOP = 1 TO REP

880 REM - CALCULATE SUMX
890 SUMRX180=SUMRX180+RX180(LOOP)
900 SUMRX90=SUMRX90+RX90(LOOP)

```

```

910 SUMRX135=SUMRX135+RX135(LOOP)
920 SUMRX45=SUMRX45+RX45(LOOP)

930 REM - CALCULATE SUMXSQUARE
940 SUMRX180SQUARE=SUMRX180SQUARE+(RX180(LOOP)^2)
950 SUMRX90SQUARE=SUMRX90SQUARE+(RX90(LOOP)^2)
960 SUMRX135SQUARE=SUMRX135SQUARE+(RX135(LOOP)^2)
970 SUMRX45SQUARE=SUMRX45SQUARE+(RX45(LOOP)^2)

980 NEXT LOOP

990 REM - CALCULATE MEANS
1000 RX180MEAN =SUMRX180/REP
1010 RX90MEAN =SUMRX90/REP
1020 RX135MEAN =SUMRX135/REP
1030 RX45MEAN =SUMRX45/REP

1040 REM - CALCULATE SUMDIFSQUARE
1050 SUMDIFRX180SQUARE=SUMRX180SQUARE-(SUMRX180^2/REP)
1060 SUMDIFRX90SQUARE=SUMRX90SQUARE-(SUMRX90^2/REP)
1070 SUMDIFRX135SQUARE=SUMRX135SQUARE-(SUMRX135^2/REP)
1080 SUMDIFRX45SQUARE=SUMRX45SQUARE-(SUMRX45^2/REP)

1090 REM - CALCULATE STANDARD DEVIATION (SD)
1100 SDRX180= SQR(SUMDIFRX180SQUARE/(REP-1))
1110 SDRX90= SQR(SUMDIFRX90SQUARE/(REP-1))
1120 SDRX135= SQR(SUMDIFRX135SQUARE/(REP-1))
1130 SDRX45= SQR(SUMDIFRX45SQUARE/(REP-1))

1140 REM - PRINTOUT
1150 CLS
1160 PRINT "MERIDIONAL RESULTS":PRINT :PRINT
1170 PRINT "MEAN K 180 = ";INT(10000*RX180MEAN)/10000
1180 PRINT "STANDARD DEVIATION ="; INT(100*SDRX180)/100: PRINT
1190 PRINT "MEAN K 90 = ";INT(10000*RX90MEAN)/10000
1200 PRINT "STANDARD DEVIATION ="; INT(100*SDRX90)/100: PRINT
1210 PRINT "MEAN K 135 = ";INT(10000*RX135MEAN)/10000
1220 PRINT "STANDARD DEVIATION ="; INT(100*SDRX135)/100: PRINT
1230 PRINT "MEAN K 45 = ";INT(10000*RX45MEAN)/10000
1240 PRINT "STANDARD DEVIATION ="; INT(100*SDRX45)/100: PRINT

1250 INPUT"ANY NUMBER TO PROCEED";NUM
1260 END

```

Appendix A2

CALCULATION OF INTERNAL OCULAR SURFACE ASTIGMATISM

Written in BASIC for the Macintosh computer using Microsoft Basic(d) (see section 4.4 for details).

```
10 PRINT "PROGRAM 2":PRINT :PRINT
20 REM - ACCEPTS MERIDIONAL RX AND K DATA FROM PROGRAM 1.

30 REM - INPUT PARAMETERS
40 CLS
50 PRINT " IF REQUIRE 180°, 90° AND 135° MERIDIANS THEN PRESS 3":PRINT
60 PRINT " IF REQUIRE 180°, 90°, 135° AND 45° MERIDIANS THEN PRESS 4":PRINT
INPUT BUG

70 REM - CORNEAL THICKNESS (D1) FIXED AT 0.5 MM
80 D1=.0005
90 CLS
100 INPUT "UNMODIFIED ACD(MM)";DD2:D2=(DD2/1000)-D1:PRINT
110 INPUT "LENS(MM)";DD3:D3=DD3/1000:PRINT
120 INPUT "VITR(MM)";DD4:D4=DD4/1000:PRINT
130 REM - PHAKOMETER WORKING DISTANCE (DS) OF 25 MM
140 DS=.025

150 FOR LOOP = 1 TO BUG
160 CLS
170 IF LOOP = 1 THEN AXIS (LOOP)=180
180 IF LOOP = 2 THEN AXIS (LOOP)=90
190 IF LOOP = 3 THEN AXIS (LOOP)=135
200 IF LOOP = 4 THEN AXIS (LOOP)=45

210 PRINT "INPUT BIOMETRIC DATA ALONG"; AXIS(LOOP);"° MERIDIAN ":PRINT
:PRINT
220 INPUT "RX(D)";FSP(LOOP)
230 INPUT "R1(MM)";RR1:R1(LOOP)=RR1/1000
240 INPUT "H1(MM)";H1(LOOP)
250 INPUT "H2(MM)";H2(LOOP)
260 INPUT "H4(MM)";H4(LOOP)
270 NEXT LOOP

280 FOR LOOP = 1 TO BUG
290 IF LOOP = 1 THEN AXIS (LOOP)=180
300 IF LOOP = 2 THEN AXIS (LOOP)=90
310 IF LOOP = 3 THEN AXIS (LOOP)=135
320 IF LOOP = 4 THEN AXIS (LOOP)=45
330 CLS
340 PRINT "PROCESSING DATA FOR";AXIS(LOOP);"° MERIDIAN":PRINT :PRINT
350 FSP=FSP(LOOP):R1=R1(LOOP):H1=H1(LOOP):H2=H2(LOOP):H4=H4(LOOP)

360 REM - ASSUMED REFRACTIVE INDICES
370 N1=1:N2=1.3771:N3=1.3374:N4=1.42:N5=1.336

380 REM - REFRACTIVE/CATOPTRIC PROPERTIES OF FRONT CORNEA
390 F1=(N2-N1)/R1:F1(LOOP)=F1
400 F1C=(-N1-N1)/R1
410 M1=(N1/-DS)/((N1/-DS)+F1C)

420 REM - REFRACTIVE/CATOPTRIC PROPERTIES OF BACK CORNEA
```

```

430 M2=(H2/H1)*M1
440 D1A=N1/((N2/D1)-F1)
450 F2C=(N1/(DS+D1A))-((N1/(DS+D1A))/M2)
460 R2A=(-N1-N1)/F2C
470 R2=(N2/((N1/(D1A+R2A))+F1))-D1:R2(LOOP)=R2
480 F2=(N3-N2)/R2:F2(LOOP)=F2

490 REM - REFRACTIVE/CATOPTRIC PROPERTIES OF LENS SURFACES

500 REM - INITIAL ESTIMATE OF FRONT LENS POWER
510 F3=8.1
520 INCR=.01

530 REM - STEP ALONG RAY TRACE TO FIND BACK LENS POWER
540 V= 0
550 F4L1=FSP/(1-V*FSP)
560 F4L1A=F4L1+F1
570 F4L2=F4L1A/(1-((D1/N2)*F4L1A))
580 F4L2A=F4L2+F2
590 F4L3=F4L2A/(1-((D2/N3)*F4L2A))
600 F4L3A=F4L3+F3
610 F4L4=F4L3A/(1-((D3/N4)*F4L3A))
620 F4L4A=N5/D4
630 F4=F4L4A-F4L4:F4(LOOP)=F4
640 R4=(N5-N4)/F4:R4(LOOP)=R4

650 REM - STEP ALONG BACK RAY TRACE FOR BACK LENS MIRROR VERTEX
660 A4AL1=N4/D3
670 A4AL1A=A4AL1-F3
680 A4AL2=A4AL1A/(1+((D2/N3)*A4AL1A))
690 A4AL2A=A4AL2-F2
700 A4AL3=A4AL2A/(1+((D1/N2)*A4AL2A))
710 A4AL3A=A4AL3-F1
720 A4A=N1/A4AL3A

730 REM - STEP ALONG BACK RAY TRACE FOR BACK LENS MIRROR CURVATURE
740 C4AL1=N4/(R4+D3)
750 C4AL1A=C4AL1-F3
760 C4AL2=C4AL1A/(1+((D2/N3)*C4AL1A))
770 C4AL2A=C4AL2-F2
780 C4AL3=C4AL2A/(1+((D1/N2)*C4AL2A))
790 C4AL3A=C4AL3-F1
800 C4A=N1/C4AL3A
810 R4A=C4A-A4A
820 F4C=(-N1-N1)/R4A

830 REM - CALCULATE ESTIMATE OF PURKINJE IV
840 M4=(N1/-(DS+A4A))/((N1/-(DS+A4A))+F4C)
850 H4EST=M4/M1

860 REM - ITERATION / OUTPUT
870 F3(LOOP)=F3
880 DIFF=-(H4/H1)-H4EST
890 IF SQR(DIFF^2)<.0005 THEN GOTO 940
900 IF DIFF < -.0005 THEN F3 = F3+INCR
910 IF DIFF <-.0005 THEN GOTO 550
920 IF DIFF >.0005 THEN F3 = F3-INCR
930 IF DIFF >.0005 THEN GOTO 550

940 CLS:PRINT "OUTPUT FOR";AXIS(LOOP);"° MERIDIAN"
950 PRINT "R1=";(INT(100*R1(LOOP)*1000)/100)
960 PRINT "F1=";(INT(100*F1(LOOP))/100):PRINT
970 PRINT "R2=";(INT(100*(R2(LOOP)*1000)/100)

```

```

980 PRINT "F2=";(INT(100*F2(LOOP))/100);PRINT
990 R3(LOOP)=(1000 *(N4-N3))/F3(LOOP);PRINT "R3=";(INT(100*R3(LOOP))/100)
1000 PRINT "F3=";(INT(100*F3(LOOP))/100);PRINT
1010 PRINT "R4=";(INT(100*(R4(LOOP)*1000))/100)
1020 PRINT "F4=";(INT(100*F4(LOOP))/100)
1030 PRINT :PRINT:INPUT"ANY NUMBER TO GO ON";ZZZ:NEXT LOOP

1040 REM MULTIMERIDIONAL ANALYSIS
1050 REM SCHEME DEVELOPED BY LONG (1974)
1060 REM WRITTEN FOR BBC MICRO BY PHIL ARMSTRONG (1991)
1070 REM ADAPTED FOR APPLE MACINTOSH BY MARK DUNNE (1991)

1080 FOR SURF=1 TO 5
1090 CLS:PRINT "MULTIMERIDIONAL ANALYSIS IN PROGRESS":PRINT :PRINT

1100 FOR LOOP=1 TO BUG

1110 IF SURF = 1 THEN POWER(LOOP) = FSP(LOOP)
1120 IF SURF = 2 THEN POWER(LOOP) = F1(LOOP)
1130 IF SURF = 3 THEN POWER(LOOP) = F2(LOOP)
1140 IF SURF = 4 THEN POWER(LOOP) = F3(LOOP)
1150 IF SURF = 5 THEN POWER(LOOP) = F4(LOOP)

1160 REM - CHANGE POWER MERIDIANS TO CYLINDER AXES
1170 IF LOOP = 1 THEN AXIS (LOOP)=90
1180 IF LOOP = 2 THEN AXIS (LOOP)=180
1190 IF LOOP = 3 THEN AXIS (LOOP)=45
1200 IF LOOP = 4 THEN AXIS (LOOP)=135

1210 NEXT LOOP
1220 REM ***** MATRIX W *****
1230 W11=BUG:W12=0:W13=0:W21=0:W22=0:W23=0:W31=0:W32=0:W33=0:V1=0:V2=0:V3=0
1240 FOR LOOP=1 TO BUG
1250 V1=V1+POWER(LOOP)
1260 V2=V2+(POWER(LOOP)*SIN(2*(AXIS(LOOP)*.01745329278#)))
1270 V3=V3+(POWER(LOOP)*COS(2*(AXIS(LOOP)*.01745329278#)))
1280 W12=W12+SIN(2*(AXIS(LOOP)*.01745329278#))
1290 W13=W13+COS(2*(AXIS(LOOP)*.01745329278#))
1300 W22=W22+SIN(2*(AXIS(LOOP)*.01745329278#))^2
1310 W23=W23+SIN(2*(AXIS(LOOP)*.01745329278#))*COS(2*(AXIS(LOOP)*.01745329278#))
1320 W33=W33+COS(2*(AXIS(LOOP)*.01745329278#))^2
1330 NEXT LOOP
1340 W21=W12:W31=W13:W32=W23

1350 REM ***** MATRIX Wt = MATRIX W *****

1360 REM ***** MATRIX W* *****
1370 COFACTORW11=1*((W22*W33)-(W23*W32))
1380 COFACTORW21=-1*((W12*W33)-(W13*W32))
1390 COFACTORW31=1*((W12*W23)-(W13*W22))
1400 COFACTORW12=-1*((W21*W33)-(W23*W31))
1410 COFACTORW22=1*((W11*W33)-(W13*W31))
1420 COFACTORW32=-1*((W11*W23)-(W13*W21))
1430 COFACTORW13=1*((W21*W32)-(W22*W31))
1440 COFACTORW23=-1*((W11*W32)-(W12*W31))
1450 COFACTORW33=1*((W11*W22)-(W12*W21))

1460 REM ***** DETERMINANT *****
1470
DETERMINANT=(W11*COFACTORW11)+(W21*COFACTORW21)+(W31*COFACTORW31)

1480 REM ***** U=W-1.V *****

```

```

1490
U1=((COFACTORW11*V1)+(COFACTORW21*V2)+(COFACTORW31*V3))/DETERMINANT:A
=U1
1500
U2=((COFACTORW12*V1)+(COFACTORW22*V2)+(COFACTORW32*V3))/DETERMINANT:B
=U2
1510
U3=((COFACTORW13*V1)+(COFACTORW23*V2)+(COFACTORW33*V3))/DETERMINANT:C
=U3

1520 REM ***** SOLVE A,B,C *****
1530 AXIS=(ATN(B/C)/.01745329278#)/2
1540 CYL=(2*C)/(COS(2*(AXIS*.01745329278#)))
1550 SPH=A-(CYL/2)

1560 REM ***CONVERT TO MINUS-CYLINDER ***
1570 IF CYL>0 THEN GOTO 1580 ELSE GOTO 1610
1580 SPH=CYL+SPH:CYL=-CYL
1590 IF AXIS>=90 THEN AXIS=AXIS-90 ELSE AXIS=AXIS+90

1600 REM ***AXIS BETWEEN 1° AND 180°***
1610 IF AXIS<.005 AND AXIS>-.005 THEN AXIS=0
1620 IF AXIS<=0 THEN AXIS=AXIS+180
1630 CLS
1640 PRINT:PRINT

1650 REM ***** PRINT TO 2 DEC PLACES *****
1660 IF SURF = 1 THEN PRINT "REFRACTIVE ERROR":PRINT :PRINT
1670 IF SURF = 2 THEN PRINT "FRONT CORNEAL SURFACE":PRINT :PRINT
1680 IF SURF = 3 THEN PRINT "REAR CORNEAL SURFACE":PRINT :PRINT
1690 IF SURF = 4 THEN PRINT "FRONT LENS SURFACE":PRINT :PRINT
1700 IF SURF = 5 THEN PRINT "REAR LENS SURFACE":PRINT :PRINT

1710 PRINT "Sphere (D) "; (INT(SPH*100))/100:PRINT
1720 PRINT "Cylinder (D) "; (INT(CYL*100))/100:PRINT
1730 PRINT "Axis (°) "; (INT(AXIS*10))/10:PRINT

1740 INPUT"ANY NUMBER TO GO ON";ZZZ
1750 NEXT SURF
1760 END

```

Appendix A3

CALCULATION OF THE CONTRIBUTION TO RESIDUAL ASTIGMATISM OF THE INTERNAL OCULAR SURFACES AND THEIR AXIAL SEPARATION

Written in BASIC for the Macintosh computer using Microsoft Basic(d) (see section 4.5 for details).

```
10 REM - PROGRAM 3: VERGENCE ANALYSIS OF RESIDUAL ASTIGMATISM
20 REM - UTILIZES SPHERO-CYLINDERS CALCULATED IN PROGRAM 2.

30 REM-EYE PARAMETERS

40 REM - INPUT SPHERO-CYLINDER POWERS

50 PRINT"ENTER SURFACE SPHERO-CYLINDERS (+ OR - CYLINDER OK)"

60 PRINT "ANTERIOR CORNEAL SURFACE"
70 INPUT "SPHERE (D)";F1S
80 INPUT "CYLINDER (D)";F1C
90 INPUT "AXIS (°)";F1A

100 PRINT "POSTERIOR CORNEAL SURFACE"
110 INPUT "SPHERE (D)";F2S
120 INPUT "CYLINDER (D)";F2C
130 INPUT "AXIS (°)";F2A

140 PRINT "ANTERIOR CRYSTALLINE LENS SURFACE"
150 INPUT "SPHERE (D)";F3S
160 INPUT "CYLINDER (D)";F3C
170 INPUT "AXIS (°)";F3A

180 PRINT "POSTERIOR CRYSTALLINE LENS SURFACE"
190 INPUT "SPHERE (D)";F4S
200 INPUT "CYLINDER (D)";F4C
210 INPUT "AXIS (°)";F4A

220 REM - INPUT AXIAL DISTANCES
230 CLS
240 PRINT "ENTER AXIAL DISTANCES (CORNEAL THICKNESS = 0.5 MM)"
250 D1=.0005

260 PRINT :INPUT "ANTERIOR CHAMBER DEPTH [WITH CORNEA] (MM)";ACD
270 D2= (ACD/1000)-D1

280 PRINT :INPUT "CRYSTALLINE LENS THICKNESS (MM)";LT
290 D3= LT/1000

300 REM - INPUT SPHERO-CYLINDER REFRACTIVE ERROR
310 CLS
320 PRINT "SPECTACLE REFRACTION"
330 INPUT "SPHERE (D)";KS
340 INPUT "CYLINDER (D)";KC
350 INPUT "AXIS (°)";KA

360 REM - ASSUMED REFRACTIVE INDICES
370 N2=1.3771
380 N3=1.3374
```


390 N4=1.42

400 REM - RADIAN CONVERSION
410 RAD=3.141592653589#/180

420 REM - REFER SPECTACLE REFRACTION TO CORNEAL VERTEX
430 REM - VERTEX DISTANCE (V) IS 0 MM
440 V= 0
450 L1SPC=(KS+KC)/(1-V*(KS+KC))
460 L1S=KS/(1-V*KS)
470 L1C=L1SPC-L1S
480 L1A=KA

490 REM - ASTIGMATIC DECOMPOSITION OF CORNEAL VERTEX REFRACTION (L1)
500 L1MRP=L1S+(L1C/2)
510 L1C0=L1C*COS(2*L1A*RAD)
520 L1C45=L1C*SIN(2*L1A*RAD)

530 REM - ASTIGMATIC DECOMPOSITION OF FRONT CORNEAL POWER (F1)
540 F1MRP=F1S+(F1C/2)
550 F1C0=F1C*COS(2*F1A*RAD)
560 F1C45=F1C*SIN(2*F1A*RAD)

570 REM - RESIDUAL ASTIGMATISM
580 RESC0=-L1C0-F1C0
590 RESC45=-L1C45-F1C45
600 RESC=SQR(RESC0^2+RESC45^2)
610 RESA=ATN((RESC-RESC0)/RESC45)/RAD
620 IF RESA<0 THEN RESA=RESA+180

630 REM - REFRACTION AT FRONT CORNEAL SURFACE
640 L1AMRP=L1MRP+F1MRP
650 L1AC0=L1C0+F1C0
660 L1AC45=L1C45+F1C45

670 REM - ASTIGMATIC RECOMPOSITION FOR PRINCIPAL VERGENCES
680 REM - AFTER FRONT CORNEA
690 L1AC=SQR(L1AC0^2+L1AC45^2)
700 L1AS=L1AMRP-(L1AC/2)
710 L1AA=ATN((L1AC-L1AC0)/L1AC45)/RAD
720 L1ASPC=L1AS+L1AC

730 REM - CHANGE IN PRINCIPAL VERGENCES DUE TO CORNEAL THICKNESS (D1)
740 L2SPC=L1ASPC/(1-((D1/N2)*L1ASPC))
750 L2S=L1AS/(1-((D1/N2)*L1AS))
760 L2C=L2SPC-L2S
770 L2A=L1AA

780 REM - ASTIGMATIC DECOMPOSITION OF VERGENCE (L2) AT REAR CORNEA
790 L2MRP=L2S+(L2C/2)
800 L2C0=L2C*COS(2*L2A*RAD)
810 L2C45=L2C*SIN(2*L2A*RAD)

820 REM - (-L1A+L2) MRP,C0,C45 GIVES CONTRIBUTION OF CORNEAL THICKNESS
830 D1MRP=-L1AMRP+L2MRP
840 D1C0=-L1AC0+L2C0
850 D1C45=-L1AC45+L2C45
860 D1C=SQR(D1C0^2+D1C45^2)
870 D1S=D1MRP-(D1C/2)
880 D1A=ATN((D1C-D1C0)/D1C45)/RAD
890 IF D1A<0 THEN D1A=D1A+180

900 REM - ASTIGMATIC DECOMPOSITION OF REAR CORNEAL POWER (F2)

910 $F2MRP = F2S + (F2C/2)$
 920 $F2C0 = F2C * \cos(2 * F2A * \text{RAD})$
 930 $F2C45 = F2C * \sin(2 * F2A * \text{RAD})$

940 REM - REFRACTION AT REAR CORNEAL SURFACE
 950 $L2AMRP = L2MRP + F2MRP$
 960 $L2AC0 = L2C0 + F2C0$
 970 $L2AC45 = L2C45 + F2C45$

980 REM - ASTIGMATIC RECOMPOSITION FOR PRINCIPAL VERGENCES
 990 REM - AFTER REAR CORNEA
 1000 $L2AC = \text{SQR}(L2AC0^2 + L2AC45^2)$
 1010 $L2AS = L2AMRP - (L2AC/2)$
 1020 $L2AA = \text{ATN}((L2AC - L2AC0) / L2AC45) / \text{RAD}$
 1030 $L2ASPC = L2AS + L2AC$

1040 REM - CHANGE IN PRINCIPAL VERGENCES DUE TO ANTERIOR CHAMBER (D3)
 1050 $L3SPC = L2ASPC / (1 - ((D2/N3) * L2ASPC))$
 1060 $L3S = L2AS / (1 - ((D2/N3) * L2AS))$
 1070 $L3C = L3SPC - L3S$
 1080 $L3A = L2AA$

1090 REM - ASTIGMATIC DECOMPOSITION OF VERGENCE (L3) AT FRONT LENS
 1100 $L3MRP = L3S + (L3C/2)$
 1110 $L3C0 = L3C * \cos(2 * L3A * \text{RAD})$
 1120 $L3C45 = L3C * \sin(2 * L3A * \text{RAD})$

1130 REM - (-L2A+L3) MRP,C0,C45 GIVES CONTRIBUTION OF ANTERIOR CHAMBER
 1140 $D2MRP = -L2AMRP + L3MRP$
 1150 $D2C0 = -L2AC0 + L3C0$
 1160 $D2C45 = -L2AC45 + L3C45$
 1170 $D2C = \text{SQR}(D2C0^2 + D2C45^2)$
 1180 $D2S = D2MRP - (D2C/2)$
 1190 $D2A = \text{ATN}((D2C - D2C0) / D2C45) / \text{RAD}$
 1200 IF $D2A < 0$ THEN $D2A = D2A + 180$

1210 REM - ASTIGMATIC DECOMPOSITION OF FRONT LENS POWER (F3)
 1220 $F3MRP = F3S + (F3C/2)$
 1230 $F3C0 = F3C * \cos(2 * F3A * \text{RAD})$
 1240 $F3C45 = F3C * \sin(2 * F3A * \text{RAD})$

1250 REM - REFRACTION AT FRONT LENS SURFACE
 1260 $L3AMRP = L3MRP + F3MRP$
 1270 $L3AC0 = L3C0 + F3C0$
 1280 $L3AC45 = L3C45 + F3C45$

1290 REM - ASTIGMATIC RECOMPOSITION FOR PRINCIPAL VERGENCES
 1300 REM - AFTER FRONT LENS
 1310 $L3AC = \text{SQR}(L3AC0^2 + L3AC45^2)$
 1320 $L3AS = L3AMRP - (L3AC/2)$
 1330 $L3AA = \text{ATN}((L3AC - L3AC0) / L3AC45) / \text{RAD}$
 1340 $L3ASPC = L3AS + L3AC$

1350 REM - CHANGE IN PRINCIPAL VERGENCES DUE TO LENS THICKNESS (D3)
 1360 $L4SPC = L3ASPC / (1 - ((D3/N4) * L3ASPC))$
 1370 $L4S = L3AS / (1 - ((D3/N4) * L3AS))$
 1380 $L4C = L4SPC - L4S$
 1390 $L4A = L3AA$

1400 REM - ASTIGMATIC DECOMPOSITION OF VERGENCE (L4) AT BACK LENS
 1410 $L4MRP = L4S + (L4C/2)$
 1420 $L4C0 = L4C * \cos(2 * L4A * \text{RAD})$
 1430 $L4C45 = L4C * \sin(2 * L4A * \text{RAD})$

```

1440 REM - (-L3A+L4) MRP,C0,C45 GIVES CONTRIBUTION OF LENS THICKNESS
1450 D3MRP=-L3AMRP+L4MRP
1460 D3C0=-L3AC0+L4C0
1470 D3C45=-L3AC45+L4C45
1480 D3C=SQR(D3C0^2+D3C45^2)
1490 D3S=D3MRP-(D3C/2)
1500 D3A=ATN((D3C-D3C0)/D3C45)/RAD
1510 IF D3A<0 THEN D3A=D3A+180

1520 REM - ASTIGMATIC DECOMPOSITION OF BACK LENS POWER (F4)
1530 F4MRP=F4S+(F4C/2)
1540 F4C0=F4C*COS(2*F4A*RAD)
1550 F4C45=F4C*SIN(2*F4A*RAD)

1560 REM - REFRACTION AT BACK LENS SURFACE
1570 L4AMRP=L4MRP+F4MRP
1580 L4AC0=L4C0+F4C0
1590 L4AC45=L4C45+F4C45

1600 REM - CHECK FOR ZERO CYLINDER AFTER BACK LENS
1610 L4AC=SQR(L4AC0^2+L4AC45^2)
1620 CLS:PRINT "L4AC SHOULD BE ZERO =";(INT(L4AC*1000000#))/1000000#
1630 INPUT XXX

1640 REM - PRINTOUT
1650 CLS
1660 PRINT "OCULAR COMPONENT CONTRIBUTIONS : "
1670 PRINT "MRP","C0","C45","CYL","AXIS"
1680 PRINT "CORNEAL DEPTH : "
1690 PRINT
INT(D1MRP*10000)/10000,INT(D1C0*10000)/10000,INT(D1C45*10000)/10000,INT(D1C*1000)/
1000,INT(D1A*1000)/1000
1700 PRINT "REAR CORNEAL SURFACE : "
1710 PRINT
INT(F2MRP*10000)/10000,INT(F2C0*10000)/10000,INT(F2C45*10000)/10000,INT(F2C*1000)/1
000,INT(F2A*1000)/1000
1720 PRINT "ANTERIOR CHAMBER : "
1730 PRINT
INT(D2MRP*10000)/10000,INT(D2C0*10000)/10000,INT(D2C45*10000)/10000,INT(D2C*1000)/
1000,INT(D2A*1000)/1000
1740 PRINT "FRONT LENS SURFACE : "
1750 PRINT
INT(F3MRP*10000)/10000,INT(F3C0*10000)/10000,INT(F3C45*10000)/10000,INT(F3C*1000)/1
000,INT(F3A*1000)/1000
1760 PRINT "LENS THICKNESS : "
1770 PRINT
INT(D3MRP*10000)/10000,INT(D3C0*10000)/10000,INT(D3C45*10000)/10000,INT(D3C*1000)/
1000,INT(D3A*1000)/1000
1780 PRINT "BACK LENS SURFACE : "
1790 PRINT
INT(F4MRP*10000)/10000,INT(F4C0*10000)/10000,INT(F4C45*10000)/10000,INT(F4C*1000)/1
000,INT(F4A*1000)/1000
1800 PRINT "RESIDUAL ASTIGMATISM : "
1810 PRINT
"N/A",INT(RESC0*10000)/10000,INT(RESC45*10000)/10000,INT(RESC*1000)/1000,INT(RESA
*1000)/1000
1820 PRINT :INPUT"HIT ANY KEY TO GO AHEAD";XXXX

1830 END

```

Appendix A4

DETERMINATION OF RANDOM EXPERIMENTAL ERRORS INVOLVED IN THE CALCULATION OF MERIDIONAL SURFACE POWERS

Written in BASIC for the Macintosh computer using Microsoft Basic(d) (see section 4.6 for details).

```
10 PRINT "PROGRAM 4":PRINT :PRINT
20 REM - DETERMINES R.M.S. ERRORS IN CALCULATION
30 REM - OF MERIDIONAL SURFACE POWERS (PROGRAM 2)

40 REM - INPUT PARAMETERS

50 REM - CORNEAL THICKNESS (D1) FIXED AT 0.5 MM
60 D1=.0005

70 INPUT "UNMODIFIED ACD(MM)";DD2:D2=(DD2/1000)-D1
80 INPUT "ACD MEASUREMENT UNCERTAINTY";SDDD2:SDD2=(SDDD2/1000):PRINT
90 INPUT "LENS(MM)";DD3:D3=DD3/1000
100 INPUT "LENS MEASUREMENT UNCERTAINTY ";SDDD3:SDD3=(SDDD3/1000):PRINT
110 INPUT "VITR(MM)";DD4:D4=DD4/1000
120 INPUT "VITR MEASUREMENT UNCERTAINTY";SDDD4:SDD4=(SDDD4/1000):PRINT

130 REM - PHAKOMETER WORKING DISTANCE (DS) OF 25 MM
140 DS=.025

150 CLS
160 INPUT "RX(D)";FSP
170 INPUT "RX MEASUREMENT UNCERTAINTY";SDFSP:PRINT
180 INPUT "R1(MM)";RR1:R1=RR1/1000
190 INPUT "R1 MEASUREMENT UNCERTAINTY";SDRR1:SDR1=SDRR1/1000:PRINT
200 INPUT "H1(MM)";H1
210 INPUT "H1 MEASUREMENT UNCERTAINTY";SDH1:PRINT
220 INPUT "H2(MM)";H2
230 INPUT "H2 MEASUREMENT UNCERTAINTY";SDH2:PRINT
240 INPUT "H4(MM)";H4
250 INPUT "H4 MEASUREMENT UNCERTAINTY";SDH4:PRINT

260 CLS
270 PRINT "PROCESSING DATA":PRINT :PRINT

280 REM - ALTER EACH PARAMETER, IN TURN, BY - THEN + MEASUREMENT
    UNCERTAINTY
290 FOR EEL = 1 TO 2
300 FOR EL = 1 TO 9
310 IF EL = 2 AND EEL = 1 THEN D2 = D2-SDD2
320 IF EL = 2 AND EEL = 2 THEN D2 = D2+SDD2
330 IF EL = 3 AND EEL = 1 THEN D3 = D3-SDD3
340 IF EL = 3 AND EEL = 2 THEN D3 = D3+SDD3
350 IF EL = 4 AND EEL = 1 THEN D4 = D4-SDD4
360 IF EL = 4 AND EEL = 2 THEN D4 = D4+SDD4
370 IF EL = 5 AND EEL = 1 THEN FSP = FSP-SDFSP
380 IF EL = 5 AND EEL = 2 THEN FSP = FSP+SDFSP
390 IF EL = 6 AND EEL = 1 THEN R1 = R1-SDR1
400 IF EL = 6 AND EEL = 2 THEN R1 = R1+SDR1
410 IF EL = 7 AND EEL = 1 THEN H1 = H1-SDH1
420 IF EL = 7 AND EEL = 2 THEN H1 = H1+SDH1
430 IF EL = 8 AND EEL = 1 THEN H2 = H2-SDH2
```

```

440 IF EL = 8 AND EEL = 2 THEN H2 = H2+SDH2
450 IF EL = 9 AND EEL = 1 THEN H4 = H4-SDH4
460 IF EL = 9 AND EEL = 2 THEN H4 = H4+SDH4

470 PRINT "ERROR LOOP =";EEL,EL:PRINT

480 REM - ASSUMED REFRACTIVE INDICES

490 N1=1:N2=1.3771:N3=1.3374:N4=1.42:N5=1.336

500 REM - REFRACTIVE/CATOPTRIC PROPERTIES OF FRONT CORNEA
510 F1=(N2-N1)/R1:F1=F1
520 F1C=(-N1-N1)/R1
530 M1=(N1/-DS)/((N1/-DS)+F1C)

540 REM - REFRACTIVE/CATOPTRIC PROPERTIES OF BACK CORNEA
550 M2=(H2/H1)*M1
560 D1A=N1/((N2/D1)-F1)
570 F2C=(N1/(DS+D1A))-((N1/(DS+D1A))/M2)
580 R2A=(-N1-N1)/F2C
590 R2=(N2/((N1/(D1A+R2A))+F1))-D1
600 F2=(N3-N2)/R2

610 REM - REFRACTIVE/CATOPTRIC PROPERTIES OF LENS SURFACES

620 REM - INITIAL ESTIMATE OF FRONT LENS POWER
630 F3=8.1
640 INCR=.01

650 REM - STEP ALONG RAY TRACE TO FIND BACK LENS POWER
660 REM - BACK VERTEX DISTANCE = 0.012 M
670 F4L1=FSP/(1- (.012*FSP))
680 F4L1A=F4L1+F1
690 F4L2=F4L1A/(1-((D1/N2)*F4L1A))
700 F4L2A=F4L2+F2
710 F4L3=F4L2A/(1-((D2/N3)*F4L2A))
720 F4L3A=F4L3+F3
730 F4L4=F4L3A/(1-((D3/N4)*F4L3A))
740 F4L4A=N5/D4
750 F4=F4L4A-F4L4
760 R4=(N5-N4)/F4

770 REM - STEP ALONG BACK RAY TRACE FOR BACK LENS MIRROR VERTEX
780 A4AL1=N4/D3
790 A4AL1A=A4AL1-F3
800 A4AL2=A4AL1A/(1+((D2/N3)*A4AL1A))
810 A4AL2A=A4AL2-F2
820 A4AL3=A4AL2A/(1+((D1/N2)*A4AL2A))
830 A4AL3A=A4AL3-F1
840 A4A=N1/A4AL3A

850 REM - STEP ALONG BACK RAY TRACE FOR BACK LENS MIRROR CURVATURE
860 C4AL1=N4/(R4+D3)
870 C4AL1A=C4AL1-F3
880 C4AL2=C4AL1A/(1+((D2/N3)*C4AL1A))
890 C4AL2A=C4AL2-F2
900 C4AL3=C4AL2A/(1+((D1/N2)*C4AL2A))
910 C4AL3A=C4AL3-F1
920 C4A=N1/C4AL3A
930 R4A=C4A-A4A
940 F4C=(-N1-N1)/R4A

950 REM - CALCULATE ESTIMATE OF PURKINJE IV

```

```

960 M4=(N1/-(DS+A4A))/((N1/-(DS+A4A))+F4C)
970 H4EST=M4/M1

```

```

980 REM - ITERATION / OUTPUT

```

```

990 DIFF=(H4/H1)-H4EST
1000 IF SQR(DIFF^2)<.0005 THEN GOTO 1050
1010 IF DIFF < -.0005 THEN F3 = F3+INCR
1020 IF DIFF <-.0005 THEN GOTO 670
1030 IF DIFF >.0005 THEN F3 = F3-INCR
1040 IF DIFF >.0005 THEN GOTO 670

```

```

1050 REM - STORE CALCULATED VALUES FOR EACH RUN

```

```

1060 FF1(EEL,EL)=F1:FF2(EEL,EL)=F2
1070 FF3(EEL,EL)=F3:FF4(EEL,EL)=F4

```

```

1080 REM - NOW CONVERT ALTERED VALUES BACK TO ORIGINAL BEFORE NEXT RUN

```

```

1090 IF EL = 2 AND EEL = 1 THEN D2 = D2+SDD2
1100 IF EL = 2 AND EEL = 2 THEN D2 = D2-SDD2
1110 IF EL = 3 AND EEL = 1 THEN D3 = D3+SDD3
1120 IF EL = 3 AND EEL = 2 THEN D3 = D3-SDD3
1130 IF EL = 4 AND EEL = 1 THEN D4 = D4+SDD4
1140 IF EL = 4 AND EEL = 2 THEN D4 = D4-SDD4
1150 IF EL = 5 AND EEL = 1 THEN FSP = FSP+SDFSP
1160 IF EL = 5 AND EEL = 2 THEN FSP = FSP-SDFSP
1170 IF EL = 6 AND EEL = 1 THEN R1 = R1+SDR1
1180 IF EL = 6 AND EEL = 2 THEN R1 = R1-SDR1
1190 IF EL = 7 AND EEL = 1 THEN H1 = H1+SDH1
1200 IF EL = 7 AND EEL = 2 THEN H1 = H1-SDH1
1210 IF EL = 8 AND EEL = 1 THEN H2 = H2+SDH2
1220 IF EL = 8 AND EEL = 2 THEN H2 = H2-SDH2
1230 IF EL = 9 AND EEL = 1 THEN H4 = H4+SDH4
1240 IF EL = 9 AND EEL = 2 THEN H4 = H4-SDH4

```

```

1250 NEXT EL
1260 NEXT EEL

```

```

1270 REM - ERRORS

```

```

1280 F1ACD=((ABS(FF1(1,2)-FF1(1,1))+ABS(FF1(2,2)-FF1(1,1)))/2)^2
1290 F2ACD=((ABS(FF2(1,2)-FF2(1,1))+ABS(FF2(2,2)-FF2(1,1)))/2)^2
1300 F3ACD=((ABS(FF3(1,2)-FF3(1,1))+ABS(FF3(2,2)-FF3(1,1)))/2)^2
1310 F4ACD=((ABS(FF4(1,2)-FF4(1,1))+ABS(FF4(2,2)-FF4(1,1)))/2)^2
1320 F1LEN=((ABS(FF1(1,3)-FF1(1,1))+ABS(FF1(2,3)-FF1(1,1)))/2)^2
1330 F2LEN=((ABS(FF2(1,3)-FF2(1,1))+ABS(FF2(2,3)-FF2(1,1)))/2)^2
1340 F3LEN=((ABS(FF3(1,3)-FF3(1,1))+ABS(FF3(2,3)-FF3(1,1)))/2)^2
1350 F4LEN=((ABS(FF4(1,3)-FF4(1,1))+ABS(FF4(2,3)-FF4(1,1)))/2)^2
1360 F1VIT=((ABS(FF1(1,4)-FF1(1,1))+ABS(FF1(2,4)-FF1(1,1)))/2)^2
1370 F2VIT=((ABS(FF2(1,4)-FF2(1,1))+ABS(FF2(2,4)-FF2(1,1)))/2)^2
1380 F3VIT=((ABS(FF3(1,4)-FF3(1,1))+ABS(FF3(2,4)-FF3(1,1)))/2)^2
1390 F4VIT=((ABS(FF4(1,4)-FF4(1,1))+ABS(FF4(2,4)-FF4(1,1)))/2)^2
1400 F1FSP=((ABS(FF1(1,5)-FF1(1,1))+ABS(FF1(2,5)-FF1(1,1)))/2)^2
1410 F2FSP=((ABS(FF2(1,5)-FF2(1,1))+ABS(FF2(2,5)-FF2(1,1)))/2)^2
1420 F3FSP=((ABS(FF3(1,5)-FF3(1,1))+ABS(FF3(2,5)-FF3(1,1)))/2)^2
1430 F4FSP=((ABS(FF4(1,5)-FF4(1,1))+ABS(FF4(2,5)-FF4(1,1)))/2)^2
1440 F1R1=((ABS(FF1(1,6)-FF1(1,1))+ABS(FF1(2,6)-FF1(1,1)))/2)^2
1450 F2R1=((ABS(FF2(1,6)-FF2(1,1))+ABS(FF2(2,6)-FF2(1,1)))/2)^2
1460 F3R1=((ABS(FF3(1,6)-FF3(1,1))+ABS(FF3(2,6)-FF3(1,1)))/2)^2
1470 F4R1=((ABS(FF4(1,6)-FF4(1,1))+ABS(FF4(2,6)-FF4(1,1)))/2)^2
1480 F1H1=((ABS(FF1(1,7)-FF1(1,1))+ABS(FF1(2,7)-FF1(1,1)))/2)^2
1490 F2H1=((ABS(FF2(1,7)-FF2(1,1))+ABS(FF2(2,7)-FF2(1,1)))/2)^2
1500 F3H1=((ABS(FF3(1,7)-FF3(1,1))+ABS(FF3(2,7)-FF3(1,1)))/2)^2
1510 F4H1=((ABS(FF4(1,7)-FF4(1,1))+ABS(FF4(2,7)-FF4(1,1)))/2)^2
1520 F1H2=((ABS(FF1(1,8)-FF1(1,1))+ABS(FF1(2,8)-FF1(1,1)))/2)^2

```

```

1530 F2H2=((ABS(FF2(1,8)-FF2(1,1))+ABS(FF2(2,8)-FF2(1,1)))/2)^2
1540 F3H2=((ABS(FF3(1,8)-FF3(1,1))+ABS(FF3(2,8)-FF3(1,1)))/2)^2
1550 F4H2=((ABS(FF4(1,8)-FF4(1,1))+ABS(FF4(2,8)-FF4(1,1)))/2)^2
1560 F1H4=((ABS(FF1(1,9)-FF1(1,1))+ABS(FF1(2,9)-FF1(1,1)))/2)^2
1570 F2H4=((ABS(FF2(1,9)-FF2(1,1))+ABS(FF2(2,9)-FF2(1,1)))/2)^2
1580 F3H4=((ABS(FF3(1,9)-FF3(1,1))+ABS(FF3(2,9)-FF3(1,1)))/2)^2
1590 F4H4=((ABS(FF4(1,9)-FF4(1,1))+ABS(FF4(2,9)-FF4(1,1)))/2)^2

1600 REM - PRINTOUT
1610 CLS
1620 PRINT "OUTPUT":PRINT :PRINT
1630 PRINT "F1 =";FF1(1,1)
1640 SDF1=SQR(F1ACD+F1LEN+F1VIT+F1FSP+F1R1+F1H1+F1H2+F1H4):PRINT "SD
=";SDF1:PRINT
1650 PRINT "F2 =";FF2(1,1)
1660 SDF2=SQR(F2ACD+F2LEN+F2VIT+F2FSP+F2R1+F2H1+F2H2+F2H4):PRINT "SD
=";SDF2:PRINT
1670 PRINT "F3 =";FF3(1,1)
1680 SDF3=SQR(F3ACD+F3LEN+F3VIT+F3FSP+F3R1+F3H1+F3H2+F3H4):PRINT "SD
=";SDF3:PRINT
1690 PRINT "F4 =";FF4(1,1)
1700 SDF4=SQR(F4ACD+F4LEN+F4VIT+F4FSP+F4R1+F4H1+F4H2+F4H4):PRINT "SD
=";SDF4:PRINT

1710 PRINT :INPUT"PRESS ANY NUMBER TO GO ON";XXX

1720 END

```

Appendix A5

DETERMINATION OF RANDOM EXPERIMENTAL ERRORS INVOLVED IN THE CALCULATION SURFACE POWERS IN SPHEROCYLINDRICAL FORM

Written in BASIC for the Macintosh computer using Microsoft Basic(d) (see section 4.7 for details).

```
10 PRINT "PROGRAM 5"
20 REM - DETERMINES R.M.S ERRORS IN CALCULATION OF SPHEROCYLINDRICAL
30 REM - SURFACE POWERS USING R.M.S ERRORS DERIVED FOR
40 REM - MERIDIONAL DATA IN PROGRAM 4

50 REM - INPUT PARAMETERS

60 PRINT"3 MERIDIANS (180°,90° AND 135°) OR"
70 INPUT"4 MERIDIANS (180°,90°,135° AND 45°)";BUG

80 FOR LOOP = 1 TO BUG
90 CLS
100 IF LOOP = 1 THEN AXIS (LOOP)=180
110 IF LOOP = 2 THEN AXIS (LOOP)=90
120 IF LOOP = 3 THEN AXIS (LOOP)=135
130 IF LOOP = 4 THEN AXIS (LOOP)=45
140 PRINT "INPUT SURFACE POWERS ALONG"; AXIS(LOOP);"° MERIDIAN ":PRINT
:PRINT
150 FOR SURF = 1 TO 4
160 PRINT "SURFACE NUMBER ";SURF
170 INPUT "POWER (D)";F(LOOP, SURF)
180 INPUT "ESTIMATED UNCERTAINTY";SDF(LOOP, SURF):PRINT
190 NEXT SURF
200 NEXT LOOP

210 REM - CHANGE POWER MERIDIANS TO POWER AXES
220 FOR LOOP=1 TO BUG
230 AXIS(LOOP)=AXIS(LOOP)-90:IF AXIS(LOOP)<0 THEN AXIS(LOOP)=AXIS(LOOP)+180
240 NEXT LOOP

250 REM - ALTER INDIVIDUAL MERIDIONAL POWERS, IN TURN, BY +/- 1 SD
260 CLS:PRINT "MERIDIONAL ANALYSIS IN PROGRESS":PRINT :PRINT
270 FOR SURF = 1 TO 4
280 FOR EL = 1 TO 9
290 PRINT "SURFACE NUMBER, ERROR LOOP ";SURF,EL
300 IF EL = 2 THEN F(1,SURF) = F(1,SURF)-SDF(1,SURF)
310 IF EL = 3 THEN F(1,SURF) = F(1,SURF)+SDF(1,SURF)
320 IF EL = 4 THEN F(2,SURF) = F(2,SURF)-SDF(2,SURF)
330 IF EL = 5 THEN F(2,SURF) = F(2,SURF)+SDF(2,SURF)
340 IF EL = 6 THEN F(3,SURF) = F(3,SURF)-SDF(3,SURF)
350 IF EL = 7 THEN F(3,SURF) = F(3,SURF)+SDF(3,SURF)
360 IF EL = 8 AND BUG=4 THEN F(4,SURF) = F(4,SURF)-SDF(4,SURF)
370 IF EL = 9 AND BUG=4 THEN F(4,SURF) = F(4,SURF)+SDF(4,SURF)

380 REM ***** MATRIX W *****
390 W11=BUG:W12=0:W13=0:W21=0:W22=0:W23=0:W31=0:W32=0:W33=0:V1=0:V2=0:V3=0
400 FOR LOOP=1 TO BUG
410 V1=V1+POWER(LOOP)
420 V2=V2+(POWER(LOOP)*SIN(2*(AXIS(LOOP)*.01745329278#)))
430 V3=V3+(POWER(LOOP)*COS(2*(AXIS(LOOP)*.01745329278#)))
```



```

440 W12=W12+SIN(2*(AXIS(LOOP)*.01745329278#))
450 W13=W13+COS(2*(AXIS(LOOP)*.01745329278#))
460 W22=W22+SIN(2*(AXIS(LOOP)*.01745329278#))^2
470 W23=W23+SIN(2*(AXIS(LOOP)*.01745329278#))*COS(2*(AXIS(LOOP)*.01745329278#))
480 W33=W33+COS(2*(AXIS(LOOP)*.01745329278#))^2
490 NEXT LOOP
500 W21=W12:W31=W13:W32=W23

510 REM ***** MATRIX Wt = MATRIX W *****

520 REM ***** MATRIX W* *****
530 COFACTORW11=1*((W22*W33)-(W23*W32))
540 COFACTORW21=-1*((W12*W33)-(W13*W32))
550 COFACTORW31=1*((W12*W23)-(W13*W22))
560 COFACTORW12=-1*((W21*W33)-(W23*W31))
570 COFACTORW22=1*((W11*W33)-(W13*W31))
580 COFACTORW32=-1*((W11*W23)-(W13*W21))
590 COFACTORW13=1*((W21*W32)-(W22*W31))
600 COFACTORW23=-1*((W11*W32)-(W12*W31))
610 COFACTORW33=1*((W11*W22)-(W12*W21))

620 REM ***** DETERMINANT *****
630
DETERMINANT=(W11*COFACTORW11)+(W21*COFACTORW21)+(W31*COFACTORW31)

640 REM ***** U=W-1.V *****
650 U1=((COFACTORW11*V1)+(COFACTORW21*V2)+(COFACTORW31*V3))
/DETERMINANT:A=U1
660 U2=((COFACTORW12*V1)+(COFACTORW22*V2)+(COFACTORW32*V3))
/DETERMINANT:B=U2
670 U3=((COFACTORW13*V1)+(COFACTORW23*V2)+(COFACTORW33*V3))
/DETERMINANT:C=U3

680 REM ***** SOLVE A,B,C *****
690 AXIS=(ATN(B/C)/.01745329278#)/2
700 CYL=(2*C)/(COS(2*(AXIS*.01745329278#)))
710 SPH=A-(CYL/2)

720 REM ***CONVERT TO MINUS-CYLINDER ***
730 IF CYL>0 THEN GOTO 740 ELSE GOTO 770
740 SPH=CYL+SPH:CYL=-CYL
750 IF AXIS>=90 THEN AXIS=AXIS-90 ELSE AXIS=AXIS+90

760 REM ***AXIS BETWEEN 1° AND 180°***
770 IF AXIS<.005 AND AXIS>-.005 THEN AXIS=0
780 IF AXIS<=0 THEN AXIS=AXIS+180

790 REM - STORE DATA CALCULATED DURING EACH RUN
800 SPH(EL,SURF)=SPH
810 CYL(EL,SURF)=CYL
820 AXI(EL,SURF)=AXIS

830 REM - RETURN ALTERED PARAMETERS TO ORIGINAL VALUES BEFORE NEXT
RUN
840 IF EL = 2 THEN F(1,SURF) = F(1,SURF)+SDF(1,SURF)
850 IF EL = 3 THEN F(1,SURF) = F(1,SURF)-SDF(1,SURF)
860 IF EL = 4 THEN F(2,SURF) = F(2,SURF)+SDF(2,SURF)
870 IF EL = 5 THEN F(2,SURF) = F(2,SURF)-SDF(2,SURF)
880 IF EL = 6 THEN F(3,SURF) = F(3,SURF)+SDF(3,SURF)
890 IF EL = 7 THEN F(3,SURF) = F(3,SURF)-SDF(3,SURF)
900 IF EL = 8 AND BUG=4 THEN F(4,SURF) = F(4,SURF)+SDF(4,SURF)
910 IF EL = 9 AND BUG=4 THEN F(4,SURF) = F(4,SURF)-SDF(4,SURF)

```

```

920 NEXT EL
930 NEXT SURF

940 REM - ROLLING SPHEROCYLINDRICAL ERRORS
950 FOR SURF = 1 TO 4

960 SPHM1(SURF)=((ABS(SPH(2,SURF)-SPH(1,SURF))+ABS(SPH(3,SURF)-
SPH(1,SURF)))/2)^2
970 CYLM1(SURF)=((ABS(CYL(2,SURF)-CYL(1,SURF))+ABS(CYL(3,SURF)-
CYL(1,SURF)))/2)^2
980 REM - SPECIAL TREATMENT FOR AXIS DIFFERENCES
990 AXDIFF1=AXI(2,SURF)-AXI(1,SURF)
1000 IF AXDIFF1>90 THEN AXDIFF1=(AXI(2,SURF)-180)-AXI(1,SURF)
1010 IF AXDIFF1<-90 THEN AXDIFF1=(AXI(2,SURF)+180)-AXI(1,SURF)
1020 AXDIFF2=AXI(3,SURF)-AXI(1,SURF)
1030 IF AXDIFF2>90 THEN AXDIFF2=(AXI(3,SURF)-180)-AXI(1,SURF)
1040 IF AXDIFF2<-90 THEN AXDIFF2=(AXI(3,SURF)+180)-AXI(1,SURF)
1050 AXIM1(SURF)=((ABS(AXDIFF1)+ABS(AXDIFF2))/2)^2

1060 SPHM2(SURF)=((ABS(SPH(4,SURF)-SPH(1,SURF))+ABS(SPH(5,SURF)-
SPH(1,SURF)))/2)^2
1070 CYLM2(SURF)=((ABS(CYL(4,SURF)-CYL(1,SURF))+ABS(CYL(5,SURF)-
CYL(1,SURF)))/2)^2
1080 REM - SPECIAL TREATMENT FOR AXIS DIFFERENCES
1090 AXDIFF1=AXI(4,SURF)-AXI(1,SURF)
1100 IF AXDIFF1>90 THEN AXDIFF1=(AXI(4,SURF)-180)-AXI(1,SURF)
1110 IF AXDIFF1<-90 THEN AXDIFF1=(AXI(4,SURF)+180)-AXI(1,SURF)
1120 AXDIFF2=AXI(5,SURF)-AXI(1,SURF)
1130 IF AXDIFF2>90 THEN AXDIFF2=(AXI(5,SURF)-180)-AXI(1,SURF)
1140 IF AXDIFF2<-90 THEN AXDIFF2=(AXI(5,SURF)+180)-AXI(1,SURF)
1150 AXIM2(SURF)=((ABS(AXDIFF1)+ABS(AXDIFF2))/2)^2

1160 SPHM3(SURF)=((ABS(SPH(6,SURF)-SPH(1,SURF))+ABS(SPH(7,SURF)-
SPH(1,SURF)))/2)^2
1170 CYLM3(SURF)=((ABS(CYL(6,SURF)-CYL(1,SURF))+ABS(CYL(7,SURF)-
CYL(1,SURF)))/2)^2
1180 REM - SPECIAL TREATMENT FOR AXIS DIFFERENCES
1190 AXDIFF1=AXI(6,SURF)-AXI(1,SURF)
1200 IF AXDIFF1>90 THEN AXDIFF1=(AXI(6,SURF)-180)-AXI(1,SURF)
1210 IF AXDIFF1<-90 THEN AXDIFF1=(AXI(6,SURF)+180)-AXI(1,SURF)
1220 AXDIFF2=AXI(7,SURF)-AXI(1,SURF)
1230 IF AXDIFF2>90 THEN AXDIFF2=(AXI(7,SURF)-180)-AXI(1,SURF)
1240 IF AXDIFF2<-90 THEN AXDIFF2=(AXI(7,SURF)+180)-AXI(1,SURF)
1250 AXIM3(SURF)=((ABS(AXDIFF1)+ABS(AXDIFF2))/2)^2

1260 IF BUG=4 THEN SPHM4(SURF)=((ABS(SPH(8,SURF)-
SPH(1,SURF))+ABS(SPH(9,SURF)-SPH(1,SURF)))/2)^2
1270 IF BUG=4 THEN CYLM4(SURF)=((ABS(CYL(8,SURF)-
CYL(1,SURF))+ABS(CYL(9,SURF)-CYL(1,SURF)))/2)^2
1280 REM - SPECIAL TREATMENT FOR AXIS DIFFERENCES
1290 IF BUG=4 THEN AXDIFF1=AXI(8,SURF)-AXI(1,SURF)
1300 IF BUG=4 AND AXDIFF1>90 THEN AXDIFF1=(AXI(8,SURF)-180)-AXI(1,SURF)
1310 IF BUG=4 AND AXDIFF1<-90 THEN AXDIFF1=(AXI(8,SURF)+180)-AXI(1,SURF)
1320 IF BUG=4 THEN AXDIFF2=AXI(9,SURF)-AXI(1,SURF)
1330 IF BUG=4 AND AXDIFF2>90 THEN AXDIFF2=(AXI(9,SURF)-180)-AXI(1,SURF)
1340 IF BUG=4 AND AXDIFF2<-90 THEN AXDIFF2=(AXI(9,SURF)+180)-AXI(1,SURF)
1350 IF BUG=4 THEN AXIM4(SURF)=((ABS(AXDIFF1)+ABS(AXDIFF2))/2)^2

1360 NEXT SURF

1370 REM - SPHEROCYLINDRICAL PRINTOUT
1380 FOR SURF = 1 TO 4
1390 CLS

```

```
1400 PRINT "OUTPUT FOR SURFACE ";SURF:PRINT :PRINT
1410 PRINT "SPHERE =";SPH(1,SURF)
1420 SDSPH(SURF)=SQR(SPHM1(SURF)+SPHM2(SURF)+SPHM3(SURF)+SPHM4(SURF)):
PRINT "SD =";SDSPH(SURF):PRINT
1430 PRINT "CYLINDER =";CYL(1,SURF)
1440 SDCYL(SURF)=SQR(CYLM1(SURF)+CYLM2(SURF)+CYLM3(SURF)+CYLM4(SURF))
:PRINT "SD =";SDCYL(SURF):PRINT
1450 PRINT "AXIS =";AXI(1,SURF)
1460 SDAXI(SURF)=SQR(AXIM1(SURF)+AXIM2(SURF)+AXIM3(SURF)+AXIM4(SURF)):
PRINT "SD =";SDAXI(SURF):PRINT
1470 INPUT"PRESS ANY NUMBER TO GO AHEAD"; XXX
1480 NEXT SURF

1490 END
```

Appendix A6

CALCULATION OF PURKINJE IMAGE POSITIONS, RATIOS AND HEIGHTS

Written in BASIC for the Macintosh computer using Microsoft Basic(d) (see section 4,8 for details).

```
10 PRINT "PROGRAM 6":PRINT
20 REM - DETERMINES PURKINJE IMAGE POSITIONS, RATIOS AND HEIGHTS
30 REM - GIVEN THE OCULAR SURFACE CURVATURES, AXIAL SEPARATIONS
40 REM - AND DISTANCE AND HEIGHT OF OBJECT LIGHT SOURCE

50 REM - INPUT PARAMETERS
60 INPUT "R1(MM)";RR1:R1=RR1/1000
70 INPUT "R2(MM)";RR2:R2=RR2/1000
80 INPUT "R3(MM)";RR3:R3=RR3/1000
90 INPUT "R4(MM)";RR4:R4=RR4/1000
100 INPUT "D1(MM)";DD1:D1=DD1/1000
110 INPUT "D2(MM)";DD2:D2=DD2/1000
120 INPUT "D3(MM)";DD3:D3=DD3/1000
130 INPUT "DS(MM)";DDS:DS=DDS/1000
140 INPUT "H(MM)"; H
150 REM - REFRACTIVE INDICES
160 INPUT" PRESS 1 FOR.DEFAULT INDICES; 2 FOR CHANGED INDICES";IND
170 IF IND=1 THEN GOTO 230
180 INPUT "N1";N1
190 INPUT "N2";N2
200 INPUT "N3";N3
210 INPUT"N4";N4
220 GOTO 240
230 N1=1:N2=1.3771:N3=1.3374:N4=1.42
240 CLS

250 REM - FRONT CORNEA
260 F1=(N2-N1)/R1
270 F1C=(-N1-N1)/R1
280 L1=N1/DS
290 L1A=L1+F1C
300 LL1A=-N1/L1A:PRINT "POSITION OF PURKINJE IMAGE I =";LL1A*1000
310 M1=L1/L1A
320 PRINT "PURKINJE IMAGE I RATIO = 1"
330 H1= H*M1 : PRINT "PURKINJE IMAGE I HEIGHT ="; H1:PRINT

340 REM - BACK CORNEA
350 L1=N2/D1
360 L1A=L1-F1
370 LL1A=N1/L1A:A2A=LL1A
380 LL1=D1+R2
390 L1=N2/LL1
400 L1A=L1-F1
410 LL1A=N1/L1A:C2A=LL1A
420 R2A=C2A-A2A
430 F2C=(-N1-N1)/R2A
440 LL1=-(DS+A2A)
450 L1=N1/LL1
460 L1A=L1+F2C
470 LL1A=-(N1/L1A):PRINT "POSITION OF PURKINJE IMAGE II =";(LL1A+A2A)*1000
480 M2=L1/L1A
490 RATIO=M2/M1:PRINT "PURKINJE IMAGE II RATIO =";RATIO
```

```

500 H2= H*M2 : PRINT "PURKINJE IMAGE II HEIGHT ="; H2:PRINT

510 REM - FRONT LENS SURFACE
520 F2=(N3-N2)/R2
530 L1=N3/D2
540 L1A=L1-F2
550 L2=L1A/(1+((D1/N2)*L1A))
560 L2A=L2-F1
570 LL2A=N1/L2A:A3A=LL2A
580 LL1=D2+R3
590 L1=N3/LL1
600 L1A = L1-F2
610 L2=L1A/(1+((D1/N2)*L1A))
620 L2A=L2-F1
630 LL2A=N1/L2A:C3A=LL2A
640 R3A=C3A-A3A
650 F3C=(-N1-N1)/R3A
660 LL1=-(DS+A3A)
670 L1=N1/LL1
680 L1A=L1+F3C
690 LL1A=-(N1/L1A):PRINT "POSITION OF PURKINJE IMAGE III =";(LL1A+A3A)*1000
700 M3=L1/L1A
710 RATIO=M3/M1:PRINT "PURKINJE IMAGE III RATIO =";RATIO
720 H3= H*M3 : PRINT "PURKINJE IMAGE III HEIGHT ="; H3:PRINT

730 REM - BACK LENS SURFACE
740 F3=(N4-N3)/R3
750 L1=N4/D3
760 L1A=L1-F3
770 L2=L1A/(1+((D2/N3)*L1A))
780 L2A=L2-F2
790 L3=L2A/(1+((D1/N2)*L2A))
800 L3A=L3-F1
810 LL3A=N1/L3A:A4A=LL3A
820 LL1=D3+R4
830 L1=N4/LL1
840 L1A=L1-F3
850 L2=L1A/(1+((D2/N3)*L1A))
860 L2A=L2-F2
870 L3=L2A/(1+((D1/N2)*L2A))
880 L3A=L3-F1
890 LL3A=N1/L3A:C4A=LL3A
900 R4A=C4A-A4A
910 F4C=(-N1-N1)/R4A
920 LL1=-(DS+A4A)
930 L1=N1/LL1
940 L1A=L1+F4C
950 LL1A=-(N1/L1A):PRINT "POSITION OF PURKINJE IMAGE IV =";(LL1A+A4A)*1000
960 M4=L1/L1A
970 RATIO=M4/M1:PRINT "PURKINJE IMAGE IV RATIO =";RATIO
980 H4= H*M4 : PRINT "PURKINJE IMAGE IV HEIGHT ="; H4

990 PRINT:PRINT:END

```

APPENDIX B
BIOMETRIC DATA

B1 Subject details

Repeat measurements were made on Subjects from 1 to 20. Subjects from 1 to 70 were included in the preliminary residual astigmatism study (chapter 5). Subjects from 1 to 66 were included in the main study (chapter 6). Subjects from (71 to 80) were included in the cycloplegic study (left eye only).

Key: M = males, F = female, A = Asian, C = Caucasian, I = Indian.

Subject NO	Age	Gender	Race
1	18	M	C
2	20	M	I
3	18	M	C
4	19	M	C
5	20	M	C
6	30	M	C
7	20	M	I
8	18	M	C
9	30	M	C
10	19	M	C
11	20	M	A
12	19	M	C
13	18	M	C
14	19	M	I
15	18	M	I
16	19	M	I
17	18	M	C
18	18	M	C
20	19	M	A
21	19	F	C
22	27	M	C
23	19	F	A
24	21	F	C
25	18	F	A
26	29	M	C
27	19	F	C
28	19	F	I
29	19	F	C
30	18	F	C
31	18	F	A
32	20	F	A
33	19	F	C
35	18	F	I
36	18	F	C
37	20	F	C
38	21	F	C
39	18	F	I
40	18	F	C
41	20	F	C
42	20	F	C
43	24	F	A
44	19	F	C
45	18	F	C
46	18	F	C

B1 Subject details (continued).

Subject NO	Age	Gender	Race
47	29	M	C
48	30	M	C
49	21	F	C
50	19	M	A
51	19	F	I
52	18	M	I
53	18	F	C
54	19	M	A
55	25	F	A
56	19	F	A
57	19	F	C
58	19	F	C
59	19	M	C
60	30	M	C
61	24	M	C
62	19	M	C
63	18	F	C
64	20	M	A
65	18	F	C
66	19	M	C
67	18	F	C
68	18	M	C
69	18	F	C
70	18	M	I
71	24	M	C
72	26	M	C
73	23	M	C
74	29	M	C
75	20	M	C
76	32	M	C
77	24	M	A
78	27	M	C
80	26	M	A

B2 NOTIONAL MERIDIONAL REFRACTIVE ERRORS

Tables B2.1 TO B2.5 show notional meridional refractive errors (mean \pm standard deviation) calculated along the 180°, 90°, 135° and 45° meridians. All values in dioptres. See section 3.2 for measurements details and 4.3.1 for calculation details.

B2.1 70 right eyes

Subjects	180°	90°	135°	45°
No				
1	-2.4566 \pm 0.25	-2.4935 \pm 0.32	-2.5851 \pm 0.26	-2.3650 \pm 0.30
2	-0.0963 \pm 0.13	-0.0538 \pm 0.10	-0.0618 \pm 0.10	-0.0883 \pm 0.12
3	-3.0173 \pm 0.03	-3.0328 \pm 0.07	-3.0013 \pm 0.01	-3.0488 \pm 0.10
4	+2.6414 \pm 0.22	+4.1085 \pm 0.19	+2.9001 \pm 0.25	+3.8498 \pm 0.15
5	+0.4912 \pm 0.00	-0.1413 \pm 0.13	+0.2466 \pm 0.06	+0.1033 \pm 0.07
6	-4.3016 \pm 0.12	-4.1485 \pm 0.14	-4.1284 \pm 0.12	-4.3170 \pm 0.14
7	-3.0320 \pm 0.00	-4.6181 \pm 0.13	-3.5985 \pm 0.06	-4.0516 \pm 0.07
8	-1.6338 \pm 0.13	-1.6663 \pm 0.14	-1.5528 \pm 0.11	-1.7473 \pm 0.17
9	-2.6496 \pm 0.13	-1.6005 \pm 0.13	-2.1355 \pm 0.09	-2.1146 \pm 0.08
10	+0.4775 \pm 0.28	+0.1724 \pm 0.24	+0.4060 \pm 0.30	+0.2439 \pm 0.21
11	-2.5024 \pm 0.00	-3.2477 \pm 0.00	-2.8716 \pm 0.04	-2.8785 \pm 0.04
12	-6.0006 \pm 0.00	-6.4995 \pm 0.00	-6.2553 \pm 0.01	-6.2448 \pm 0.01
13	-0.8471 \pm 0.12	-0.3030 \pm 0.01	-0.7523 \pm 0.10	-0.3978 \pm 0.03
14	-0.5281 \pm 0.10	-0.2220 \pm 0.20	-0.4545 \pm 0.14	-0.2956 \pm 0.17
15	-0.3047 \pm 0.11	-0.5954 \pm 0.13	-0.4183 \pm 0.10	-0.4818 \pm 0.12
16	-0.9104 \pm 0.35	-1.3897 \pm 0.31	-1.1082 \pm 0.28	-1.1919 \pm 0.39
17	+0.3135 \pm 0.17	+0.2864 \pm 0.12	+0.2647 \pm 0.17	+0.3352 \pm 0.12
18	-7.9118 \pm 0.24	-9.0383 \pm 0.65	-8.5726 \pm 0.55	-8.3880 \pm 0.32
19	-4.2631 \pm 0.12	-4.1870 \pm 0.15	-4.0042 \pm 0.17	-4.4459 \pm 0.11
20	-1.5846 \pm 0.12	-0.4655 \pm 0.02	-1.1520 \pm 0.11	-0.8981 \pm 0.13
21	-0.8000 \pm 0.11	-0.8000 \pm 0.11	-0.8000 \pm 0.11	-0.8000 \pm 0.11
22	+0.3168 \pm 0.11	+0.6813 \pm 0.11	+0.5826 \pm 0.08	+0.4173 \pm 0.09
23	-0.6629 \pm 0.01	-0.3372 \pm 0.01	-0.3113 \pm 0.01	-0.6888 \pm 0.01
24	-0.3708 \pm 0.19	-0.4793 \pm 0.26	-0.3168 \pm 0.21	-0.5330 \pm 0.26
25	+0.0260 \pm 0.02	+0.1739 \pm 0.09	+0.1642 \pm 0.09	+0.0357 \pm 0.02
26	-0.9735 \pm 0.25	-0.3766 \pm 0.12	-0.5757 \pm 0.24	-0.7744 \pm 0.17
27	-3.8909 \pm 0.40	-4.7592 \pm 0.41	-3.9678 \pm 0.37	-4.6023 \pm 0.36
28	+0.2558 \pm 0.17	+0.4941 \pm 0.11	+0.4100 \pm 0.17	+0.3399 \pm 0.17
29	+0.6043 \pm 0.41	+1.2456 \pm 0.31	+0.9560 \pm 0.31	+0.8939 \pm 0.40
30	-10.5759 \pm 0.23	-12.5242 \pm 0.53	-11.7130 \pm 0.53	-11.386 \pm 0.25
31	-3.0710 \pm 0.25	-0.8930 \pm 0.46	-0.4129 \pm 0.29	-0.7872 \pm 0.40
32	-0.3191 \pm 0.27	-0.6310 \pm 0.28	-0.4010 \pm 0.27	-0.5491 \pm 0.27
33	-0.3278 \pm 0.24	-0.0723 \pm 0.31	+0.0070 \pm 0.25	-0.4071 \pm 0.29
34	+0.3500 \pm 0.13	+0.3500 \pm 0.13	+0.3500 \pm 0.13	+0.3500 \pm 0.13
35	-4.9335 \pm 0.19	-5.7666 \pm 0.47	-5.4971 \pm 0.31	-5.2030 \pm 0.35
36	+3.1249 \pm 1.08	+3.1249 \pm 1.08	+3.2000 \pm 0.94	+3.0500 \pm 1.24
37	+0.7000 \pm 0.11	+0.7499 \pm 0.00	+0.7232 \pm 0.05	+0.7267 \pm 0.05
38	-0.0240 \pm 0.20	+0.2739 \pm 0.11	+0.0360 \pm 0.17	+0.2139 \pm 0.13
39	+0.2419 \pm 0.01	-0.0424 \pm 0.11	+0.0848 \pm 0.04	+0.1147 \pm 0.09
40	+0.3113 \pm 0.11	+0.5886 \pm 0.21	+0.4979 \pm 0.16	+0.4020 \pm 0.12
41	+0.4987 \pm 0.00	+0.2509 \pm 0.00	+0.3791 \pm 0.01	+0.3704 \pm 0.01
42	+0.8638 \pm 0.11	+0.8861 \pm 0.06	+0.9970 \pm 0.00	+0.7529 \pm 0.17
43	+0.6196 \pm 0.13	+0.7303 \pm 0.24	+0.5655 \pm 0.13	+0.7844 \pm 0.25

B2.1 70 right eyes (continued)

Subjects	180°	90°	135°	45°
No				
44	-1.1442 ± 0.13	-0.9059 ± 0.13	-0.9882 ± 0.13	-1.0619 ± 0.13
45	+0.1529 ± 0.23	+0.2470 ± 0.26	+0.0077 ± 0.25	+0.3922 ± 0.28
46	-3.8112 ± 0.12	-3.9389 ± 0.25	-3.9404 ± 0.18	-3.8097 ± 0.17
47	-0.2795 ± 0.23	-0.1706 ± 0.21	-0.1136 ± 0.22	-0.3365 ± 0.22
48	-0.2069 ± 0.21	-0.4432 ± 0.26	-0.2848 ± 0.20	-0.3653 ± 0.24
49	+2.2336 ± 0.12	+2.8663 ± 0.20	+2.6929 ± 0.22	+2.4070 ± 0.10
50	-0.8395 ± 0.32	-0.6606 ± 0.14	-0.7194 ± 0.21	-0.7807 ± 0.27
51	-0.2840 ± 0.02	-0.4161 ± 0.24	-0.4269 ± 0.40	-0.2732 ± 0.06
52	-0.6932 ± 0.37	-0.6069 ± 0.41	-0.6261 ± 0.40	-0.6740 ± 0.37
53	+0.1630 ± 0.12	+0.2369 ± 0.02	+0.2268 ± 0.40	+0.1731 ± 0.10
54	+0.1544 ± 0.02	+0.0955 ± 0.02	+0.0064 ± 0.00	+0.2435 ± 0.00
55	+0.7882 ± 0.10	+0.2617 ± 0.17	+0.6013 ± 0.11	+0.4486 ± 0.09
56	+0.1999 ± 0.11	+0.1500 ± 0.22	+0.1758 ± 0.16	+0.1741 ± 0.16
57	-2.2500 ± 0.82	-2.2500 ± 0.82	-2.2500 ± 0.82	-2.2500 ± 0.82
58	-2.4655 ± 0.25	-2.4846 ± 0.50	-2.2190 ± 0.35	-2.7311 ± 0.40
59	-6.2127 ± 0.13	-5.1374 ± 0.02	-5.2682 ± 0.04	-6.0819 ± 0.10
60	-1.9526 ± 0.11	-2.3475 ± 0.13	-2.1232 ± 0.10	-2.1769 ± 0.10
61	-3.5715 ± 0.11	-4.0786 ± 0.13	-3.9284 ± 0.12	-3.7217 ± 0.10
62	-1.3917 ± 0.21	-0.9084 ± 0.36	-1.2513 ± 0.06	-1.0871 ± 0.17
63	+0.7376 ± 0.00	+0.2623 ± 0.00	+0.5753 ± 0.01	+0.4246 ± 0.01
64	-1.7575 ± 0.20	-0.5326 ± 0.01	-0.9485 ± 0.06	-1.3516 ± 0.14
65	-1.7026 ± 0.17	-3.1475 ± 0.29	-1.1981 ± 0.20	-3.6520 ± 0.25
66	+0.2025 ± 0.10	+0.3974 ± 0.13	+0.3207 ± 0.10	+0.2792 ± 0.11
67	-3.1909 ± 0.19	-2.8092 ± 0.21	-3.0413 ± 0.23	-2.9588 ± 0.17
68	-5.2559 ± 0.17	-5.7442 ± 0.17	-5.4586 ± 0.14	-5.5415 ± 0.20
69	-1.7044 ± 0.01	-1.4457 ± 0.11	-1.4600 ± 0.10	-1.6901 ± 0.03
70	-6.8622 ± 0.13	-7.7879 ± 0.11	-7.4223 ± 0.11	-7.4227 ± 0.12

B2.2 20 right eyes repeated

Subject	180°	90°	135°	45°
No				
1	-2.1818 ± 0.14	-2.3683 ± 0.18	-2.4174 ± 0.20	-2.1327 ± 0.15
2	-0.0556 ± 0.10	-0.1945 ± 0.10	-0.0997 ± 0.09	-0.1504 ± 0.09
3	-3.200 ± 0.11	-3.2000 ± 0.11	-3.2000 ± 0.11	-3.2000 ± 0.11
4	+3.2751 ± 0.52	+4.724 ± 0.51	+3.5603 ± 0.44	+4.4396 ± 0.58
5	+0.4981 ± 0.00	-0.1982 ± 0.20	+0.1256 ± 0.12	+0.1743 ± 0.09
6	-4.1910 ± 0.01	-4.0591 ± 0.01	-4.0195 ± 0.00	-4.2306 ± 0.00
7	-3.0357 ± 0.00	-4.7144 ± 0.00	-3.6280 ± 0.01	-4.1221 ± 0.01
8	-1.5432 ± 0.05	-1.6069 ± 0.11	-1.5150 ± 0.02	-1.6351 ± 0.12
9	-2.5997 ± 0.13	-1.7504 ± 0.00	-2.1794 ± 0.08	-2.1707 ± 0.05
10	+0.0914 ± 0.51	-0.2915 ± 0.60	-0.0567 ± 0.58	-0.1434 ± 0.52
11	-2.4568 ± 0.27	-3.6433 ± 0.22	-3.0308 ± 0.15	-3.0693 ± 0.31
12	-6.1511 ± 0.13	-6.4490 ± 0.20	-6.3096 ± 0.15	-6.2905 ± 0.18
13	-0.5178 ± 0.11	+0.0670 ± 0.12	-0.3659 ± 0.09	-0.0842 ± 0.12
14	-0.5945 ± 0.27	-0.3056 ± 0.13	-0.7015 ± 0.21	-0.1986 ± 0.16
15	-1.6733 ± 0.18	-1.6768 ± 0.19	-1.6001 ± 0.13	-1.7500 ± 0.24
16	-1.2084 ± 0.11	-1.4417 ± 0.10	-1.2935 ± 0.09	-1.3566 ± 0.13
17	+0.2494 ± 0.43	-0.0495 ± 0.32	+0.1069 ± 0.36	+0.0930 ± 0.37
18	-8.0032 ± 0.00	-8.9969 ± 0.00	-8.4478 ± 0.02	-8.5523 ± 0.02
19	-4.1932 ± 0.07	-4.2069 ± 0.15	-4.1085 ± 0.14	-4.2916 ± 0.14
20	-1.4882 ± 0.17	-0.5119 ± 0.00	-1.1056 ± 0.09	-0.8945 ± 0.08

B2.3 70 left eyes.

Subject	180°	90°	135°	45°
N0				
1	-2.2959 ± 0.17	-2.8042 ± 0.21	-2.1204 ± 0.21	-2.9797 ± 0.19
2	-0.0470 ± 0.20	+0.0469 ± 0.11	-0.0171 ± 0.17	+0.017 ± 0.13
3	-3.0217 ± 0.02	-3.1284 ± 0.11	-3.2350 ± 0.02	-3.1266 ± 0.11
4	+1.5108 ± 0.17	+3.9391 ± 0.20	+2.5631 ± 0.18	+2.8868 ± 0.18
5	-0.1104 ± 0.03	-0.5897 ± 0.02	-0.0969 ± 0.02	-0.6032 ± 0.02
6	-4.5961 ± 0.12	-4.4540 ± 0.13	-4.6216 ± 0.12	-4.4285 ± 0.11
7	-3.5153 ± 0.00	-4.9848 ± 0.00	-4.1046 ± 0.04	-4.3955 ± 0.04
8	-1.5010 ± 0.00	-1.5491 ± 0.00	-1.5182 ± 0.00	-1.5319 ± 0.00
9	-1.4000 ± 0.22	-1.4000 ± 0.22	-1.4000 ± 0.22	-1.4000 ± 0.22
10	+0.1738 ± 0.09	+0.0761 ± 0.09	+0.1818 ± 0.10	+0.0681 ± 0.10
11	-2.6818 ± 0.14	-3.5118 ± 0.21	-3.2533 ± 0.16	-2.9468 ± 0.13
12	-3.5241 ± 0.11	-3.9760 ± 0.09	-3.5536 ± 0.08	-3.9465 ± 0.11
13	+0.1137 ± 0.11	+0.2362 ± 0.11	+0.4421 ± 0.11	-0.0922 ± 0.13
14	-0.4868 ± 0.17	-0.2133 ± 0.10	-0.4109 ± 0.12	-0.2892 ± 0.40
15	-1.5680 ± 0.11	-1.6033 ± 0.10	-1.4546 ± 0.11	-1.6955 ± 0.11
16	-0.7913 ± 0.14	-1.5588 ± 0.19	-1.0079 ± 0.13	-1.3422 ± 0.16
17	+0.3628 ± 0.13	+0.2871 ± 0.10	+0.435 ± 0.10	+0.2149 ± 0.12
18	-7.2035 ± 0.32	-8.1966 ± 0.37	-7.6461 ± 0.34	-7.7540 ± 0.33
19	-2.5000 ± 0.00	-2.5000 ± 0.00	-2.5000 ± 0.00	-2.5000 ± 0.00
20	-1.5945 ± 0.13	-1.1556 ± 0.13	-1.3767 ± 0.09	-1.3734 ± 0.16
21	-0.4897 ± 0.22	-0.3604 ± 0.19	-0.3236 ± 0.22	-0.5265 ± 0.19
22	+2.1061 ± 0.43	+1.7938 ± 0.47	+1.7013 ± 0.44	+2.1986 ± 0.48
23	-0.7994 ± 0.00	-0.5007 ± 0.00	-0.6225 ± 0.01	-0.6276 ± 0.01
24	-0.2500 ± 0.00	-0.3000 ± 0.11	-0.2751 ± 0.05	-0.2750 ± 0.05
25	-0.0371 ± 0.13	+0.0370 ± 0.11	-0.1451 ± 0.13	+0.1450 ± 0.13
26	-0.4884 ± 0.25	-0.3617 ± 0.21	-0.4626 ± 0.19	-0.3875 ± 0.23
27	-5.5049 ± 0.14	-5.4952 ± 0.11	-5.3574 ± 0.13	-5.6427 ± 0.13
28	+0.4500 ± 0.11	+0.4500 ± 0.11	+0.4500 ± 0.11	+0.4500 ± 0.11
29	+1.2000 ± 0.35	+1.499 ± 0.32	+1.2239 ± 0.39	+1.4760 ± 0.33
30	-8.3372 ± 0.31	-10.962 ± 0.33	-9.3478 ± 0.27	-9.9523 ± 0.30
31	-0.7015 ± 0.11	-1.5486 ± 0.20	-1.0972 ± 0.15	-1.1529 ± 0.15
32	+0.0898 ± 0.13	-0.2899 ± 0.11	-0.0383 ± 0.12	-0.1618 ± 0.09
33	-0.0080 ± 0.29	-0.2421 ± 0.35	+0.0050 ± 0.28	-0.2506 ± 0.35
34	+6.3360 ± 0.61	+2.4789 ± 2.21	+4.2147 ± 1.31	+4.6002 ± 1.31
35	-5.0014 ± 0.00	-5.7487 ± 0.00	-5.3542 ± 0.02	-5.3959 ± 0.02
36	+5.3935 ± 0.13	+5.2564 ± 0.01	+5.3001 ± 0.05	+5.3498 ± 0.09
37	+0.5375 ± 0.01	+0.7124 ± 0.01	+0.5368 ± 0.01	+0.7131 ± 0.01
38	-0.1471 ± 0.22	+0.4970 ± 0.00	+0.1642 ± 0.14	+0.1857 ± 0.07
39	+0.6378 ± 0.13	+0.4621 ± 0.10	+0.6677 ± 0.09	+0.4322 ± 0.14
40	+0.2073 ± 0.11	+0.3926 ± 0.13	+0.2864 ± 0.08	+0.3135 ± 0.14
41	+0.4918 ± 0.00	+0.2581 ± 0.00	+0.4104 ± 0.02	+0.3395 ± 0.02
42	+0.5008 ± 0.17	+0.6991 ± 0.11	+0.5887 ± 0.13	+0.6112 ± 0.13
43	-0.3972 ± 0.33	+0.2971 ± 0.20	-0.8040 ± 0.24	-0.0197 ± 0.27
44	-1.6249 ± 0.14	-1.4752 ± 0.08	-1.4875 ± 0.12	-1.6126 ± 0.10
45	+0.4171 ± 0.12	+0.5328 ± 0.10	+0.5212 ± 0.10	+0.4287 ± 0.12
46	-3.5008 ± 0.00	-3.9993 ± 0.00	-3.7588 ± 0.01	-3.7413 ± 0.01
47	+0.5850 ± 0.11	+0.7649 ± 0.12	+0.7468 ± 0.11	+0.6031 ± 0.11
48	+0.0540 ± 0.12	-0.2541 ± 0.24	-0.2259 ± 0.22	+0.0258 ± 0.14
49	+1.5228 ± 0.21	+1.4271 ± 0.26	+1.5320 ± 0.21	+1.4179 ± 0.27
50	-0.4836 ± 0.18	-0.4665 ± 0.19	-0.4516 ± 0.20	-0.4985 ± 0.17
51	-0.3581 ± 0.03	-0.3920 ± 0.03	-0.2552 ± 0.00	-0.4949 ± 0.00

B2.3 70 left eyes (continued).

Subject	180°	90°	135°	45°
N0				
52	-0.2641 ± 0.03	-0.2860 ± 0.08	-0.2975 ± 0.10	-0.2526 ± 0.00
53	+0.4319 ± 0.11	+0.4680 ± 0.10	+0.5476 ± 0.13	+0.3522 ± 0.13
54	-0.0207 ± 0.04	-0.0294 ± 0.06	-0.0004 ± 0.00	-0.0497 ± 0.11
55	+0.7912 ± 0.10	+0.3087 ± 0.11	+0.6101 ± 0.13	+0.4898 ± 0.09
56	+0.2870 ± 0.10	+0.1129 ± 0.13	+0.2453 ± 0.12	+0.1546 ± 0.11
57	-0.4493 ± 0.15	-0.6008 ± 0.13	-0.4401 ± 0.14	+0.6100 ± 0.13
58	-2.5051 ± 0.00	-3.4450 ± 0.11	-3.0305 ± 0.04	-2.9196 ± 0.08
59	-6.4244 ± 0.11	-5.2757 ± 0.00	-6.0229 ± 0.06	-5.6772 ± 0.04
60	-2.0619 ± 0.11	-2.2882 ± 0.11	-2.1247 ± 0.11	-2.2254 ± 0.11
61	-5.0747 ± 0.11	-5.2754 ± 0.10	-5.1070 ± 0.10	-5.2431 ± 0.12
62	-1.6500 ± 0.13	-1.6500 ± 0.13	-1.6500 ± 0.13	-1.6500 ± 0.13
63	+0.7484 ± 0.00	+0.4015 ± 0.13	+0.5941 ± 0.06	+0.5558 ± 0.07
64	-1.4322 ± 0.20	-0.2679 ± 0.00	-0.9925 ± 0.14	+0.7076 ± 0.07
65	-2.7717 ± 0.11	-3.1784 ± 0.16	-3.1571 ± 0.16	-2.7930 ± 0.12
66	+0.1592 ± 0.12	+0.2907 ± 0.16	+0.3243 ± 0.12	+0.1256 ± 0.14
67	-3.5180 ± 0.24	-2.6821 ± 0.16	-2.8286 ± 0.13	-3.3715 ± 0.28
68	-7.0226 ± 0.01	-7.6275 ± 0.23	-7.2211 ± 0.14	-7.4290 ± 0.08
69	-1.4656 ± 0.11	-1.6345 ± 0.12	-1.6028 ± 0.12	-1.4973 ± 0.10
70	-5.653 ± 0.09	-7.4227 ± 0.12	-5.9638 ± 0.15	-6.7363 ± 0.22

B2.4 20 left eyes repeated

Subject	180°	90°	135°	45°
N0				
1	-2.7100 ± 0.06	-3.1316 ± 0.08	-2.5550 ± 0.01	-3.2951 ± 0.01
2	+0.1457 ± 0.13	+ 0.1042 ± 0.13	+0.1110 ± 0.12	+0.1389 ± 0.12
3	-3.0553 ± 0.05	-3.0948 ± 0.08	-3.0031 ± 0.00	-3.1470 ± 0.13
4	+1.7401 ± 0.20	+4.2134 ± 0.17	+2.6751 ± 0.22	+3.2748 ± 0.15
5	+0.2438 ± 0.01	-0.2939 ± 0.13	+0.1532 ± 0.11	-0.2033 ± 0.11
6	-4.4462 ± 0.13	-4.4039 ± 0.16	-4.4080 ± 0.17	-4.3593 ± 0.13
7	-3.5525 ± 0.11	-5.0476 ± 0.11	-4.2425 ± 0.10	-4.3576 ± 0.12
8	-1.5010 ± 0.00	-1.5491 ± 0.10	-1.5182 ± 0.04	-1.5319 ± 0.07
9	-1.3500 ± 0.13	-1.3500 ± 0.13	-1.3500 ± 0.13	-1.3500 ± 0.13
10	+0.1794 ± 0.11	+0.0705 ± 0.19	+0.1763 ± 0.12	+0.0736 ± 0.19
11	-2.6406 ± 0.14	-3.5595 ± 0.12	-3.2931 ± 0.16	-2.9070 ± 0.11
12	-3.4096 ± 0.13	-3.8405 ± 0.14	-3.4567 ± 0.12	-3.7934 ± 0.12
13	+0.0717 ± 0.09	+0.4282 ± 0.14	+0.5481 ± 0.10	-0.0482 ± 0.13
14	-0.3264 ± 0.15	-0.0737 ± 0.18	-0.2683 ± 0.13	-0.1318 ± 0.21
15	-1.5544 ± 0.05	-1.5957 ± 0.08	-1.5032 ± 0.00	-1.6469 ± 0.13
16	-0.9965 ± 0.14	-2.0036 ± 0.12	-1.7510 ± 0.11	-1.8250 ± 0.14
17	+0.3704 ± 0.12	+0.2295 ± 0.12	+0.3652 ± 0.13	+0.2347 ± 0.11
18	-7.4051 ± 0.13	-8.7450 ± 0.17	-7.9950 ± 0.15	-8.1551 ± 0.13
19	-2.4119 ± 0.14	-2.6887 ± 0.19	-2.5006 ± 0.12	-2.5995 ± 0.21
20	-1.7480 ± 0.17	-1.2521 ± 0.25	-1.5270 ± 0.19	-1.4730 ± 0.19

B2.5 10 left eyes with and without cycloplegia

Subject	180°	90°	135°	45°
N0				
Without				
71	- 1.6974 ± 0.20	- 1.5027 ± 0.00	-1 .6199 ± 0.13	- 1.5802 ± 0.07
72	+0.7255 ± 0.01	+0.2744 ± 0.01	+0.6024 ± 0.03	+0.3975 ± 0.07
73	+0.5530 ± 0.12	- 0.5031 ± 0.11	+0.2515 ± 0.13	- 0.2016 ± 0.08
74	+3.3809 ± 0.10	+2.8610 ± 0.13	+2.9398 ± 0.06	+3.3101 ± 0.11
75	+0.4539 ± 0.17	+0.2460 ± 0.25	+0.4610 ± 0.17	+0.2389 ± 0.30
76	- 0.6512 ± 0.14	- 0.4989 ± 0.15	- 0.7310 ± 0.17	- 0.4191 ± 0.12
77	+0.4726 ± 0.08	+0.3773 ± 0.13	+0.5377 ± 0.11	+0.3122 ± 0.10
78	- 1.3598 ± 0.12	- 1.3403 ± 0.21	- 1.3246 ± 0.17	- 1.3755 ± 0.16
79	+0.6457 ± 0.13	+0.3542 ± 0.22	+0.4681 ± 0.18	+0.5318 ± 0.17
80	- 0.4420 ± 0.11	+0.0919 ± 0.13	- 0.1121 ± 0.13	- 0.2380 ± 0.09
With				
71	-1.6998 ± 0.02	- 1.5003 ± 0.00	- 1.6070 ± 0.11	- 1.5931 ± 0.09
72	+0.9835 ± 0.00	+0.5164 ± 0.00	+0.8368 ± 0.02	+0.6631 ± 0.02
73	+1.1949 ± 0.01	+0.1550 ± 0.13	+0.9198 ± 0.09	+0.4301 ± 0.10
74	+4.6393 ± 0.13	+4.1106 ± 0.10	+4.1907 ± 0.10	+4.5592 ± 0.07
75	+1.4187 ± 0.02	+1.1408 ± 0.12	+1.4187 ± 0.03	+1.1812 ± 0.11
76	- 0.6452 ± 0.20	- 0.4549 ± 0.21	- 0.7808 ± 0.20	- 0.3193 ± 0.20
77	+0.8089 ± 0.14	+0.6410 ± 0.13	+0.8169 ± 0.13	+0.6330 ± 0.14
78	- 1.3000 ± 0.11	- 1.3000 ± 0.11	- 1.3000 ± 0.11	- 1.3000 ± 0.11
79	+1.3953 ± 0.13	+0.9046 ± 0.13	+1.1049 ± 0.13	+1.1950 ± 0.14
80	- 0.1852 ± 0.52	+0.2351 ± 0.01	+0.1042 ± 0.18	- 0.0543 ± 0.35

B3 NOTIONAL MERIDIONAL ANTERIOR CORNEAL CURVATURE

RADII

Tables B3.1 to B3.5 show notional meridional anterior corneal surface radii (mean and standard deviation) calculated along the 180, 90, 135 and 45 meridians. All values in millimetres. See section 3.3 for measurements details and 4.3.2 for calculations.

B3.1 70 right eyes

Subject	180°	90°	135°	45°
N0				
1	7.5721 ± 0.06	7.4311 ± 0.05	7.4628 ± 0.04	7.5405 ± 0.02
2	8.0293 ± 0.02	7.9473 ± 0.05	7.9952 ± 0.03	7.9813 ± 0.03
3	8.4457 ± 0.03	8.3109 ± 0.03	8.4101 ± 0.04	8.3464 ± 0.02
4	8.4937 ± 0.02	8.7095 ± 0.00	8.5322 ± 0.02	8.6710 ± 0.00
5	8.1153 ± 0.03	7.9112 ± 0.01	8.0275 ± 0.02	7.9991 ± 0.02
6	7.8197 ± 0.03	7.7302 ± 0.00	7.7926 ± 0.01	7.7573 ± 0.01
7	7.3160 ± 0.03	7.0239 ± 0.03	7.1645 ± 0.02	7.1754 ± 0.04
8	8.5491 ± 0.00	8.5041 ± 0.02	8.5151 ± 0.01	8.5381 ± 0.01
9	8.0937 ± 0.01	8.2095 ± 0.01	8.1725 ± 0.00	8.1307 ± 0.01
10	7.8627 ± 0.04	7.7672 ± 0.04	7.8108 ± 0.05	7.8191 ± 0.03
11	8.0505 ± 0.03	7.8094 ± 0.02	7.8310 ± 0.02	7.9868 ± 0.02
12	7.7997 ± 0.00	7.6436 ± 0.04	7.7210 ± 0.03	7.7223 ± 0.01
13	7.7970 ± 0.03	7.9268 ± 0.03	7.9113 ± 0.02	7.9953 ± 0.03
14	8.2340 ± 0.06	8.2059 ± 0.05	8.2122 ± 0.08	8.2277 ± 0.03
15	8.0009 ± 0.02	7.8457 ± 0.02	7.9086 ± 0.02	7.9379 ± 0.03
16	8.0734 ± 0.06	7.9565 ± 0.06	8.0197 ± 0.07	8.0102 ± 0.06
17	8.0163 ± 0.05	7.9070 ± 0.09	7.9417 ± 0.09	7.9816 ± 0.03
18	7.6783 ± 0.02	7.5049 ± 0.04	7.5530 ± 0.03	7.6279 ± 0.03
19	8.4440 ± 0.02	8.3226 ± 0.14	8.4513 ± 0.07	8.3153 ± 0.09
20	7.9140 ± 0.02	7.8925 ± 0.00	7.8943 ± 0.02	7.9123 ± 0.02
21	7.3022 ± 0.01	7.1311 ± 0.00	7.1808 ± 0.00	7.2524 ± 0.02
22	7.7263 ± 0.02	7.7069 ± 0.01	7.7105 ± 0.03	7.7226 ± 0.02
23	7.3930 ± 0.00	7.3403 ± 0.01	7.3544 ± 0.01	7.3788 ± 0.00
24	7.8842 ± 0.01	7.7057 ± 0.03	7.8145 ± 0.01	7.7754 ± 0.02
25	7.7538 ± 0.00	7.6761 ± 0.01	7.7224 ± 0.01	7.7075 ± 0.02
26	7.7236 ± 0.05	7.5863 ± 0.03	7.6718 ± 0.04	7.6381 ± 0.04
27	7.6363 ± 0.01	7.3069 ± 0.01	7.4695 ± 0.02	7.4737 ± 0.01
28	7.9791 ± 0.04	7.9941 ± 0.02	8.0217 ± 0.04	7.9515 ± 0.03
29	7.5171 ± 0.01	7.5361 ± 0.04	7.5268 ± 0.01	7.5264 ± 0.04
30	7.8460 ± 0.00	7.6672 ± 0.05	7.7053 ± 0.02	7.8080 ± 0.07
31	7.8324 ± 0.01	7.6342 ± 0.00	7.7598 ± 0.04	7.7068 ± 0.03
32	7.6058 ± 0.00	7.4607 ± 0.01	7.5233 ± 0.00	7.5432 ± 0.01
33	7.6416 ± 0.03	7.5217 ± 0.03	7.5929 ± 0.03	7.5704 ± 0.02
34	8.3954 ± 0.03	8.2645 ± 0.03	8.3190 ± 0.03	8.3409 ± 0.02
35	7.8691 ± 0.02	7.6975 ± 0.00	7.7148 ± 0.01	7.8518 ± 0.01
36	8.1121 ± 0.00	8.0045 ± 0.03	8.0550 ± 0.02	8.0616 ± 0.01
37	7.6970 ± 0.01	7.6429 ± 0.04	7.6506 ± 0.03	7.6893 ± 0.01
38	8.0741 ± 0.02	8.0124 ± 0.03	8.0553 ± 0.01	8.0313 ± 0.02
39	7.8659 ± 0.02	7.6174 ± 0.04	7.7329 ± 0.03	7.7503 ± 0.04
40	7.7352 ± 0.20	7.7014 ± 0.07	7.7347 ± 0.06	7.7019 ± 0.04
41	7.7304 ± 0.02	7.6280 ± 0.05	7.6723 ± 0.04	7.7009 ± 0.04
42	7.7750 ± 0.20	7.7349 ± 0.02	7.7612 ± 0.02	7.7487 ± 0.02
43	7.6769 ± 0.03	7.6230 ± 0.02	7.6590 ± 0.02	7.6409 ± 0.03
44	8.2441 ± 0.03	8.1924 ± 0.01	8.2250 ± 0.02	8.2116 ± 0.02
45	7.6935 ± 0.01	7.6264 ± 0.00	7.6293 ± 0.02	7.6906 ± 0.02

B3.1 70 right eyes (continued)

Subject	180°	90°	135°	45°
N0				
46	7.7595 ± 0.06	7.6271 ± 0.03	7.7065 ± 0.06	7.6801 ± 0.03
47	7.8160 ± 0.03	7.6806 ± 0.03	7.7446 ± 0.04	7.7520 ± 0.02
48	8.0696 ± 0.03	7.9703 ± 0.02	7.9951 ± 0.03	8.0448 ± 0.02
49	7.9326 ± 0.00	7.9639 ± 0.04	7.9169 ± 0.02	7.9797 ± 0.02
50	7.3764 ± 0.11	7.2868 ± 0.10	7.3347 ± 0.08	7.3286 ± 0.13
51	8.1813 ± 0.07	8.1353 ± 0.02	8.1437 ± 0.11	8.1729 ± 0.03
52	7.6141 ± 0.00	7.5691 ± 0.01	7.5872 ± 0.02	7.5961 ± 0.00
53	7.7569 ± 0.02	7.5896 ± 0.00	7.6907 ± 0.02	7.6559 ± 0.01
54	9.1084 ± 0.03	9.0682 ± 0.03	8.9994 ± 0.01	9.1772 ± 0.05
55	7.7319 ± 0.04	7.5013 ± 0.04	7.6489 ± 0.03	7.5843 ± 0.05
56	7.5017 ± 0.02	7.4749 ± 0.03	7.4913 ± 0.04	7.4853 ± 0.02
57	7.8234 ± 0.02	7.7532 ± 0.00	7.7940 ± 0.01	7.7826 ± 0.02
58	8.0955 ± 0.03	7.8744 ± 0.04	7.9993 ± 0.03	7.9706 ± 0.04
59	7.8781 ± 0.03	7.8984 ± 0.03	7.9626 ± 0.04	7.8140 ± 0.03
60	7.9699 ± 0.02	7.9134 ± 0.01	7.9509 ± 0.03	7.9324 ± 0.00
61	7.9434 ± 0.01	7.9165 ± 0.02	7.9213 ± 0.01	7.9386 ± 0.04
62	7.9116 ± 0.00	7.8806 ± 0.01	7.8937 ± 0.00	7.9028 ± 0.00
63	7.6328 ± 0.01	7.4604 ± 0.03	7.5135 ± 0.03	7.5797 ± 0.02
64	7.6491 ± 0.03	7.6708 ± 0.03	7.6802 ± 0.03	7.6397 ± 0.03
65	7.5656 ± 0.00	7.3377 ± 0.01	7.5567 ± 0.01	7.3466 ± 0.01
66	8.0891 ± 0.00	8.0042 ± 0.03	8.0261 ± 0.04	8.0671 ± 0.01
67	7.6527 ± 0.03	7.6739 ± 0.02	7.6656 ± 0.01	7.6610 ± 0.04
68	8.1653 ± 0.03	8.0980 ± 0.01	8.1091 ± 0.00	8.1541 ± 0.04
69	7.7441 ± 0.03	7.6724 ± 0.03	7.7058 ± 0.03	7.7107 ± 0.02
70	7.8330 ± 0.01	7.7769 ± 0.01	7.7801 ± 0.02	7.8298 ± 0.02

B3.2 20 right eyes repeated

Subject	180°	90°	135°	45°
N0				
1	7.6400 ± 0.01	7.4243 ± 0.03	7.4670 ± 0.01	7.5998 ± 0.02
2	8.0425 ± 0.02	7.9841 ± 0.01	8.0151 ± 0.02	8.0114 ± 0.00
3	8.3832 ± 0.02	8.2400 ± 0.02	8.3482 ± 0.01	8.2750 ± 0.03
4	8.4507 ± 0.01	8.6759 ± 0.02	8.4983 ± 0.01	8.6283 ± 0.01
5	8.0832 ± 0.02	7.8767 ± 0.02	7.9808 ± 0.01	7.9791 ± 0.01
6	7.7841 ± 0.02	7.7391 ± 0.01	7.7705 ± 0.02	7.7527 ± 0.03
7	7.3187 ± 0.01	7.0212 ± 0.00	7.1783 ± 0.00	7.1616 ± 0.03
8	8.5797 ± 0.00	8.5102 ± 0.00	8.5194 ± 0.02	8.5705 ± 0.01
9	8.1640 ± 0.01	8.2359 ± 0.05	8.1900 ± 0.03	8.2099 ± 0.04
10	7.9157 ± 0.01	7.8142 ± 0.01	7.8583 ± 0.01	7.7816 ± 0.00
11	8.0048 ± 0.06	7.7651 ± 0.03	7.8499 ± 0.04	7.9200 ± 0.06
12	7.7849 ± 0.02	7.6483 ± 0.03	7.7253 ± 0.01	7.7080 ± 0.04
13	7.9603 ± 0.02	8.0296 ± 0.01	7.9587 ± 0.02	8.0312 ± 0.00
14	8.2502 ± 0.01	8.1931 ± 0.03	8.2303 ± 0.00	8.2129 ± 0.01
15	8.0132 ± 0.00	7.6900 ± 0.28	7.8198 ± 0.16	7.8834 ± 0.12
16	8.1031 ± 0.02	7.9801 ± 0.00	8.0236 ± 0.01	8.0596 ± 0.01
17	8.0607 ± 0.00	7.9392 ± 0.02	7.9856 ± 0.01	8.0143 ± 0.01
18	7.6815 ± 0.02	7.4218 ± 0.02	7.4966 ± 0.04	7.6066 ± 0.00
19	8.4218 ± 0.00	8.1781 ± 0.05	8.3887 ± 0.04	8.2112 ± 0.00
20	7.8437 ± 0.01	7.9329 ± 0.06	7.8700 ± 0.02	7.9066 ± 0.04

B3.3 70 left eyes

Subject	180°	90°	135°	45°
N0				
1	7.4819 ± 0.10	7.3214 ± 0.30	7.4156 ± 0.50	7.3876 ± 0.20
2	7.9473 ± 0.00	7.8526 ± 0.02	7.8949 ± 0.01	7.9026 ± 0.03
3	8.3056 ± 0.00	7.1743 ± 0.02	8.2280 ± 0.00	8.2519 ± 0.01
4	8.3492 ± 0.04	8.6673 ± 0.01	8.5330 ± 0.03	8.4836 ± 0.02
5	8.1753 ± 0.00	7.9612 ± 0.02	8.1180 ± 0.01	8.0186 ± 0.00
6	7.7675 ± 0.03	7.6291 ± 0.04	7.6811 ± 0.04	7.7154 ± 0.04
7	7.3317 ± 0.02	7.0588 ± 0.02	7.1859 ± 0.04	7.1877 ± 0.01
8	8.4804 ± 0.01	8.4862 ± 0.03	8.4820 ± 0.02	8.4846 ± 0.02
9	8.1817 ± 0.01	8.1081 ± 0.03	8.1143 ± 0.03	8.1756 ± 0.00
10	7.8352 ± 0.03	7.6714 ± 0.17	7.7943 ± 0.03	7.7123 ± 0.15
11	7.7974 ± 0.01	7.7360 ± 0.03	7.8085 ± 0.00	7.9014 ± 0.00
12	7.7726 ± 0.03	7.6540 ± 0.02	7.7350 ± 0.03	7.6916 ± 0.02
13	8.0459 ± 0.03	7.9307 ± 0.01	8.0354 ± 0.02	7.9411 ± 0.02
14	8.1920 ± 0.04	8.1512 ± 0.04	8.1295 ± 0.04	8.2137 ± 0.04
15	7.8924 ± 0.05	7.8342 ± 0.12	7.8834 ± 0.02	7.8431 ± 0.06
16	8.1360 ± 0.01	7.9706 ± 0.02	8.0787 ± 0.02	8.0279 ± 0.01
17	8.1196 ± 0.02	8.0336 ± 0.04	8.1131 ± 0.02	8.0402 ± 0.04
18	7.7528 ± 0.03	7.5604 ± 0.04	7.6301 ± 0.03	7.6831 ± 0.04
19	8.3658 ± 0.06	8.2174 ± 0.07	8.2676 ± 0.08	8.3157 ± 0.05
20	7.8386 ± 0.02	7.9013 ± 0.00	7.8852 ± 0.02	7.8547 ± 0.00
21	7.2869 ± 0.01	7.1464 ± 0.01	7.2353 ± 0.02	7.1979 ± 0.19
22	7.7486 ± 0.00	7.6913 ± 0.02	7.6603 ± 0.01	7.7796 ± 0.00
23	7.2859 ± 0.03	7.2840 ± 0.02	7.2655 ± 0.03	7.3044 ± 0.03
24	7.8355 ± 0.02	7.7011 ± 0.00	7.7597 ± 0.01	7.7769 ± 0.01
25	7.7442 ± 0.01	7.6624 ± 0.00	7.6935 ± 0.01	7.7131 ± 0.01
26	7.7022 ± 0.04	7.5311 ± 0.04	7.6299 ± 0.04	7.6034 ± 0.04
27	7.4884 ± 0.02	7.3149 ± 0.02	7.3859 ± 0.02	7.4173 ± 0.02
28	7.9358 ± 0.04	7.9007 ± 0.02	7.8716 ± 0.03	7.9649 ± 0.02
29	7.5392 ± 0.01	7.5407 ± 0.00	7.5361 ± 0.01	7.5438 ± 0.00
30	7.9484 ± 0.04	7.6015 ± 0.06	7.7854 ± 0.06	7.7645 ± 0.03
31	7.7395 ± 0.05	7.5138 ± 0.01	7.6166 ± 0.01	7.6366 ± 0.02
32	7.5861 ± 0.02	7.4104 ± 0.00	7.4985 ± 0.01	7.4981 ± 0.01
33	7.7609 ± 0.02	7.5856 ± 0.03	7.7041 ± 0.01	7.6424 ± 0.03
34	8.8977 ± 0.05	7.9256 ± 0.03	8.2900 ± 0.04	8.5333 ± 0.06
35	7.9468 ± 0.03	7.7931 ± 0.03	7.8379 ± 0.03	7.9020 ± 0.03
36	8.1313 ± 0.01	7.9620 ± 0.01	8.0484 ± 0.01	8.0449 ± 0.02
37	7.7063 ± 0.01	7.6336 ± 0.00	7.6627 ± 0.01	7.6772 ± 0.02
38	8.1461 ± 0.00	8.1571 ± 0.01	8.1510 ± 0.00	8.1522 ± 0.02
39	7.8469 ± 0.12	7.6530 ± 0.13	7.7267 ± 0.13	7.7320 ± 0.13
40	7.7622 ± 0.02	7.7210 ± 0.01	7.7403 ± 0.00	7.7429 ± 0.03
41	7.7263 ± 0.01	7.5769 ± 0.03	7.6503 ± 0.03	7.6529 ± 0.01
42	7.7751 ± 0.00	7.7615 ± 0.01	7.7449 ± 0.00	7.7917 ± 0.01
43	7.6833 ± 0.00	7.7133 ± 0.00	7.6712 ± 0.02	7.7254 ± 0.01
44	8.2971 ± 0.01	8.2195 ± 0.02	8.2572 ± 0.02	8.2594 ± 0.02
45	7.6966 ± 0.07	7.5900 ± 0.00	7.6624 ± 0.05	7.6242 ± 0.02
46	7.7756 ± 0.02	7.6376 ± 0.01	7.6986 ± 0.04	7.7147 ± 0.01
47	7.8381 ± 0.04	7.7684 ± 0.02	7.7598 ± 0.02	7.8468 ± 0.03
48	8.1098 ± 0.02	7.9467 ± 0.04	8.0422 ± 0.05	8.0144 ± 0.01
49	8.0098 ± 0.01	7.9235 ± 0.01	7.9516 ± 0.02	7.9816 ± 0.01

B3.3 70 left eyes (continued)

Subject	180°	90°	135°	45°
NO				
50	7.4682 ± 0.02	7.3583 ± 0.04	7.3928 ± 0.04	7.4337 ± 0.02
51	8.1503 ± 0.02	8.0562 ± 0.04	8.0834 ± 0.03	8.1232 ± 0.05
52	7.5332 ± 0.03	7.5401 ± 0.04	7.5301 ± 0.05	7.5432 ± 0.04
53	7.7579 ± 0.00	7.5620 ± 0.01	7.6302 ± 0.01	7.6897 ± 0.02
54	9.1044 ± 0.01	9.0289 ± 0.02	9.0922 ± 0.00	9.0411 ± 0.01
55	7.7454 ± 0.04	7.6045 ± 0.03	7.6628 ± 0.00	7.6871 ± 0.01
56	7.4863 ± 0.03	7.4403 ± 0.02	7.4704 ± 0.01	7.4561 ± 0.05
57	7.7951 ± 0.02	7.7782 ± 0.08	7.7594 ± 0.06	7.8138 ± 0.06
58	8.2229 ± 0.03	7.8570 ± 0.03	8.0337 ± 0.04	8.0462 ± 0.02
59	7.8552 ± 0.03	7.9480 ± 0.01	7.8494 ± 0.00	7.9538 ± 0.03
60	7.9885 ± 0.03	7.9547 ± 0.04	7.9463 ± 0.04	7.9969 ± 0.03
61	7.9376 ± 0.02	7.8256 ± 0.01	7.8968 ± 0.01	7.8665 ± 0.00
62	7.9729 ± 0.02	7.8537 ± 0.02	7.9172 ± 0.02	7.9094 ± 0.02
63	7.6265 ± 0.01	7.4834 ± 0.06	7.5971 ± 0.06	7.5128 ± 0.00
64	7.8200 ± 0.02	7.9066 ± 0.00	7.8470 ± 0.01	7.8795 ± 0.01
65	7.5627 ± 0.01	7.4805 ± 0.01	7.5208 ± 0.01	7.5225 ± 0.01
66	8.0941 ± 0.02	8.0292 ± 0.03	8.0651 ± 0.01	8.0581 ± 0.03
67	7.6411 ± 0.02	7.7055 ± 0.03	7.6769 ± 0.03	7.6697 ± 0.02
68	8.1963 ± 0.06	8.1502 ± 0.06	8.2099 ± 0.06	8.1366 ± 0.06
69	7.7848 ± 0.05	7.7697 ± 0.04	7.7697 ± 0.05	7.7835 ± 0.04
70	7.8500 ± 0.0	7.7632 ± 0.00	7.8525 ± 0.01	7.7608 ± 0.01

B3.4 20 left eyes repeated

Subject	180°	90°	135°	45°
NO				
1	7.5503 ± 0.02	7.3529 ± 0.06	7.4607 ± 0.00	7.4426 ± 0.07
2	7.9943 ± 0.02	7.8790 ± 0.01	7.9356 ± 0.02	7.9377 ± 0.02
3	8.2983 ± 0.02	8.2016 ± 0.01	8.2608 ± 0.01	8.2319 ± 0.01
4	8.3614 ± 0.03	8.6852 ± 0.04	8.5410 ± 0.05	8.5056 ± 0.02
5	8.1560 ± 0.02	7.9772 ± 0.01	8.1178 ± 0.02	8.0154 ± 0.01
6	7.7620 ± 0.03	7.6146 ± 0.02	7.6786 ± 0.03	7.6979 ± 0.02
7	7.3343 ± 0.02	7.0389 ± 0.02	7.1655 ± 0.04	7.2078 ± 0.01
8	8.4763 ± 0.00	8.4736 ± 0.00	8.4670 ± 0.00	8.4829 ± 0.00
9	8.2502 ± 0.01	8.1730 ± 0.01	8.1829 ± 0.00	8.2404 ± 0.01
10	7.7758 ± 0.05	7.6975 ± 0.01	7.7586 ± 0.01	7.7147 ± 0.05
11	7.9717 ± 0.01	7.7248 ± 0.03	7.8134 ± 0.01	7.8832 ± 0.00
12	7.7718 ± 0.02	7.6348 ± 0.02	7.7288 ± 0.00	7.6777 ± 0.00
13	8.0001 ± 0.01	7.9365 ± 0.02	8.0129 ± 0.01	7.9237 ± 0.02
14	8.1558 ± 0.04	8.1741 ± 0.07	8.1226 ± 0.05	8.2073 ± 0.09
15	7.9921 ± 0.03	7.8278 ± 0.05	7.9069 ± 0.03	7.9130 ± 0.05
16	8.1189 ± 0.02	7.9476 ± 0.03	8.0377 ± 0.00	8.0288 ± 0.02
17	8.1534 ± 0.01	8.0198 ± 0.03	8.0884 ± 0.05	8.0848 ± 0.00
18	7.7183 ± 0.02	7.4849 ± 0.01	7.5971 ± 0.03	7.6061 ± 0.02
19	8.3980 ± 0.02	8.1852 ± 0.01	8.2765 ± 0.03	8.3067 ± 0.01
20	7.7905 ± 0.03	7.8694 ± 0.01	7.8360 ± 0.01	7.8239 ± 0.02

B3.5 10 left eyes with and without cycloplegia

Subject	180°	90°	135°	45°
NO				
Without				
71	7.7966 ± 0.01	7.7966 ± 0.01	7.7966 ± 0.01	7.7966 ± 0.01
72	7.7299 ± 0.03	7.6167 ± 0.02	7.6761 ± 0.02	7.6705 ± 0.01
73	8.3081 ± 0.03	7.8552 ± 0.06	8.1107 ± 0.04	8.0525 ± 0.04
74	7.7831 ± 0.00	7.6401 ± 0.03	7.7160 ± 0.01	7.7073 ± 0.02
75	8.1499 ± 0.04	8.0267 ± 0.02	8.0855 ± 0.03	8.0855 ± 0.02
76	7.9066 ± 0.02	7.8900 ± 0.01	7.8988 ± 0.02	7.8978 ± 0.02
77	7.9632 ± 0.01	7.8134 ± 0.01	7.8914 ± 0.00	7.8851 ± 0.00
78	8.2714 ± 0.05	8.1275 ± 0.04	8.2107 ± 0.01	8.1892 ± 0.01
79	7.8766 ± 0.00	7.7000 ± 0.00	7.7893 ± 0.01	7.7893 ± 0.01
80	7.8033 ± 0.01	7.8499 ± 0.02	7.8258 ± 0.02	7.8274 ± 0.02
with				
71	7.8433 ± 0.01	7.8433 ± 0.01	7.8433 ± 0.01	7.8433 ± 0.01
72	7.7265 ± 0.01	7.5700 ± 0.01	7.6490 ± 0.01	7.6475 ± 0.00
73	8.1995 ± 0.01	7.8737 ± 0.01	8.0462 ± 0.00	8.0270 ± 0.01
74	7.7763 ± 0.04	7.6602 ± 0.01	7.7234 ± 0.03	7.7132 ± 0.03
75	8.1732 ± 0.04	7.9934 ± 0.01	8.0869 ± 0.01	8.0797 ± 0.01
76	7.9232 ± 0.00	7.8733 ± 0.00	7.8994 ± 0.00	7.8971 ± 0.00
77	7.9599 ± 0.03	7.8167 ± 0.00	7.8871 ± 0.01	7.8895 ± 0.02
78	8.2431 ± 0.92	8.1535 ± 0.03	8.1963 ± 0.20	8.2003 ± 0.02
79	7.8799 ± 0.00	7.7134 ± 0.01	7.7944 ± 0.00	7.7088 ± 0.00
80	7.8066 ± 0.01	7.8533 ± 0.02	7.8296 ± 0.01	7.8303 ± 0.01

B4 PRELIMINARY STUDY: RESIDUAL ASTIGMATIC POWER

Tables B4.1 to B4.4 show calculated residual astigmatic power in terms of its orthogonal (C_0) and oblique (C_{45}) components of astigmatic decomposition, its cylinder (C) and axis (\emptyset) as well as calculated torsion (T). See section 5.2 for details.

B4.1 70 right eyes

Subject NO	C_0	C_{45}	C	\emptyset Corneal	T
1	- 0.73	- 0.29	0.79	100.90	+6.45
2	- 0.45	+0.06	0.46	086.46	- 2.16
3	- 0.49	- 0.17	0.52	099.60	- 22.26
4	- 0.49	+0.31	0.58	073.60	- 90.00
5	- 0.45	0.00	0.45	089.79	- 3.79
6	- 0.62	- 0.01	0.62	090.50	- 11.47
7	- 0.36	- 0.52	0.63	117.80	- 26.78
8	- 0.16	- 0.31	0.35	121.20	- 15.86
9	- 0.63	+0.23	0.67	080.19	- 70.49
10	- 0.17	- 0.19	0.26	113.90	- 21.60
11	- 0.50	- 0.61	0.79	115.50	- 12.79
12	- 0.39	+0.02	0.40	088.33	+1.27
13	- 1.07	- 0.48	1.17	102.20	+16.81
14	- 0.02	+0.11	0.11	050.71	- 55.04
15	- 0.54	- 0.22	0.58	101.00	- 5.70
16	- 0.18	- 0.04	0.18	096.20	- 8.21
17	- 0.38	+0.47	0.61	064.56	+4.44
18	+0.13	- 0.27	0.30	147.70	- 46.05
19	- 0.58	+0.36	0.68	074.36	- 13.03
20	- 1.07	+0.03	1.07	089.11	+53.56
21	- 1.13	- 0.46	1.22	01010	0.00
22	- 0.14	- 0.17	0.22	115.20	+64.09
23	- 0.66	- 0.54	0.85	109.70	- 6.69
24	- 0.81	- 0.02	0.81	090.80	- 7.61
25	- 0.15	- 0.13	0.20	110.50	- 25.50
26	- 1.10	- 0.77	1.34	107.60	- 17.25
27	- 0.78	- 0.17	0.80	096.20	- 12.54
28	- 0.15	+0.28	0.32	058.72	- 21.05
29	- 0.43	+0.03	0.43	088.12	- 78.45
30	- 0.85	- 0.32	0.91	169.70	- 65.73
31	- 1.72	+0.66	1.85	079.49	+3.51
32	- 0.56	- 0.28	0.62	103.20	- 9.24
33	- 0.94	- 0.28	0.98	098.30	- 14.30
34	- 0.66	- 0.12	0.67	095.00	0.00
35	- 0.11	- 0.41	0.43	127.30	- 17.97
36	- 0.56	- 0.18	0.59	099.00	- 7.31
37	- 0.33	- 0.18	0.38	104.40	+2.28
38	- 0.64	+0.29	0.71	077.65	+3.35
39	- 1.10	- 0.02	1.10	090.50	+1.52
40	- 0.27	+0.34	0.43	064.56	- 19.86
41	- 0.23	- 0.18	0.29	109.40	- 9.37
42	- 0.28	- 0.15	0.31	104.20	- 24.83
43	- 0.22	- 0.12	0.25	104.40	- 23.40
44	- 0.51	+0.04	0.51	087.57	- 9.24
45	- 0.53	+0.02	0.54	088.81	+21.19
46	- 0.64	+0.29	0.70	077.94	+9.06
47	- 0.89	- 0.27	0.93	098.50	- 6.81

B4.1 70 right eyes (continued).

Subject NO	C _o	C ₄₅	C	Ø Corneal	T
48	- 0.33	- 0.34	0.47	112.70	- 10.72
49	- 0.49	- 0.67	0.82	117.00	+29.02
50	- 0.81	+0.02	0.81	089.42	- 2.42
51	- 0.60	- 0.38	0.71	106.00	- 10.29
52	- 0.38	- 0.07	0.38	094.90	- 3.26
53	+0.74	- 0.34	0.81	167.80	- 83.47
54	- 0.11	- 0.46	0.48	128.50	- 0.17
55	- 0.80	+0.20	0.83	082.95	- 0.62
56	- 0.02	+0.02	0.03	066.44	+14.89
57	- 0.43	+0.10	0.44	083.66	0.00
58	- 1.20	- 0.40	1.26	099.10	- 12.80
59	- 1.17	- 1.48	1.88	115.80	- 74.82
60	+0.09	+0.01	0.09	003.66	+80.01
61	- 0.34	- 0.26	0.43	108.60	- 4.27
62	- 0.69	+0.06	0.69	087.51	+10.16
63	- 0.57	- 0.53	0.78	111.50	- 11.53
64	- 1.13	- 0.20	1.15	095.00	- 63.68
65	+0.11	- 1.17	1.18	137.70	- 69.12
66	- 0.69	- 0.18	0.71	097.40	+0.56
67	- 0.22	+0.10	0.25	077.64	- 73.37
68	+0.23	- 0.21	0.31	159.10	- 64.45
69	- 0.75	- 0.35	0.83	102.70	- 6.00
70	+0.54	- 0.10	0.55	174.60	- 65.27

B4.2 20 right eyes repeated

Subj	C _o	C ₄₅	C	Ø Corneal	T
1	- 1.09	- 0.53	1.21	102.90	+3.11
2	- 0.17	- 0.05	0.18	098.40	- 8.36
3	- 0.69	+0.35	0.77	076.37	0.00
4	- 0.43	+0.29	0.52	073.03	- 88.03
5	- 0.35	+0.01	0.35	089.00	+0.67
6	- 0.44	- 0.09	0.45	095.60	- 16.62
7	+0.14	- 0.28	0.31	148.30	- 44.00
8	- 0.26	- 0.38	0.46	117.60	- 29.31
9	- 0.28	- 0.35	0.45	115.70	- 9.73
10	- 0.46	- 0.07	0.47	094.40	+79.89
11	- 0.20	- 0.18	0.27	110.90	- 17.24
12	- 0.09	- 0.43	0.44	129.10	- 31.06
13	- 0.48	+0.11	0.49	083.43	+3.24
14	- 0.20	- 0.15	0.25	107.80	+48.15
15	- 0.57	+0.57	0.81	067.59	+18.41
16	- 0.88	- 0.34	0.94	100.50	- 4.48
17	- 0.40	- 0.27	0.48	106.80	- 8.17
18	- 0.31	- 0.16	0.35	103.90	- 6.90
19	- 0.52	- 0.74	0.90	117.50	- 16.12
20	- 0.39	- 0.02	0.39	091.40	+76.94

B4.3 70 left eyes

Subject NO	C ₀	C ₄₅	C	Ø Corneal	T
1	- 0.46	- 0.76	0.88	119.50	- 32.45
2	- 0.62	- 0.05	0.62	092.40	+2.25
3	- 0.58	- 0.17	0.60	098.10	- 5.46
4	- 0.97	+0.56	1.12	075.06	- 70.46
5	- 0.63	+0.02	0.63	089.14	- 11.81
6	- 0.90	+0.04	0.90	088.70	+7.63
7	- 0.33	- 0.38	0.50	114.20	- 22.89
8	+0.14	+0.01	0.14	001.33	0.00
9	- 0.37	- 0.27	0.45	108.00	0.00
10	- 0.87	+0.29	0.92	080.76	-2.09
11	- 0.51	+0.22	0.55	101.60	-0.58
12	- 0.23	- 0.15	0.27	106.10	-26.07
13	- 0.74	- 0.04	0.74	091.50	-21.13
14	- 0.57	- 0.27	0.63	102.80	13.84
15	- 0.31	- 0.14	0.34	102.30	-20.27
16	- 1.65	- 0.85	1.86	103.50	-3.87
17	- 0.04	- 0.04	0.06	113.40	-32.04
18	- 0.05	- 0.39	0.39	131.50	-33.84
19	- 0.74	- 0.23	0.78	098.70	0.00
20	- 0.08	+0.21	0.22	055.26	- 40.26
21	- 1.06	+0.03	1.07	089.11	- 6.44
22	+0.01	- 0.21	0.21	136.20	- 13.51
23	- 0.27	- 0.32	0.42	114.80	+22.83
24	- 0.65	- 0.21	0.68	098.90	+57.07
25	- 0.72	- 0.09	0.72	093.60	- 0.23
26	- 0.66	+0.09	0.66	085.90	- 13.40
27	- 0.64	+0.04	0.64	088.33	0.00
28	- 1.20	+0.24	1.22	084.28	+1.39
29	- 1.10	- 0.50	1.21	102.30	- 6.93
30	- 0.19	- 0.50	0.53	124.70	0.00
31	- 0.19	- 0.28	0.34	062.04	- 55.37
32	+0.71	- 0.45	0.84	164.00	- 75.98
33	- 0.53	- 0.17	0.55	098.70	- 6.41
34	- 0.68	- 0.12	0.69	094.90	- 4.90
35	- 0.79	+0.09	0.79	086.69	- 6.36
36	+0.04	- 0.72	0.72	136.70	- 39.67
37	- 0.05	- 0.37	0.38	131.50	- 30.18
38	- 0.73	+0.06	0.74	087.61	+2.06
39	- 0.62	+0.10	0.63	085.27	+9.40
40	- 0.50	- 0.06	0.51	093.30	+79.06
41	+0.01	- 0.28	0.28	136.10	- 39.42
42	- 0.47	+0.05	0.48	087.06	+0.94
43	- 0.61	- 0.08	0.62	093.80	- 3.48
44	- 0.28	- 0.24	0.37	110.40	+15.92
45	- 0.49	- 0.19	0.52	100.50	+53.48
46	- 0.59	- 0.15	0.61	097.10	- 5.72
47	- 0.71	+0.10	0.72	085.96	- 4.96
48	- 0.34	- 0.09	0.35	097.50	- 3.85
49	- 0.56	- 0.64	0.85	114.40	+1.91
50	- 0.55	+0.41	0.69	071.67	+13.00
51	- 0.35	- 0.27	0.44	108.60	- 9.24
52	- 0.70	- 0.30	0.76	101.80	- 1.43
53	- 0.34	- 0.03	0.34	092.40	+8.55
54	+0.09	- 0.12	0.15	154.40	- 7.45
55	- 1.13	- 0.57	1.27	103.40	- 5.04
56	- 0.25	- 0.03	0.25	903.20	- 21.56
57	- 0.59	- 0.27	0.65	102.40	- 8.40

B4.3 70 left eyes (continued)

Subject NO	C ₀	C ₄₅	C	Ø Corneal	T
58	- 0.23	- 0.01	0.23	090.70	- 6.65
59	- 0.01	- 0.59	0.59	134.70	- 11.04
60	- 0.91	+0.05	0.92	088.30	+2.70
61	- 0.00	- 0.39	0.39	135.20	- 19.19
62	- 0.41	+0.04	0.41	087.38	- 5.38
63	- 0.59	+0.54	0.80	068.89	+5.11
64	- 0.71	+0.11	0.72	085.79	+83.54
65	- 0.06	+0.36	0.36	049.75	+40.58
66	- 0.48	- 0.12	0.50	096.90	- 14.2
67	- 0.46	- 0.47	0.66	113.10	+70.92
68	+0.43	- 0.05	0.44	176.50	+69.13
69	+0.17	- 0.06	0.18	170.40	- 35.12
70	+0.89	- 0.29	0.94	171.00	+75.96

B4.4 20 left eyse repeated

Subject NO	C ₀	C ₄₅	C	Ø Corneal	T
1	- 0.78	- 0.68	1.04	110.6	- 21.94
2	- 0.59	- 0.01	0.59	090.40	+1.23
3	- 0.69	+0.14	0.71	084.32	- 4.99
4	- 0.97	+0.76	1.23	071.04	- 68.04
5	- 0.44	+0.20	0.48	077.43	- 2.43
6	- 0.88	+0.02	0.89	089.20	+4.80
7	+0.36	+0.14	0.39	010.47	+50.86
8	- 0.42	- 0.38	0.57	111.20	- 17.21
9	+0.07	- 0.05	0.09	162.10	- 10.74
10	- 0.39	- 0.30	0.49	108.70	0.00
11	- 0.36	+0.19	0.41	076.06	- 2.06
12	- 0.43	- 0.00	0.43	090.00	+7.99
13	- 0.25	- 0.08	0.26	098.90	- 19.53
14	- 0.69	- 0.13	0.70	095.40	- 32.77
15	+0.27	- 0.31	0.41	155.30	+4.67
16	- 0.81	- 0.19	0.83	096.70	- 5.06
17	+0.13	- 0.65	0.66	140.70	- 50.69
18	- 0.55	- 0.07	0.55	093.80	- 5.47
19	- 0.04	+0.22	0.23	129.50	- 38.21
20	- 0.07	- 0.12	0.14	058.97	- 54.97

B5 ULTRASONIC MEASUREMENTS OF AXIAL DISTANCES

Tales B5.1 to B5.5 show ultrasonic measurements of axial distances(mean \pm standard deviation) including the anterior chamber depth (d_1), crystalline lens thickness (d_2) and vitreous depth (d_3), All values in millimetres. See section 3.4 for measurements details.

B5.1 66 right eyes

Subject NO	d_1	d_2	d_3
1	3.61 \pm 0.21	3.32 \pm 0.20	16.12 \pm 0.13
2	3.69 \pm 0.19	3.37 \pm 0.25	16.82 \pm 0.10
3	3.35 \pm 0.24	3.52 \pm 0.12	18.47 \pm 0.05
4	3.13 \pm 0.15	3.29 \pm 0.25	16.34 \pm 0.17
5	3.57 \pm 0.21	3.28 \pm 0.20	16.56 \pm 0.07
6	3.23 \pm 0.21	4.04 \pm 0.30	17.68 \pm 0.09
7	3.34 \pm 0.05	3.41 \pm 0.11	15.99 \pm 0.20
8	3.72 \pm 0.25	3.60 \pm 0.26	18.50 \pm 0.11
9	3.13 \pm 0.11	4.22 \pm 0.15	17.93 \pm 0.06
10	3.78 \pm 0.08	3.65 \pm 0.04	15.85 \pm 0.15
11	3.47 \pm 0.19	3.65 \pm 0.20	17.65 \pm 0.19
12	3.48 \pm 0.06	3.37 \pm 0.04	18.71 \pm 0.07
13	3.80 \pm 0.11	3.29 \pm 0.11	17.51 \pm 0.20
14	3.33 \pm 0.15	3.62 \pm 0.19	17.12 \pm 0.14
15	3.38 \pm 0.08	3.47 \pm 0.09	16.69 \pm 0.07
16	3.50 \pm 0.13	3.42 \pm 0.26	17.38 \pm 0.27
17	3.69 \pm 0.19	3.49 \pm 0.18	16.49 \pm 0.05
18	3.51 \pm 0.22	3.82 \pm 0.07	17.65 \pm 0.09
19	3.86 \pm 0.18	3.41 \pm 0.06	19.87 \pm 0.15
20	3.77 \pm 0.12	3.31 \pm 0.10	16.22 \pm 0.10
21	3.82 \pm 0.16	3.54 \pm 0.12	14.85 \pm 0.13
22	3.43 \pm 0.13	3.63 \pm 0.20	15.22 \pm 0.05
23	2.86 \pm 0.17	3.38 \pm 0.05	15.88 \pm 0.14
24	3.52 \pm 0.04	3.47 \pm 0.10	15.86 \pm 0.12
25	3.32 \pm 0.10	3.26 \pm 0.07	15.68 \pm 0.10
26	3.75 \pm 0.21	3.44 \pm 0.17	16.80 \pm 0.14
27	3.52 \pm 0.08	3.52 \pm 0.03	17.11 \pm 0.13
28	3.20 \pm 0.10	3.73 \pm 0.05	15.65 \pm 0.05
29	3.11 \pm 0.11	3.85 \pm 0.26	16.57 \pm 0.26
30	3.23 \pm 0.05	3.65 \pm 0.05	19.92 \pm 0.07
31	3.82 \pm 0.08	3.26 \pm 0.12	16.48 \pm 0.12
32	3.31 \pm 0.31	3.92 \pm 0.21	15.12 \pm 0.09
33	3.59 \pm 0.13	3.57 \pm 0.07	15.35 \pm 0.07
34	2.98 \pm 0.26	3.52 \pm 0.04	17.44 \pm 0.13
35	3.53 \pm 0.27	3.52 \pm 0.33	17.39 \pm 0.08
36	3.23 \pm 0.05	3.55 \pm 0.10	14.98 \pm 0.07
37	3.52 \pm 0.15	3.56 \pm 0.06	15.83 \pm 0.15
38	3.85 \pm 0.09	3.57 \pm 0.08	16.21 \pm 0.15
39	3.61 \pm 0.28	3.07 \pm 0.18	16.11 \pm 0.15
40	3.49 \pm 0.11	3.41 \pm 0.06	16.25 \pm 0.10
41	3.30 \pm 0.09	3.57 \pm 0.10	15.78 \pm 0.26

B5.1 66 right eyes (continued)

Subject NO	d ₁	d ₂	d ₃
42	3.61 ± 0.21	4.02 ± 0.24	15.53 ± 0.19
43	2.62 ± 0.24	3.71 ± 0.22	15.68 ± 0.23
44	3.66 ± 0.32	3.82 ± 0.23	18.12 ± 0.27
45	3.24 ± 0.28	3.95 ± 0.30	15.18 ± 0.20
46	3.64 ± 0.19	3.74 ± 0.18	16.70 ± 0.38
47	3.69 ± 0.09	4.04 ± 0.07	15.45 ± 0.10
48	3.59 ± 0.14	3.95 ± 0.20	16.81 ± 0.09
49	3.20 ± 0.21	4.06 ± 0.12	14.44 ± 0.06
50	3.65 ± 0.13	3.08 ± 0.18	15.14 ± 0.18
51	3.10 ± 0.09	3.22 ± 0.26	17.28 ± 0.26
52	3.59 ± 0.10	3.18 ± 0.06	15.90 ± 0.16
53	3.51 ± 0.17	3.30 ± 0.17	15.97 ± 0.09
54	3.57 ± 0.10	3.31 ± 0.09	18.87 ± 0.20
55	3.37 ± 0.14	3.55 ± 0.10	15.50 ± 0.10
56	3.30 ± 0.13	3.70 ± 0.16	15.45 ± 0.08
57	3.81 ± 0.24	3.70 ± 0.22	16.20 ± 0.06
58	3.48 ± 0.11	3.70 ± 0.08	17.39 ± 0.07
59	3.99 ± 0.10	3.09 ± 0.13	18.72 ± 0.25
60	3.50 ± 0.10	3.86 ± 0.12	17.29 ± 0.07
61	3.93 ± 0.09	3.90 ± 0.24	17.34 ± 0.24
62	3.52 ± 0.26	3.39 ± 0.14	17.12 ± 0.28
63	3.30 ± 0.17	3.16 ± 0.21	15.84 ± 0.15
64	3.83 ± 0.12	3.46 ± 0.12	16.70 ± 0.12
65	3.65 ± 0.14	3.20 ± 0.14	16.19 ± 0.09
66	3.38 ± 0.05	3.68 ± 0.10	15.93 ± 0.17

B5.2 20 right eyes repeated

Subject NO	d ₁	d ₂	d ₃
1	3.65 ± 0.17	3.32 ± 0.18	16.04 ± 0.15
2	3.76 ± 0.11	3.30 ± 0.13	16.81 ± 0.15
3	3.49 ± 0.19	3.44 ± 0.13	18.45 ± 0.17
4	3.24 ± 0.11	3.44 ± 0.29	16.24 ± 0.18
5	3.48 ± 0.11	3.19 ± 0.12	16.58 ± 0.09
6	2.94 ± 0.05	4.51 ± 0.15	17.45 ± 0.12
7	3.45 ± 0.08	3.43 ± 0.15	15.93 ± 0.34
8	3.69 ± 0.11	3.63 ± 0.18	18.47 ± 0.11
9	3.08 ± 0.12	4.19 ± 0.22	17.88 ± 0.22
10	3.75 ± 0.15	3.65 ± 0.28	15.83 ± 0.14
11	3.48 ± 0.11	3.64 ± 0.16	17.54 ± 0.05
12	3.56 ± 0.06	3.47 ± 0.08	18.75 ± 0.12
13	3.91 ± 0.15	3.19 ± 0.09	17.60 ± 0.16
14	3.37 ± 0.07	3.62 ± 0.17	17.15 ± 0.23
15	3.49 ± 0.05	3.51 ± 0.14	16.59 ± 0.20
16	3.54 ± 0.03	4.49 ± 0.09	17.57 ± 0.07
17	3.64 ± 0.18	3.56 ± 0.25	16.43 ± 0.13
18	3.50 ± 0.08	3.91 ± 0.25	17.54 ± 0.19
19	3.89 ± 0.07	3.37 ± 0.14	19.68 ± 0.20
20	3.77 ± 0.15	3.45 ± 0.22	16.26 ± 0.10

B5.3 66 left eyes

Subject N0	d ₁	d ₂	d ₃
1	3.31 ± 0.26	3.31 ± 0.12	16.39 ± 0.20
2	3.71 ± 0.27	3.36 ± 0.18	16.50 ± 0.10
3	3.54 ± 0.21	3.44 ± 0.08	18.61 ± 0.23
4	3.04 ± 0.21	3.51 ± 0.14	16.79 ± 0.32
5	3.54 ± 0.09	3.37 ± 0.15	16.86 ± 0.19
6	3.00 ± 0.11	4.01 ± 0.27	17.48 ± 0.30
7	3.09 ± 0.15	3.78 ± 0.11	15.90 ± 0.08
8	3.50 ± 0.15	3.50 ± 0.04	18.50 ± 0.20
9	2.76 ± 0.15	3.89 ± 0.29	18.95 ± 0.23
10	3.53 ± 0.10	3.65 ± 0.22	15.53 ± 0.31
11	3.62 ± 0.05	3.55 ± 0.05	17.86 ± 0.14
12	3.53 ± 0.19	3.33 ± 0.21	17.55 ± 0.30
13	3.51 ± 0.09	3.13 ± 0.07	16.95 ± 0.09
14	3.50 ± 0.14	3.34 ± 0.13	17.09 ± 0.13
15	3.76 ± 0.24	3.36 ± 0.12	16.85 ± 0.22
16	3.55 ± 0.20	3.36 ± 0.14	17.57 ± 0.25
17	3.64 ± 0.08	3.68 ± 0.07	16.91 ± 0.14
18	3.61 ± 0.30	3.74 ± 0.09	17.38 ± 0.34
19	3.82 ± 0.18	3.43 ± 0.12	19.15 ± 0.16
20	3.47 ± 0.09	3.37 ± 0.03	16.61 ± 0.20
21	3.73 ± 0.11	3.64 ± 0.06	14.64 ± 0.34
22	3.44 ± 0.12	3.53 ± 0.18	14.28 ± 0.22
23	3.44 ± 0.25	3.02 ± 0.09	15.04 ± 0.19
24	3.16 ± 0.19	3.79 ± 0.24	15.82 ± 0.19
25	3.33 ± 0.08	3.30 ± 0.15	15.74 ± 0.29
26	3.79 ± 0.12	3.58 ± 0.08	16.71 ± 0.13
27	3.16 ± 0.16	3.14 ± 0.16	16.75 ± 0.21
28	2.83 ± 0.14	3.69 ± 0.04	15.93 ± 0.07
29	3.09 ± 0.07	3.54 ± 0.14	15.55 ± 0.15
30	3.21 ± 0.14	3.62 ± 0.07	19.83 ± 0.11
31	3.66 ± 0.15	3.57 ± 0.13	16.50 ± 0.18
32	3.38 ± 0.28	3.77 ± 0.09	14.91 ± 0.15
33	3.50 ± 0.14	3.51 ± 0.09	15.44 ± 0.19
34	3.25 ± 0.16	3.27 ± 0.13	15.69 ± 0.16
35	2.99 ± 0.17	3.57 ± 0.04	17.96 ± 0.17
36	3.07 ± 0.25	3.51 ± 0.20	14.19 ± 0.17
37	3.25 ± 0.15	3.53 ± 0.06	15.95 ± 0.12
38	3.46 ± 0.08	3.78 ± 0.04	16.35 ± 0.14
39	3.45 ± 0.18	3.09 ± 0.09	16.07 ± 0.12
40	3.72 ± 0.12	3.55 ± 0.15	15.86 ± 0.11
41	3.61 ± 0.13	3.51 ± 0.10	16.20 ± 0.25
42	3.39 ± 0.10	3.66 ± 0.08	15.80 ± 0.06
43	2.13 ± 0.08	3.82 ± 0.11	15.48 ± 0.16
44	3.44 ± 0.10	3.41 ± 0.05	18.31 ± 0.11
45	3.27 ± 0.25	3.73 ± 0.15	15.14 ± 0.20
46	3.55 ± 0.22	3.72 ± 0.08	17.06 ± 0.22
47	3.70 ± 0.08	4.16 ± 0.20	15.20 ± 0.07
48	3.60 ± 0.13	3.71 ± 0.12	16.82 ± 0.13
49	2.74 ± 0.23	4.16 ± 0.33	14.53 ± 0.09
50	3.63 ± 0.22	3.31 ± 0.18	15.14 ± 0.16
51	3.07 ± 0.22	3.40 ± 0.11	17.12 ± 0.32
52	3.59 ± 0.25	3.33 ± 0.09	15.87 ± 0.09
53	3.18 ± 0.09	3.33 ± 0.05	16.10 ± 0.11
54	3.29 ± 0.22	3.45 ± 0.09	18.96 ± 0.20
55	3.30 ± 0.09	3.57 ± 0.10	15.78 ± 0.26
56	3.73 ± 0.19	3.72 ± 0.10	15.28 ± 0.17

B5.3 66 left eyes (continued).

Subject NO	d ₁	d ₂	d ₃
57	3.79 ± 0.10	3.57 ± 0.08	16.38 ± 0.08
58	3.58 ± 0.09	3.53 ± 0.10	17.69 ± 0.13
59	3.56 ± 0.12	3.38 ± 0.09	19.29 ± 0.24
60	3.05 ± 0.14	3.76 ± 0.08	17.80 ± 0.16
61	3.65 ± 0.15	3.76 ± 0.18	17.63 ± 0.24
62	3.44 ± 0.22	3.28 ± 0.08	17.45 ± 0.22
63	2.86 ± 0.17	3.38 ± 0.05	15.88 ± 0.14
64	3.63 ± 0.11	3.46 ± 0.12	17.00 ± 0.12
65	3.62 ± 0.12	3.52 ± 0.09	16.87 ± 0.13
66	3.47 ± 0.20	3.73 ± 0.07	16.53 ± 0.11

B5.4 20 left eyes repeated

Subject NO	d ₁	d ₂	d ₃
1	3.36 ± 0.19	3.41 ± 0.07	16.42 ± 0.18
2	3.68 ± 0.16	3.37 ± 0.07	16.46 ± 0.13
3	3.73 ± 0.12	3.46 ± 0.04	18.54 ± 0.13
4	3.34 ± 0.09	3.53 ± 0.28	16.83 ± 0.12
5	3.61 ± 0.12	3.40 ± 0.05	16.69 ± 0.18
6	2.99 ± 0.15	4.05 ± 0.23	17.55 ± 0.25
7	3.40 ± 0.07	3.69 ± 0.04	15.98 ± 0.12
8	3.57 ± 0.08	3.44 ± 0.06	18.54 ± 0.07
9	2.81 ± 0.07	3.94 ± 0.21	18.94 ± 0.22
10	3.61 ± 0.06	3.74 ± 0.07	15.61 ± 0.16
11	3.61 ± 0.14	3.55 ± 0.05	17.74 ± 0.16
12	3.55 ± 0.11	3.41 ± 0.09	17.77 ± 0.19
13	3.60 ± 0.19	3.31 ± 0.16	16.82 ± 0.26
14	3.55 ± 0.13	3.48 ± 0.16	17.13 ± 0.12
15	3.50 ± 0.15	3.46 ± 0.05	17.04 ± 0.12
16	3.59 ± 0.21	3.51 ± 0.06	17.65 ± 0.09
17	3.40 ± 0.12	3.78 ± 0.05	16.90 ± 0.13
18	3.11 ± 0.02	3.94 ± 0.23	17.24 ± 0.17
19	3.84 ± 0.07	3.36 ± 0.07	19.30 ± 0.15
20	3.67 ± 0.07	3.43 ± 0.06	16.44 ± 0.20

B5.5 10 left eyes with and without cycloplegia

Subject NO	d ₁	d ₂	d ₃
Without			
71	3.72 ± 0.04	3.35 ± 0.12	17.69 ± 0.18
72	3.50 ± 0.07	3.68 ± 0.07	15.57 ± 0.11
73	3.80 ± 0.04	3.74 ± 0.09	16.37 ± 0.17
74	3.24 ± 0.03	3.90 ± 0.14	14.53 ± 0.17
75	3.18 ± 0.08	3.73 ± 0.04	16.85 ± 0.06
76	3.92 ± 0.05	3.68 ± 0.06	17.07 ± 0.03
77	3.49 ± 0.07	3.63 ± 0.09	16.09 ± 0.06
78	3.42 ± 0.13	3.98 ± 0.27	18.96 ± 0.17
79	3.77 ± 0.14	3.51 ± 0.26	16.41 ± 0.20
80	3.55 ± 0.11	3.92 ± 0.12	15.81 ± 0.08
With			
71	3.86 ± 0.04	3.31 ± 0.04	17.81 ± 0.10
72	3.85 ± 0.13	3.74 ± 0.08	15.41 ± 0.18
73	3.89 ± 0.03	3.73 ± 0.08	16.01 ± 0.08
74	3.76 ± 0.15	3.69 ± 0.17	13.81 ± 0.20
75	3.78 ± 0.08	3.71 ± 0.10	15.82 ± 0.04
76	3.83 ± 0.05	3.67 ± 0.14	16.56 ± 0.33
77	3.72 ± 0.25	3.51 ± 0.05	16.93 ± 0.34
78	3.19 ± 0.10	4.10 ± 0.21	18.50 ± 0.49
79	3.66 ± 0.12	3.37 ± 0.06	16.38 ± 0.20
80	3.74 ± 0.10	3.76 ± 0.08	15.60 ± 0.06

B6 OPHTHALMOPHAKOMETRIC MEASUREMENTS OF PURKINJE IMAGE HEIGHTS

Tables B6.1.1 to B6.3.5 show ophthalmophakometric measurements of Purkinje image heights (mean and standard deviation) measured along 180, 90, 135 and 45 meridians. All values are in millimetres and must be scaled down by X37.5 to obtain heights. See section 3.5 for measurements details.

B6. I PURKINJE IMAGE I (ANTERIOR CORNEAL SURFACE)

B6.1.1 66 right eyes

Subject	180°	90°	135°	45°
N0				
1	71.50 ± 0.87	78.17 ± 0.76	81.67 ± 0.76	80.33 ± 0.58
2	76.00 ± 0.87	81.33 ± 0.58	90.00 ± 0.00	86.33 ± 0.58
3	82.50 ± 1.32	86.33 ± 1.15	92.83 ± 0.76	89.17 ± 1.61
4	80.17 ± 0.29	88.83 ± 1.26	92.67 ± 0.29	93.33 ± 0.58
5	75.00 ± 0.50	78.83 ± 1.26	88.00 ± 1.00	83.33 ± 0.58
6	72.83 ± 0.29	75.50 ± 0.50	81.17 ± 0.29	80.33 ± 1.15
7	66.50 ± 1.73	69.00 ± 1.73	73.50 ± 1.32	74.67 ± 1.15
8	76.33 ± 0.58	87.33 ± 0.76	91.17 ± 0.76	90.17 ± 0.76
9	80.00 ± 1.00	89.50 ± 0.50	93.17 ± 0.76	91.00 ± 1.00
10	76.00 ± 0.50	78.67 ± 0.58	84.33 ± 0.29	83.67 ± 0.29
11	74.33 ± 1.15	75.50 ± 0.87	82.50 ± 0.50	84.00 ± 1.00
12	73.00 ± 0.76	76.00 ± 0.50	81.67 ± 0.29	80.75 ± 0.35
13	75.33 ± 0.29	79.33 ± 1.53	85.00 ± 1.00	83.33 ± 1.15
14	81.17 ± 1.61	86.83 ± 0.76	89.33 ± 1.53	88.67 ± 1.15
15	77.17 ± 1.04	80.83 ± 1.26	86.17 ± 0.29	84.50 ± 0.50
16	74.83 ± 1.61	79.00 ± 1.73	86.33 ± 1.53	82.33 ± 1.53
17	80.17 ± 0.29	81.67 ± 0.58	89.33 ± 0.58	85.00 ± 1.00
18	74.50 ± 0.87	77.83 ± 0.29	85.33 ± 1.53	83.33 ± 0.58
19	80.67 ± 1.53	87.67 ± 0.58	89.67 ± 0.58	90.33 ± 0.58
20	75.17 ± 1.15	81.33 ± 1.15	85.33 ± 0.58	86.67 ± 0.58
21	73.18 ± 0.29	77.00 ± 0.00	82.00 ± 0.00	81.67 ± 0.58
22	73.00 ± 0.00	73.00 ± 1.00	81.00 ± 0.00	81.17 ± 0.76
23	71.50 ± 0.50	79.33 ± 0.58	80.00 ± 0.00	79.67 ± 0.29
24	75.00 ± 0.87	78.67 ± 0.58	86.33 ± 0.58	83.33 ± 0.58
25	75.17 ± 0.29	84.67 ± 0.58	90.33 ± 0.15	88.00 ± 0.00
26	74.17 ± 0.29	79.00 ± 0.00	85.33 ± 0.58	81.83 ± 0.67
27	72.33 ± 0.29	75.00 ± 1.00	81.50 ± 0.87	81.33 ± 1.53
28	75.17 ± 0.58	76.67 ± 0.58	84.17 ± 1.04	82.00 ± 0.00
29	73.00 ± 0.50	79.00 ± 0.00	83.83 ± 0.29	83.67 ± 0.58
30	73.00 ± 0.50	77.67 ± 0.58	84.33 ± 2.00	73.00 ± 0.50
31	79.00 ± 0.87	81.33 ± 0.58	89.00 ± 0.00	86.33 ± 1.15
32	73.33 ± 0.76	74.83 ± 0.76	82.50 ± 0.29	80.83 ± 0.76
33	69.67 ± 0.29	77.00 ± 0.00	81.00 ± 1.00	80.00 ± 0.00
34	77.50 ± 0.50	81.67 ± 0.58	88.00 ± 0.00	87.00 ± 0.00
35	77.00 ± 0.50	79.00 ± 0.00	86.33 ± 0.58	85.83 ± 0.29
36	77.17 ± 1.04	83.83 ± 0.29	88.67 ± 0.58	89.33 ± 0.58
37	70.67 ± 0.58	76.33 ± 0.58	81.33 ± 0.58	80.33 ± 0.58
38	74.67 ± 0.29	81.33 ± 0.58	86.33 ± 1.15	85.00 ± 1.00

B6.1.1 66 right eyes (continued).

Subject	180°	90°	135°	45°
N0				
39	73.83 ± 0.58	75.17 ± 0.29	83.33 ± 0.58	81.33 ± 0.58
40	73.50 ± 0.50	76.83 ± 0.29	82.50 ± 0.50	81.00 ± 1.00
41	75.00 ± 1.00	78.17 ± 1.76	84.00 ± 1.73	82.67 ± 1.15
42	76.00 ± 1.32	79.00 ± 1.00	85.00 ± 1.00	83.67 ± 0.58
43	69.33 ± 1.15	73.33 ± 0.58	80.33 ± 0.58	79.67 ± 0.58
44	78.33 ± 0.58	82.67 ± 0.58	89.00 ± 0.00	90.00 ± 1.00
45	73.50 ± 0.50	79.17 ± 0.76	84.00 ± 0.00	80.00 ± 0.00
46	72.33 ± 0.58	74.33 ± 0.58	80.83 ± 1.44	79.50 ± 0.50
47	71.00 ± 0.50	78.17 ± 0.76	81.33 ± 0.58	79.50 ± 0.50
48	77.67 ± 1.53	84.00 ± 0.00	92.33 ± 0.58	89.67 ± 1.00
49	77.00 ± 0.00	80.83 ± 0.76	85.00 ± 0.00	85.83 ± 0.29
50	68.00 ± 0.50	70.33 ± 0.58	75.00 ± 1.46	75.33 ± 1.53
51	76.33 ± 0.29	81.67 ± 0.58	88.33 ± 1.15	84.00 ± 1.00
52	73.67 ± 0.58	77.00 ± 0.00	83.33 ± 0.58	82.67 ± 0.58
53	74.33 ± 1.04	78.67 ± 1.15	81.33 ± 2.00	82.33 ± 2.00
54	81.17 ± 2.00	86.83 ± 2.00	92.00 ± 1.73	93.33 ± 0.58
55	76.17 ± 1.26	77.67 ± 0.58	84.17 ± 0.29	83.33 ± 1.53
56	73.33 ± 1.26	79.00 ± 2.00	82.00 ± 1.73	81.67 ± 1.53
57	77.67 ± 0.58	84.33 ± 0.58	92.33 ± 0.58	89.83 ± 2.00
58	78.83 ± 0.29	79.83 ± 0.29	88.83 ± 0.29	84.83 ± 0.29
59	78.00 ± 0.50	82.67 ± 2.00	90.33 ± 0.58	85.33 ± 1.15
60	76.83 ± 1.61	75.17 ± 2.00	83.67 ± 1.04	80.33 ± 2.00
61	80.00 ± 0.50	81.67 ± 0.29	89.67 ± 0.29	85.00 ± 0.58
62	74.67 ± 0.76	80.17 ± 0.29	87.00 ± 0.00	84.00 ± 0.00
63	67.67 ± 0.58	71.83 ± 0.29	78.83 ± 0.29	78.00 ± 0.01
64	77.33 ± 0.25	81.33 ± 1.15	88.33 ± 1.15	84.67 ± 1.53
65	72.00 ± 1.00	74.50 ± 0.50	80.83 ± 1.04	77.33 ± 2.00
66	75.83 ± 0.58	81.67 ± 0.58	86.83 ± 1.04	87.83 ± 1.04

B6.1.2 20 right eyes repeated

Subject	180°	90°	135°	45°
N0				
1	71.17 ± 1.26	78.33 ± 0.58	82.33 ± 0.58	81.00 ± 1.73
2	78.33 ± 0.76	85.33 ± 0.58	92.83 ± 0.29	89.00 ± 1.00
3	80.67 ± 1.04	81.50 ± 0.50	92.50 ± 1.50	87.67 ± 1.15
4	79.67 ± 0.00	87.33 ± 0.58	93.33 ± 1.15	91.33 ± 2.00
5	75.67 ± 0.29	79.00 ± 0.00	83.17 ± 0.76	83.67 ± 0.58
6	74.17 ± 1.04	76.67 ± 0.58	81.67 ± 0.58	79.67 ± 0.58
7	69.17 ± 0.29	71.17 ± 1.26	77.33 ± 0.58	77.33 ± 0.67
8	77.50 ± 1.00	86.50 ± 1.80	91.00 ± 1.32	90.17 ± 1.04
9	75.83 ± 0.29	82.00 ± 1.00	86.83 ± 0.58	86.67 ± 0.76
10	76.83 ± 0.76	80.67 ± 0.58	87.00 ± 1.00	87.00 ± 1.00
11	72.67 ± 0.29	73.33 ± 0.58	81.33 ± 0.58	81.17 ± 0.29
12	75.00 ± 1.32	79.33 ± 0.58	84.00 ± 1.15	84.00 ± 0.00
13	75.50 ± 0.00	79.33 ± 1.53	85.33 ± 1.15	83.50 ± 0.87
14	78.83 ± 1.04	81.83 ± 1.61	88.67 ± 1.15	86.67 ± 0.58
15	73.67 ± 1.04	78.33 ± 0.29	83.83 ± 1.26	84.00 ± 1.00
16	77.67 ± 1.53	81.00 ± 1.73	85.33 ± 0.58	86.83 ± 0.76
17	81.50 ± 0.50	81.33 ± 0.58	89.67 ± 0.58	84.33 ± 1.53
18	75.33 ± 0.76	78.67 ± 0.58	86.67 ± 1.15	82.67 ± 0.58
19	79.50 ± 0.87	88.00 ± 1.00	89.83 ± 0.76	90.33 ± 0.58
20	76.67 ± 1.15	81.83 ± 0.76	87.50 ± 0.87	85.67 ± 1.53

B6.1.3 66 left eyes

Subject	180°	90°	135°	45°
NO				
1	71.17 ± 1.26	77.00 ± 1.00	84.17 ± 0.76	81.33 ± 1.53
2	78.17 ± 0.76	80.33 ± 0.58	86.17 ± 1.04	85.17 ± 0.76
3	76.17 ± 1.61	80.00 ± 1.00	88.00 ± 1.00	82.67 ± 0.58
4	75.33 ± 0.58	87.00 ± 1.00	92.00 ± 1.00	88.33 ± 0.58
5	74.50 ± 0.50	78.50 ± 0.50	87.25 ± 0.35	84.67 ± 0.58
6	77.00 ± 1.00	78.67 ± 1.15	83.67 ± 1.15	85.33 ± 1.15
7	67.17 ± 0.29	70.33 ± 0.58	74.00 ± 1.00	75.00 ± 1.00
8	81.33 ± 0.58	87.00 ± 1.00	91.67 ± 0.58	93.67 ± 0.58
9	80.50 ± 1.32	85.17 ± 0.58	91.67 ± 0.29	87.33 ± 1.15
10	76.00 ± 0.50	79.35 ± 0.58	84.67 ± 0.58	83.00 ± 1.00
11	75.00 ± 0.50	78.33 ± 0.58	85.67 ± 1.15	83.00 ± 1.00
12	75.00 ± 0.87	79.00 ± 1.00	87.83 ± 0.76	82.67 ± 1.15
1	72.00 ± 0.87	78.50 ± 0.50	85.00 ± 1.00	83.17 ± 1.04
14	79.67 ± 0.58	81.33 ± 0.58	87.67 ± 1.15	85.83 ± 1.26
15	75.33 ± 0.58	79.33 ± 0.58	86.67 ± 1.35	84.67 ± 1.15
16	74.33 ± 0.29	78.00 ± 1.00	84.67 ± 0.58	82.33 ± 0.58
17	80.00 ± 1.00	81.67 ± 1.53	89.83 ± 1.26	85.67 ± 0.58
18	74.83 ± 0.76	78.50 ± 0.50	86.00 ± 0.58	82.67 ± 0.58
19	79.00 ± 0.50	88.33 ± 0.58	90.67 ± 1.15	90.33 ± 1.15
20	75.67 ± 0.76	80.83 ± 1.44	86.83 ± 1.26	85.33 ± 0.58
21	73.83 ± 0.76	78.17 ± 0.76	82.50 ± 0.50	81.67 ± 0.58
22	72.67 ± 0.58	72.33 ± 0.58	79.67 ± 0.58	80.67 ± 1.53
23	70.33 ± 0.29	79.67 ± 0.58	81.17 ± 0.76	79.17 ± 0.76
24	75.17 ± 0.58	80.33 ± 1.53	85.83 ± 0.76	84.00 ± 1.00
25	78.67 ± 0.58	82.67 ± 0.58	88.67 ± 0.58	88.67 ± 0.58
26	76.17 ± 0.58	81.33 ± 1.15	84.00 ± 0.00	85.00 ± 1.00
27	72.67 ± 0.29	77.50 ± 0.50	84.33 ± 0.58	82.33 ± 0.58
28	71.67 ± 0.76	75.33 ± 0.58	83.00 ± 0.50	80.00 ± 0.00
29	74.00 ± 0.87	79.83 ± 1.04	83.33 ± 0.58	84.67 ± 0.58
30	76.50 ± 1.32	81.67 ± 0.58	89.00 ± 2.00	88.33 ± 1.53
31	73.33 ± 0.58	76.00 ± 1.00	82.83 ± 0.76	80.67 ± 1.53
32	71.17 ± 0.29	79.00 ± 0.00	84.00 ± 0.50	81.50 ± 0.50
33	75.00 ± 0.00	78.00 ± 1.00	84.00 ± 1.00	83.67 ± 0.58
34	82.17 ± 0.29	78.17 ± 0.76	86.67 ± 0.58	87.50 ± 0.50
35	77.17 ± 0.58	80.33 ± 0.76	86.67 ± 0.58	85.33 ± 0.58
36	76.00 ± 1.00	80.00 ± 1.00	88.33 ± 0.58	84.33 ± 1.15
37	69.50 ± 0.50	75.00 ± 1.00	80.67 ± 0.58	79.00 ± 1.00
38	75.10 ± 0.76	81.67 ± 0.58	86.83 ± 0.29	85.33 ± 0.58
39	77.17 ± 0.58	78.17 ± 0.29	86.67 ± 0.58	85.00 ± 0.00
40	72.50 ± 0.00	74.00 ± 1.00	81.50 ± 0.50	78.83 ± 0.76
41	72.50 ± 0.87	76.00 ± 1.00	82.00 ± 1.00	79.67 ± 0.58
42	76.50 ± 0.50	80.67 ± 0.58	85.33 ± 1.15	84.67 ± 0.76
43	69.33 ± 0.29	75.00 ± 0.00	79.00 ± 0.00	78.67 ± 0.58
44	76.17 ± 0.29	81.33 ± 0.58	86.33 ± 0.58	89.00 ± 0.00
45	72.67 ± 0.29	78.67 ± 0.58	85.00 ± 0.00	80.17 ± 0.89
46	71.83 ± 0.76	76.83 ± 0.76	80.17 ± 0.76	79.33 ± 0.76
47	73.33 ± 0.76	83.00 ± 0.00	86.67 ± 0.58	86.67 ± 0.58
48	77.50 ± 0.87	84.50 ± 0.50	92.67 ± 0.58	88.67 ± 1.53
49	77.83 ± 0.76	81.67 ± 0.00	89.33 ± 0.58	86.00 ± 0.00
50	70.50 ± 0.87	75.33 ± 2.00	79.33 ± 1.53	81.33 ± 1.21
51	77.67 ± 1.04	81.33 ± 1.53	89.00 ± 1.35	86.00 ± 1.00
52	73.67 ± 0.58	77.00 ± 2.00	84.00 ± 2.00	83.33 ± 0.58
53	74.17 ± 1.26	79.00 ± 1.00	80.33 ± 1.53	82.00 ± 1.73
54	81.50 ± 1.80	88.33 ± 0.58	91.67 ± 2.00	94.33 ± 0.58
55	74.83 ± 0.76	77.83 ± 0.29	84.33 ± 0.58	82.00 ± 1.00
56	73.00 ± 0.50	78.67 ± 0.58	82.33 ± 0.58	81.67 ± 1.44
57	80.00 ± 2.00	81.50 ± 0.50	89.33 ± 2.00	88.67 ± 0.58

B6.1.3 66 left eyes (continued)

Subject	180°	90°	135°	45°
N0				
58	76.67 ± 0.29	79.67 ± 0.58	86.67 ± 0.58	84.67 ± 0.58
59	72.33 ± 0.29	78.33 ± 1.53	83.33 ± 2.00	84.00 ± 1.00
60	77.67 ± 0.58	80.33 ± 1.61	86.17 ± 1.76	88.67 ± 2.00
61	77.00 ± 1.00	82.67 ± 0.50	89.83 ± 0.29	84.00 ± 1.00
62	73.00 ± 0.50	78.33 ± 0.58	83.33 ± 0.29	82.83 ± 0.76
63	68.17 ± 0.29	72.83 ± 0.29	79.00 ± 0.00	79.67 ± 0.58
64	78.67 ± 0.76	81.00 ± 1.00	91.00 ± 1.53	85.17 ± 0.76
65	69.83 ± 0.29	73.67 ± 0.58	79.33 ± 1.15	79.00 ± 0.00
66	76.67 ± 0.29	80.00 ± 0.00	86.67 ± 1.53	87.83 ± 0.76

B6.1.4 20 left eyes repeated

Subject	180°	90°	135°	45°
N0				
1	71.33 ± 0.58	76.50 ± 0.50	83.50 ± 1.32	81.00 ± 1.00
2	77.67 ± 0.29	81.67 ± 1.53	86.33 ± 1.00	86.33 ± 1.00
3	80.33 ± 0.29	82.17 ± 0.76	92.50 ± 0.50	87.67 ± 0.58
4	74.50 ± 0.00	86.33 ± 1.53	92.00 ± 0.00	88.00 ± 1.00
5	75.83 ± 0.29	77.67 ± 1.53	88.00 ± 0.00	81.67 ± 0.58
6	76.17 ± 0.29	78.67 ± 0.58	84.00 ± 1.00	84.33 ± 1.00
7	67.00 ± 0.87	71.00 ± 1.00	75.33 ± 0.58	76.67 ± 0.58
8	76.00 ± 1.73	87.67 ± 0.58	92.83 ± 0.76	90.33 ± 0.58
9	77.67 ± 0.29	85.33 ± 1.15	90.67 ± 0.58	89.67 ± 1.15
10	75.50 ± 0.50	81.33 ± 0.58	87.33 ± 0.58	86.67 ± 1.53
11	74.33 ± 0.58	78.33 ± 0.58	82.50 ± 0.50	81.83 ± 0.76
12	77.17 ± 0.76	79.67 ± 0.58	86.33 ± 0.58	85.00 ± 1.00
13	72.83 ± 0.58	78.33 ± 0.58	85.00 ± 1.00	82.67 ± 0.58
14	78.00 ± 0.00	81.83 ± 0.76	87.50 ± 0.50	89.00 ± 1.00
15	72.83 ± 1.04	77.33 ± 0.58	83.00 ± 1.00	83.67 ± 0.58
16	74.17 ± 0.58	77.00 ± 0.00	84.83 ± 0.29	81.67 ± 0.58
17	81.00 ± 0.00	81.00 ± 1.00	90.17 ± 0.76	85.83 ± 0.29
18	75.33 ± 0.29	78.00 ± 0.00	86.00 ± 1.00	81.67 ± 0.58
19	80.00 ± 0.50	87.67 ± 0.58	91.50 ± 0.50	90.33 ± 1.15
20	75.50 ± 0.50	81.67 ± 0.58	86.17 ± 1.04	85.67 ± 0.58

B6.1.5 10 left eyes with and without cycloplegia

Subject	180°	90°	135°	45°
N0				
Without				
71	111.67 ± 0.58	135.50 ± 0.50	143.00 ± 0.00	130.33 ± 0.58
72	109.33 ± 1.53	132.33 ± 1.04	141.00 ± 1.00	126.67 ± 0.58
73	116.00 ± 1.00	142.33 ± 0.58	152.33 ± 1.15	135.33 ± 0.58
74	111.67 ± 1.04	128.33 ± 0.58	142.00 ± 1.00	128.00 ± 1.00
75	117.67 ± 0.58	140.00 ± 1.00	151.33 ± 0.58	137.33 ± 0.58
76	115.67 ± 1.04	139.33 ± 0.58	149.00 ± 2.00	136.67 ± 0.58
77	114.00 ± 1.00	141.00 ± 1.00	151.50 ± 0.87	133.33 ± 0.58
78	115.00 ± 1.00	144.33 ± 0.58	152.00 ± 1.00	139.33 ± 0.58
79	112.17 ± 0.29	135.33 ± 0.58	146.00 ± 1.00	131.00 ± 1.00
80	114.50 ± 0.50	143.33 ± 0.87	151.00 ± 1.00	137.67 ± 0.58
With				
71	109.67 ± 0.29	133.67 ± 0.58	141.67 ± 0.58	130.00 ± 0.00
72	109.83 ± 1.04	133.00 ± 0.00	141.33 ± 0.58	127.33 ± 0.58
73	117.33 ± 0.58	142.67 ± 1.15	152.67 ± 0.58	136.33 ± 0.58
74	112.00 ± 0.00	127.17 ± 0.96	143.00 ± 1.00	127.83 ± 0.58
75	118.50 ± 0.50	140.67 ± 0.58	152.67 ± 0.52	137.33 ± 1.15
76	117.00 ± 1.00	141.00 ± 1.00	150.00 ± 1.00	137.33 ± 0.58
77	113.17 ± 1.04	139.67 ± 0.58	151.67 ± 0.67	133.33 ± 1.15
78	115.67 ± 0.58	145.00 ± 0.00	153.67 ± 0.58	140.00 ± 0.58
79	112.67 ± 0.58	135.67 ± 1.15	147.00 ± 1.73	132.67 ± 0.58
80	115.17 ± 0.29	143.00 ± 1.00	152.33 ± 0.58	136.67 ± 0.58

B6.2 PURKINJE IMAGE II (POSTERIOR CORNEAL SURFACE)

B6.2.1 66 right eyes.

Subject	180°	90°	135°	45°
N0				
1	61.17 ± 1.04	66.33 ± 0.76	68.33 ± 0.58	65.83 ± 0.29
2	66.33 ± 1.15	69.67 ± 0.58	75.67 ± 0.58	73.33 ± 1.15
3	68.50 ± 0.50	68.50 ± 0.50	75.33 ± 1.15	73.33 ± 0.58
4	66.83 ± 0.29	73.00 ± 1.00	77.17 ± 1.04	74.50 ± 0.50
5	64.50 ± 0.50	67.67 ± 1.15	76.00 ± 1.15	71.33 ± 0.58
6	63.17 ± 0.29	61.00 ± 1.73	69.00 ± 1.00	67.83 ± 0.76
7	55.50 ± 1.00	58.50 ± 1.33	64.33 ± 1.53	63.17 ± 0.76
8	65.50 ± 0.50	74.00 ± 1.00	79.17 ± 0.76	75.33 ± 1.15
9	67.00 ± 1.00	70.83 ± 0.76	75.17 ± 1.04	73.17 ± 0.76
10	65.33 ± 0.76	67.00 ± 0.00	75.33 ± 0.58	72.67 ± 0.58
11	63.83 ± 1.04	62.50 ± 0.50	72.00 ± 1.00	67.67 ± 0.58
12	61.83 ± 0.29	61.83 ± 0.76	68.83 ± 1.26	66.50 ± 1.00
13	64.33 ± 0.58	66.67 ± 0.58	72.33 ± 0.58	68.50 ± 1.32
14	68.67 ± 1.15	69.50 ± 0.87	75.00 ± 1.73	74.67 ± 0.58
15	66.33 ± 0.58	65.33 ± 0.58	70.17 ± 0.76	71.00 ± 1.00
16	62.17 ± 1.04	61.67 ± 1.53	69.00 ± 1.73	67.50 ± 0.87
17	69.00 ± 0.50	69.00 ± 1.00	78.00 ± 1.00	71.50 ± 0.87
18	64.83 ± 0.29	64.50 ± 0.50	69.33 ± 0.58	69.67 ± 0.58
19	70.17 ± 1.89	67.33 ± 1.15	77.67 ± 0.58	76.33 ± 1.00
20	60.50 ± 0.87	66.00 ± 1.00	72.33 ± 0.58	70.33 ± 1.15
21	62.67 ± 0.29	63.33 ± 0.58	70.17 ± 0.29	67.67 ± 0.58
22	62.17 ± 0.29	63.67 ± 0.58	69.00 ± 1.00	69.00 ± 1.00
23	60.17 ± 0.29	64.50 ± 0.50	69.67 ± 0.58	65.50 ± 0.50
24	62.67 ± 0.29	64.17 ± 0.29	74.67 ± 0.58	68.33 ± 0.58
25	63.17 ± 0.29	69.00 ± 0.00	75.00 ± 1.00	72.50 ± 0.50
26	62.67 ± 0.67	62.83 ± 0.29	69.83 ± 0.29	68.17 ± 0.29
27	62.83 ± 0.58	62.67 ± 0.58	72.00 ± 1.00	68.33 ± 1.15
28	65.50 ± 0.87	63.33 ± 0.76	69.67 ± 1.04	70.00 ± 0.00
29	60.33 ± 0.29	64.17 ± 0.76	70.17 ± 0.76	67.67 ± 0.58
30	60.17 ± 0.29	61.67 ± 0.58	66.00 ± 0.00	60.17 ± 0.29
31	65.17 ± 0.29	67.67 ± 0.58	71.83 ± 1.26	72.67 ± 0.58
32	63.50 ± 0.50	64.83 ± 0.50	70.67 ± 0.58	69.67 ± 0.58
33	59.50 ± 1.00	63.00 ± 0.00	69.67 ± 0.58	67.00 ± 0.00
34	65.00 ± 0.50	64.83 ± 0.29	70.67 ± 0.58	70.00 ± 1.00
35	66.00 ± 0.50	65.67 ± 0.58	71.67 ± 0.58	71.33 ± 0.58
36	65.67 ± 0.76	68.67 ± 0.58	75.67 ± 0.58	74.33 ± 1.53
37	59.83 ± 0.29	64.33 ± 0.58	70.67 ± 0.58	67.67 ± 0.58
38	63.67 ± 0.58	67.33 ± 1.53	71.33 ± 2.00	70.67 ± 1.53
39	65.50 ± 0.50	64.67 ± 0.76	73.00 ± 0.00	69.67 ± 0.58
40	61.33 ± 0.58	63.67 ± 0.58	67.00 ± 1.00	68.50 ± 0.50
41	64.17 ± 1.00	68.67 ± 1.15	77.00 ± 1.00	72.17 ± 1.15
42	63.00 ± 1.00	68.67 ± 0.58	70.00 ± 0.00	74.50 ± 0.50
43	56.50 ± 0.50	60.00 ± 0.00	65.33 ± 0.58	63.33 ± 0.58
44	64.83 ± 0.29	66.33 ± 1.15	75.67 ± 0.58	70.67 ± 0.58
45	60.17 ± 0.29	64.33 ± 0.58	69.83 ± 1.04	69.33 ± 0.58
46	57.83 ± 1.26	57.00 ± 1.00	63.83 ± 0.76	60.67 ± 0.58
47	61.00 ± 0.50	65.17 ± 0.76	69.33 ± 0.58	66.83 ± 0.29
48	66.17 ± 1.04	73.00 ± 1.00	79.67 ± 0.58	76.33 ± 1.15
49	63.17 ± 0.29	69.00 ± 0.00	69.83 ± 0.29	71.67 ± 0.58
50	56.33 ± 0.58	61.67 ± 1.53	64.00 ± 1.00	66.33 ± 1.89
51	63.33 ± 0.29	66.67 ± 1.15	71.83 ± 0.76	71.00 ± 0.00

B6.2.1 66 right eyes (continued).

Subject	180°	90°	135°	45°
N0				
52	62.50 ± 0.50	65.17 ± 0.29	69.67 ± 0.58	69.33 ± 0.58
53	62.67 ± 1.15	63.00 ± 1.00	69.33 ± 2.00	68.67 ± 1.15
54	69.83 ± 1.89	73.33 ± 1.53	76.67 ± 1.53	77.67 ± 0.58
55	63.50 ± 1.73	65.33 ± 0.58	72.33 ± 1.53	72.50 ± 2.00
56	60.17 ± 1.53	63.00 ± 1.73	66.67 ± 1.15	66.00 ± 2.00
57	66.17 ± 1.04	73.00 ± 1.15	79.00 ± 1.00	76.33 ± 0.29
58	65.83 ± 0.76	64.83 ± 0.29	76.83 ± 0.29	71.17 ± 0.76
59	63.83 ± 2.00	68.67 ± 1.53	74.50 ± 1.32	74.33 ± 2.00
60	64.67 ± 0.29	61.33 ± 1.15	67.17 ± 0.76	66.00 ± 2.00
61	69.00 ± 0.50	69.00 ± 0.76	78.00 ± 0.00	71.50 ± 0.00
62	65.83 ± 0.58	67.17 ± 0.58	75.50 ± 0.50	72.17 ± 0.29
63	59.00 ± 0.50	58.83 ± 0.29	65.17 ± 0.29	65.83 ± 0.29
64	67.00 ± 1.53	64.83 ± 1.61	75.50 ± 1.35	67.33 ± 0.58
65	63.17 ± 1.04	71.00 ± 1.00	72.67 ± 0.58	68.33 ± 2.00
66	63.00 ± 0.87	66.50 ± 0.50	74.67 ± 0.58	72.67 ± 0.58

B6.2.2. 20 right eyes repeated

Subject	180°	90°	135°	45°
N0				
1	61.50 ± 0.50	66.17 ± 0.76	69.00 ± 0.00	66.67 ± 1.53
2	68.00 ± 1.00	70.67 ± 0.58	79.00 ± 0.00	74.83 ± 0.58
3	65.00 ± 1.32	68.33 ± 2.00	78.33 ± 1.53	72.17 ± 0.29
4	70.00 ± 0.50	72.00 ± 0.00	76.67 ± 1.53	76.33 ± 1.53
5	65.17 ± 0.76	67.33 ± 2.00	72.83 ± 0.29	71.67 ± 1.53
6	64.00 ± 0.00	62.17 ± 1.26	70.00 ± 0.00	67.67 ± 0.58
7	60.00 ± 0.87	59.00 ± 1.00	66.33 ± 0.58	63.00 ± 2.00
8	66.00 ± 1.00	74.00 ± 1.00	78.50 ± 0.50	76.00 ± 1.00
9	64.33 ± 0.76	66.17 ± 0.76	74.33 ± 0.58	68.50 ± 0.50
10	66.33 ± 0.29	68.00 ± 0.00	73.33 ± 1.15	73.67 ± 0.76
11	62.33 ± 1.04	60.33 ± 0.58	67.00 ± 1.00	67.17 ± 0.29
12	62.50 ± 0.50	66.00 ± 0.00	71.00 ± 0.58	71.00 ± 1.15
13	64.17 ± 0.76	66.17 ± 0.76	72.33 ± 0.58	69.00 ± 0.50
14	68.33 ± 0.58	69.17 ± 0.29	74.67 ± 0.76	74.17 ± 0.76
15	64.50 ± 0.50	62.67 ± 0.58	69.33 ± 0.58	68.33 ± 0.58
16	64.83 ± 1.26	64.00 ± 1.00	72.00 ± 1.00	71.26 ± 0.37
17	69.83 ± 0.29	69.00 ± 1.00	79.67 ± 0.58	72.00 ± 1.00
18	63.50 ± 1.00	64.67 ± 0.58	68.33 ± 0.58	69.33 ± 1.15
19	69.17 ± 0.76	68.00 ± 1.00	77.00 ± 0.00	74.33 ± 1.15
20	61.83 ± 0.29	69.83 ± 0.76	72.50 ± 0.87	70.33 ± 1.15

B6.2.3 66 left eyes

Subject	180°	90°	135°	45°
N0				
1	61.00 ± 1.00	65.00 ± 1.00	71.50 ± 0.50	69.00 ± 1.00
2	68.17 ± 0.29	69.33 ± 0.58	74.00 ± 1.00	71.67 ± 0.58
3	63.33 ± 1.35	64.33 ± 0.58	72.67 ± 1.26	67.33 ± 0.58
4	65.33 ± 0.58	72.67 ± 0.58	74.67 ± 0.58	73.67 ± 0.58
5	64.33 ± 1.26	66.67 ± 0.58	75.17 ± 1.04	70.00 ± 0.00
6	66.83 ± 0.29	64.67 ± 0.58	72.33 ± 1.15	74.00 ± 1.00
7	56.33 ± 0.29	58.00 ± 1.00	64.67 ± 1.53	63.33 ± 1.15
8	70.83 ± 0.76	75.00 ± 1.00	78.67 ± 0.58	80.00 ± 1.00
9	67.83 ± 0.29	67.67 ± 1.26	76.00 ± 1.00	70.17 ± 1.04
10	64.67 ± 0.58	66.83 ± 1.04	74.67 ± 0.58	72.17 ± 1.04
11	65.33 ± 0.29	62.00 ± 1.00	70.67 ± 0.58	67.67 ± 1.15
12	64.67 ± 1.04	62.00 ± 0.50	74.17 ± 1.61	68.15 ± 1.26
13	61.33 ± 1.26	64.67 ± 1.15	74.83 ± 0.29	69.67 ± 1.15
14	67.00 ± 1.73	68.00 ± 1.73	72.33 ± 1.15	70.83 ± 0.76
15	64.33 ± 1.15	66.50 ± 1.32	75.00 ± 1.00	69.83 ± 0.76
16	61.33 ± 0.29	61.00 ± 0.00	69.33 ± 0.58	67.00 ± 0.00
17	68.50 ± 0.50	69.33 ± 1.53	79.00 ± 1.00	71.83 ± 0.29
18	65.17 ± 0.29	63.67 ± 1.53	68.17 ± 0.29	68.17 ± 0.29
19	69.67 ± 0.58	67.33 ± 0.58	78.00 ± 0.00	75.67 ± 0.58
20	62.00 ± 0.50	64.83 ± 1.04	70.83 ± 1.61	68.33 ± 0.58
21	61.83 ± 0.58	64.00 ± 1.00	70.00 ± 0.50	68.50 ± 0.50
22	63.67 ± 1.15	63.33 ± 0.58	70.33 ± 1.15	69.33 ± 1.15
23	59.83 ± 0.76	64.83 ± 0.76	70.83 ± 0.76	64.67 ± 1.15
24	64.00 ± 0.00	65.67 ± 0.58	74.00 ± 0.00	69.67 ± 0.58
25	66.33 ± 0.58	66.83 ± 0.29	73.67 ± 0.58	71.50 ± 0.87
26	64.50 ± 0.50	64.67 ± 1.53	71.83 ± 0.58	70.50 ± 0.50
27	63.00 ± 0.50	64.00 ± 0.00	71.33 ± 0.58	70.00 ± 0.00
28	62.00 ± 0.50	62.00 ± 0.50	71.17 ± 0.29	67.33 ± 0.58
29	60.00 ± 0.50	64.67 ± 0.58	70.67 ± 0.58	68.67 ± 0.58
30	63.17 ± 0.58	67.83 ± 1.26	78.00 ± 0.50	68.00 ± 1.00
31	60.50 ± 0.50	62.00 ± 0.00	69.33 ± 1.53	66.33 ± 0.58
32	61.67 ± 0.76	66.67 ± 0.29	73.83 ± 0.29	69.50 ± 0.29
33	64.17 ± 0.29	62.83 ± 0.29	69.00 ± 1.00	68.83 ± 0.00
34	70.67 ± 0.58	65.83 ± 0.29	73.00 ± 1.00	74.00 ± 0.00
35	65.67 ± 0.58	68.17 ± 0.76	76.33 ± 0.76	72.00 ± 1.00
36	64.17 ± 1.04	67.33 ± 0.58	74.00 ± 1.00	71.67 ± 0.58
37	58.33 ± 0.29	63.33 ± 0.58	70.67 ± 1.15	67.67 ± 0.58
38	63.00 ± 0.50	68.67 ± 0.58	70.67 ± 0.58	70.83 ± 0.76
39	67.83 ± 0.29	68.00 ± 0.50	75.33 ± 0.58	72.67 ± 0.58
40	60.00 ± 0.00	60.33 ± 0.58	66.83 ± 0.76	63.33 ± 0.58
41	60.50 ± 0.87	60.33 ± 1.53	67.67 ± 1.53	66.67 ± 1.53
42	64.33 ± 0.58	68.17 ± 0.29	71.33 ± 0.58	74.50 ± 0.50
43	57.50 ± 0.50	58.33 ± 0.58	65.17 ± 0.76	61.33 ± 0.58
44	63.00 ± 0.50	65.83 ± 0.76	75.00 ± 0.00	69.33 ± 0.58
45	59.33 ± 0.76	65.00 ± 0.50	70.33 ± 0.58	70.67 ± 0.58
46	59.00 ± 0.50	57.67 ± 1.26	63.00 ± 1.00	59.83 ± 0.29
47	62.83 ± 0.58	67.50 ± 0.50	73.17 ± 0.29	70.67 ± 0.58
48	66.50 ± 1.32	72.33 ± 0.58	79.50 ± 0.50	75.00 ± 1.53

B6.2.3 66 left eyes (continued)

Subject	180°	90°	135°	45°
N0				
49	64.17 ± 0.29	69.67 ± 0.58	80.50 ± 1.00	72.00 ± 1.00
50	61.00 ± 0.50	61.00 ± 1.73	65.33 ± 0.58	67.00 ± 1.15
51	64.00 ± 0.50	75.33 ± 0.58	75.33 ± 1.32	71.50 ± 1.32
52	62.00 ± 0.87	66.33 ± 0.58	70.33 ± 1.15	70.33 ± 0.58
53	61.83 ± 1.04	62.67 ± 1.53	68.00 ± 1.73	68.67 ± 0.56
54	70.00 ± 1.00	75.00 ± 1.73	76.67 ± 1.00	77.00 ± 0.00
55	61.50 ± 1.80	66.67 ± 2.00	72.00 ± 1.00	71.33 ± 2.00
56	59.33 ± 0.29	62.33 ± 0.58	67.67 ± 0.58	65.67 ± 1.26
57	69.00 ± 1.00	68.00 ± 0.00	76.50 ± 0.50	73.67 ± 1.53
58	65.33 ± 1.04	66.33 ± 0.58	77.00 ± 0.00	71.00 ± 0.00
59	61.00 ± 0.87	62.67 ± 0.58	67.33 ± 1.15	68.67 ± 0.58
60	67.00 ± 0.50	66.00 ± 2.00	74.67 ± 1.53	71.67 ± 1.53
61	65.67 ± 0.29	69.17 ± 1.61	77.33 ± 1.15	73.50 ± 0.87
62	62.83 ± 0.29	64.83 ± 0.29	70.00 ± 0.00	69.67 ± 0.58
63	60.50 ± 0.50	59.83 ± 0.29	66.33 ± 0.58	66.33 ± 0.58
64	66.50 ± 0.87	73.83 ± 0.76	74.67 ± 0.76	72.00 ± 1.00
65	62.17 ± 1.15	65.00 ± 0.50	70.83 ± 0.76	69.67 ± 0.58
66	64.33 ± 0.58	66.33 ± 0.58	73.17 ± 0.29	71.67 ± 2.00

B6.2.4 20 left eyes repeated

Subject	180°	90°	135°	45°
N0				
1	60.17 ± 0.29	64.17 ± 1.04	71.83 ± 0.29	69.00 ± 1.00
2	66.17 ± 0.58	69.67 ± 0.58	74.33 ± 0.76	73.00 ± 0.76
3	65.67 ± 0.76	69.00 ± 1.73	77.67 ± 0.58	74.00 ± 1.80
4	65.33 ± 0.58	71.83 ± 1.76	75.00 ± 0.76	73.67 ± 0.58
5	65.83 ± 0.29	67.67 ± 1.15	76.00 ± 0.00	70.67 ± 0.58
6	65.33 ± 1.15	63.67 ± 0.58	74.33 ± 2.00	69.00 ± 1.00
7	58.67 ± 0.29	58.00 ± 1.00	63.83 ± 0.29	63.83 ± 0.76
8	65.00 ± 1.44	74.50 ± 0.50	80.00 ± 1.00	76.00 ± 1.73
9	68.50 ± 0.50	66.67 ± 0.58	74.67 ± 0.29	75.33 ± 0.58
10	66.17 ± 0.29	68.67 ± 0.58	77.33 ± 0.58	69.00 ± 0.00
11	63.50 ± 1.32	61.33 ± 0.58	71.17 ± 1.89	67.00 ± 1.00
12	66.17 ± 0.76	65.00 ± 1.32	72.17 ± 1.04	70.67 ± 0.58
13	62.83 ± 0.58	64.17 ± 0.76	74.67 ± 0.58	68.67 ± 1.15
14	69.17 ± 0.29	69.67 ± 0.58	75.17 ± 0.76	77.33 ± 0.58
15	64.33 ± 0.58	62.17 ± 1.04	69.00 ± 1.73	68.67 ± 1.53
16	63.17 ± 0.29	61.67 ± 0.58	69.17 ± 0.76	67.00 ± 0.29
17	69.00 ± 0.00	69.00 ± 1.00	79.00 ± 1.00	72.33 ± 0.58
18	64.33 ± 0.29	64.33 ± 0.58	68.00 ± 1.00	69.17 ± 0.76
19	69.83 ± 0.29	67.33 ± 0.58	78.00 ± 0.00	75.17 ± 0.29
20	61.83 ± 0.76	69.00 ± 0.00	71.17 ± 0.29	70.67 ± 1.15

B6.2.5 10 left eyes with and without cycloplegia

Subject	180°	90°	135°	45°
N0				
Without				
71	97.50 ± 0.50	112.33 ± 0.58	123.00 ± 0.00	111.00 ± 0.00
72	95.83 ± 1.04	109.67 ± 0.58	121.67 ± 1.53	105.67 ± 0.58
73	100.33 ± 0.58	117.17 ± 0.76	128.67 ± 0.58	113.00 ± 1.00
74	93.50 ± 0.50	110.50 ± 0.50	130.33 ± 1.53	112.33 ± 0.58
75	105.33 ± 0.58	120.33 ± 0.58	133.33 ± 0.58	119.33 ± 0.58
76	99.83 ± 1.04	120.67 ± 1.53	128.00 ± 1.04	117.00 ± 1.00
77	96.83 ± 1.26	112.00 ± 1.00	127.00 ± 1.00	109.67 ± 0.58
78	94.33 ± 0.58	122.00 ± 1.00	126.00 ± 1.00	118.33 ± 0.58
79	96.00 ± 2.00	115.00 ± 1.00	126.00 ± 1.00	114.17 ± 0.76
80	99.50 ± 0.87	120.00 ± 1.73	126.33 ± 0.58	116.67 ± 1.15
With				
71	95.33 ± 0.58	112.33 ± 0.58	121.00 ± 1.00	109.00 ± 1.00
72	95.50 ± 0.50	109.67 ± 0.58	119.67 ± 0.58	106.67 ± 0.58
73	101.83 ± 0.29	119.00 ± 1.00	129.33 ± 0.58	113.67 ± 0.58
74	94.00 ± 1.00	111.33 ± 0.58	132.00 ± 1.00	112.33 ± 1.15
75	105.00 ± 0.00	120.83 ± 1.61	134.33 ± 1.15	119.00 ± 1.00
76	100.00 ± 0.87	121.00 ± 1.00	128.67 ± 1.15	117.67 ± 0.58
77	95.17 ± 1.04	111.67 ± 0.58	125.33 ± 0.58	110.37 ± 0.58
78	94.67 ± 0.58	122.67 ± 0.58	126.00 ± 1.00	119.00 ± 1.00
79	95.83 ± 0.29	115.33 ± 0.58	125.67 ± 0.58	115.33 ± 0.58
80	98.50 ± 0.87	121.33 ± 0.58	125.33 ± 0.58	116.33 ± 1.15

B6.3 PURKINJE IMAGE IV (POSTERIOR LENS SURFACE).

B6.3.1 66 right eyes.

Subject	180°	90°	135°	45°
N0				
1	49.83 ± 0.76	62.83 ± 0.29	62.33 ± 0.58	61.83 ± 1.04
2	54.50 ± 0.50	66.17 ± 1.04	66.83 ± 0.76	65.00 ± 1.00
3	52.33 ± 0.58	57.33 ± 0.58	58.67 ± 1.15	59.00 ± 1.00
4	54.50 ± 0.50	62.67 ± 0.76	65.00 ± 1.00	61.50 ± 0.87
5	52.00 ± 0.00	59.33 ± 1.53	63.00 ± 0.00	59.33 ± 0.58
6	54.17 ± 1.04	49.67 ± 0.58	59.33 ± 0.58	58.17 ± 0.76
7	49.17 ± 0.76	59.17 ± 0.76	60.17 ± 1.44	59.17 ± 0.76
8	48.67 ± 0.58	60.33 ± 0.58	62.00 ± 0.50	59.33 ± 0.58
9	57.00 ± 0.76	69.83 ± 0.29	70.33 ± 0.76	66.17 ± 1.04
10	50.67 ± 0.29	57.00 ± 0.00	58.67 ± 0.58	58.83 ± 0.29
11	52.00 ± 0.87	60.00 ± 0.00	62.50 ± 0.50	61.00 ± 0.00
12	59.83 ± 0.76	66.67 ± 0.58	68.67 ± 1.15	67.67 ± 0.58
13	58.67 ± 0.58	67.00 ± 1.00	63.83 ± 0.29	65.33 ± 1.15
14	51.83 ± 1.61	58.67 ± 1.15	59.00 ± 1.00	59.33 ± 1.53
15	53.83 ± 0.76	60.33 ± 0.58	61.76 ± 0.58	61.17 ± 0.76
16	49.50 ± 1.32	59.33 ± 1.53	62.33 ± 0.58	58.33 ± 1.53
17	53.83 ± 0.58	61.00 ± 1.00	64.67 ± 0.58	61.00 ± 1.00
18	51.83 ± 0.29	58.83 ± 0.29	60.33 ± 0.58	62.50 ± 0.50
19	58.33 ± 0.58	66.67 ± 0.58	68.00 ± 0.00	69.00 ± 0.00
20	48.67 ± 0.58	60.00 ± 0.00	59.67 ± 0.58	59.00 ± 0.00
21	53.50 ± 0.00	63.67 ± 0.29	63.33 ± 0.29	63.00 ± 0.00
22	51.67 ± 0.29	62.00 ± 1.00	60.00 ± 1.00	60.67 ± 0.58
23	49.83 ± 0.58	57.67 ± 1.15	58.33 ± 0.58	58.33 ± 0.58
24	49.83 ± 0.29	57.67 ± 0.58	59.33 ± 0.58	56.50 ± 0.50
25	48.17 ± 0.67	59.00 ± 1.00	62.00 ± 1.00	59.00 ± 0.00
26	52.67 ± 0.67	63.67 ± 0.29	63.33 ± 0.58	63.00 ± 0.00
27	49.00 ± 0.50	60.00 ± 1.00	61.33 ± 0.58	58.83 ± 1.04
28	50.67 ± 0.29	58.33 ± 0.58	61.17 ± 0.29	58.33 ± 0.58
29	49.17 ± 0.58	56.83 ± 0.29	58.83 ± 0.29	58.17 ± 0.76
30	51.83 ± 0.75	61.00 ± 1.00	60.00 ± 1.00	51.83 ± 0.75
31	53.83 ± 0.76	62.67 ± 0.58	67.00 ± 0.00	62.17 ± 0.76
32	46.33 ± 0.29	51.83 ± 0.29	54.50 ± 0.50	52.83 ± 0.29
33	51.00 ± 0.00	58.33 ± 0.58	60.67 ± 0.58	58.33 ± 0.58
34	47.00 ± 0.00	56.00 ± 0.00	58.00 ± 1.00	55.67 ± 0.58
35	54.67 ± 0.76	59.67 ± 0.50	64.67 ± 0.58	60.67 ± 0.58
36	46.50 ± 0.87	55.33 ± 0.58	57.17 ± 0.29	55.00 ± 0.00
37	49.17 ± 0.76	57.50 ± 0.50	60.50 ± 0.50	57.50 ± 0.50
38	48.00 ± 1.00	54.33 ± 1.15	57.33 ± 1.73	54.33 ± 1.15
39	49.50 ± 0.50	55.00 ± 0.50	60.33 ± 0.76	53.17 ± .29
40	53.67 ± 0.58	62.50 ± 0.50	64.00 ± 0.50	62.00 ± 0.00
41	50.33 ± 0.58	57.00 ± 1.00	59.00 ± 0.00	58.50 ± 0.50
42	45.33 ± 1.89	54.17 ± 0.76	57.00 ± 1.00	54.50 ± 1.50
43	43.50 ± 0.50	48.33 ± 1.15	48.33 ± 1.53	49.67 ± 0.58
44	51.67 ± 0.58	59.67 ± 1.15	62.00 ± 1.00	61.33 ± 1.15
45	50.67 ± 0.29	55.67 ± 0.58	57.00 ± 0.00	56.33 ± 0.58
46	56.17 ± 0.76	62.50 ± 0.50	63.33 ± 0.58	63.50 ± 1.00
47	43.00 ± 0.76	51.00 ± 0.00	52.33 ± 0.29	51.33 ± 0.58
48	55.33 ± 0.76	65.50 ± 0.87	67.00 ± 1.00	66.00 ± 0.00
49	50.17 ± 0.29	60.00 ± 0.00	60.67 ± 0.58	59.00 ± 0.00
50	42.00 ± 0.50	45.00 ± 0.00	50.33 ± 0.58	45.67 ± 0.58
51	48.88 ± 0.25	57.67 ± 1.15	59.00 ± 0.00	57.00 ± 1.00

B6.3.1 66 right eyes (continued).

Subject	180°	90°	135°	45°
N0				
52	51.67 ± 0.58	60.00 ± 1.00	61.67 ± 0.58	59.67 ± 0.58
53	49.67 ± 0.29	56.33 ± 0.58	57.67 ± 0.58	57.00 ± 1.00
54	52.00 ± 2.00	56.33 ± 0.58	58.33 ± 0.58	54.67 ± 0.58
55	55.17 ± 1.15	60.33 ± 1.53	63.33 ± 1.53	61.33 ± 1.15
56	50.50 ± 0.00	60.17 ± 1.89	62.00 ± 1.73	59.00 ± 1.73
57	55.50 ± 0.00	65.50 ± 0.58	67.00 ± 1.00	66.00 ± 0.00
58	47.67 ± 0.29	57.33 ± 0.58	60.33 ± 0.58	56.33 ± 0.58
59	55.50 ± 0.50	60.00 ± 0.00	65.67 ± 0.50	61.00 ± 0.00
60	54.83 ± 0.76	60.17 ± 0.76	62.00 ± 1.00	60.00 ± 2.00
61	53.00 ± 0.58	61.00 ± 0.00	64.67 ± 0.00	61.00 ± 0.58
62	52.83 ± 0.58	62.33 ± 0.58	63.83 ± 0.29	63.33 ± 0.58
63	45.50 ± 0.50	53.33 ± 0.58	55.33 ± 0.58	53.33 ± 0.58
64	59.67 ± 0.58	67.67 ± 0.58	70.67 ± 0.58	68.33 ± 0.58
65	54.17 ± 1.89	63.17 ± 1.04	65.33 ± 0.58	62.17 ± 1.89
66	47.33 ± 0.76	53.17 ± 0.29	56.00 ± 0.50	55.67 ± 0.58

B6.3.2 20 right eyes repeated.

Subject	180°	90°	135°	45°
N0				
1	50.50 ± 1.00	63.00 ± 0.00	62.00 ± 1.00	61.33 ± 0.58
2	56.33 ± 0.58	69.33 ± 0.58	68.00 ± 1.00	69.33 ± 0.58
3	58.67 ± 1.04	59.17 ± 0.29	63.00 ± 1.00	58.50 ± 0.50
4	53.00 ± 0.87	63.00 ± 0.00	65.33 ± 0.58	62.67 ± 1.53
5	50.17 ± 0.29	55.33 ± 0.58	59.67 ± 0.58	57.17 ± 0.76
6	53.67 ± 0.58	58.50 ± 0.50	60.33 ± 1.15	57.67 ± 0.58
7	50.67 ± 0.58	59.67 ± 0.50	61.00 ± 0.00	59.67 ± 0.58
8	49.17 ± 0.76	60.83 ± 1.76	62.00 ± 0.00	58.33 ± 0.58
9	56.33 ± 1.26	66.00 ± 0.00	69.00 ± 1.00	62.67 ± 0.58
10	50.83 ± 0.29	57.83 ± 1.61	59.67 ± 0.58	59.00 ± 0.00
11	52.50 ± 0.50	59.67 ± 0.58	62.67 ± 0.58	60.67 ± 0.58
12	60.50 ± 0.50	66.50 ± 1.00	69.00 ± 1.00	67.00 ± 0.58
13	57.33 ± 0.29	67.00 ± 1.00	63.67 ± 0.58	65.00 ± 1.00
14	54.83 ± 0.76	63.00 ± 1.00	65.00 ± 0.00	59.67 ± 1.15
15	52.33 ± 0.58	60.00 ± 1.00	61.33 ± 0.29	61.50 ± 1.32
16	50.67 ± 0.29	60.00 ± 1.00	63.00 ± 1.00	58.67 ± 0.58
17	53.67 ± 0.29	61.00 ± 1.04	63.67 ± 0.58	61.33 ± 0.58
18	51.17 ± 0.29	58.00 ± 1.00	60.67 ± 0.58	61.00 ± 0.00
19	59.00 ± 0.50	66.33 ± 1.15	67.67 ± 0.58	69.33 ± 0.58
20	49.33 ± 0.29	59.33 ± 1.15	61.33 ± 1.15	59.67 ± 1.15

B6.3.3 66 left eyes.

Subject	180°	90°	135°	45°
N0				
1	50.17 ± 0.76	62.17 ± 0.76	64.17 ± 0.76	60.83 ± 0.76
2	54.17 ± 0.29	64.00 ± 1.00	65.83 ± 1.44	62.50 ± 0.50
3	49.83 ± 1.26	56.17 ± 1.61	55.83 ± 1.89	54.33 ± 1.53
4	53.83 ± 0.76	63.33 ± 0.58	65.67 ± 1.53	63.00 ± 1.00
5	53.17 ± 0.29	59.33 ± 1.61	62.00 ± 1.73	60.00 ± 0.00
6	55.33 ± 0.58	62.33 ± 0.58	64.33 ± 1.00	62.00 ± 0.58
7	49.17 ± 0.29	58.67 ± 0.58	60.67 ± 0.58	59.00 ± 1.00
8	50.33 ± 0.58	61.00 ± 2.00	60.00 ± 1.00	62.83 ± 0.76
9	57.83 ± 1.04	66.33 ± 0.29	66.67 ± 1.53	66.33 ± 0.58
10	49.83 ± 0.58	57.67 ± 0.58	59.67 ± 0.50	58.67 ± 1.53
11	53.50 ± 0.00	60.33 ± 0.58	63.17 ± 0.29	61.33 ± 1.15
12	61.67 ± 0.58	67.67 ± 0.58	70.50 ± 1.00	69.33 ± 1.15
13	57.33 ± 0.76	69.33 ± 0.58	67.67 ± 1.53	66.00 ± 1.00
14	51.00 ± 1.53	55.67 ± 2.00	54.33 ± 1.53	56.67 ± 1.53
15	54.00 ± 1.26	56.83 ± 1.26	65.00 ± 1.00	63.00 ± 0.50
16	49.83 ± 0.29	59.67 ± 0.58	62.83 ± 0.76	59.33 ± 0.58
17	53.00 ± 1.00	61.67 ± 1.53	64.00 ± 0.50	61.33 ± 1.15
18	52.83 ± 0.76	57.67 ± 0.58	59.00 ± 1.00	62.00 ± 1.00
19	57.83 ± 0.29	67.33 ± 0.58	69.67 ± 1.53	69.33 ± 1.15
20	49.00 ± 0.87	57.62 ± 0.58	58.33 ± 0.58	57.67 ± 0.58
21	52.83 ± 0.58	62.17 ± 0.76	63.33 ± 0.58	62.33 ± 0.58
22	52.00 ± 0.87	61.67 ± 0.58	61.33 ± 1.15	59.00 ± 1.00
23	49.00 ± 0.00	57.67 ± 0.58	59.83 ± 0.29	58.67 ± 0.58
24	50.33 ± 0.29	59.33 ± 0.58	61.00 ± 1.00	59.67 ± 0.58
25	50.50 ± 0.50	57.50 ± 0.50	59.33 ± 0.58	58.33 ± 0.58
26	51.67 ± 0.29	59.00 ± 0.00	55.17 ± 0.76	59.33 ± 0.58
27	50.33 ± 0.58	59.33 ± 0.50	61.67 ± 0.58	59.00 ± 0.00
28	47.17 ± 0.29	55.00 ± 1.00	57.17 ± 0.76	54.83 ± 0.29
29	49.83 ± 0.58	57.33 ± 0.58	58.33 ± 0.58	59.00 ± 1.00
30	50.83 ± 1.26	61.33 ± 1.26	60.00 ± 0.00	62.00 ± 0.00
31	52.17 ± 0.76	60.67 ± 0.58	63.00 ± 0.00	61.67 ± 0.58
32	47.00 ± 0.50	53.83 ± 0.50	55.17 ± 0.29	54.00 ± 0.00
33	53.67 ± 0.29	60.00 ± 0.00	63.00 ± 0.00	60.83 ± 0.29
34	49.33 ± 0.76	57.67 ± 0.29	59.33 ± 0.58	57.83 ± 0.29
35	55.00 ± 0.50	61.83 ± 1.25	63.67 ± 0.76	62.33 ± 0.76
36	45.67 ± 0.76	53.67 ± 1.15	55.67 ± 1.15	53.67 ± 1.15
37	49.33 ± 0.29	57.83 ± 0.29	59.67 ± 0.58	57.33 ± 0.58
38	47.83 ± 0.76	54.00 ± 1.00	57.33 ± 1.00	53.83 ± 1.26
39	49.83 ± 0.29	57.33 ± 0.58	58.83 ± 0.76	57.00 ± 0.50
40	54.50 ± 1.00	63.00 ± 0.00	64.33 ± 0.76	62.83 ± 0.29
41	55.33 ± 1.53	61.67 ± 0.29	62.50 ± 1.18	65.00 ± 0.50
42	46.00 ± 0.87	54.33 ± 1.15	57.33 ± 0.58	54.33 ± 1.53
43	45.00 ± 1.80	50.00 ± 0.00	52.17 ± 0.29	51.50 ± 0.50
44	50.17 ± 0.50	58.50 ± 0.87	62.83 ± 0.29	61.00 ± 0.00
45	50.33 ± 0.29	56.17 ± 0.79	58.33 ± 0.58	57.00 ± 1.00
46	56.00 ± 0.58	62.67 ± 0.58	63.17 ± 0.76	63.33 ± 0.76
47	44.33 ± 0.58	54.17 ± 0.29	56.17 ± 0.29	53.00 ± 0.00
48	54.17 ± 0.58	65.67 ± 0.58	66.67 ± 0.58	65.33 ± 0.58
49	49.50 ± 0.00	59.83 ± 0.76	60.67 ± 0.58	58.33 ± 0.58
50	52.67 ± 1.15	49.67 ± 2.00	52.67 ± 1.15	52.33 ± 1.53
51	50.67 ± 0.76	59.33 ± 1.53	59.00 ± 1.53	59.00 ± 1.00
52	51.00 ± 1.32	60.67 ± 1.15	61.33 ± 1.53	60.67 ± 1.15
53	49.33 ± 1.53	55.83 ± 0.76	57.17 ± 1.26	56.50 ± 0.87
54	52.67 ± 0.29	57.00 ± 1.15	58.00 ± 1.00	55.33 ± 0.58

B6.3.3 66 left eyes (continued).

Subject	180°	90°	135°	45°
N0				
55	54.00 ± 0.87	60.00 ± 2.00	62.67 ± 1.53	60.33 ± 2.00
56	50.00 ± 0.50	59.33 ± 1.04	61.67 ± 0.58	60.67 ± 1.15
57	51.33 ± 2.00	58.67 ± 0.58	61.00 ± 2.00	58.67 ± 0.58
58	46.17 ± 0.29	56.00 ± 1.00	58.83 ± 0.29	55.67 ± 0.58
59	50.17 ± 0.29	55.33 ± 0.58	58.67 ± 0.58	57.83 ± 0.29
60	57.33 ± 0.76	64.67 ± 0.58	67.33 ± 2.00	63.33 ± 2.00
61	46.33 ± 1.04	58.33 ± 0.29	60.33 ± 0.58	56.50 ± 0.50
62	53.50 ± 0.50	62.83 ± 0.29	65.33 ± 0.29	62.17 ± 0.76
63	46.33 ± 0.29	53.67 ± 0.58	56.75 ± 0.50	54.83 ± 0.29
64	60.50 ± 0.50	65.67 ± 0.58	69.67 ± 0.58	66.67 ± 1.15
65	51.83 ± 0.76	60.33 ± 1.15	61.67 ± 0.58	58.83 ± 0.29
66	46.67 ± 1.61	53.83 ± 0.76	55.17 ± 0.29	55.00 ± 1.00

B6.3.4 20 left eyes repeated.

Subject	180°	90°	135°	45°
N0				
1	51.00 ± 0.87	62.00 ± 0.00	64.00 ± 0.00	60.83 ± 0.29
2	53.83 ± 0.29	63.00 ± 1.00	66.33 ± 1.53	62.67 ± 0.58
3	52.67 ± 0.58	58.67 ± 0.58	62.17 ± 1.89	58.83 ± 1.00
4	52.00 ± 0.50	62.67 ± 0.58	65.33 ± 0.58	62.00 ± 0.00
5	49.83 ± 0.58	55.17 ± 0.29	60.33 ± 0.52	57.17 ± 0.29
6	56.50 ± 0.87	62.67 ± 0.58	64.00 ± 1.00	63.00 ± 1.73
7	49.83 ± 0.29	58.00 ± 0.00	61.67 ± 0.58	57.00 ± 0.00
8	48.17 ± 0.29	60.67 ± 0.58	61.67 ± 1.53	58.67 ± 0.58
9	56.33 ± 0.29	67.33 ± 0.50	69.67 ± 0.58	66.33 ± 0.58
10	50.67 ± 1.04	58.67 ± 1.53	61.00 ± 0.00	56.00 ± 1.73
11	53.33 ± 0.29	61.00 ± 0.00	62.67 ± 0.58	62.67 ± 0.58
12	63.00 ± 0.50	71.67 ± 1.15	73.67 ± 0.58	71.75 ± 1.33
13	57.50 ± 0.50	68.33 ± 0.58	67.50 ± 0.87	66.67 ± 0.58
14	54.83 ± 0.29	64.67 ± 0.58	64.67 ± 0.58	62.67 ± 0.58
15	51.33 ± 0.76	60.00 ± 1.00	61.00 ± 1.00	60.50 ± 0.50
16	49.33 ± 0.76	59.67 ± 0.58	61.67 ± 0.58	58.83 ± 0.76
17	52.83 ± 0.29	61.33 ± 0.58	63.67 ± 0.58	61.67 ± 1.15
18	51.83 ± 0.76	58.00 ± 1.00	60.00 ± 1.00	61.00 ± 1.73
19	58.17 ± 0.29	67.00 ± 0.00	67.00 ± 1.73	69.33 ± 1.15
20	48.83 ± 0.76	58.33 ± 0.58	61.67 ± 0.58	58.67 ± 0.58

B6.3.5 10 left eyes with and without cycloplegia.

Subject	180°	90°	135°	45°
N0				
Without				
71	85.00 ± 0.00	108.00 ± 0.00	111.67 ± 0.58	101.00 ± 0.00
72	73.67 ± 1.15	94.00 ± 1.00	97.00 ± 1.00	89.33 ± 0.58
73	75.50 ± 0.50	100.00 ± 1.00	98.33 ± 0.58	94.67 ± 0.58
74	78.00 ± 0.00	99.67 ± 0.50	101.00 ± 0.00	96.00 ± 1.00
75	81.33 ± 0.58	102.00 ± 1.00	107.33 ± 0.58	97.33 ± 0.58
76	82.17 ± 1.35	102.33 ± 1.53	106.00 ± 1.00	96.00 ± 2.00
77	72.17 ± 0.76	96.67 ± 1.15	87.00 ± 0.00	87.00 ± 0.00
78	85.33 ± 0.58	108.00 ± 1.00	110.33 ± 0.58	103.67 ± 0.58
79	75.67 ± 0.58	99.33 ± 0.58	100.33 ± 0.58	97.00 ± 0.00
80	82.33 ± 0.29	105.00 ± 0.58	107.67 ± 0.50	100.00 ± 0.00
with				
71	87.33 ± 0.58	108.33 ± 0.58	112.00 ± 1.00	102.33 ± 0.58
72	81.17 ± 1.61	102.00 ± 1.00	105.00 ± 0.00	97.00 ± 1.00
73	84.33 ± 0.58	106.33 ± 0.58	105.50 ± 0.50	101.67 ± 0.58
74	80.83 ± 0.58	102.00 ± 1.00	105.00 ± 0.00	99.33 ± 0.58
75	91.17 ± 0.76	113.33 ± 0.58	117.00 ± 1.00	99.67 ± 0.58
76	83.67 ± 0.58	109.00 ± 0.58	109.00 ± 1.00	102.67 ± 0.58
77	78.67 ± 0.58	102.33 ± 0.58	104.67 ± 0.58	96.00 ± 1.00
78	90.33 ± 0.58	117.33 ± 1.15	117.67 ± 0.58	111.33 ± 0.58
79	85.60 ± 1.15	105.00 ± 1.00	107.33 ± 0.58	104.67 ± 0.58
80	84.83 ± 0.29	108.67 ± 1.15	112.00 ± 1.00	103.00 ± 1.00

B7 COMPUTED OCULAR SURFACE ASTIGMATISM

Tables B7.1 to B7.5 show computed ocular surface astigmatism in spherocylindrical form; where the sphere (s) and cylinder (c) components values are given in dioptres and cylinder axis (\emptyset) in degrees. Values shown for the anterior corneal surface (F₁), posterior corneal surface (F₂), anterior lens surface (F₃) and posterior lens surface (F₄). See section 4.4 for calculation details.

B7.1 20 right eyes repeated on two occasions.

Subj ectt NO	F ₁			F ₂			F ₃			F ₄		
	S	C	\emptyset	S	C	\emptyset	S	C	\emptyset	S	C	\emptyset
1st												
1	50.81	-1.08	104.4	-6.19	-0.17	171.9	12.62	-0.98	62.4	15.17	-2.10	173.6
2	47.45	-0.50	85.1	-5.72	-0.16	7.6	10.84	-0.83	89.6	13.98	-1.77	177.1
3	45.41	-0.81	77.3	-5.60	-0.33	2.0	10.42	-0.15	19.6	15.00	-0.80	153.9
4	44.49	-1.31	163.6	-5.50	-0.14	119.3	13.17	-0.77	134.2	13.56	-1.18	17.4
5	47.66	-1.22	86.0	-5.67	-0.18	168.8	11.15	-0.25	172.9	14.14	-0.87	4.8
6	48.80	-0.61	79.2	-5.81	-0.45	175.9	10.22	-1.98	177.6	15.91	-2.27	86.9
7	53.67	-2.15	91.0	-6.37	-0.26	158.0	12.24	-0.76	69.9	14.87	-1.75	8.3
8	44.35	-0.27	103.5	-5.35	-0.20	148.8	9.43	-0.80	81.5	14.71	-1.29	10.7
9	46.61	-0.70	9.9	-5.85	-0.22	173.4	10.22	-1.25	107.7	14.17	-1.78	10.7
10	48.69	-0.78	91.8	-5.76	-0.20	158.6	10.18	-0.72	61.1	15.71	-1.15	174.5
11	48.36	-1.60	102.6	-5.68	-0.50	159.3	10.71	-1.13	61.1	14.31	-1.52	7.5
12	49.33	-0.99	90.2	-5.96	-0.37	170.1	11.27	-0.26	76.2	12.22	-0.67	1.3
13	47.71	-0.60	118.8	-5.82	-0.17	158.3	9.50	-0.99	40.9	13.19	-1.37	160.7
14	46.02	-0.20	72.0	-5.62	-0.31	179.4	10.42	-0.71	113.9	15.45	-1.09	16.0
15	48.07	-0.95	95.3	-5.76	-0.48	11.5	10.99	-0.38	70.7	14.27	-0.80	172.3
16	47.39	-0.69	87.6	-5.70	-0.64	5.7	10.71	-1.39	97.7	14.34	-1.18	8.1
17	47.71	-0.70	100.0	-5.70	-0.24	158.9	10.22	-0.66	72.1	14.89	-1.51	0.7
18	50.29	-1.24	101.4	-5.99	-0.46	14.2	13.16	-1.40	66.4	15.81	-1.56	154.6
19	45.47	-0.98	65.8	-5.27	-0.74	171.7	9.12	-0.48	107.3	12.74	-0.58	7.2
20	47.79	-0.17	109.9	-5.98	-0.22	131.3	12.39	-0.22	129.6	15.89	-2.24	5.1
2nd												
1	50.62	-1.41	106.0	-6.08	-0.27	179.7	13.33	-1.07	43.1	14.69	-1.37	171.8
2	47.23	-0.35	88.1	-5.68	-0.29	173.5	11.7	-1.53	73.7	13.84	-1.87	164.8
3	45.81	-0.88	76.4	-5.62	-0.22	121.2	11.64	-1.46	167.4	13.81	-0.57	62.2
4	44.71	-1.34	165.0	-5.37	-0.23	23.5	11.88	-1.07	107.7	13.91	-1.69	0.9
5	47.87	-1.23	89.7	-5.65	-0.24	165.8	11.04	-0.55	139.2	14.74	-0.91	30.4
6	48.73	-0.31	79.2	-5.85	-0.37	175.2	9.7	-0.51	95.7	14.90	-0.88	12.8
7	53.69	-2.19	88.3	-6.25	-0.61	164.9	12.12	-1.03	75.7	15.26	-1.53	7.7
8	44.35	-0.45	108.1	-5.33	-0.09	143.3	9.5	-0.79	91.8	14.92	-1.70	14.3
9	46.19	-0.42	172.2	-5.60	-0.44	148.6	10.98	-0.81	104.0	13.66	-1.91	22.4
10	48.25	-0.63	93.7	-5.70	-0.31	155.2	11.28	-0.86	76.4	15.86	-1.15	3.6
11	48.58	-1.52	98.1	-5.81	-0.41	5.5	11.22	-1.04	83.3	13.93	-1.35	6.9
12	49.30	-0.88	86.1	-6.04	-0.12	176.4	10.54	-0.65	154.3	12.78	-0.55	29.9
13	47.46	-0.60	156.8	-5.84	-0.09	150.0	9.28	-1.44	70.6	13.49	-1.87	167.3
14	46.03	-0.34	81.5	-5.54	-0.19	15.0	11.81	-1.51	125.1	14.10	-1.65	14.0
15	48.01	-0.94	96.0	-5.71	-0.59	176.9	11.62	-0.79	71.1	14.09	-0.89	177.5
16	47.26	-0.75	98.1	-5.76	-0.40	171.5	9.87	-1.32	101.6	15.28	-2.25	18.1
17	47.50	-0.74	96.6	-5.64	-0.23	154.2	11.11	-1.29	70.9	15.14	-1.93	172.9
18	50.87	-1.87	101.4	-6.06	-0.57	25.4	12.8	-1.36	42.4	16.26	-1.42	151.3
19	46.26	-1.66	71.9	-5.31	-0.84	168.6	9.42	-1.11	161.3	12.65	-0.22	80.6
20	48.07	-0.59	168.8	-5.86	-0.37	91.5	11.84	-0.72	88.3	16.07	-2.29	0.0

B7.2 20 left eyes repeated on two occasions.

Subj ectt NO	F ₁			F ₂			F ₃			F ₄		
	S	C	Ø	S	C	Ø	S	C	Ø	S	C	Ø
1st												
1	51.51	-1.13	85.0	-6.18	-0.23	176.0	11.32	-1.02	74.9	15.19	-1.92	6.0
2	48.02	-0.58	92.5	-5.76	-0.16	160.8	10.95	-0.84	100.5	14.55	-2.09	8.3
3	46.13	-0.75	95.3	-5.70	-0.28	173.3	9.49	-0.88	51.9	15.13	-1.10	161.6
4	45.16	-1.68	4.4	-5.49	-0.11	52.7	11.83	-1.08	150	13.03	-0.88	3.2
5	47.42	-1.37	77.5	-5.58	-0.37	155.0	10.16	-0.37	4.7	14.09	-0.51	15.2
6	49.44	-0.91	96.9	-5.82	-0.40	3.1	10.84	-0.63	127	14.74	-1.53	16.5
7	53.40	-1.92	88.8	-6.32	-0.40	164.4	12.55	-0.76	91.9	15.14	-1.67	12.7
8	44.46	-0.04	167.9	-5.39	-0.05	167.1	9.82	-1.66	83.7	15.14	-2.04	174.4
9	46.57	-0.55	109.8	-5.72	-0.38	170.9	7.87	-1.32	61.1	13.41	-1.30	162.2
10	49.21	-1.15	76.7	-5.83	-0.23	161.7	11.64	-0.43	132.2	15.85	-1.41	2.0
11	48.79	-1.57	100.6	-5.74	-0.69	0.4	9.55	-0.74	66.9	14.16	-0.75	170.1
12	49.28	-0.80	79.8	-5.89	-0.59	172.0	12.25	-0.98	65.6	12.54	-0.75	155.3
13	47.64	-0.88	70.3	-5.63	-0.41	154.5	11.77	-0.30	69.5	12.30	-1.24	5.2
14	46.41	-0.53	122	-5.76	-0.09	23.4	10.82	-1.36	49.8	15.78	-1.65	154.5
15	48.17	-0.44	72.6	-5.79	-0.32	148.2	10.90	-0.37	13.9	14.05	-0.26	62.3
16	47.33	-0.01	81.4	-5.81	-0.43	175.2	10.72	-1.59	95.4	14.43	-1.83	8.8
17	47.01	-0.66	69.8	-5.58	-0.31	145.0	9.35	-1.00	88.5	15.01	-1.91	1.0
18	49.89	-1.29	97.6	-5.95	-0.60	13.0	13.86	-1.48	50.6	15.89	-1.68	138.5
19	45.90	-0.86	98.9	-5.29	-0.85	176.7	8.59	-0.58	58.9	12.68	-0.36	173.7
20	48.12	-0.43	12.9	-6.10	-0.14	148.7	11.94	-1.40	91.2	15.95	-1.83	179.4
2nd												
1	51.01	-1.08	88.9	-6.12	-0.21	162.1	11.59	-0.90	66.8	14.90	-1.76	9.2
2	47.86	-0.70	90.5	-5.79	-0.12	155.8	11.13	-0.66	119.3	14.40	-1.70	15.6
3	45.99	-0.56	81.6	-5.69	-0.07	87.5	9.24	-0.22	105.7	14.88	-1.16	2.2
4	45.09	-1.70	3.1	-5.46	-0.12	34.7	10.8	-1.33	141.0	13.49	-1.24	4.2
5	47.34	-1.20	75.1	-5.61	-0.13	164.9	9.51	-0.22	111.5	14.82	-0.89	176.7
6	49.52	-0.95	93.7	-5.82	-0.58	158.7	10.47	-0.38	38.8	14.21	-0.88	8.4
7	53.57	-2.18	94.0	-6.21	-0.67	177.4	11.63	-0.63	117.3	15.58	-1.73	31.2
8	44.53	-0.09	130.1	-5.42	-0.11	143.6	9.47	-1.17	90.2	14.87	-1.45	6.6
9	46.19	-0.54	108.3	-5.44	-0.68	5.9	8.05	-1.07	92.9	13.10	-1.18	11.1
10	49.02	-0.57	75.3	-5.74	-0.48	151	10.75	-0.69	104.8	16.18	-1.37	19.1
11	48.84	-1.58	97.8	-5.72	-0.70	170.9	10.13	-0.80	66.9	13.90	-0.83	169
12	49.42	-0.93	79.7	-5.95	-0.38	174.6	11.17	-0.72	95.2	12.42	-1.15	6.5
13	47.65	-0.66	62.7	-5.62	-0.47	155.9	11.45	-0.71	62.8	12.57	-1.30	178.4
14	46.43	-0.50	141.0	-5.50	-0.22	15.9	11.18	-1.41	92.8	14.15	-1.93	8.8
15	47.97	-0.80	93.8	-5.68	-0.59	177.3	11.30	-0.75	79.3	14.28	-1.28	4.9
16	47.44	-1.01	88.5	-5.74	-0.45	1.6	10.36	-2.13	82.3	14.79	-2.07	2.4
17	47.01	-0.78	89.2	-5.61	-0.22	148.1	9.68	-1.04	73.0	15.11	-2.13	176.1
18	50.37	-1.53	91.1	-5.99	-0.54	22.6	14.12	-0.81	63.7	15.77	-1.40	151.1
19	45.84	-0.23	114.3	-5.41	-0.69	173.6	8.54	-1.94	74.9	13.17	-0.95	160.5
20	48.40	-0.50	4.3	-5.96	-0.23	92.0	11.86	-1.38	105.8	16.05	-2.09	10.9

B7.3 10 left eyes with and without cycloplegia.

Subjec	F ₁			F ₂			F ₃			F ₄			
	N0	S	C	Ø	S	C	Ø	S	C	Ø	S	C	Ø
witho													
ut 71	48.36	0.00	0.0	-5.82	-0.28	174.6	8.48	-0.64	93.1	13.39	-0.73	4.3	
72	49.50	-0.73	88.5	-5.86	-0.43	167.3	10.57	-0.96	64.0	15.79	-0.78	163.1	
73	47.99	-2.64	86.3	-5.52	-0.59	175.0	10.91	-1.62	23.0	15.72	-1.25	140.4	
74	49.35	-0.91	88.2	-5.79	-0.23	132.0	11.86	-0.58	73.8	15.27	-1.66	163.5	
75	46.98	-0.72	90.0	-5.46	-0.29	173.3	9.93	-0.39	56.5	14.15	-0.60	0.4	
76	47.79	-0.11	88.2	-5.82	-0.02	127.3	7.70	-0.55	132.8	14.80	-0.55	11.2	
77	48.26	-0.91	88.7	-5.81	-0.49	173.7	9.90	-0.65	41.8	16.33	-0.66	161.7	
78	46.40	-0.83	85.7	-5.70	-0.12	57.1	6.57	-1.20	0.7	13.33	-0.38	121.2	
79	48.96	-1.10	90.0	-5.83	-0.19	7.9	8.45	-0.77	41.6	15.53	-1.59	154.5	
80	48.32	-0.29	179.0	-5.88	-0.17	11.8	11.23	-0.37	61.8	14.85	-0.55	163.3	
With													
71	48.07	0.00	0.0	-5.83	-0.20	165.5	8.35	-0.18	81.8	12.78	-0.28	6.9	
72	49.81	-1.01	89.7	-5.92	-0.41	175.9	10.48	-0.59	44.0	14.60	-0.48	150.1	
73	47.88	-1.91	88.3	-5.59	-0.45	173.3	11.69	-1.62	32.9	14.65	-1.20	131.4	
74	49.22	-0.74	87.4	-5.73	-0.28	121.6	13.17	-0.69	76.1	14.90	-1.71	163.3	
75	47.17	-1.04	88.8	-5.48	-0.29	172	12.08	-0.43	161.2	13.48	-0.94	34.7	
76	47.89	-0.31	88.6	-5.84	-0.02	168.3	9.95	-0.34	115.5	14.55	-1.23	168.8	
77	48.24	-0.87	90.4	-5.88	-0.38	0.6	10.84	-0.78	43.8	14.90	-0.90	153.7	
78	46.24	-0.51	91.2	-5.67	-0.21	59.6	8.26	-0.54	10.9	12.54	-0.63	150.5	
79	48.88	-1.04	90.7	-5.85	-0.16	16.8	9.41	-0.91	25.1	13.94	-1.21	133.0	
80	48.30	-0.29	179.5	-5.89	-0.18	44.2	12.30	-0.43	70.3	14.54	-0.81	165.2	

B8. COMPUTED INTERNAL OCULAR COMPONENT CONTRIBUTIONS TO RESIDUAL ASTIGMATISM

Tables B8.1.1 to B8.6.3 show computed internal ocular surface component contributions to residual astigmatism. Where orthogonal (C_0) and oblique (C_{45}) components of astigmatic decomposition are shown along with cylinders (C) and cylinder axis (\emptyset). Powers are shown in dioptres and axes in degrees. See section 4.5 for calculation details.

B8.1 CORNEAL THICKNESS.

B8.1.1 66 right and left eyes.

Subject N0	Right eyes				Left eyes			
	C_0	C_{45}	C	\emptyset	C_0	C_{45}	C	\emptyset
1	+0.03	+0.01	+0.03	9.30	+0.02	+0.02	+0.03	22.05
2	+0.02	+0.00	+0.02	177.19	+0.02	0.00	+0.02	0.70
3	+0.02	- 0.01	+0.02	168.54	+0.02	+0.01	+0.02	9.91
4	+0.02	- 0.01	+0.02	163.28	+0.03	- 0.02	+0.04	163.59
5	+0.03	0.00	+0.03	179.19	+0.03	0.00	+0.03	177.07
6	+0.02	0.00	+0.02	178.10	+0.03	+0.00	+0.03	1.21
7	+0.03	+0.02	+0.03	18.20	+0.02	+0.01	+0.02	8.48
8	+0.01	+0.01	+0.01	28.09	0.00	0.00	+0.00	70.03
9	+0.01	- 0.01	+0.01	161.38	+0.01	+0.01	+0.02	19.80
10	+0.02	+0.01	+0.02	12.34	+0.03	- 0.01	+0.04	168.39
11	+0.02	+0.02	+0.03	21.63	+0.02	+0.01	+0.02	11.28
12	+0.02	0.00	+0.02	179.89	+0.01	0.00	+0.01	6.93
13	+0.03	+0.01	+0.03	5.14	+0.03	0.00	+0.03	179.27
14	+0.01	0.00	+0.02	174.81	+0.02	+0.01	+0.02	17.59
15	+0.02	+0.01	+0.02	10.34	+0.01	0.00	+0.01	178.46
16	+0.01	0.00	+0.01	3.27	+0.01	0.00	+0.01	3.73
17	+0.02	+0.01	+0.03	7.32	+0.01	-0.01	+0.02	167.46
18	+0.01	+0.01	+0.01	28.09	+0.01	+0.01	+0.02	23.16
19	+0.02	- 0.01	+0.03	167.65	+0.03	+0.01	+0.03	9.03
20	+0.04	0.00	+0.04	176.74	0.00	- 0.01	+0.01	140.79
21	+0.05	+0.02	+0.05	11.30	+0.04	0.00	+0.04	178.37
22	+0.02	+0.01	+0.02	13.15	0.00	+0.01	+0.01	40.61
23	+0.03	+0.02	+0.03	19.08	+0.01	+0.01	+0.01	21.28
24	+0.04	0.00	+0.04	179.33	+0.02	0.00	+0.03	3.87
25	+0.02	0.00	+0.02	1.48	+0.03	- 0.01	+0.03	174.43
26	+0.05	0.00	+0.05	0.79	+0.05	- 0.01	+0.05	174.26
27	+0.05	+0.02	+0.06	12.52	+0.04	+0.02	+0.04	10.64
28	+0.01	- 0.01	+0.01	146.69	+0.01	+0.02	+0.02	34.60
29	+0.02	0.00	+0.02	3.21	+0.01	- 0.01	+0.01	162.83
30	- 0.01	+0.01	+0.02	66.83	0.00	+0.01	+0.01	40.74
31	+0.02	+0.00	+0.02	1.49	+0.02	+0.01	+0.02	7.99
32	+0.02	+0.01	+0.03	11.57	+0.03	0.00	+0.03	4.28
33	+0.04	+0.01	+0.04	7.00	+0.03	+0.01	+0.03	175.53
34	+0.02	0.00	+0.02	4.70	+0.03	+0.03	+0.05	22.18
35	+0.01	+0.02	+0.02	30.48	+0.01	+0.01	+0.02	28.39
36	+0.02	+0.01	+0.02	8.79	+0.03	0.00	+0.03	177.29
37	+0.02	+0.01	+0.02	15.37	+0.02	0.00	+0.02	176.16
38	+0.02	- 0.01	+0.02	167.03	+0.02	0.00	+0.02	179.26
39	+0.05	0.00	+0.05	1.77	+0.04	+0.02	+0.04	13.58

B8.1.1 66 right and left eyes (continued).

Subject N0	Right eyes				Left eyes			
	C0	C45	C	Ø	C0	C45	C	Ø
40	+0.02	0.00	+0.02	173.79	+0.02	0.00	+0.02	179.30
41	+0.01	+0.01	+0.02	12.62	+0.03	0.00	+0.03	3.41
42	+0.01	+0.01	+0.01	15.90	+0.01	+0.01	+0.01	21.74
43	+0.02	- 0.01	+0.02	161.73	+0.01	- 0.02	+0.02	159.50
44	+0.02	0.00	+0.02	179.76	+0.02	0.00	+0.02	6.59
45	+0.02	0.00	+0.02	0.39	+0.03	- 0.01	+0.03	174.58
46	+0.02	- 0.01	+0.03	168.99	+0.01	- 0.02	+0.02	153.95
47	+0.03	+0.01	+0.04	8.32	+0.02	+0.02	+0.03	23.98
48	+0.01	+0.01	+0.02	23.19	+0.02	+0.01	+0.03	13.56
49	+0.02	+0.03	+0.03	27.07	+0.02	+0.01	+0.02	17.68
50	+0.03	0.00	+0.03	0.54	+0.03	+0.01	+0.03	11.48
51	+0.00	0.00	+0.00	1.93	+0.02	+0.02	+0.02	21.47
52	+0.01	0.00	+0.02	7.61	0.00	0.00	+0.00	73.58
53	+0.04	0.00	+0.04	175.92	+0.05	+0.02	+0.05	11.83
54	+0.00	+0.02	+0.02	38.86	+0.01	- 0.01	+0.01	166.14
55	+0.04	- 0.01	+0.04	172.21	+0.02	+0.01	+0.02	16.79
56	+0.01	0.00	+0.01	171.69	+0.01	0.00	+0.01	178.83
57	+0.02	0.00	+0.02	175.50	0.00	- 0.03	+0.03	133.07
58	+0.04	+0.01	+0.04	6.96	+0.04	0.00	+0.04	179.21
59	+0.03	- 0.01	+0.03	173.50	+0.01	+0.01	+0.01	24.75
60	0.00	0.00	+0.00	120.21	0.00	+0.01	+0.01	45.78
61	- 0.01	0.00	+0.01	97.57	+0.02	0.00	+0.02	176.61
62	+0.02	0.00	+0.02	175.71	+0.02	0.00	+0.02	177.34
63	+0.02	+0.02	+0.03	20.86	+0.02	- 0.02	+0.02	159.39
64	+0.03	0.00	+0.04	3.46	+0.02	- 0.05	+0.06	146.35
65	+0.01	+0.03	+0.03	39.26	+0.01	- 0.01	+0.01	148.40
66	+0.02	+0.01	+0.02	10.98	0.00	+0.01	+0.01	50.55

B8.1.2 20 right and left eyes repeated.

Subject N0	Right eyes				Left eyes			
	C ₀	C ₄₅	C	∅	C ₀	C ₄₅	C	∅
1	+0.03	+0.02	+0.04	14.67	+0.02	+0.03	+0.03	24.16
2	+0.01	+0.00	+0.01	3.87	+0.02	0.00	+0.02	179.06
3	+0.02	- 0.01	+0.03	166.13	+0.02	+0.00	+0.02	178.44
4	+0.02	- 0.01	+0.02	162.55	+0.03	- 0.03	+0.05	159.64
5	+0.02	0.00	+0.02	176.67	+0.02	- 0.01	+0.02	167.33
6	+0.01	0.00	+0.01	5.43	+0.03	+0.00	+0.03	2.18
7	+0.02	+0.01	+0.03	12.93	+0.03	+0.01	+0.03	13.53
8	+0.01	+0.01	+0.02	26.03	+00.0	0.00	+0.00	55.53
9	+0.01	+0.00	+0.10	7.28	+0.01	- 0.01	+0.02	18.30
10	+0.01	+0.01	+0.01	17.86	+0.01	- 0.01	+0.02	167.75
11	+0.01	+0.02	+0.02	26.33	+0.02	0.00	+0.02	2.91
12	+0.02	0.00	+0.02	173.76	+0.02	0.00	+0.02	179.10
13	+0.01	+0.01	+0.01	21.49	+0.03	0.00	+0.03	2.51
14	+0.02	- 0.02	+0.03	157.81	+00.0	+0.01	+0.01	33.74
15	+0.02	+0.01	+0.02	12.72	+0.03	+0.01	+0.30	10.60
16	+0.02	+0.01	+0.02	14.64	+00.0	+0.02	+0.02	42.84
17	+0.01	+0.01	+0.02	11.81	+0.02	0.00	+0.02	5.18
18	+0.03	+0.03	+0.04	20.97	+0.01	+0.01	+0.01	12.60
19	+0.04	- 0.02	+0.05	164.32	- 0.01	+0.01	+0.01	64.88
20	+0.01	+0.00	+0.01	1.07	00.0	0.00	+0.00	131.67

B8.1.3 10 left eyes with and without cycloplegia.

Subject N0	Without Cycloplegia				With Cycloplegia			
	C ₀	C ₄₅	C	∅	C ₀	C ₄₅	C	∅
71	+0.01	0.00	+0.01	174.20	+0.01	0.00	+0.01	178.00
72	+0.01	+0.01	+0.01	16.29	+0.02	+0.01	+0.02	8.69
73	+0.05	0.00	+0.05	2.14	+0.03	+0.01	+0.03	12.26
74	+0.01	- 0.02	+0.02	152.99	+0.01	- 0.02	+0.02	143.20
75	+0.02	+0.01	+0.02	12.14	+0.03	+0.01	+0.03	8.02
76	+0.01	- 0.01	+0.01	154.73	+0.02	- 0.02	+0.20	158.28
77	+0.03	+0.01	+0.03	6.27	+0.03	+0.01	+0.03	8.00
78	+0.03	0.00	+0.03	177.7	+0.02	0.00	+0.02	1.20
79	+0.03	0.00	+0.03	177.72	+0.02	0.00	+0.02	176.41
80	+0.01	0.00	+0.01	14.53	0.00	+0.01	+0.01	25.60

B8.2 POSTERIOR CORNEAL SURFACE.

B8.2.1 66 right and left eyes.

Subject NO	Right eyes				Left eyes			
	C ₀	C ₄₅	C	Ø	C ₀	C ₄₅	C	Ø
1	- 0.16	+0.05	-0.17	171.9	- 0.23	+0.03	-0.23	17.6
2	- 0.15	- 0.04	-0.16	7.6	- 0.13	+0.10	-0.16	160.8
3	- 0.33	- 0.02	-0.33	2.0	- 0.27	+0.06	-0.28	173.3
4	+0.07	+0.12	-0.14	119.3	+0.03	- 0.11	-0.11	52.7
5	- 0.17	+0.07	-0.18	168.8	- 0.24	+0.28	-0.37	155.0
6	- 0.45	+0.06	-0.45	175.9	- 0.40	- 0.04	-0.40	3.1
7	- 0.19	+0.18	-0.26	158.0	- 0.34	+0.21	-0.40	164.4
8	- 0.09	+0.18	-0.20	148.8	- 0.05	+0.02	-0.05	167.1
9	- 0.21	+0.05	-0.22	173.4	- 0.36	+0.12	-0.38	170.9
10	- 0.15	+0.14	-0.20	158.6	- 0.18	+0.14	-0.23	161.7
11	- 0.38	+0.33	-0.50	159.3	- 0.69	- 0.01	-0.69	0.4
12	- 0.35	+0.13	-0.37	170.1	-0.57	+0.16	-0.59	172
13	- 0.12	+0.12	-0.17	158.3	- 0.26	+0.32	-0.41	154.5
14	- 0.31	+0.01	-0.31	179.4	- 0.06	- 0.07	-0.09	23.4
15	- 0.44	- 0.19	-0.48	11.5	+0.14	+0.29	-0.32	148.2
16	- 0.63	- 0.13	-0.64	5.7	- 0.42	+0.07	-0.43	175.2
17	- 0.18	+0.16	-0.24	158.9	- 0.11	+0.29	-0.31	145.0
18	- 0.40	- 0.22	-0.46	14.2	- 0.54	- 0.26	-0.60	13.0
19	- 0.71	+0.21	-0.74	171.7	- 0.84	+0.10	-0.85	176.7
20	+0.03	+0.22	-0.22	131.3	- 0.06	+0.12	-0.14	148.7
21	- 0.38	+0.11	-0.40	171.7	- 0.26	+0.10	-0.28	169.5
22	+0.07	00.00	-0.07	90.5	- 0.05	+0.05	-0.07	159.0
23	- 0.24	+0.29	-0.38	154.6	- 0.25	+0.33	-0.42	153.6
24	- 0.27	+0.31	-0.41	155.6	- 0.33	+0.19	-0.38	164.8
25	- 0.23	+0.06	-0.24	173.3	- 0.33	+0.15	-0.36	167.9
26	- 0.45	- 0.07	-0.45	4.3	- 0.49	+0.15	-0.51	171.5
27	- 0.47	+0.26	-0.54	165.5	- 0.42	- 0.05	-0.42	3.7
28	- 0.26	- 0.10	-0.28	11.0	- 0.29	+0.03	-0.29	177.5
29	- 0.08	+0.19	-0.21	146.3	0.00	+0.24	-0.24	135.4
30	- 0.35	- 0.37	-0.51	23.2	- 0.24	+0.71	-0.75	144.5
31	- 0.12	- 0.18	-0.22	28.9	- 0.26	+0.08	-0.27	171.2
32	- 0.12	- 0.05	-0.13	11.3	- 0.29	+0.16	-0.33	165.5
33	- 0.33	+0.16	-0.37	167.1	- 0.47	+0.04	-0.47	177.3
34	- 0.37	- 0.02	-0.37	1.9	- 0.75	- 0.18	-0.77	6.8
35	- 0.30	-0.11	-0.32	10.6	- 0.14	+0.17	-0.22	154
36	- 0.27	+0.12	-0.30	167.9	- 0.14	- 0.07	-0.16	13.2
37	- 0.07	+0.13	-0.15	148.7	- 0.03	+0.11	-0.11	142.2
38	- 0.20	- 0.10	-0.20	2.0	+0.02	- 0.11	-0.11	50.4
39	- 0.36	+0.10	-0.37	171.9	- 0.20	+0.05	-0.21	173.1
40	- 0.06	- 0.19	-0.20	35.6	+0.12	+0.11	-0.16	158.1
41	+0.06	+0.22	-0.23	128.0	- 0.40	- 0.08	-0.41	5.4
42	+0.22	- 0.40	-0.45	59.3	+0.01	- 0.30	-0.30	46.2
43	- 0.02	+0.15	-0.15	139.6	- 0.33	+0.27	-0.43	160.4
44	- 0.20	+0.42	-0.46	147.6	- 0.16	+0.44	-0.47	145.2
45	- 0.01	- 0.27	-0.29	35.0	- 0.02	- 0.30	-0.30	42.7
46	- 0.36	+0.22	-0.42	164.0	- 0.63	+0.31	-0.70	166.9
47	- 0.27	+0.07	-0.28	173.1	- 0.33	+0.12	-0.35	170.3
48	- 0.03	+0.03	-0.05	114.9	- 0.14	0.00	-0.14	0.6
49	+0.23	- 0.14	-0.27	74.9	+0.11	+0.34	-0.36	126.1
50	+0.24	- 0.16	-0.29	72.4	- 0.46	- 0.04	-0.46	2.3
51	- 0.12	- 0.22	-0.25	30.9	+0.51	+0.06	-0.51	93.4

B8.2.1 66 right and left eyes (continued).

Subject NO	Right eyes				Left eyes			
	C ₀	C ₄₅	C	∅	C ₀	C ₄₅	C	∅
52	- 0.05	- 0.03	-0.06	12.7	+0.13	- 0.05	-0.14	78.6
53	- 0.42	+0.14	-0.44	170.5	+0.44	+0.01	-0.44	179.4
54	- 0.11	- 0.10	-0.15	21.1	- 0.10	- 0.47	0.48	39.2
55	- 0.15	- 0.02	-0.15	4.6	+0.11	- 0.12	-0.16	66.1
56	- 0.19	+0.04	-0.19	173.9	- 0.19	+0.11	-0.22	164.9
57	- 0.11	+0.18	-0.21	151.5	- 0.19	+0.12	-0.22	164.0
58	- 0.31	+0.18	-0.36	165.4	- 0.39	+0.28	-0.48	162.2
59	+0.10	- 0.17	-0.20	59.7	- 0.21	- 0.15	-0.26	17.5
60	- 0.21	- 0.11	-0.24	13.9	- 0.27	+0.32	-0.42	155.3
61	- 0.13	+0.18	-0.22	152.7	- 0.19	- 0.06	-0.20	8.8
62	- 0.29	+0.04	-0.29	175.6	- 0.29	0.00	-0.29	0.1
63	- 0.48	- 0.17	-0.51	9.6	+0.53	+0.12	0.54	173.7
64	- 0.43	+0.43	-0.61	157.6	+0.44	- 0.18	-0.48	78.7
65	+0.23	+0.26	-0.35	114.4	- 0.11	+0.06	-0.13	165.6
66	- 0.17	+0.17	-0.24	157.7	- 0.04	+0.19	-0.19	141.3

B8.2.2 20 right and left eyes repeated.

Subject NO	Right eyes				Left eyes			
	C ₀	C ₄₅	C	∅	C ₀	C ₄₅	C	∅
1	-0.27	0.00	-0.27	179.7	-0.17	+0.12	-0.21	162.1
2	-0.28	+0.07	-0.29	173.5	-0.08	+0.09	-0.12	155.8
3	0.10	+0.19	-0.22	121.2	0.07	- 0.01	-0.07	87.5
4	-0.16	- 0.17	-0.23	23.5	-0.04	- 0.11	-0.12	34.7
5	-0.21	+0.11	-0.24	165.8	-0.11	+0.06	-0.13	164.9
6	-0.36	+0.06	-0.37	175.2	-0.43	+0.39	-0.58	158.7
7	-0.53	+0.31	-0.61	164.9	-0.67	+0.06	-0.67	177.4
8	-0.03	+0.09	-0.09	143.3	-0.03	+0.11	-0.11	143.6
9	-0.20	+0.39	-0.44	148.6	-0.67	- 0.14	-0.68	5.9
10	-0.20	+0.24	-0.31	155.2	-0.25	+0.41	-0.48	151.0
11	-0.40	- 0.08	-0.41	5.5	-0.67	+0.22	-0.70	170.9
12	-0.12	+0.02	-0.12	176.4	-0.37	+0.07	-0.38	174.6
13	-0.05	+0.08	-0.09	150.0	-0.31	+0.35	-0.47	155.9
14	-0.16	- 0.10	-0.19	15.0	-0.19	- 0.12	-0.22	15.9
15	+0.59	+0.06	-0.59	176.9	-0.59	+0.06	-0.59	177.3
16	-0.38	+0.12	-0.40	171.5	-0.45	- 0.03	-0.45	1.6
17	-0.14	+0.18	-0.23	154.2	-0.10	+0.20	-0.22	148.1
18	-0.36	- 0.44	-0.57	25.4	-0.38	- 0.38	-0.54	22.6
19	-0.77	+0.33	-0.84	168.6	-0.70	+0.15	-0.69	173.6
20	+0.37	+0.02	-0.37	91.5	+0.23	+0.02	-0.23	92.0

B8.2.3 10 left eyes with and without cycloplegia.

Subject N0	Without Cycloplegia				With Cycloplegia			
	C ₀	C ₄₅	C	∅	C ₀	C ₄₅	C	∅
71	- 0.28	+0.05	-0.28	174.6	- 0.18	+0.10	-0.20	165.5
72	- 0.39	+0.18	-0.43	167.3	- 0.41	+0.06	-0.41	175.9
73	- 0.58	+0.10	-0.59	175	- 0.44	+0.10	-0.45	173.3
74	+0.02	+0.23	-0.23	132	+0.13	+0.25	-0.28	121.6
75	- 0.28	+0.07	-0.29	173.3	- 0.28	+0.08	-0.29	172.0
76	+0.01	+0.02	-0.02	127.3	- 0.02	+0.01	-0.20	168.3
77	- 0.48	+0.11	+0.49	173.7	- 0.38	- 0.01	-0.38	0.6
78	+0.05	- 0.11	-0.12	57.1	+0.10	- 0.18	-0.21	59.6
79	- 0.18	- 0.05	-0.19	7.9	- 0.13	- 0.09	-0.16	16.8
80	- 0.16	- 0.07	-0.17	11.8	- 0.01	- 0.18	-0.18	44.2

B8.3 ANTERIOR CHAMBER DEPTH.

B8.3.1 66 right and left eyes.

Subject NO	Right eyes				Left eyes			
	C ₀	C ₄₅	C	∅	C ₀	C ₄₅	C	∅
1	+0.18	+0.08	+0.20	12.54	+0.10	+0.14	+0.17	28.66
2	+0.10	- 0.02	+0.10	173.29	+0.14	+0.03	+0.14	5.76
3	+0.07	- 0.06	+0.09	160.37	+0.08	+0.06	+0.10	19.03
4	+0.11	- 0.04	+0.12	169.77	+0.18	- 0.13	+0.23	161.89
5	+0.16	+0.01	+0.16	1.74	+0.12	+0.04	+0.13	10.12
6	+0.05	+0.00	+0.05	1.55	+0.11	+0.00	+0.11	0.05
7	+0.12	+0.15	+0.19	26.56	+0.05	+0.07	+0.09	28.01
8	+0.03	+0.11	+0.11	38.07	- 0.02	+0.01	+0.02	73.36
9	+0.02	- 0.04	+0.04	151.12	+0.01	+0.07	+0.07	40.45
10	+0.09	+0.09	+0.12	23.36	+0.18	- 0.06	+0.19	170.18
11	+0.08	+0.21	+0.23	34.70	0.00	+0.06	+0.06	43.93
12	+0.04	+0.02	+0.05	14.23	- 0.05	+0.05	+0.07	65.72
13	+0.19	+0.07	+0.20	9.99	+0.13	+0.07	+0.14	13.68
14	+0.03	- 0.02	+0.04	167.33	+0.10	+0.06	+0.12	16.65
15	+0.05	+0.01	+0.05	7.96	+0.04	+0.06	+0.08	28.47
16	- 0.08	- 0.02	+0.09	97.03	- 0.04	+0.02	+0.05	76.62
17	+0.11	+0.08	+0.14	17.50	+0.08	+0.02	+0.08	7.19
18	- 0.04	+0.02	+0.04	74.81	- 0.02	+0.04	+0.04	61.03
19	+0.01	- 0.03	+0.03	142.07	0.00	+0.08	+0.08	45.7
20	+0.31	+0.02	+0.31	1.62	- 0.01	- 0.02	+0.02	125.49
21	+0.25	+0.18	+0.31	17.82	+0.25	+0.01	+0.25	0.97
22	+0.13	+0.06	+0.14	11.79	0.00	+0.07	+0.07	46.45
23	+0.09	+0.16	+0.18	30.4	+0.02	+0.15	+0.15	41.96
24	+0.17	+0.06	+0.18	10.14	+0.09	+0.06	+0.11	16.01
25	+0.09	+0.02	+0.10	5.78	+0.12	- 0.01	+0.12	178.71
26	+0.27	- 0.01	+0.27	179.34	+0.20	- 0.03	+0.21	175.99
27	+0.22	+0.21	+0.30	21.61	+0.15	+0.08	+0.17	13.71
28	- 0.02	- 0.09	+0.09	128.79	- 0.01	+0.10	+0.10	48.21
29	+0.10	+0.05	+0.11	14.26	+0.06	+0.00	+0.06	2.22
30	- 0.11	+0.01	+0.11	88.51	- 0.03	+0.17	+0.17	50.03
31	+0.15	- 0.04	+0.15	172.78	+0.10	+0.06	+0.12	16.92
32	+0.12	+0.05	+0.13	11.63	+0.12	+0.06	+0.14	13.86
33	+0.18	+0.10	+0.21	14.87	+0.11	- 0.02	+0.11	173.77
34	+0.06	+0.02	+0.07	7.37	+0.04	+0.16	+0.16	38.08
35	+0.01	+0.10	+0.10	42.60	+0.02	+0.10	+0.10	37.96
36	+0.08	+0.07	+0.11	20.52	+0.15	- 0.03	+0.15	173.99
37	+0.08	+0.09	+0.13	23.62	+0.14	0.00	+0.14	0.70
38	+0.12	- 0.09	+0.15	162.23	+0.13	- 0.03	+0.13	174.40
39	+0.23	+0.04	+0.24	5.42	+0.20	+0.14	+0.24	17.26
40	+0.10	- 0.07	+0.13	163.15	+0.09	+0.02	+0.09	7.93
41	+0.10	+0.09	+0.14	20.78	+0.09	0.00	+0.09	1.11
42	+0.12	- 0.05	+0.13	168.48	+0.07	0.00	+0.07	178.57
43	+0.07	- 0.03	+0.08	167.72	+0.02	- 0.02	+0.03	157.97
44	+0.08	+0.09	+0.12	25.01	+0.09	+0.11	+0.14	26.64
45	+0.09	- 0.06	+0.11	164.77	+0.18	- 0.10	+0.20	165.25
46	+0.09	- 0.02	+0.09	174.12	- 0.04	- 0.05	+0.07	116.82
47	+0.17	+0.09	+0.20	13.32	+0.08	+0.21	+0.22	34.50
48	+0.09	+0.10	+0.13	23.33	+0.12	+0.08	+0.14	16.36
49	+0.16	+0.12	+0.20	18.75	+0.09	+0.11	+0.14	25.03
50	+0.27	- 0.04	+0.28	176.03	+0.09	+0.08	+0.11	20.62
51	+00.0	- 0.04	+0.04	136.60	+0.19	+0.10	+0.21	140.03

B8.3.1 66 right and left eyes (continued).

Subject N0	Right eyes				Left eyes			
	C ₀	C ₄₅	C	∅	C ₀	C ₄₅	C	∅
52	+0.09	+0.02	+0.09	6.79	+0.01	0.00	+0.01	175.82
53	+0.18	- 0.01	+0.18	178.95	+0.19	+0.12	+0.22	16.71
54	+0.00	+0.10	+0.10	43.94	+0.04	- 0.11	+0.12	145.51
55	+0.19	- 0.07	+0.20	170.22	+0.12	+0.04	+0.12	8.65
56	- 0.01	+0.00	+0.01	91.08	- 0.01	+0.03	+0.03	57.32
57	+0.08	+0.02	+0.08	8.33	- 0.06	- 0.16	+0.17	124.55
58	+0.21	+0.10	+0.23	13.19	0.19	+0.05	+0.19	7.49
59	+0.20	- 0.08	+0.21	169.32	+0.02	+0.04	+0.04	33.90
60	- 0.05	- 0.04	+0.06	107.59	- 0.05	+0.13	+0.14	55.57
61	- 0.10	+0.02	+0.10	83.76	+0.07	- 0.03	+0.07	169.62
62	+0.10	- 0.01	+0.10	175.79	+0.09	- 0.01	+0.10	175.82
63	+0.05	+0.10	+0.11	32.48	+0.02	- 0.08	+0.08	140.99
64	+0.17	+0.14	+0.22	20.31	+0.25	- 0.40	+0.47	151.12
65	+0.10	+0.28	+0.30	35.31	+0.01	- 0.06	+0.07	141.00
66	+0.11	+0.10	+0.15	19.98	- 0.02	+0.08	+0.08	50.95

B8.3.2 20 right and left eyes repeated.

Subject N0	Right eyes				Left eyes			
	C ₀	C ₄₅	C	∅	C ₀	C ₄₅	C	∅
1	+0.20	+0.15	+0.24	18.36	+0.11	+0.19	+0.21	30.10
2	- 0.02	+0.02	+0.03	62.51	+0.14	+0.02	+0.14	3.26
3	+0.17	- 0.04	+0.18	173.49	+0.12	- 0.01	+0.12	178.33
4	+0.06	- 0.10	+0.12	150.8	+0.20	- 0.20	+0.29	157.29
5	+0.07	+0.01	+0.07	4.23	+0.09	- 0.04	+0.10	168.04
6	+0.01	+0.02	+0.20	34.06	+0.10	+0.08	+0.12	19.28
7	+0.03	+0.14	+0.14	38.41	+0.04	+0.10	+0.11	35.45
8	+0.06	+0.10	+0.12	29.78	- 0.02	+0.04	+0.05	54.59
9	+0.04	+0.08	+0.09	33.37	- 0.03	+0.03	+0.04	69.18
10	+0.01	+0.10	+0.10	42.00	+0.04	+0.05	+0.06	28.37
11	- 0.01	+0.08	+0.08	47.69	+0.00	+0.06	+0.06	42.91
12	+0.10	- 0.02	+0.10	173.16	+0.02	+0.01	+0.03	12.80
13	+0.03	+0.06	+0.07	31.00	+0.11	+0.10	+0.14	21.20
14	+0.09	- 0.14	+0.17	151.6	- 0.01	+0.05	+0.05	49.03
15	0.00	+0.08	+0.08	43.55	+0.04	+0.08	+0.09	30.40
16	+0.03	+0.08	+0.09	36.60	- 0.09	+0.13	+0.15	62.35
17	+0.07	+0.09	+0.11	25.87	+0.12	+0.07	+0.13	14.81
18	+0.11	+0.07	+0.13	17.36	+0.01	- 0.03	+0.03	142.39
19	+0.13	- 0.11	+0.17	159.72	- 0.20	+0.10	+0.22	77.29
20	+0.19	+0.01	+0.19	1.27	+0.05	- 0.03	+0.06	165.66

B8.3.3 10 left eyes with and without cycloplegia.

Subject NO	Without Cycloplegia				With Cycloplegia			
	C ₀	C ₄₅	C	∅	C ₀	C ₄₅	C	∅
71	- 0.20	0.00	+0.02	85.59	+0.01	+0.02	+0.02	37.02
72	- 0.03	+0.08	+0.09	53.39	+0.04	+0.06	+0.07	28.80
73	+0.25	+0.05	+0.26	6.09	+0.11	+0.13	+0.17	24.39
74	+0.08	- 0.06	+0.10	163.07	+0.08	- 0.07	+0.11	158.87
75	+0.05	+0.06	+0.08	25.70	+0.11	+0.07	+0.14	16.29
76	+0.07	- 0.08	+0.11	155.86	+0.12	- 0.12	+0.17	157.99
77	+0.08	+0.07	+0.10	19.53	+0.08	+0.05	+0.10	15.06
78	+0.18	- 0.04	+0.18	174.40	+0.11	- 0.03	+0.12	172.81
79	+0.17	+0.03	+0.17	174.84	+0.10	- 0.04	+0.11	169.68
80	+0.02	+0.02	+0.03	18.39	+0.03	0.00	+0.03	177.69

B8.4 ANTERIOR CRYSTALLINE LENS SURFACE.

B8.4.1 66 right and left eyes.

Subject N0	Right eyes				Left eyes			
	C0	C45	C	Ø	C0	C45	C	Ø
1	+0.56	- 0.80	-0.98	62.4	+0.88	- 0.51	-1.02	74.9
2	+0.83	- 0.01	-0.83	89.6	+0.78	+0.30	-0.84	100.5
3	- 0.12	- 0.09	-0.15	19.6	+0.21	- 0.85	-0.88	51.9
4	+0.02	+0.77	-0.77	134.2	- 0.54	+0.94	-1.08	150
5	- 0.24	+0.06	-0.25	172.9	- 0.37	- 0.06	-0.37	4.7
6	- 1.97	+0.17	-1.98	177.6	+0.17	+0.61	-0.63	127.0
7	+0.58	- 0.49	-0.76	69.9	+0.76	+0.05	-0.76	91.9
8	+0.77	- 0.23	-0.80	81.5	+1.62	- 0.36	-1.66	83.7
9	+1.02	+0.72	-1.25	107.7	+0.70	- 1.12	-1.32	61.1
10	+0.38	- 0.61	-0.72	61.1	+0.04	+0.43	-0.43	132.2
11	+0.60	- 0.95	-1.13	61.1	+0.51	-0.53	-0.74	66.9
12	+0.23	- 0.12	-0.26	76.2	+0.65	- 0.74	-0.98	65.6
13	- 0.14	- 0.98	-0.99	40.9	+0.23	- 0.20	-0.30	69.5
14	+0.48	+0.53	-0.71	113.9	+0.23	- 1.34	-1.36	49.8
15	+0.30	- 0.24	-0.38	70.7	- 0.33	- 0.17	-0.37	13.9
16	+1.34	+0.37	-1.39	97.7	+1.56	+0.30	-1.59	95.4
17	+0.54	- 0.39	-0.66	72.1	+1.00	- 0.05	-1.00	88.5
18	+0.95	- 1.03	-1.40	66.4	+0.29	- 1.45	-1.48	50.6
19	+0.40	+0.27	-0.48	107.3	+0.27	- 0.51	-0.58	58.9
20	+0.04	+0.22	-0.22	129.6	+1.40	+0.06	-1.40	91.2
21	+0.04	- 0.98	-0.98	46.1	- 0.12	+0.12	-0.17	157.5
22	+1.31	- 0.43	-1.38	80.9	+1.87	+0.03	-1.87	90.4
23	- 0.11	- 1.11	-1.12	42.1	+0.45	- 0.95	-1.05	57.7
24	- 0.02	- 0.12	-0.12	39.8	+0.38	- 0.39	-0.55	67.1
25	+0.45	+0.22	-0.50	103.2	+0.18	+0.21	-0.28	114.6
26	- 0.05	- 0.34	-0.34	40.6	- 0.44	- 0.63	-0.77	27.5
27	+0.25	- 0.67	-0.72	55.2	+0.01	- 0.31	-0.31	45.9
28	+1.57	+0.92	-1.82	105.2	+1.26	- 0.81	-1.50	73.7
29	+0.31	- 0.20	-0.37	73.5	+0.45	0.00	-0.45	90.0
30	+1.79	- 0.19	-1.80	86.9	+1.13	- 1.77	-2.10	61.3
31	+0.44	+0.84	-0.95	121.1	+0.46	- 0.43	-0.63	68.4
32	+0.24	- 0.18	-0.30	71.5	- 0.61	- 0.47	-0.77	19.0
33	- 0.72	- 0.17	-0.74	6.7	+0.02	+0.62	-0.62	134.0
34	+0.91	+0.21	-0.93	96.5	+0.73	- 0.82	-1.10	65.8
35	+0.40	- 0.12	-0.42	81.6	+0.48	- 0.76	-0.90	61.3
36	+0.54	+0.18	-0.57	99.2	+0.23	+0.07	-0.24	98.8
37	+0.71	- 0.09	-0.72	86.3	+0.08	+0.18	-0.20	123
38	- 0.20	+0.98	-1.00	140.8	- 0.25	+0.72	-0.76	144.6
39	- 0.55	+1.08	-1.21	148.6	+0.22	- 0.66	-0.70	54.2
40	+0.64	+0.59	-0.87	111.5	+0.89	- 0.24	-0.92	82.3
41	+0.26	- 0.66	-0.71	55.7	+0.01	- 0.80	-0.80	45.3
42	+1.11	+0.69	-1.31	105.9	+1.11	+0.55	-1.24	103.1
43	+0.03	- 0.24	-0.24	48.7	+0.22	+0.19	-0.28	111.7
44	+0.58	- 0.24	-0.63	78.7	+0.44	- 0.27	-0.52	74.2
45	- 0.42	- 0.25	-0.49	15.6	- 0.80	+0.20	-0.83	172.9
46	+0.20	- 0.09	-0.22	77.3	+0.54	+0.28	-0.61	103.7
47	- 0.15	- 0.53	-0.55	36.9	+0.52	- 0.43	-0.68	70.2
48	+0.37	- 0.75	-0.84	58.1	+0.29	- 0.86	-0.91	54.3
49	+0.68	- 0.17	-0.70	82.8	+0.88	- 0.80	-1.19	68.9
50	- 1.03	+1.73	-2.01	150.4	- 2.29	- 0.02	-2.29	0.2
51	+1.12	+0.00	-1.12	90.0	- 0.03	- 1.14	-1.14	44.2

B8.4.1 66 right and left eyes (continued).

Subject N0	Right eyes				Left eyes			
	C ₀	C ₄₅	C	∅	C ₀	C ₄₅	C	∅
52	+0.99	+0.20	-1.01	95.7	+1.53	+0.02	-1.54	90.3
53	- 0.35	+0.41	-0.54	155.5	- 0.65	- 0.43	-0.78	16.7
54	+0.07	+0.13	-0.15	120.8	- 0.41	+1.78	-1.83	141.4
55	- 0.63	+0.75	-0.98	155.0	- 0.13	- 0.13	-0.19	22.5
56	+1.26	+0.55	-1.37	101.8	+1.29	+0.00	-1.29	90.0
57	+1.16	+0.34	-1.21	98.1	+1.73	+1.05	-2.03	105.6
58	- 1.99	- 0.26	-2.01	3.7	+0.27	+0.07	-0.28	97.2
59	- 0.86	+0.96	-1.29	155.9	+0.31	- 0.13	-0.34	78.6
60	+1.51	+0.15	-1.52	92.8	+1.26	+0.07	-1.26	91.6
61	+0.65	- 0.05	-0.65	87.7	+1.53	+0.20	-1.55	93.7
62	+0.56	- 0.26	-0.62	77.5	+0.31	+0.60	-0.68	121.3
63	+0.70	- 0.32	-0.77	77.7	+0.70	+1.20	-1.39	119.7
64	+0.10	- 0.74	-0.75	48.8	- 0.61	+1.83	-1.93	144.2
65	+0.46	- 1.02	-1.12	57.1	+0.96	+0.86	-1.29	111.0
66	- 0.26	- 0.41	-0.49	28.8	+1.43	- 0.21	-1.44	85.9

B8.4.2 20 right and left eyes repeated.

Subject N0	Right eyes				Left eyes			
	C ₀	C ₄₅	C	∅	C ₀	C ₄₅	C	∅
1	- 0.07	- 1.07	-1.07	43.1	+0.62	- 0.65	-0.90	66.8
2	+1.29	- 0.82	-1.53	73.7	+0.34	+0.56	-0.66	119.3
3	- 1.32	+0.62	-1.46	167.4	+0.19	+0.11	-0.22	105.7
4	+0.87	+0.62	-1.07	107.7	- 0.28	+1.30	-1.33	141.0
5	- 0.08	+0.54	-0.55	139.2	+0.16	+0.15	-0.22	111.5
6	+0.50	+0.10	-0.51	95.7	- 0.08	- 0.37	-0.38	38.8
7	+0.90	- 0.49	-1.03	75.7	+0.36	+0.51	-0.63	117.3
8	+0.79	+0.05	-0.79	91.8	+1.17	+0.01	-1.17	90.2
9	+0.72	+0.38	-0.81	104	+1.06	+0.11	-1.07	92.9
10	+0.76	- 0.39	-0.86	76.4	+0.58	+0.33	-0.67	104.8
11	+1.01	- 0.24	-1.04	83.3	+0.55	- 0.58	-0.80	66.9
12	- 0.41	+0.51	-0.65	154.3	+0.71	+0.13	-0.72	95.2
13	+1.12	- 0.90	-1.44	70.6	+0.41	- 0.58	-0.71	62.8
14	+0.51	+1.42	-1.51	125.1	+1.40	+0.14	-1.41	92.8
15	+0.62	- 0.48	-0.79	71.1	+0.70	- 0.27	-0.75	79.3
16	+1.21	+0.52	-1.32	101.6	+2.05	- 0.57	-2.13	82.3
17	+1.01	- 0.80	-1.29	70.9	+0.86	- 0.58	-1.04	73.0
18	- 0.12	- 1.35	-1.36	42.4	+0.49	- 0.64	-0.81	63.7
19	- 0.88	- 0.67	-1.11	161.3	+1.68	- 0.98	-1.94	74.9
20	+0.72	- 0.04	-0.72	88.3	+1.18	+0.72	-1.38	105.8

B8.4.3 10 left eyes with and without cycloplegia.

Subject NO	Without Cycloplegia				With Cycloplegia			
	C ₀	C ₄₅	C	∅	C ₀	C ₄₅	C	∅
71	+0.64	+0.07	-0.64	93.1	+0.17	-0.05	-0.18	81.8
72	+0.59	- 0.76	-0.96	64.0	- 0.02	-0.59	-0.59	44.0
73	- 1.13	- 1.17	-1.62	23.0	- 0.66	-1.48	-1.62	32.9
74	+0.49	- 0.31	-0.58	73.8	+0.61	-0.32	-0.69	76.1
75	+0.15	- 0.36	-0.39	56.5	- 0.34	0.26	-0.43	161.2
76	+0.04	+0.55	-0.55	132.8	+0.21	0.26	-0.34	115.5
77	- 0.07	- 0.65	-0.65	41.8	- 0.03	-0.78	-0.78	43.8
78	- 1.20	- 0.03	-1.20	0.7	- 0.50	-0.20	-0.54	10.9
79	- 0.09	- 0.76	-0.77	41.6	- 0.58	-0.70	-0.91	25.1
80	+0.20	- 0.31	-0.37	61.8	+0.33	-0.27	-0.43	70.3

B8.5 CRYSTALLINE LENS THICKNESS.

B8.5.1 66 right and left eyes.

Subject NO	Right eyes				Left eyes			
	C ₀	C ₄₅	C	Ø	C ₀	C ₄₅	C	Ø
1	+0.53	+0.13	+0.54	173.41	+0.47	+0.10	+0.48	5.94
2	+0.45	- 0.04	+0.45	177.18	+0.51	+0.15	+0.54	8.31
3	+0.11	- 0.15	+0.19	153.9	+0.20	- 0.15	+0.25	161.6
4	+0.25	+0.18	+0.30	17.74	+0.23	+0.03	+0.23	3.17
5	+0.21	+0.04	+0.22	5.09	+0.11	+0.07	+0.13	15.73
6	- 0.61	+0.07	+0.62	86.79	+0.36	+0.23	+0.43	16.59
7	+0.45	+0.14	+0.47	8.52	+0.43	+0.21	+0.48	12.86
8	+0.29	+0.12	+0.31	11.03	+0.46	- 0.09	+0.47	174.53
9	+0.47	+0.19	+0.50	10.88	+0.27	- 0.19	+0.33	162.26
10	+0.31	- 0.06	+0.32	174.39	+0.40	+0.03	+0.04	2.43
11	+0.37	+0.11	+0.39	8.13	+0.17	- 0.06	+0.18	169.94
12	+0.15	+0.01	+0.15	1.49	+0.12	- 0.14	+0.19	155.30
13	+0.26	- 0.20	+0.33	160.94	+0.29	+0.05	+0.30	5.08
14	+0.24	- 0.15	+0.28	16.01	+0.25	- 0.31	+0.40	154.39
15	+0.20	- 0.06	+0.21	172.20	- 0.04	+0.05	+0.06	62.25
16	+0.28	+0.08	+0.29	8.08	+0.42	+0.13	+0.44	8.84
17	+0.40	+0.01	+0.40	0.63	+0.51	+0.02	+0.51	1.08
18	+0.26	- 0.32	+0.41	154.6	+0.05	- 0.43	+0.44	138.49
19	+0.13	+0.03	+0.14	7.18	+0.08	- 0.02	+0.08	173.28
20	+0.56	+0.10	+0.57	5.29	+0.46	- 0.01	+0.46	179.43
21	+0.49	- 0.06	+0.49	176.49	+0.46	+0.07	+0.46	4.26
22	+0.84	- 0.05	+0.84	178.33	+0.81	+0.17	+0.83	5.84
23	+0.16	- 0.03	+0.17	173.96	+0.18	- 0.06	+0.19	171.09
24	+0.34	+0.08	+0.35	7.02	+0.39	- 0.01	+0.39	179.04
25	+0.34	+0.11	+0.36	9.32	+0.29	+0.06	+0.30	6.08
26	+0.45	- 0.13	+0.47	172.16	+0.20	- 0.27	+0.33	153.1
27	+0.50	+0.16	+0.53	9.10	+0.31	+0.06	+0.31	5.73
28	+0.59	+0.15	+0.61	7.02	+0.46	- 0.04	+0.47	177.70
29	+0.34	+0.04	+0.34	3.47	+0.32	+0.01	+0.32	1.01
30	+0.27	- 0.04	+0.28	175.46	+0.26	- 0.15	+0.30	164.87
31	+0.39	+0.22	+0.44	14.57	+0.35	- 0.03	+0.35	177.10
32	+0.40	+0.05	+0.40	3.50	+0.02	- 0.05	+0.06	147.5
33	+0.09	+0.15	+0.17	29.44	+0.23	+0.19	+0.30	20.01
34	+0.45	+0.11	+0.46	6.78	+0.34	+0.02	+0.34	1.77
35	+0.15	+0.16	+0.22	23.18	+0.22	- 0.02	+0.22	178.02
36	+0.40	+0.23	+0.46	15.05	+0.47	- 0.05	+0.47	177.07
37	+0.44	+0.15	+0.46	9.23	+0.32	+0.08	+0.33	6.58
38	+0.15	+0.20	+0.25	26.59	+0.19	+0.22	+0.29	24.17
39	+0.20	+0.41	+0.46	31.81	+0.41	+0.02	+0.41	1.71
40	+0.43	+0.08	+0.44	5.20	+0.51	- 0.05	+0.52	177.40
41	+0.31	- 0.06	+0.32	174.92	+0.17	- 0.29	+0.33	149.86
42	+0.75	+0.18	+0.77	6.82	+0.57	+0.20	+0.61	9.74
43	+0.22	- 0.19	+0.29	159.73	+0.17	0.00	+0.17	179.68
44	+0.35	+0.09	+0.36	7.26	+0.29	+0.13	+0.32	11.85
45	+0.06	- 0.25	+0.26	141.16	+0.08	- 0.15	+0.17	149.70
46	+0.26	- 0.07	+0.27	172.03	+0.12	- 0.01	+0.12	177.45
47	+0.33	- 0.03	+0.33	177.25	+0.42	+0.28	+0.51	16.78
48	+0.34	- 0.09	+0.36	172.45	+0.35	- 0.17	+0.39	167.30
49	+0.78	+0.26	+0.82	9.07	+0.76	- 0.02	+0.76	179.25
50	+0.11	+0.51	+0.52	38.98	- 0.67	+0.13	+0.69	84.46
51	+0.35	+0.08	+0.36	173.79	+0.39	- 0.16	+0.42	168.78

B8.5.1 66 right and left eyes (continued).

Subject N0	Right eyes				Left eyes			
	C ₀	C ₄₅	C	∅	C ₀	C ₄₅	C	∅
52	+0.48	+0.10	+0.50	6.04	+0.57	+0.00	+0.57	0.10
53	+0.21	+0.13	+0.25	15.40	+0.15	+0.10	+0.18	16.73
54	+0.03	+0.20	+0.21	14.32	- 0.03	+0.30	+0.30	48.11
55	+0.16	+0.15	+0.22	21.18	+0.20	+0.03	+0.20	3.81
56	+0.49	+0.22	+0.54	12.24	+0.51	+0.05	+0.51	3.07
57	+0.60	+0.18	+0.62	8.16	+0.52	+0.10	+0.53	5.46
58	- 0.27	+0.12	+0.30	77.70	+0.44	+0.12	+0.46	7.44
59	+0.08	+0.14	+0.15	30.47	+0.11	+0.03	+0.12	6.72
60	+0.46	- 0.02	+0.46	178.52	+0.33	+0.33	+0.47	22.64
61	+0.05	+0.02	+0.05	15.34	+0.66	+0.02	+0.66	0.74
62	+0.36	- 0.11	+0.38	171.36	+0.27	+0.16	+0.32	15.55
63	+0.34	+0.08	+0.33	6.66	+0.29	+0.25	+0.38	20.31
64	+0.32	- 0.01	+0.33	178.77	+0.25	- 0.10	+0.27	169.05
65	+0.33	+0.15	+0.36	12.46	+0.36	+0.18	+0.40	13.31
66	+0.15	+0.05	+0.16	9.68	+0.49	+0.08	+0.50	4.65

B8.5.2 20 right and left eyes repeated.

Subject N0	Right eyes				Left eyes			
	C ₀	C ₄₅	C	∅	C ₀	C ₄₅	C	∅
1	+0.34	- 0.10	+0.35	171.54	+0.43	+0.14	+0.45	9.29
2	+0.40	- 0.24	+0.47	73.70	+0.37	+0.22	+0.44	15.48
3	- 0.07	+0.11	+0.13	61.40	+0.27	+0.02	+0.27	2.34
4	+0.45	+0.01	+0.45	0.77	+0.32	+0.04	+0.32	3.73
5	+0.11	+0.20	+0.22	30.68	+0.22	- 0.02	+0.22	176.7
6	+0.25	+0.12	+0.27	12.59	+0.23	+0.07	+0.24	8.13
7	+0.39	+0.10	+0.41	7.28	+0.22	+0.43	+0.48	31.37
8	+0.36	+0.20	+0.41	14.62	+0.32	+0.08	+0.33	6.87
9	+0.39	+0.39	+0.55	22.46	+0.28	+0.12	+0.31	11.07
10	+0.32	+0.05	+0.32	4.16	+0.31	+0.25	+0.39	19.26
11	+0.34	+0.08	+0.35	6.98	+0.19	- 0.08	+0.21	169.3
12	+0.06	+0.11	+0.13	29.86	+0.28	+0.06	+0.29	6.55
13	+0.39	- 0.18	+0.43	167.36	+0.33	- 0.02	+0.33	178.17
14	+0.38	+0.20	+0.43	13.93	+0.46	+0.15	+0.48	8.98
15	+0.23	- 0.02	+0.23	177.49	+0.32	+0.06	+0.33	4.96
16	+0.44	+0.33	+0.55	18.22	+0.51	+0.05	+0.52	2.61
17	+0.50	+0.12	+0.52	173.03	+0.58	- 0.07	+0.58	176.33
18	+0.20	- 0.32	+0.38	151.13	+0.21	- 0.32	+0.38	151.33
19	- 0.05	+0.02	+0.05	80.17	+0.16	- 0.13	+0.21	160.89
20	+0.60	0.00	+0.60	0.01	+0.50	+0.20	+0.54	10.97

B8.5.3 10 left eyes with and without cycloplegia.

Subject N0	Without Cycloplegia				With Cycloplegia			
	C ₀	C ₄₅	C	∅	C ₀	C ₄₅	C	∅
71	+0.17	+0.03	+0.17	4.46	+0.06	+0.02	+0.07	7.29
72	+0.18	- 0.12	+0.22	162.97	+0.07	- 0.12	+0.14	149.65
73	+0.06	- 0.34	+0.34	140.14	- 0.04	- 0.33	+0.33	131.39
74	+0.44	- 0.29	+0.53	163.45	+0.46	- 0.31	+0.55	163.15
75	+0.16	0.00	+0.16	0.23	+0.09	+0.26	+0.27	34.97
76	+0.14	+0.06	+0.15	11.21	+0.31	- 0.13	+0.34	169.06
77	+0.14	- 0.11	+0.17	161.18	+0.15	- 0.20	+0.24	153.40
78	- 0.04	- 0.08	+0.09	121.35	+0.09	- 0.15	+0.17	150.85
79	+0.26	- 0.33	+0.42	154.21	- 0.02	- 0.31	+0.31	133.17
80	+0.14	- 0.09	+0.17	162.88	+0.21	- 0.12	+0.24	165.00

B8.6 POSTERIOR CRYSTALLINE LENS SURFACE

B8.6.1 66 right and left eyes.

Subject NO	Right eyes				Left eyes			
	C ₀	C ₄₅	C	Ø	C ₀	C ₄₅	C	Ø
1	-2.05	+0.47	-2.10	173.6	-1.88	- 0.40	-1.92	6.0
2	-1.76	+0.18	-1.77	177.1	-2.00	- 0.60	-2.09	8.3
3	-0.49	+0.63	-0.80	153.9	-0.88	+0.66	-1.10	161.6
4	-0.97	- 0.67	-1.18	17.4	-0.87	- 0.10	-0.88	3.2
5	-0.86	- 0.15	-0.87	4.8	-0.44	- 0.26	-0.51	15.2
6	+2.26	- 0.25	-2.27	86.9	-1.28	- 0.83	-1.53	16.5
7	-1.68	- 0.50	-1.75	8.3	-1.51	- 0.72	-1.67	12.7
8	-1.20	- 0.47	-1.29	10.7	-2.00	+0.40	-2.04	174.4
9	-1.66	- 0.65	-1.78	10.7	-1.06	+0.76	-1.30	162.2
10	-1.13	+0.22	-1.15	174.5	-1.41	- 0.10	-1.41	2.0
11	-1.47	- 0.39	-1.52	7.5	-0.71	+0.25	-0.75	170.1
12	-0.67	- 0.03	-0.67	1.3	-0.49	+0.57	-0.75	155.3
13	-1.07	+0.85	-1.37	160.7	-1.22	- 0.22	-1.24	5.2
14	-0.92	- 0.58	-1.09	16.0	-1.04	+1.28	-1.65	154.5
15	-0.77	+0.21	-0.80	172.3	0.15	- 0.21	-0.26	62.3
16	-1.13	- 0.33	-1.18	8.1	-1.74	- 0.55	-1.83	8.8
17	-1.51	- 0.04	-1.51	0.7	-1.91	- 0.07	-1.91	1.0
18	-0.99	+1.21	-1.56	154.6	-0.20	+1.66	-1.68	138.5
19	-0.56	- 0.14	-0.58	7.2	-0.35	+0.08	-0.36	173.7
20	-2.20	- 0.40	-2.24	5.1	-1.83	+0.04	-1.83	179.4
21	-1.69	+0.20	-1.70	176.6	-1.52	- 0.21	-1.53	4.0
22	-2.85	+0.17	-2.86	178.3	-2.66	- 0.55	-2.72	5.8
23	-0.61	+0.14	-0.63	173.7	-0.72	+0.23	-0.76	171
24	-1.26	- 0.31	-1.30	7.0	-1.38	+0.05	-1.38	179
25	-1.31	- 0.44	-1.38	9.3	-1.15	- 0.24	-1.17	5.9
26	-1.75	+0.50	-1.82	172.1	-0.76	+1.04	-1.29	153.1
27	-2.00	- 0.66	-2.10	9.1	-1.30	- 0.26	-1.33	5.8
28	-2.04	- 0.52	-2.10	7.1	-1.65	+0.13	-1.66	177.7
29	-1.22	- 0.14	-1.23	3.3	-1.14	- 0.03	-1.14	0.7
30	-1.20	+0.20	-1.22	175.4	-1.18	+0.68	-1.36	165.1
31	-1.56	- 0.87	-1.79	14.6	-1.33	+0.14	-1.34	177.1
32	-1.33	- 0.16	-1.34	3.4	-0.09	+0.18	-0.20	149
33	-0.31	- 0.51	-0.60	29.5	-0.82	- 0.68	-1.06	19.8
34	-1.78	- 0.43	-1.83	6.8	-1.29	- 0.07	-1.29	1.5
35	-0.62	- 0.64	-0.89	22.9	-0.88	+0.06	-0.88	177.9
36	-1.40	- 0.81	-1.62	15.1	-1.56	+0.16	-1.57	177
37	-1.57	- 0.53	-1.66	9.3	-1.19	- 0.27	-1.22	6.4
38	-0.56	- 0.74	-0.93	26.4	-0.71	- 0.79	-1.06	24.1
39	-0.88	- 1.71	-1.92	31.4	-1.72	- 0.10	-1.72	1.6
40	-1.61	- 0.29	-1.64	5.1	-1.83	+0.17	-1.84	177.4
41	-1.16	+0.21	-1.18	174.8	-0.62	+1.06	-1.23	150.2
42	-2.47	- 0.61	-2.55	6.9	-2.00	- 0.73	-2.19	9.7
43	-0.78	+0.66	-1.02	159.8	-0.59	+0.02	-0.59	179.1
44	-1.35	- 0.35	-1.39	7.3	-1.25	- 0.54	-1.36	11.8
45	-0.19	+0.82	-0.84	141.6	-0.26	+0.51	-0.57	148.7
46	-0.94	+0.26	-0.98	172.3	-0.43	+0.04	-0.43	177.4
47	-1.10	+0.11	-1.10	177.3	-1.33	- 0.88	-1.59	16.7
48	-1.18	+0.34	-1.23	172	-1.31	+0.60	-1.44	167.6
49	-2.33	- 0.78	-2.46	9.2	-2.25	+0.07	-2.25	179.1
50	-0.41	- 2.05	-2.09	39.4	+2.53	- 0.49	-2.58	84.5
51	-1.50	+0.32	-1.53	174.0	-1.57	+0.65	-1.70	168.7

B8.6.1 66 right and left eyes (continued).

Subject N0	Right eyes				Left eyes			
	C0	C45	C	Ø	C0	C45	C	Ø
52	-1.91	-0.41	-1.95	6.0	-2.17	-0.01	-2.17	0.1
53	-0.82	-0.49	-0.95	15.4	-0.60	+0.41	-0.73	17.2
54	-0.13	-0.93	-0.94	41.1	+0.14	-1.31	-1.32	48.1
55	-0.59	-0.53	-0.80	21.1	-0.72	-0.11	-0.73	4.3
56	-1.68	-0.77	-1.85	12.3	-1.74	-0.18	-1.75	2.9
57	-2.18	-0.64	-2.27	8.1	-1.97	-0.36	-2.00	5.2
58	+1.03	-0.46	-1.13	78.0	-1.82	-0.48	-1.88	7.4
59	-0.37	-0.66	-0.76	30.3	-0.54	-0.13	-0.56	6.9
60	-1.68	+0.08	-1.68	178.7	-1.24	-1.25	-1.76	22.6
61	-0.15	-0.08	-0.17	14.4	-2.60	-0.06	-2.60	0.7
62	-1.44	+0.46	-1.51	171.2	-1.13	-0.68	-1.32	15.5
63	-1.28	-0.30	-1.31	6.6	-1.10	-0.94	-1.45	20.2
64	-1.27	+0.06	-1.27	178.7	-0.95	+0.41	-1.04	168.3
65	-1.31	-0.60	-1.44	12.3	-1.39	-0.70	-1.56	13.3
66	-0.56	-0.19	-0.59	9.5	-1.85	-0.30	-1.87	4.6

B8.6.2 20 right and left eyes repeated

Subject N0	Right eyes				Left eyes			
	C0	C45	C	Ø	C0	C45	C	Ø
1	-1.31	+0.39	-1.37	171.8	-1.67	-0.56	-1.76	9.2
2	-1.61	+0.95	-1.87	164.8	-1.45	-0.88	-1.70	15.6
3	0.32	-0.47	-0.57	62.2	-1.16	-0.09	-1.16	2.2
4	-1.69	-0.05	-1.69	0.9	-1.23	-0.18	-1.24	4.2
5	-0.44	-0.79	-0.91	30.4	-0.88	+0.10	-0.89	176.7
6	-0.79	-0.38	-0.88	12.8	-0.84	-0.25	-0.88	8.4
7	-1.48	-0.41	-1.53	7.7	-0.80	-1.53	-1.73	31.2
8	-1.49	-0.81	-1.70	14.3	-1.41	-0.33	-1.45	6.6
9	-1.36	-1.35	-1.91	22.4	-1.09	-0.45	-1.18	11.1
10	-1.14	-1.14	-1.15	3.6	-1.08	-0.85	-1.37	19.1
11	-1.31	-0.32	-1.35	6.9	-0.77	+0.31	-0.83	169
12	-0.28	-0.48	-0.55	29.9	-1.12	-0.26	-1.15	6.5
13	-1.69	+0.80	-1.87	167.3	-1.30	+0.08	-1.30	178.3
14	-1.46	-0.77	-1.65	14	-1.83	-0.58	-1.93	8.8
15	-0.88	-0.08	-0.89	177.5	-1.26	-0.22	-1.28	4.9
16	-1.82	-1.33	-2.25	18.1	-2.06	-0.17	-2.07	2.4
17	-1.87	+0.47	-1.93	172.9	-2.11	+0.29	-2.13	176.1
18	-0.77	+1.20	-1.42	151.3	-0.75	+1.18	-1.40	151.1
19	+0.21	-0.07	-0.22	80.6	-0.74	+0.60	-0.95	160.5
20	-2.29	0.00	-2.29	0.00	-1.94	-0.78	-2.09	10.9

B8.6.3 10 left eyes with and without cycloplegia.

Subject N0	Without Cycloplegia				With Cycloplegia			
	C0	C45	C	Ø	C0	C45	C	Ø
71	-0.72	- 0.11	-0.73	4.3	-0.27	- 0.07	-0.28	6.9
72	-0.65	+0.43	-0.78	163.1	-0.24	+0.41	-0.48	150.1
73	-0.23	+1.23	-1.25	140.4	0.15	+1.19	-1.20	131.4
74	-1.39	+0.90	-1.66	163.5	-1.43	+0.94	-1.71	163.3
75	-0.60	- 0.01	-0.60	0.4	-0.33	- 0.88	-0.94	34.7
76	-0.51	- 0.21	+0.55	11.2	-1.14	+0.47	-1.23	168.8
77	-0.53	+0.40	-0.66	161.7	-0.55	+0.70	-0.90	153.7
78	+0.18	+0.34	-0.38	121.2	-0.32	+0.54	-0.63	150.5
79	-1.00	+1.12	-1.59	154.5	+0.08	+1.21	-1.21	133.0
80	-0.46	+0.30	-0.55	163.3	-0.70	+0.40	-0.81	165.2

B9. POPULATION STUDY: RESIDUAL ASTIGMATIC (RAP) POWER.

Tables B9.1 to B9.3 show computed residual astigmatism in terms of its orthogonal (C_0) and oblique (C_{45}) components of astigmatic decomposition, its cylinder (C) and axis (\emptyset).

B9.1 66 right and left eyes.

Subject N0	Right eyes				Left eyes			
	C_0	C_{45}	C	\emptyset	C_0	C_{45}	C	\emptyset
1	- 0.91	- 0.31	+0.96	99.30	- 0.63	- 0.61	+0.88	112.05
2	- 0.54	+0.05	+0.55	87.19	- 0.67	- 0.02	+0.67	90.70
3	- 0.72	+0.30	+0.78	78.54	- 0.64	- 0.23	+0.68	99.91
4	- 0.49	+0.33	+0.59	73.28	- 0.94	+0.60	+1.11	73.59
5	- 0.85	+0.02	+0.86	89.19	- 0.76	+0.08	+0.77	87.07
6	- 0.71	+0.05	+0.71	88.10	- 1.01	- 0.04	+1.01	91.21
7	- 0.70	- 0.51	+0.87	108.20	- 0.59	- 0.18	+0.61	98.48
8	- 0.21	- 0.31	+0.38	118.09	+0.04	- 0.04	+0.05	160.03
9	- 0.34	+0.26	+0.43	71.38	- 0.42	- 0.35	+0.55	109.78
10	- 0.47	- 0.21	+0.51	102.34	- 0.93	+0.40	+1.01	78.35
11	- 0.75	- 0.70	+1.03	111.63	- 0.68	- 0.28	+0.73	101.28
12	- 0.56	+0.00	+0.56	89.89	- 0.34	- 0.08	+0.35	96.93
13	- 0.86	- 0.16	+0.87	95.14	- 0.80	+0.02	+0.80	89.27
14	- 0.47	+0.09	+0.47	84.81	- 0.50	- 0.36	+0.62	107.59
15	- 0.65	- 0.24	+0.69	100.34	- 0.31	+0.02	+0.31	88.46
16	- 0.22	- 0.03	+0.22	93.27	- 0.22	- 0.03	+0.22	93.73
17	- 0.63	- 0.16	+0.65	97.32	- 0.42	+0.20	+0.47	77.46
18	- 0.21	- 0.32	+0.38	118.09	- 0.41	- 0.43	+0.60	113.16
19	- 0.72	+0.33	+0.79	77.65	- 0.81	- 0.26	+0.85	99.03
20	- 1.22	+0.14	+1.23	86.74	- 0.04	- 0.19	+0.19	50.79
21	- 1.25	- 0.52	+1.35	101.30	- 1.16	+0.07	+1.16	88.37
22	- 0.50	- 0.26	+0.55	103.15	- 0.04	- 0.23	+0.24	130.61
23	- 0.69	- 0.55	+0.88	109.08	- 0.31	- 0.28	+0.42	111.28
24	- 1.00	+0.02	+1.00	89.33	- 0.78	- 0.11	+0.79	93.87
25	- 0.65	- 0.03	+0.65	91.48	- 0.84	+0.17	+0.86	84.43
26	- 1.48	- 0.04	+1.48	90.79	- 1.24	+0.25	+1.27	84.26
27	- 1.44	- 0.67	+1.59	102.52	- 1.21	- 0.47	+1.30	100.64
28	- 0.15	+0.35	+0.38	56.69	- 0.21	- 0.56	+0.60	124.6
29	- 0.53	- 0.06	+0.53	93.21	- 0.30	+0.21	+0.37	72.83
30	+0.38	- 0.40	+0.55	156.83	- 0.05	- 0.35	+0.36	130.74
31	- 0.67	- 0.04	+0.68	91.49	- 0.64	- 0.18	+0.66	97.99
32	- 0.66	- 0.28	+0.72	101.57	- 0.80	- 0.21	+0.81	94.28
33	- 1.05	- 0.26	+1.08	97.00	- 0.90	+0.14	+0.91	85.53
34	- 0.72	- 0.12	+0.73	94.70	- 0.89	- 0.87	+1.25	112.18
35	- 0.33	- 0.59	+0.68	120.48	- 0.28	- 0.43	+0.51	118.39
36	- 0.62	- 0.19	+0.66	98.79	- 0.83	+0.08	+0.83	87.29
37	- 0.41	- 0.24	+0.48	105.37	- 0.65	+0.09	+0.65	86.16
38	- 0.66	+0.32	+0.74	77.30	- 0.58	+0.01	+0.58	89.26
39	- 1.28	- 0.08	+1.28	91.77	- 1.04	- 0.54	+1.17	103.58
40	- 0.50	+0.11	+0.51	83.79	- 0.45	+0.01	+0.45	89.30
41	- 0.40	- 0.19	+0.45	102.62	- 0.73	- 0.09	+0.73	93.41
42	- 0.28	- 0.17	+0.33	105.9	- 0.29	- 0.27	+0.40	111.74
43	- 0.46	+0.34	+0.58	71.73	- 0.50	+0.43	+0.66	69.5

B9.1 66 right and left eyes (continued).

Subject N0	Right eyes				Left eyes			
	C ₀	C ₄₅	C	∅	C ₀	C ₄₅	C	∅
44	- 0.53	0.00	+0.52	89.76	- 0.58	- 0.14	+0.59	96.59
45	- 0.53	- 0.01	+0.53	90.39	- 0.81	+0.16	+0.83	84.58
46	- 0.73	+0.30	+0.79	78.99	- 0.43	+0.55	+0.69	63.95
47	- 0.97	- 0.29	+1.01	98.32	- 0.63	- 0.70	+0.94	113.98
48	- 0.36	- 0.37	+0.52	113.19	- 0.65	- 0.33	+0.73	103.56
49	- 0.49	- 0.68	+0.84	117.07	- 0.42	- 0.29	+0.52	107.68
50	- 0.82	- 0.02	+0.82	90.54	- 0.78	- 0.33	+0.84	101.48
51	- 0.13	- 0.01	+0.13	91.93	- 0.51	- 0.47	+0.70	111.47
52	- 0.40	- 0.11	+0.42	97.61	+0.07	- 0.04	+0.08	163.58
53	- 1.16	+0.17	+1.17	85.92	- 1.30	- 0.57	+1.42	101.83
54	- 0.13	- 0.58	+0.59	128.86	- 0.34	+0.18	+0.38	76.14
55	- 0.96	+0.27	+1.00	82.21	- 0.42	- 0.28	+0.50	106.79
56	- 0.14	+0.04	+0.14	81.69	- 0.14	+0.01	+0.14	88.83
57	- 0.44	+0.07	+0.45	85.50	+0.05	+0.71	+0.71	43.07
58	- 1.29	- 0.32	+1.33	96.96	- 1.26	+0.03	+1.26	89.21
59	- 0.82	+0.19	+0.84	83.50	- 0.28	- 0.33	+0.43	114.75
60	+0.03	+0.06	+0.07	30.21	+0.01	- 0.40	+0.40	164.23
61	+0.30	+0.08	+0.31	7.57	- 0.50	+0.06	+0.51	86.50
62	- 0.70	+0.11	+0.71	85.71	- 0.72	+0.07	+0.72	87.34
63	- 0.67	- 0.59	+0.89	110.86	- 0.59	+0.52	+0.79	69.39
64	- 1.05	- 1.28	+1.06	93.46	- 0.62	+1.48	+1.61	56.35
65	- 0.18	- 0.90	+0.91	129.46	- 0.17	+0.33	+0.37	58.40
66	- 0.69	+0.28	+0.75	100.98	+0.03	- 0.16	+0.16	140.55

B9.2 20 right and left eyes repeated.

Subject N0	Right eyes				Left eyes			
	C ₀	C ₄₅	C	∅	C ₀	C ₄₅	C	∅
1	-1.07	- 0.60	+1.23	104.67	- 0.65	- 0.73	+0.98	114.16
2	-0.21	- 0.03	+0.21	93.87	- 0.65	+0.02	+0.65	89.06
3	-0.78	+0.39	+0.88	76.67	- 0.50	+0.03	+0.50	88.44
4	-0.44	+0.31	+0.54	72.55	- 0.97	+0.84	+1.28	69.64
5	-0.53	+0.06	+0.53	86.67	- 0.50	+0.24	+0.55	77.33
6	-0.41	- 0.08	+0.42	95.43	- 0.98	- 0.08	+0.99	92.18
7	-0.65	- 0.32	+0.72	102.93	- 0.81	- 0.41	+0.91	103.53
8	-0.30	- 0.39	+0.49	116.03	+0.04	- 0.10	+0.11	145.53
9	-0.40	- 0.10	+0.42	97.28	- 0.43	- 0.32	+0.54	108.30
10	-0.24	- 0.17	+0.29	107.86	- 0.39	+0.18	+0.43	77.75
11	-0.35	- 0.46	+0.58	116.33	- 0.66	- 0.07	+0.67	92.91
12	-0.61	+0.14	+0.63	83.76	- 0.47	+0.01	+0.47	89.10
13	-0.16	- 0.15	+0.23	111.49	- 0.75	- 0.07	+0.75	92.51
14	-0.61	+0.60	+0.85	67.81	- 0.15	- 0.35	+0.38	123.46
15	-0.58	- 0.28	+0.65	102.72	- 0.76	- 0.30	+0.82	100.60
16	-0.49	- 0.27	+0.56	104.64	- 0.04	- 0.59	+0.59	132.84
17	-0.42	- 0.18	+0.46	101.81	- 0.63	- 0.12	+0.64	95.18
18	-0.91	- 0.81	+1.22	110.97	- 0.42	- 0.20	+0.46	102.60
19	-1.33	+0.81	+1.55	74.32	+0.22	- 0.27	+0.35	154.88
20	-0.41	- 0.02	+0.41	90.07	+0.02	+0.13	+0.13	41.67

B9.3 10 left eyes with and without cycloplegia.

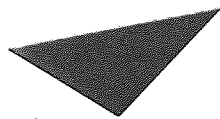
Subject N0	Without Cycloplegia				With Cycloplegia			
	C ₀	C ₄₅	C	∅	C ₀	C ₄₅	C	∅
71	- 0.19	+0.04	+0.19	84.20	- 0.19	+0.01	+0.19	88.00
72	- 0.27	- 0.17	+0.32	106.33	- 0.53	- 0.17	+0.59	98.69
73	- 1.56	- 0.12	+1.57	92.14	- 0.85	- 0.39	+0.94	102.26
74	- 0.33	+0.46	+0.57	62.99	- 0.14	+0.48	+0.50	53.27
75	- 0.51	- 0.23	+0.56	102.14	- 0.71	- 0.20	+0.74	98.02
76	+0.26	+0.32	+0.41	64.73	- 0.50	+0.47	+0.69	68.30
77	+0.81	- 0.18	+0.83	96.27	- 0.70	- 0.20	+0.73	98.00
78	- 0.82	+0.07	+0.82	87.70	- 0.51	- 0.02	+0.51	91.20
79	- 0.80	+0.06	+0.81	87.72	- 0.53	+0.07	+0.54	86.41
80	- 0.24	- 0.14	+0.28	104.53	- 0.13	+0.16	+0.21	115.60

APPENDIX C
SUPPORTING PUBLICATIONS

A study of the axis
of orientation of residual astigmatism

Mark C. M. Dunne, Mohamed E. A. Elawad
and Derek A. Barnes

Ophthalmic and Physiological Optics Research Group,
Department of Vision Sciences, Aston University, Birmingham, U.K.



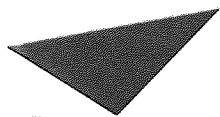
Aston University

Content has been removed for copyright reasons

A clinical trial of the SUN SK-2000 computer-assisted videokeratoscope

Trusit N. Dave,* Colin W. Fowler,† Mohammed E. A. Elawad and Mark C. M. Dunne*

Department of Vision Sciences, University of Aston, Birmingham B4 7ET, UK



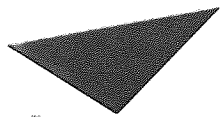
Aston University

Content has been removed for copyright reasons

Measurement of astigmatism arising from the internal ocular surfaces

Mark C. M. Dunne, Mohamed E. A. Elawad
and Derek A. Barnes

Ophthalmic and Physiological Optics Research Group,
Department of Vision Sciences, Aston University, Birmingham, U.K.



Aston University

Content has been removed for copyright reasons